TOPICS IN SUPERSYMMETRY AND PHYSICS BEYOND THE STANDARD MODEL

BY JEAN-FRANÇOIS FORTIN

A dissertation submitted to the

Graduate School—New Brunswick

Rutgers, The State University of New Jersey

in partial fulfillment of the requirements

for the degree of

Doctor of Philosophy

Graduate Program in Physics and Astronomy

Written under the direction of

Professor Thomas Banks

and approved by

____

____

____

____

____

New Brunswick, New Jersey

October, 2009

ABSTRACT OF THE DISSERTATION

Topics in Supersymmetry and Physics Beyond the Standard Model

by Jean-François Fortin

Dissertation Director: Professor Thomas Banks

In this thesis we explore different aspects related to the central concepts of supersymmetry and physics beyond the Standard Model. We start by investigating fine-tuning in the minimal supersymmetric extension of the Standard Model, where the regions with the minimal amount of fine-tuning of electroweak symmetry breaking are found. Afterwards, we concentrate on a more formal aspect of supersymmetry, studying spontaneous symmetry breaking in supersymmetry using the superspace formalism. Thereafter we direct our attention to supersymmetry as physics beyond the Standard Model, looking more specifically at supersymmetry breaking in metastable states. First, we discuss possible undetected Higgs decays in the Pentagon model with renormalizable lepton number violating couplings which also explain neutrino masses. Second, we generalize metastable supersymmetry breaking in supersymmetric quantum chromodynamics to phenomenologically viable models of direct gauge mediation by adding single and multitrace deformations. Third, we introduce a new model of physics beyond the Standard Model, the Pyramid Scheme, and study its implications, focusing on dark matter and its astrophysical signatures in particular. Four, we examine tunneling constraints in models of Cosmological Supersymmetry Breaking, arguing that these models can have no supersymmetric vacuum states in the infinite Planck mass limit. Finally, we present a general study of the possible gamma ray signatures coming from dark matter annihilation or decay.

Acknowledgements

In the first place, I wish to thank my advisor Professor Tom Banks for his support and guidance, and for sharing his profound knowledge of physics. It has been a great intellectual challenge and privilege to work with him and I have learned a great deal from him.

I am also indebted to all professors from Rutgers University, University of California in Santa Cruz and Laval University. In particular, I would like to thank several professors for many enlightening discussions over the years, especially Professors Scott Thomas, Matthew Strassler and Pierre Mathieu. Moreover, I am grateful to Michael Dine, Kenneth Intriligator, Nathan Seiberg, and also to the members of my PhD committee, for their interest and useful discussions. A special thank you also goes to my graduate director, Ronald Ransome.

It is my pleasure to thank many friends and colleagues at Rutgers University, SCIPP and other places for interesting discussions from which I learned. A very partial list includes Evgeny Andriyash, Manjul Apratim, Louis-Francois Arsenault, Aatish Bhatia, Dmitriy Belov, Linda Carpenter, Carl-Johan Eklund, Rouven Essig, Adam Falkowski, Guido Festuccia, Alberto García Raboso, Deepak Iyer, José Juknevich, Michael Kavic, Semyon Klevtsov, Zohar Komargodski, Sergio Lukic, Dmitry Malyshev, John Mason, Jan Manschot, Dmitry Melnikov, Samuel Monnier, Alexander Morisse, Haile Owusu, Guang Pan, Stefano Profumo, Shidhar Ramanujam, Robert Schabinger, Jesse Shelton, David Shih, Warren Siegel, Kuver Sinha, Martin Roček, Gonzalo Torroba, Brian Vancil, Dieter van den Bleeken, Korneel van den Broek, Peter van Nieuwenhuizen, Yi Zhang, Yue Zhao and Iskander Ziyatdinov.

I gratefully acknowledge the hospitality of the members of SCIPP at University of California in Santa Cruz during the month of May 2008. Also a special word of gratitude to Diane Soyak.

Finally, I would like to thank my parents, my siblings and Silvia for their care and patience.

Dedication

Pour

mes parents,

mon frère, ma soeur

&

mon amour

Table of Contents

List of Tables

List of Figures

Chapter 1

Introduction

1.1 Supersymmetry and Physics Beyond the Standard Model

1.1.1 Supersymmetry

The Standard Model (SM) of particle physics is one of the greatest achievements of the 20th century in physics. It describes physics up to energies of the order of the electroweak scale $\Lambda_{\rm EW}$. Although very successful, the SM is likely not to be a good description of physics all the way up to the Planck scale $\Lambda_{\rm P}$, where quantum gravitational effects are expected to generate large corrections. However, from the modern effective field theory point of view, the SM high-energy bound could in principle be pushed up to a larger scale Λ, like the grand unified theory (GUT) scale $\Lambda_{\rm GUT}$ or even the Planck scale, but quantum corrections would destabilize the electroweak scale. Indeed the correct electroweak scale would be obtained by fine-tuning the bare Higgs mass at the level of $\frac{\Lambda}{\Lambda_{\rm EW}}$. This hierarchy problem [1], which comes from a sensitivity of the SM scalar boson sector to new physics, leads to SM scenarios with high-energy bound $\Lambda \gg \Lambda_{\rm EW}$ which are not natural.

Naturalness [2] states that all dimensionful parameters in an effective field theory Lagrangian valid up to an energy scale Λ must be of the order of Λ to the appropriate exponent. Small dimensionful parameters with respect to Λ are only allowed if some symmetry is restored when one small parameter is taken to zero. From this criterion, one can immediately conclude that the SM seen as an effective field theory valid up to $\Lambda \gg \Lambda_{\rm EW}$ is not natural. Either a precise cancellation is needed between the bare Higgs mass and quantum corrections and the theory is fine-tuned or new physics appears at the appropriate scale and stabilizes the theory preserving naturalness.

One of the most popular solutions to the hierarchy problem is supersymmetry (SUSY) [3, 4, 5]. SUSY introduces new physics at a given scale and enlarges the symmetry group of the theory such that scalar field masses are protected against large quantum corrections. In supersymmetric theories, each field comes with a superpartner which has a different spin statistics, and these two fields are combined into a supermultiplet. Thus scalar boson mass terms are protected by the chiral properties of their fermionic superpartners. In other words, there are new contributions to the quantum corrections of the scalar boson mass terms coming from the fermionic superpartners which cancel the otherwise large scalar boson contributions.

The SM can be extended in several ways and the minimal supersymmetric Standard Model (MSSM) is the minimal extension of the SM. It contains all SM particles together with SUSY partners carrying the same quantum numbers but opposite spin statistics. Moreover, due to SUSY and/or anomalies, the MSSM Higgs sector contains two Higgs doublets.

If SUSY were unbroken, the superpartners would share the same mass than their corresponding SM particles. Therefore quantum corrections would cancel exactly and the holomorphic Higgs mass would remain the same. However there is no experimental evidence for the superpartners and SUSY must be a broken symmetry. In order to explain the large hierarchy between the Planck scale and the electroweak scale, one would like to break SUSY dynamically, which would then naturally generate the appropriate small number by dimensional transmutation [6]. There are several ways to dynamically break SUSY and mediate this breaking to the MSSM (e.g. gauge mediation, gravity mediation).

In the MSSM the SUSY breaking sector and the messenger sector are however not specified. Instead one introduces a set of soft SUSY breaking terms and uses renormalization group (RG) equations to determine the electroweak scale superpartner spectrum in function of these high-scale soft SUSY breaking terms. The form of the messenger sector nevertheless dictates the dominant contributions to the high-scale soft SUSY breaking terms.

Moreover, the scale of SUSY breaking dictates the size of the quantum corrections to the Higgs mass and thus is related to the amount of fine-tuning re-introduced in the theory. Indeed, the MSSM predicts a light Higgs boson at tree-level and significant quantum corrections are needed to evade the LEP SM-like Higgs mass bound of 114.4 GeV [7]. This supersymmetric little hierarchy problem, while nowhere as severe as the original hierarchy problem, has led to many theoretical investigations, some of which will be discussed in this thesis (see [8, 9, 10]). For example one can scan the MSSM parameter space to localize the regions with minimal amount of fine-tuning [8]. Rather than doing a total scan of the MSSM parameter space to find the minimally fine-tuned regions, one can also look directly for ways to evade the LEP bound by allowing for a light Higgs bosons which decays in novel ways [9]. Finally one can explore models of gauge mediation where large Higgs mass quantum corrections do not lead to extremely split superpartner spectra [10].

Supersymmetric extensions of the SM come with many virtues. Indeed, one of the most interesting properties of supersymmetric extensions of the SM is gauge coupling unification. At one-loop, the $SU(3)_C \times SU(2)_L \times U(1)_Y$ gauge couplings run with the energy scale and converge for high energy scales. However the gauge coupling constants in the SM context do not merge at any scale while the gauge coupling constants in the MSSM context merge successfully at the GUT scale (see for example [11]). This fact is sometimes seen as the most appealing hint for SUSY as physics beyond the SM. Although very appealing, for this property to hold the messenger sector and/or the SUSY breaking sector must be engineered such that the theory does not develop SM Landau poles before the GUT scale (as in [10]).

Moreover, due to the strong constraints from dynamical SUSY breaking in stable states [6], attempts to build complete theories of dynamical SUSY breaking in stable states usually lead to very baroque models (see e.g. [12]). Indeed, generic models do not exhibit SUSY breaking in stable states unless there is a $U(1)_R$ R-symmetry (necessary condition) which is spontaneously broken (sufficient condition) [13]. Dynamical SUSY breaking in metastable states [14] does not suffer from the constraints on dynamical SUSY breaking in stable states, although the relationship between SUSY breaking and R-symmetry breaking is preserved. In order to simplify SUSY breaking models, dynamical SUSY breaking in metastable states is therefore a promising direction which will be discussed in this thesis [15]. In [15], a simple phenomenologically viable model of dynamical SUSY breaking in metastable states is investigated, where SUSY breaking is mediated directly to the SM by gauge interactions. Direct gauge mediation simplifies the model by eliminating the messenger sector and by offering a straightforward solution to the SUSY flavor problem.

However, dynamical SUSY breaking in metastable states is not always desired. Indeed, the idea of cosmological SUSY breaking (CSB) [16], which conjectures a relation between the cosmological constant and the scale of SUSY breaking, is not compatible with dynamical SUSY breaking in metastable states [17]. The idea of CSB comes from M-theory in asymptotically flat space, which is conjectured to be supersymmetric, hence the aforementioned relation between the cosmological constant and the SUSY breaking scale. In CSB the cosmological constant is seen as an input parameter determining the total number of quantum states of the asymptotically flat de Sitter space, which is represented by the Bekenstein-Hawking entropy [18, 19, 20]. The cosmological constant/SUSY breaking scale relation also leads to a relation between the gravitino mass and the cosmological constant, which constrains SUSY breaking to be gauge-mediated in the low-energy effective theory, resulting in sub-Planckian distances in field space between vacua. Moreover, for the low-energy effective theory to be a theory of stable de Sitter space, it must be above the Great Divide [21], i.e. that transitions from the de Sitter space to other vacua can be seen as highly improbable Poincaré recurrences. This is however impossible for flat space field theory models with different vacua at sub-Planckian distances in field space [17], forcing the low-energy effective theory of CSB to exhibit SUSY breaking in stable states only.

Another flaw of the SM is related to neutrinos: it does not explain neutrino masses. SUSY models with R-parity violating terms offer a simple solution to this problem without introducing right-handed neutrinos. Indeed, neutrino masses can be generated radiatively from renormalizable R-parity violating terms and this will be discussed here [9].

1.1.2 Physics beyond the Standard Model

The SM also suffers problems related to cosmology. One of the main cosmological problems of the SM is dark matter (DM). Another virtue of (R-parity conserving) supersymmetric extensions of the SM is the presence of weakly interactive massive particles (WIMP) with the appropriate mass and relic density to be good DM candidates. This WIMP miracle has excited a lot of theoretical interests, although gauge-mediated SUSY breaking models do not have standard WIMP DM candidates, the gravitino being too light. However, non-thermal production of baryon-like states of the hidden sector can account for the observed DM density and thus give good DM candidates [22]. Moreover, in analogy with QCD, when DM annihilates to pseudo Nambu-Goldstone bosons, there is a possibility to explain the positron excess seen in recent experiments [23, 24, 25, 26, 27]. Indeed, if the pseudo Nambu-Goldstone bosons are light enough, they would decay only to electron-positron pairs, neutrinos and photons, in agreement with the recent observations [10].

Nevertheless, with or without SUSY as physics beyond the SM, a determination of the particle nature of DM is very important for physics beyond the SM. A promising way is to look for cosmic gamma rays. Indeed, if the measured positron excess is due to DM annihilation or decay, the irreducible background of gamma ray photons produced by final state radiation would be diffuse, in constrast with other primary sources of positrons like pulsars which would lead to local gamma ray photon backgrounds. Different photon spectra are expected for different DM annihilation or decay scenarios and a knowleddge of the achievable spectra could help determine the particle nature of DM, as will be discussed here [28].

1.2 Outline of the Thesis and Summary of the Results

1.2.1 Fine-tuning in the MSSM

In chapter 2 (see [8]), the regions in the Minimal Supersymmetric Standard Model (MSSM) with the minimal amount of fine-tuning of electroweak symmetry breaking are presented for general messenger scale. No a priori relations among the soft supersymmetry breaking parameters are assumed and fine-tuning is minimized with respect to all the important parameters which affect electroweak symmetry breaking. The main results are: quite distinctive superpartner spectra in the minimally tuned region of parameter space with large stop mixing at the low scale and negative squark soft masses at the high scale and enormous increase in the minimal amount of tuning for a Higgs mass beyond roughly 120 GeV.

1.2.2 Spontaneous Symmetry Breaking in Supersymmetry

In chapter 3 (see [29]), the analysis of spontaneous gauge symmetry breaking of $N = 1$ supersymmetric $SU(N_c)$ Yang-Mills theory with matter is performed. The supersymmetric R_ξ-gauge is used and its non-local effects investigated. Superpropagators and vertices are computed, and it is shown that the non-local terms introduced by the R_ξ-gauge-fixing are well-behaved in general gauge at one-loop. It is also argued that this feature generalizes to multiple loops.

1.2.3 Undetected Higgs Decays in Supersymmetry

In chapter 4 (see [9]), we discuss SUSY models in which renormalizable lepton number violating couplings hide the decay of the Higgs through $h \to \chi_1^0 \chi_1^0$ followed by $\chi_1^0 \to \tau j j$ or $\chi_1^0 \to \nu_\tau j j$ and also explain neutrino masses. This mechanism can be made compatible with gauge mediated SUSY breaking.

1.2.4 Metastable Supersymmetry Breaking

In chapter 5 (see [15]), metastable vacua in supersymmetric QCD in the presence of single and multitrace deformations of the superpotential are explored, with the aim of obtaining an acceptable phenomenology. The metastable vacua appear at one loop, have a broken R-symmetry, and a magnetic gauge group that is completely Higgsed. With only a single trace deformation, the adjoint fermions from the meson superfield are approximately massless at one loop, even though they are massive at tree level and R-symmetry is broken. Consequently, if charged under the standard model, they are unacceptably light. A multitrace quadratic deformation generates fermion masses proportional to the deformation parameter. Phenomenologically viable models of direct gauge mediation can then be obtained, and some of their features are discussed.

1.2.5 A Pyramid Scheme for Particle Physics

In chapter 6 (see [10]), we introduce a new model, the Pyramid Scheme, of direct mediation of SUSY breaking, which is compatible with the idea of Cosmological SUSY Breaking (CSB). It uses the trinification scheme of grand unification and avoids problems with Landau poles in standard model gauge couplings. It also avoids problems, which have recently come to light, associated with rapid stellar cooling due to emission of the pseudo Nambu-Goldstone Boson (PNGB) of spontaneously broken hidden sector baryon-like number. With a certain pattern of R-symmetry breaking masses, a pattern more or less required by CSB, the Pyramid Scheme leads to a dark matter candidate that decays predominantly into leptons, with cross sections compatible with a variety of recent observations. The dark matter particle is not a thermal WIMP but a particle with new strong interactions, produced in the late decay of some other scalar, perhaps the superpartner of the QCD axion, with a reheat temperature in the TeV range. This is compatible with a variety of scenarios for baryogenesis, including some novel ones which exploit specific features of the Pyramid Scheme.

1.2.6 Tunneling Constraints in Cosmological Supersymmetry Breaking

In chapter 7 (see [17]), we argue that effective field theories compatible with the idea of Cosmological SUSY Breaking (CSB), can have no supersymmetric vacuum states in the $M_P \to \infty$ limit. We introduce a revised version of the Pyramid Scheme, which satisfies this criterion. Combining the criteria for CSB with results of Nelson and Seiberg, any such Lagrangian is non-generic, but we argue that this is plausible in the context of CSB, where R-violating terms in the Lagrangian come from interactions with the horizon, rather than integrating out short distance degrees of freedom. We also point out a Landau pole in the hidden sector gauge group of the Pyramid Scheme, and propose an unique mechanism for avoiding it.

1.2.7 Gamma Ray Spectra from Dark Matter Annihilation and Decay

In chapter 8 (see [28]), we study gamma ray spectra for various scenarios of dark matter annihilation and decay. We focus on processes which generate only high-energy photons or leptons and photons, but no proton-antiproton pairs, to be compatible with PAMELA's data. We investigate photons produced directly from two-body decay chains and photons produced together with charged particles. For the former case we also include the process DM(+DM) $\rightarrow N\phi \rightarrow 2N\gamma$ which can arise from specific strongly-coupled dark matter scenarios. For the latter case, photons are either generated by final state radiation from high-energy leptons or are directly generated from contact interactions represented by higher-order (non-renormalizable) operators obtained after integrating out heavy modes. We compare their overall annihilation cross-sections/decay rates taking into account chiral suppression (in the s-wave approximation), dimension of operators and dark matter particle properties. A rough estimate shows that, for a dark matter particle with a mass of $\mathcal{O}(1\,\mathrm{TeV})$, the hard photon spectra in direct electron-positron-photon final states arising from either scalar boson dark matter annihilation/decay or Majorana fermion dark matter annihilation are dominated by higher-order operators if the scale of the leading operator is lower than $\mathcal{O}(1000\,\mathrm{TeV})$. Otherwise, all the photon spectra arising in this way are dominated by final state radiation. Among the spectra studied, the higher-order operators spectrum is the hardest while the final state radiation spectrum with an intermediate decay is the softest.

Chapter 2
Fine-tuning in the MSSM

2.1 Introduction

In this chapter we discuss in detail the findings of the work done in collaboration with R. Essig [8].

The Minimal Supersymmetric Standard Model (MSSM) is a well-motivated candidate for physics beyond the Standard Model (SM). The gauge couplings within the MSSM unify to within a few percent at the grand unified theory (GUT) scale, $M_{\rm GUT} \simeq 2 \times 10^{16}$ GeV, and the lightest supersymmetric particle is a good dark matter candidate provided that R-parity is conserved. Supersymmetry (SUSY) can also naturally stabilize the hierarchy between the electroweak (EW) and the GUT or Planck scale. It does this by providing a radiative mechanism for electroweak symmetry breaking (EWSB) where large quantum fluctuations of the scalar top squarks due to the large Yukawa coupling destabilize the origin of the Higgs potential. In much of the MSSM parameter space this quite naturally leads to the right EWSB scale, as long as the soft SUSY breaking parameters lie near it.

The absence of any direct experimental evidence from collider searches for the MSSM scalar particles and the Higgs boson has, however, ruled out significant regions in the MSSM parameter space. Indirect evidence from EW precision measurements and searches for flavor changing neutral currents, CP violating effects and rare decays has not been forthcoming either, providing additional severe constraints. As a result, the soft SUSY breaking parameters must lie well above the EW scale in order to satisfy the experimental constraints, especially the constraints on the Higgs mass from the results of the CERN LEP collider ($m_h \gtrsim 114.4$ GeV [7]).

Soft SUSY breaking parameters well above the EW scale reintroduce a small hierarchy and require some fine-tuning (FT) among the SUSY parameters in order to obtain EWSB [30]-[50]. This is usually referred to as the supersymmetric little hierarchy problem.

Different choices for the soft SUSY breaking parameters lead to different amounts of FT. This paper presents the minimally tuned MSSM (or MTMSSM), i.e. the MSSM parameter region that has the least model-independent FT of EWSB. Model-independent means that no relations are assumed between the soft SUSY breaking parameters at the scale at which they are generated (which will be referred to as the messenger scale). Rather, each of them is taken to be an independent parameter which is free at the messenger scale, and which therefore can contribute to the total FT of the EWSB scale. The messenger scale itself is varied between 2 TeV and $M_{\rm GUT}$ and the effect of this on the minimal FT is discussed.

In Section 2.2, EWSB in the MSSM will be reviewed. Section 2.3 discusses the tuning measure used in this paper. The parameters taken to contribute to the tuning are $|\mu|^2$, $m^2_{H_u}$, the gaugino masses M_1, M_2 and M_3, the stop soft masses $m^2_{\tilde{t}_L}$ and $m^2_{\tilde{t}_R}$, and the stop soft trilinear coupling A_t.

Section 2.4 contains some of the main results. The low- and high-scale MSSM spectrum which leads to the least model-independent FT is found. This is done for various messenger scales by numerically minimizing the FT expression subject to constraints on the Higgs, stop, and gaugino masses. The results are then motivated analytically. The least FT is found to be about 5% if the messenger scale coincides with the GUT scale. An important feature of the least FT region is negative stop soft masses at the messenger scale (first pointed out in [47]). Even for messenger scales as low as 2 TeV, the stop soft masses are tachyonic at the messenger scale (threshold effects in the RG-running were neglected throughout). This does not lead to any problems with charge and/or color breaking minima. Another feature of the least FT region is that the trilinear stop soft coupling, A_t, is negative and lies near "natural" maximal mixing, i.e. $A_t \simeq -2m_{\tilde{t}}$, where $m_{\tilde{t}}$ is the average of the two stop soft masses. This value for A_t maximizes the radiative corrections to m_h. The large stop mixing leads to a sizeable splitting between the two stop mass eigenstates. Moreover, the gluino mass, M_3, is much smaller than the wino mass, M_2, at the high scale. The wino mass, in turn, is much smaller than the bino mass M_1. Phenomenological consequences of the low-scale spectrum are briefly summarized.

Section 2.5 contains the rest of the main results of the paper. The FT is minimized as a function of the lower bound on the Higgs mass (with the messenger scale set to $M_{\rm GUT}$). Although the numerical minimization procedure contains the dominant one-loop expression for m_h as a constraint, the resulting least FT spectra are used to calculate m_h more accurately with the program `FeynHiggs` [51, 52, 53, 54, 55]. The result is a plot of the minimal FT as a function of m_h, where m_h now includes all the important higher order corrections. There are several striking features of this plot. First of all, for m_h larger than a certain value, the FT increases very rapidly and at least as fast as an exponential. Secondly, around this m_h, the value of A_t in the least FT region makes a sudden transition from lying near $-2m_{\tilde{t}}$ to lying near $+2m_{\tilde{t}}$. The third striking feature is that this value of m_h is surprisingly low. The precise value is only slightly dependent on the parameters in the Higgs sector and can be taken to lie around 120 GeV. It has been mentioned before that the FT increases exponentially as a function of m_h, see for example [36, 42]. Previously, these results were obtained by assuming a specific set of boundary conditions at the messenger scale and without taking into account important higher-order corrections to the Higgs mass which are included in `FeynHiggs`. The results here do not assume particular boundary values for any of the important parameters contributing to EWSB - rather, the spectrum that leads to the least amount of tuning is found. Moreover, the higher-order Higgs mass corrections are included. It is shown that the *minimal* amount of tuning still increases at least as fast as an exponential.

Section 2.6 contains a summary of the results and the conclusions. Appendix 2.7 reviews the semi-numerical solutions of the MSSM one-loop renormalization - group (RG) equations. These are used to calculate the expression for the FT employed in this paper. Appendix 2.8 contains a list of expressions for the FT with respect to various parameters.

2.2 Electroweak Symmetry Breaking

In the Higgs decoupling limit of the MSSM, the lower bound on the mass of the lighter CP-even Higgs mass eigenstate h coincides with the 114.4 GeV bound on the mass of the SM Higgs boson [7]. The mass of h may be approximated by

$$m_h^2 \simeq m_Z^2 \cos^2 2\beta + \frac{3}{4\pi^2}\frac{m_t^4}{v^2}\left[\log\frac{m_{\tilde{t}}^2}{m_t^2} + \frac{X_t^2}{m_{\tilde{t}}^2}\left(1 - \frac{X_t^2}{12 m_{\tilde{t}}^2}\right)\right] \tag{2.1}$$

which, in addition to the tree-level Higgs mass, includes the dominant one-loop quantum corrections coming from top and stop loops [56, 57, 58, 59, 60, 61]. Here m_t is the top mass, $m_{\tilde{t}}^2$ is the arithmetic mean of the two squared stop masses and $v = \sqrt{2}m_W/g \simeq 174.1$ GeV where g is the $SU(2)$ gauge coupling and m_W is the mass of the W-boson. Furthermore, equation (2.1) assumes $m_{\tilde{t}} \gg m_t$. The stop mixing parameter is given by $X_t = A_t - \mu\cot\beta$ ($\simeq A_t$ for large $\tan\beta$), where A_t denotes the stop soft trilinear coupling and μ is the supersymmetric Higgsino mass parameter. The first term in equation (2.1) is the tree-level contribution to the Higgs mass. The first term in square brackets comes from renormalization group running of the Higgs quartic coupling below the stop mass scale and vanishes in the limit of exact supersymmetry. It grows logarithmically with the stop mass. The second term in square brackets is only present for non-zero stop mixing and comes from a finite threshold correction to the Higgs quartic coupling at the stop mass scale. It is independent of the stop mass for fixed $X_t/m_{\tilde{t}}$, and grows as $(X_t/m_{\tilde{t}})^2$ for small $X_t/m_{\tilde{t}}$.

Equation (2.1) implies a combination of three things which are required to satisfy the bound on m_h, namely a large tree-level contribution, large stop masses and/or large stop mixing[1]. A large tree-level contribution to m_h requires $\tan\beta$ to be at least of a moderate size ($\gtrsim 5-10$). Although the stop masses must be rather large, their lower bound is very sensitive to the size of the stop mixing, with larger mixing allowing for much smaller stop masses (see [62] for a recent study on this). The reason for this sensitive dependence is due to the Higgs mass depending logarithmically on the stop masses in contrast to the polynomial dependence on the stop mixing.

The soft masses are not only directly constrained from the LEP Higgs bounds but also indirectly by constraints on flavor changing neutral currents, electroweak precision measurements and CP-violation. Besides these, however, the Higgs sector parameters are also constrained by requiring that the electroweak symmetry is broken. This leads to the following two tree-level relations at the low scale

$$\sin 2\beta = \frac{2m_{12}^2}{m_{H_u}^2 + m_{H_d}^2 + 2|\mu|^2} = \frac{2m_{12}^2}{m_A^2} \tag{2.2}$$

$$\frac{m_Z^2}{2} = -|\mu|^2 + \frac{m_{H_d}^2 - m_{H_u}^2 \tan^2\beta}{\tan^2\beta - 1}, \tag{2.3}$$

where m_A is the CP-odd Higgs mass, and β is determined from the ratio of the two vacuum expectation values $v_u \equiv \langle \mathrm{Re}(H_u^0)\rangle$ and $v_d \equiv \langle \mathrm{Re}(H_d^0)\rangle$ as $\tan\beta = v_u/v_d$. The masses $m_{H_u}^2$, $m_{H_d}^2$ and m_{12}^2 are the three soft mass parameters in the MSSM Higgs sector. For a given value of $\tan\beta$, m_{12}^2 may be eliminated in favor of m_A^2 with equation (2.2). Equation (2.3) gives an expression for m_Z^2 in terms of the supersymmetric mass parameter μ and the soft masses $m_{H_u}^2$ and $m_{H_d}^2$. Since $\tan\beta$ should be sizeable, the contribution from $m_{H_d}^2$ to the expression for m_Z^2 may be neglected and (2.3) simplifies to

$$m_Z^2 = -2|\mu|^2 - 2m_{H_u}^2. \tag{2.4}$$

Close to the Higgs decoupling limit, m_A is relatively large. However, since $|\mu|^2, m_{H_u}^2 \sim \mathcal{O}(m_Z^2)$ to avoid large cancellations, m_A may not be too large, otherwise $m_{H_d}^2$ would also be sizeable and equation (2.4) would break down (unless the value of $\tan\beta$ is increased accordingly). By choosing $\tan\beta = 10$ and $m_A = 250$ GeV in the numerical analysis throughout, equation (2.4) holds to a very good approximation.

---

[1] Although it is not obvious, it is important to note that these statements remain the same even away from the Higgs decoupling limit, see e.g. [62]. Moreover, as mentioned in [62], the fine-tuning in the Higgs decoupling limit is comparable to the fine-tuning in the Higgs non-decoupling limit. Thus the least fine-tuned regions found in this paper do not depend in an essential way on the fact that the analysis is done in the Higgs decoupling limit.

Equation (2.4) holds at tree-level, and although quantum corrections may add $\mathcal{O}(10\text{ GeV})$ to the right hand side of (2.4), this has negligible impact on the amount of fine-tuning to be discussed below.

The parameters $m_{H_u}^2$ and $|\mu|^2$ in equation (2.4) are evaluated at the scale m_Z. Since the fine-tuning of EWSB is a measure of the sensitivity of some low-scale EWSB parameter (usually taken to be m_Z^2) to a change in high-scale input parameters, $|\mu|^2$ and $m_{H_u}^2$ need to be evolved to a high scale using their RG equations (the one-loop RG equations will be sufficient for the purposes of discussing fine-tuning). Under RG running many of the soft parameters mix, and as a result of this mixing, the expression for m_Z^2 in terms of parameters that are evaluated at the messenger scale M_S differs significantly from the simple form given in (2.4). The RG-equations may be integrated (see Appendix 2.7) and the expression for m_Z^2 may generically be written as [63, 64]

$$m_Z^2 = \sum_{i,j} c_{ij}(\tan\beta, M_S)\, m_i(M_S)\, m_j(M_S). \tag{2.5}$$

For moderate and not too large values of $\tan\beta$ with an appropriate m_A, the simplified expression for m_Z^2 is applicable (equation (2.4)) and contributions from the bottom/sbottom and tau/stau sectors may still be neglected[2]. The most important parameters appearing in (2.5) then are μ^2, $m_{H_u}^2$, the gaugino masses M_1, M_2 and M_3, the stop soft masses $m_{\tilde{t}_L}^2$ and $m_{\tilde{t}_R}^2$, and the stop soft trilinear coupling A_t. The coefficients c_{ij} depend on $\tan\beta$ and the messenger scale M_S. The most important coefficients are shown in Figure 2.1 for $\tan\beta = 10$ as a function of M_S.

At the scale m_Z, the coefficients of $m_{H_u}^2$ and μ^2 are -2 while the coefficients of the other soft parameters are zero in agreement with equation (2.4). Since μ^2 is a supersymmetric parameter, it gets renormalized multiplicatively and its RG evolution does not give rise to soft parameters (see equation (2.45)). Figure 2.1 shows that the coefficient of μ^2 does not vary much and remains close to -2 all the way up to the GUT scale. The RG evolution of $m_{H_u}^2$ to higher messenger scales, however, generates non-zero coefficients for the other soft parameters. The β-function of $m_{H_u}^2$,

$$8\pi^2\beta_{m_{H_u}^2} = 3\lambda_t^2(m_{H_u}^2 + m_{\tilde{t}_L}^2 + m_{\tilde{t}_R}^2 + |A_t|^2) - 3g_2^2|M_2|^2 - g_Y^2|M_1|^2 - \frac{1}{2}g_Y^2 S_Y, \tag{2.6}$$

depends on the stop sector parameters $\{m_{\tilde{t}_L}^2, m_{\tilde{t}_R}^2, A_t\}$, the wino and bino masses M_2 and M_1, and $S_Y \equiv \frac{1}{2}\mathrm{Tr}(Y_i m_i^2)$, which thus get generated immediately under RG evolution. The

[2] For large $\tan\beta$, bottom/sbottom and tau/stau sector contributions must be included. Large $\tan\beta$ allows the tree-level Higgs mass to be increased by about 2 GeV compared to its value for $\tan\beta = 10$. Higher-order corrections to the Higgs mass from the bottom/sbottom sector, however, can in some regions lead to rather large negative contributions. The effect on the least fine-tuned regions found in this paper will not be discussed in detail, but it is unlikely that the main features of the least fine-tuned spectrum will change.

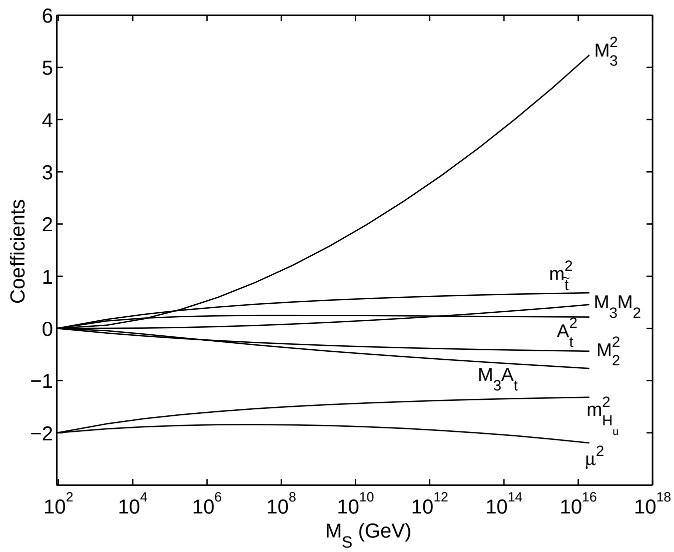

Figure 2.1: The coefficients c_{ij} defined in equation (2.5) for $\tan\beta = 10$ as a function of the messenger scale M_S.

coefficients of M_2 and especially M_1 and S_Y in (2.6) are small and lead to small coefficients in the expression for m_Z^2 (2.5). Although $\beta_{m^2_{H_u}}$ does not explicitly depend on the gluino mass, a non-zero coefficient for M_3 is generated indirectly since the stop sector β-functions depend on M_3. Moreover, M_3 appears with a large coefficient in these β-functions, and thus the coefficient of M_3 in equation (2.5) dominates after a few decades of RG evolution. For example, at a messenger scale of $M_S = M_{\rm GUT} \equiv 2\times 10^{16}$ GeV, the expression for m_Z^2 (for $\tan\beta = 10$) is

$$\begin{aligned} m_Z^2 \quad = \quad & -2.19\,\hat\mu^2 - 1.32\,\hat m^2_{H_u} + 0.68\,\hat m^2_{\tilde t_L} + 0.68\,\hat m^2_{\tilde t_R} + 5.24\,\hat M_3^2 - 0.44\,\hat M_2^2 \\ & - 0.01\hat M_1^2 + 0.22\,\hat A_t^2 - 0.77\,\hat A_t\,\hat M_3 - 0.17\,\hat A_t\,\hat M_2 - 0.02\,\hat A_t\,\hat M_1 \\ & + 0.46\,\hat M_3\,\hat M_2 + 0.07\,\hat M_3\,\hat M_1 + 0.01\,\hat M_2\,\hat M_1 + 0.05\,\hat S_Y, \end{aligned} \tag{2.7}$$

where the hatted parameters on the right-hand side are all evaluated at M_S. This expression may be used to calculate the FT as discussed next.

2.3 The Tuning Measure

A variety of tuning measures have been used in the literature (a list of references has been provided in the Introduction). Since the concept of fine-tuning (FT) is inherently subjective, there is no absolute definition of a FT measure. The most common definition of the sensitivity of an observable $\mathcal{O}(\{a_i\})$ on a parameter a_i, denoted by $\Delta(\mathcal{O}, a_i)$, is given by [30, 31]

$$\Delta(\mathcal{O}, a_i) = \left| \frac{\partial \log \mathcal{O}}{\partial \log a_i} \right| = \left| \frac{a_i}{\mathcal{O}} \frac{\partial \mathcal{O}}{\partial a_i} \right| . \tag{2.8}$$

$\Delta(\mathcal{O}, a_i)$ thus measures the percentage variation of the observable under a percentage variation of the parameter. A large value of $\Delta(\mathcal{O}, a_i)$ signifies that a small change in the parameter leads to a large change in the observable, and suggests that the observable is fine-tuned with respect to that parameter. In the literature, the FT of $\mathcal{O}$ is often defined to be $\max_i \Delta(\mathcal{O}(a_i))$, e.g. [30, 31]. This FT measure arguably underestimates the "total amount" of FT if there is more than one parameter a_i. This can be a drawback especially if there are many parameters that are tuned by roughly the same amount. This motivates the use of a FT measure which considers the tuning of all the parameters simultaneously. Assuming that the individual $\Delta(\mathcal{O}, a_i)$ are uncorrelated, the following FT measure may be used (see also [44, 65])

$$\mathcal{F}(\mathcal{O}) = \sqrt{\sum_i \Big(\Delta(\mathcal{O}, a_i)\Big)^2}. \tag{2.9}$$

Of interest in this paper is to quantify the sensitivity of EWSB in the MSSM on (soft) supersymmetric parameters at the messenger scale M_S. To this end, the observable to consider is m_Z^2 as a function of the supersymmetric Higgsino mass squared and the soft supersymmetry breaking parameters, collectively denoted by $m_i^2(M_S)$ (in the FT measure, all parameters are taken to have mass dimension two). The sensitivity of m_Z^2 with respect to each parameter may be calculated as in (2.8) with $\mathcal{O} = m_Z^2$, and the total FT of m_Z^2 on parameters evaluated at the messenger scale M_S may be quantified by

$$\mathcal{F}(m_Z^2; M_S) = \sqrt{\sum_i \Big(\Delta\big(m_Z^2, m_i^2(M_S)\big)\Big)^2}. \tag{2.10}$$

$\mathcal{F}(m_Z^2; M_S)$ may be interpreted as the length of a "fine-tuning vector" with components $\Delta(m_Z^2, m_i^2(M_S))$. This fine-tuning vector is formally a vector field defined by the gradient of the scalar field $\log m_Z^2$, a function of $\log m_i^2$, along surfaces of constant $\log m_Z^2$.

There are several possible drawbacks to this FT measure, see for example [50, 66]. One of these is that the individual $\Delta(m_Z^2, m_i^2(M_S))$ are assumed to be uncorrelated. Within a given model of supersymmetry breaking, there may be relations among the parameters at the messenger scale. This would imply that the FT vector is projected onto a subspace, and the resulting FT is necessarily less. In other words, the tuning of one parameter is correlated with the tuning of another, so that the total FT is less[3] than that given by (2.10). Moreover,

[3]Note, however, that if a given model assumes relations among the high scale parameters which do not allow the parameters to fall within the least fine-tuned regions found in this paper, then the FT of such a model will most likely be substantially larger than the model-independent minimal FT, *despite* there being relations among the high scale parameters.

within a given model the values of the parameters at the messenger scale may be restricted to certain ranges, whereas (2.10) assumes that all values are equally likely. However, no model for supersymmetry breaking will be assumed here. Instead, the minimal FT will be found as a function of the messenger scale M_S assuming no relations or restrictions among the high-scale input parameters. For this "model-independent" tuning it is satisfactory to use the FT measure (2.10).

Note that to find the tuning of a model, one should in principle consider the tuning of all observables, since the absence of tuning in one observable does not necessarily imply it is small in others, see e.g. [45]. In this paper, however, only the tuning of EWSB will be considered.

Finally, note that the FT with respect to a single parameter is by definition (2.8) zero if that parameter happens to be zero at the messenger scale. An extreme version of this is found in the no-scale model [67], where all scalar soft masses are much smaller than the gaugino masses at the high scale. Setting them to zero, and using (2.8) and (2.10) the FT could be expected to be small. However, it may be shown that this does not minimize the FT, since M_3 and μ need to be quite large at the high scale to satisfy all the low-energy experimental bounds (see [41]). In the results presented in this paper, no parameter is found to be zero at the high scale.

2.4 Minimal Model Independent Tuning

In this section the minimal model independent tuning will be found as a function of the messenger scale.

2.4.1 Discussion of Minimization Procedure and Constraints

The FT given by equation (2.10) is written in terms of parameters evaluated at the messenger scale. In order to find the minimal FT (MFT) for a given messenger scale that is consistent with low-energy experimental constraints, it is easiest to rewrite the FT expression in terms of parameters that are evaluated at the low scale. This can be done by expressing each high-scale parameter in terms of low-scale parameters, see Appendix 2.7. Once the FT is written in terms of low-scale parameters, $m_{H_u}^2(m_Z)$ may be eliminated by using equation (2.4) (neglecting contributions from $m_{H_d}^2$).

The low-energy constraints considered in this paper include bounds on the (physical) sparticle masses, on the gaugino masses, and on the Higgs mass[4]. The physical top quark mass

[4]Constraints from measurements of $B \to X_s\gamma$ or the electroweak S- and T-parameter do not significantly affect the results presented below, since an experimentally consistent value can be obtained by only small

$m_t^{\rm pole}$ is set to the central value of the latest Tevatron mass measurement of 170.9 $\pm$ 1.8 GeV [68]. The physical stop masses are required to be at least 100 GeV which is illustrative of the actual, slightly model dependent, lower bound obtained from the Tevatron [69]. It is found that the region of MFT does not quite saturate this bound, although a slightly larger value for the top mass would allow the lighter stop to be as low as 100 GeV. The gaugino masses M_1 and M_2, as well as μ, are taken to have a lower bound of 100 GeV. The gluino mass is found to be never smaller than 335 GeV in the numerical results presented in this section, and this does not generically violate any experimental bounds.

The most important constraint is the Higgs mass bound of 114.4 GeV (valid in the decoupling limit), since it turns out that this bound is always saturated when minimizing the FT. In the numerical results presented in this paper, the Higgs mass is calculated using the formulas found in [70] (see also [56, 57, 58, 59, 60, 71]). These formulas include the one-loop corrections coming from the top/stop sector and are simple enough to be used as constraints in the FT minimization (but note that the sign convention used here for A_t is that of [11]). In order to capture some of the important leading two-loop contributions to the Higgs mass, a running top mass $m_t(m_t) \simeq 162.5$ GeV (evaluated in the $\overline{MS}$-scheme) is used instead of the physical top mass $m_t^{\rm pole}$. There are, however, further higher-order corrections to the Higgs mass that play a very important role, and more accurate Higgs masses may be obtained with the program `FeynHiggs` which includes many of them. These additional corrections often tend to lower the Higgs mass, and the one-loop formula used in the minimization procedure here does not capture this effect. In order to compensate for some of these additional higher-order corrections and thus obtain a more accurate estimate of the MFT, a lower bound for the Higgs mass of 121.5 GeV is used in the FT minimization, instead of the SM lower bound of 114.4 GeV. It turns out that the typical low energy sparticle spectrum obtained in the analysis below then leads to a Higgs mass that lies just above 114.4 GeV when these additional corrections are taken into account (calculated with `FeynHiggs`, version 2.6.0, assuming real parameters). The issue of higher-order corrections to the Higgs mass will be revisited in Section 2.5.

Sequential Quadratic Programming (SQP) in Maple is used as a minimization algorithm. Given the FT function (2.10) written in terms of low scale parameters, as well as linear constraints on the gaugino masses and μ, non-linear constraints on the physical stop and Higgs masses, and an initial guess, SQP generates a less FT point until the minimum is found. Unlike other minimization algorithms, SQP can handle arbitrary constraints which is essential here

adjustments (if at all necessary) in the least fine-tuned parameters - see also [62].

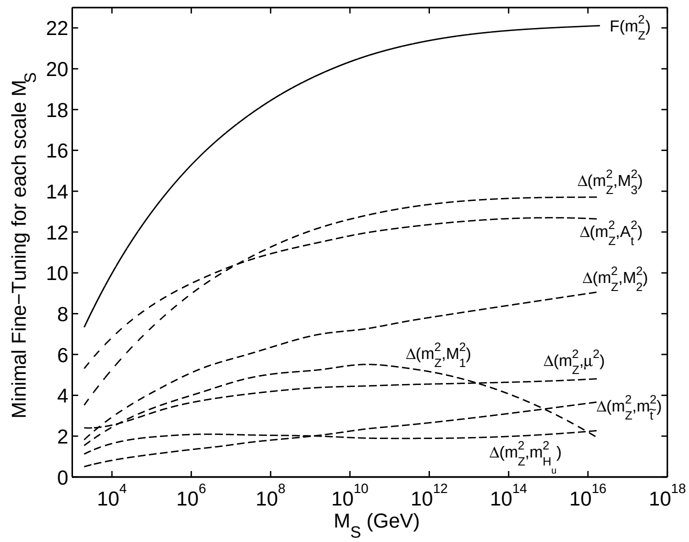

Figure 2.2: The minimal fine-tuning as a function of the messenger scale M_S for $\tan\beta = 10$. The top black line is the total minimal fine-tuning as defined in equation (2.10) which includes all the individual contributions. The individual contributions to the fine-tuning from μ^2, $m^2_{H_u}$, the gaugino masses M_1^2, M_2^2 and M_3^2, and the stop soft trilinear coupling A_t^2 are included. Moreover, the average fine-tuning of the stop soft masses $m^2_{\tilde{t}_L}$ and $m^2_{\tilde{t}_R}$ is included as in equation (2.11).

due to the highly non-linear physical stop mass and Higgs mass constraints.

2.4.2 Numerical Results

Figure 2.2 shows a plot of the MFT as a function of the messenger scale M_S. Shown are the individual contributions $\Delta\big(m_Z^2, m_i^2(M_S)\big)$ to the FT, with m_i^2 given by M_3^2, M_2^2, M_1^2, A_t^2, μ^2, or $m^2_{H_u}$. The FT of $m^2_{\tilde{t}_L}$ and $m^2_{\tilde{t}_R}$ have been included as

$$\Delta(m_Z^2, m_{\tilde{t}}^2) = \left(\frac{1}{2}\Big[\Big(\Delta(m_Z^2, m^2_{\tilde{t}_L})\Big)^2 + \Big(\Delta(m_Z^2, m^2_{\tilde{t}_R})\Big)^2\Big]\right)^{1/2}. \tag{2.11}$$

The (top) black line shows the total FT as defined by (2.10).

From the plot it is clear that the MFT increases as a function of the messenger scale M_S. This is expected since a higher messenger scale implies more RG running to the low scale so that small differences in high-scale input parameters are magnified. For $M_S = M_{\rm GUT}$, the total MFT is about 22, i.e. 4.5%. (As an aside, for $\tan\beta = 30$ and $m_A = 1000$, the MFT for a Higgs mass of 114 GeV is about 11, i.e. 9%.) The largest contribution to the total minimal FT comes from M_3^2 and A_t^2 which are both comparable for all values of M_S. The next most important contribution is that from M_2^2. The contributions from μ^2, as well as $m^2_{\tilde{t}_L}$ and $m^2_{\tilde{t}_R}$ are less important and increase only slightly as a function of M_S. The FT from $m^2_{H_u}$ is very

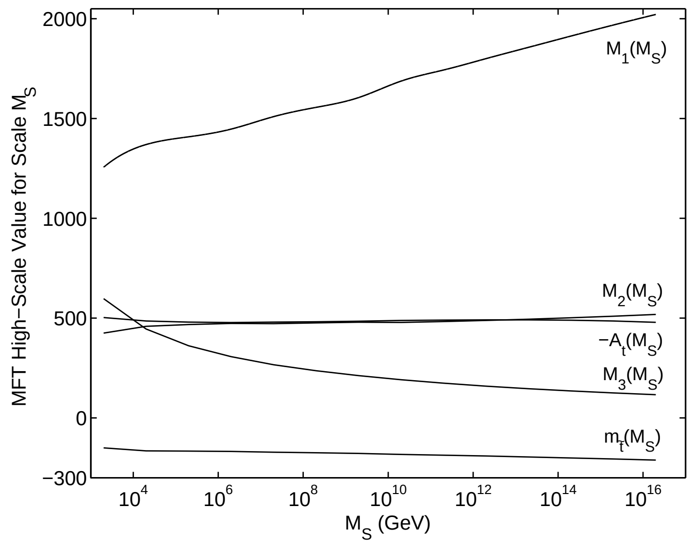

Figure 2.3: The messenger scale values of M_3, M_2, M_1, A_t and the average of the stop soft masses squared, $m_{\tilde{t}}$, that give the minimal fine-tuning (MFT) as a function of the messenger scale M_S and for $\tan\beta = 10$. The high-scale values of M_2 and A_t, and to a lesser extent M_1 and $m_{\tilde{t}}$, in the minimal fine-tuned region are roughly constant. The high-scale value of M_3, however, decreases significantly as the messenger scale is increased. The reason for this is that the coefficient of M_3^2 in the expression for m_Z^2 increases as a function of M_S, and thus the minimal fine-tuned region requires the value of M_3 to decrease as M_S increases.

small for all messenger scales while the contribution from M_1^2 is negligible for small and large M_S but larger for intermediate messenger scales.

The large contribution from M_3^2 is mainly because it has the largest (in magnitude) coefficient in the expression for m_Z^2, at least for $M_S \gtrsim 10^{10}$ GeV, see Figure 2.1. The coefficients of the cross-terms A_tM_3, M_2M_3 and M_1M_3 are smaller (see Appendix 2.8), but together still contribute about 40% of the FT with respect to M_3^2 for $M_S = M_{\mathrm{GUT}}$. The reason that the cross-term contributions are so large is that the MFT values of A_t, M_2, and M_1 are rather sizeable at the messenger scale when compared with M_3 (at least for $M_S \gtrsim 10^4$ GeV). This is depicted in Figure 2.3.

The FT of m_Z^2 with respect to A_t^2 is also very large even though the coefficients of A_t^2 and the cross-terms A_tM_3, A_tM_2 and A_tM_1 in the expression for m_Z^2 are rather small (for $M_S = M_{\mathrm{GUT}}$, about 50% of the FT comes from the cross-terms). This is again because A_t, M_2 and M_1 are sizeable at M_S. The contribution to the FT from M_2^2 is large for similar reasons.

The FT with respect to μ^2 increases only slightly as a function of M_S since the coefficient of μ^2 in the expression for m_Z^2 does not vary much, and since the high-scale value of μ^2 increases only slightly as M_S is increased. The contribution from μ^2 is smaller than those from M_3^2, M_2^2

A_t	$\sqrt{\frac{1}{2}(m^2_{\tilde{t}_L} + m^2_{\tilde{t}_R})}$	$m_{\tilde{t}_1}$	$m_{\tilde{t}_2}$
-610 GeV	305 GeV	110 GeV	475 GeV

Table 2.1: Low-scale values for the stop soft trilinear coupling, the average of the left- and right-handed stop soft masses and the two physical stop masses. These low scale values give the minimal fine-tuning for arbitrary messenger scales.

and A_t^2 because the value of μ is comparatively small and also because there are no cross-terms in the FT expression that involve μ and other (large) soft parameters. Similar reasoning holds for the contributions from $m^2_{H_u}$, $m^2_{\tilde{t}_L}$ and $m^2_{\tilde{t}_R}$.

The low-energy spectrum that gives the MFT for a given messenger scale remains roughly unchanged as the messenger scale changes. The value of the stop soft trilinear coupling at the low scale is always about -610 GeV, with the two physical stop masses around 110 GeV and 475 GeV, respectively, see Table 2.1 and Figure 2.4. These values of the stop-sector parameters are essentially determined by the constraint on the Higgs mass and from the minimization of $\Delta(m_Z^2, m^2_{H_u}(M_S))$. The ratio $X_t/m_{\tilde{t}}$ is approximately -2, where $X_t \equiv A_t - \mu \cot\beta$, and $m_{\tilde{t}} \equiv \sqrt{\frac{1}{2}(m^2_{\tilde{t}_L} + m^2_{\tilde{t}_R})}$. The MFT is thus found for the *natural maximal-mixing* scenario which approximately maximizes the radiative corrections to the Higgs sector for a given set of parameters and for *negative* A_t [62, 72, 73, 74]. Small deviations of A_t (and to a lesser extent $m_{\tilde{t}_L}$ and $m_{\tilde{t}_R}$) from its MFT value at the low scale lead to a very large increase in the FT, mainly from $\Delta(m_Z^2, m^2_{H_u}(M_S))$. This can be seen from (2.23), which shows that the largest coefficients in the expression for $m^2_{H_u}(M)$ in terms of low-scale parameters all involve powers of A_t. Note that for generic points in the still allowed parameter space, $\Delta(m_Z^2, m^2_{H_u})$ would give one of the largest contribution to the FT. To minimize the FT it is thus best to minimize $\Delta(m_Z^2, m^2_{H_u}(M_S))$ which essentially determines the values of the stop-sector parameters (see the discussion in Section 2.4.3). The other contributions to the FT are then not at their minimum, but they are much smaller and less sensitive to variations in the parameters.

The low-scale values of the gaugino masses that give the MFT for a given messenger scale are shown in Figure 2.4. While the value of M_2 that gives the MFT is roughly the same for all M_S, the values of M_1 and M_3 decrease for larger M_S. Changing M_1 away from its MFT value does affect the FT but not excessively so, while a change in M_3 has a larger effect. The μ-parameter is always found to be less than 150 GeV for the MFT region at any messenger scale. Choosing it to be closer to 100 GeV instead has a negligible impact on the FT, and allows a neutralino to be the lightest SM superpartner (LSP), instead of the lighter stop, which is found to be the LSP in the numerical minimization procedure.

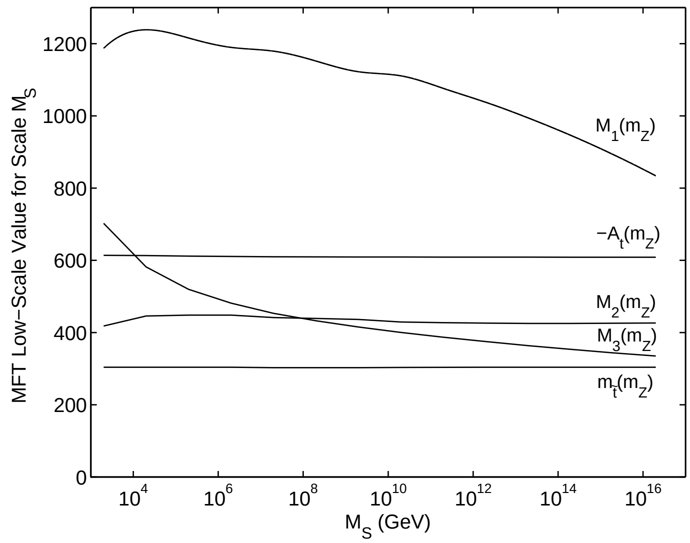

Figure 2.4: The low-scale values of the gaugino masses M_1, M_2 and M_3, the stop soft trilinear coupling A_t and the average of the stop soft masses squared $m_{\tilde{t}}$ that give the minimal fine-tuning (MFT) for the messenger scale M_S (with $\tan\beta = 10$). While the low-scale values of M_2, A_t and $m_{\tilde{t}}$ that give the minimal fine-tuning are roughly the same for all M_S, the values of M_1 and M_3 decrease for larger M_S.

Negative A_t may be expected to lead to less FT than positive A_t because A_t has a strongly attractive infrared quasi-fixed point near [75, 76]

$$A_t \simeq -M_3. \tag{2.12}$$

(This relation is strictly valid only at the Pendleton-Ross quasi-fixed point for the top Yukawa [77], and neglecting $SU(2)_L$ and $U(1)_Y$ gauge interactions.) Because of this it is most natural for A_t and M_3 to have opposite sign and be comparable in magnitude at low scales due to renormalization group evolution, see Figure 2.5. For positive A_t and maximal-mixing in the stop-sector, A_t would have to be an order of magnitude larger then M_3 at the messenger scale (see Figure 2.5) which would lead to a much more FT parameter region. The MFT region here does not satisfy (2.12) exactly, but instead $A_t/M_3 \simeq -1.8$ at the low scale, for $M_S = M_{\mathrm{GUT}}$. In order to satisfy (2.12) exactly, M_3 would have to be larger (assuming A_t remains fixed). This would increase the size of the stop masses under RG evolution as can be seen from their β-functions, see (2.50) and (2.51), which would lead to increased FT.

The MTMSSM has negative soft squark squared masses at the messenger scale (see also [47]). This remains the case even if the messenger scale is very low and only on the order of a few TeV (for very low messenger scales, finite threshold corrections should really be included). Under RG-evolution the masses get driven positive very quickly within about a decade of running.

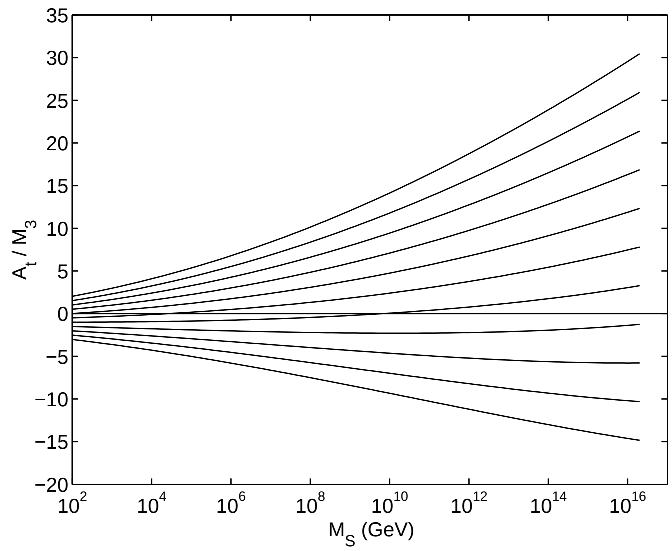

Figure 2.5: The RG-evolution of A_t/M_3 for various low-scale boundary conditions $A_t(m_Z)/M_3(m_Z) = \{-2.0, -1.5, \ldots, 1.5, 2.0\}$ and $\tan\beta = 10$. The strongly attractive infrared quasi-fixed point near $A_t/M_3 \simeq -1$ is clearly visible. The gaugino masses have been set to their minimal fine-tuned values for the case $M_S = M_{\rm GUT}$, i.e. $M_3(m_Z) \simeq 335$ GeV, $M_2(m_Z) \simeq 430$ GeV, and $M_1(m_Z) \simeq 830$ GeV.

It is the sizeable values of the gaugino masses that pull them up towards positive values. For smaller messenger scales the MFT region has a larger gluino mass, which drives the squark masses to positive values even faster while running towards the infrared. Equations (2.22) and (2.24) or (2.25) in Appendix 2.7 show that negative squarks at the messenger scale lead to more stop-mixing at the low scale, as was pointed out in [47]. Figure 2.6 shows the RG-trajectories of the MFT region if the messenger scale is M_S=$M_{\rm GUT}$.

The presence of tachyonic squarks at the messenger scale [78, 79] and/or very large A_t [80, 81] may lead to dangerous color and/or charge breaking (CCB) minima.

Very large A_t may result in dangerous CCB minima around the EW scale. These CCB minima occur in the $(\tilde{t}_L, \tilde{t}_R, H_u)$ plane [82]. The condition that the EW minimum is the global minimum may be estimated by going along the D-flat direction $|\tilde{t}_L| = |\tilde{t}_R| = |H_u|$ and is given by [83]

$$A_t^2 + 3\mu^2 \ \lesssim\ 3(m^2_{\tilde{t}_L} + m^2_{\tilde{t}_R}). \tag{2.13}$$

Assuming instead that the EW minimum is only metastable but has a large enough lifetime gives the weaker constraint [83]

$$A_t^2 + 3\mu^2 \ \lesssim\ 7.5(m^2_{\tilde{t}_L} + m^2_{\tilde{t}_R}). \tag{2.14}$$

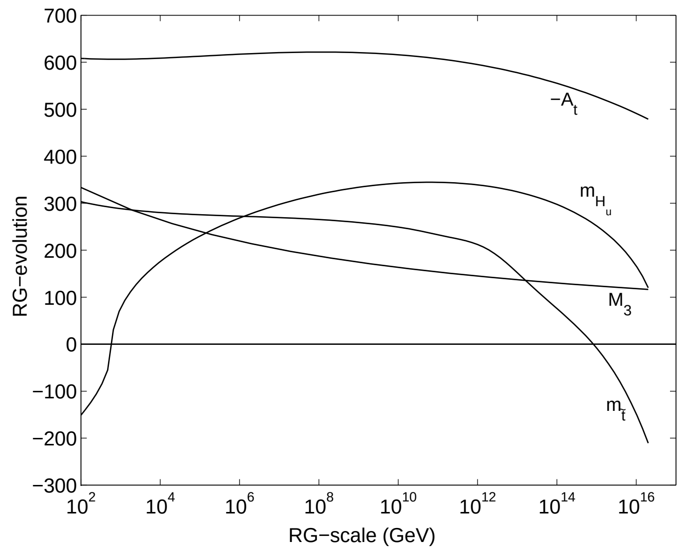

Figure 2.6: The RG-trajectories of the minimal fine-tuned region if the messenger scale is M_S=$M_{\rm GUT}$ ($\tan\beta$ has been set to 10). At the scale m_Z, the parameter values are $m_{\tilde{t}} \simeq 305$ GeV, $m_{\tilde{t}_1} \simeq 110$ GeV, $m_{\tilde{t}_2} \simeq 475$ GeV, $M_3(m_Z) \simeq 335$ GeV, and $\mu(m_Z) = 140$ GeV. The minimal fine-tuned value is obtained for *natural maximal-mixing*, i.e. $A_t \simeq -2m_{\tilde{t}}$.

The MTMSSM easily satisfies the second condition, as well as satisfying the first condition. There are thus no dangerous CCB minima resulting from large A_t.

Tachyonic stops at the messenger scale may result in an unbounded from below potential along D-flat directions involving the stop fields, as well as first and/or second generation squark fields or slepton fields. Loop corrections give rise to an effective potential which is not unbounded from below, but they generically introduce a CCB minimum with a vacuum expectation value (VEV) on the order of the messenger scale. The MTMSSM may thus have CCB minima with a VEV around the EW scale if the messenger scale is low, or CCB minima with a VEV large compared to the EW scale if the messenger scale is high. Since the EW minimum is metastable and long-lived for $m_{\tilde{t}} \gtrsim \frac{1}{6}M_3$ [84], it turns out that these CCB minima are not dangerous in the MTMSSM. Moreover, the MTMSSM does not determine the masses of the sleptons or first and second generation squarks since these do not play an important role in the FT. It is thus always possible to choose them in such a way to avoid CCB minima without changing the above FT results.

Finally, it is interesting to note that there are several near degenerate parameter subspaces along which the FT does not change much. The first and second generation particles and their superpartners do not contribute much to the FT because in equation (2.5) they appear only with a small coefficient. The parameter S_Y is also not very important for the same reason.

A more interesting near degenerate subspace is that the FT is rather insensitive to changes in the *difference* of the two stop soft mass squared parameters at the low scale as long as their sum is kept fixed. This may be understood from the expression for m_Z^2, e.g. equation (2.7), in which only their sum appears (using the one-loop RG equations). However, even with only one-loop RG equations this degeneracy is not exact since small discrepancies appear in the FT measure from equations (2.24) and (2.25). Moreover, the difference in the two stop soft mass squared parameters appears in the calculation of the physical stop masses and this affects the size of the Higgs mass, which is the most crucial low-energy constraint when calculating the FT. The FT only starts to change by an order one number when $\sqrt{|m_{\tilde{t}_L}^2 - m_{\tilde{t}_R}^2|} \sim 300$ GeV for $M_S = M_{\mathrm{GUT}}$.

2.4.3 Analytic Motivation for Numerical Results

The numerical results presented in section 2.4.2 may be motivated analytically. The discussion will for now assume $M_S = M_{\mathrm{GUT}}$, but generalizes to arbitrary M_S with a few caveats discussed below.

In order to get a physical Higgs mass satisfying the experimental bound without generating large FT for the EWSB, it is natural to maximize the radiative corrections to m_h. Due to the strongly attractive quasi-fixed point for A_t, this is achieved for negative A_t near (natural) maximal mixing (at least for m_h not too large, see Section 2.5).

The most important contribution to the FT comes from $\Delta(m_Z^2, m_{H_u}^2(M_S))$ since it has the largest coefficients, see Appendix 2.8. Eliminating $\hat{m}_{H_u}^2$ with the EWSB equation (2.7) and using the average stop soft mass squared $\hat{m}_{\tilde{t}}^2 = (\hat{m}_{\tilde{t}_L}^2 + \hat{m}_{\tilde{t}_R}^2)/2$ gives

$$\begin{aligned} m_Z^2 \Delta(m_Z^2, \hat{m}_{H_u}^2) \quad = \quad & |- m_Z^2 - 2.19\,\hat{\mu}^2 + 1.36\,\hat{m}_{\tilde{t}}^2 + 5.24\,\hat{M}_3^2 \\ & - 0.44\,\hat{M}_2^2 + 0.46\,\hat{M}_3\,\hat{M}_2 - 0.77\,\hat{A}_t\,\hat{M}_3 - 0.17\,\hat{A}_t\,\hat{M}_2 \\ & - 0.01\hat{M}_1^2 + 0.22\,\hat{A}_t^2|. \end{aligned} \tag{2.15}$$

It is possible to have cancelations among the various terms in this expression. $\Delta(m_Z^2, M_3^2(M_S))$ also has large coefficients, but cancelations among its terms are impossible since $\hat{A}_t$ is negative (see Appendix 2.8).

Ignoring $\hat{\mu}^2$, cancelation of the largest terms in equation (2.15), i.e. the gluino term and the average stop soft mass squared term, decreases the FT by setting $\hat{m}_{H_u}^2 \simeq m_{H_u}^2$ and leads to tachyonic squarks at the messenger scale [47]

$$\hat{m}_{\tilde{t}}^2 \simeq -3.9\hat{M}_3^2. \tag{2.16}$$

Next, the four terms on the second line of equation (2.15) can cancel by taking

$$\hat{M}_3 \simeq \frac{0.96\hat{M}_2 + 0.37\hat{A}_t}{1 - 1.67\frac{\hat{A}_t}{\hat{M}_2}}. \tag{2.17}$$

Assuming $\hat{M}_2 \simeq -\hat{A}_t$, this simplifies to $\hat{M}_2 \simeq 4.5\hat{M}_3$. Furthermore, keeping only the most important terms, the natural maximal-mixing scenario implies

$$\begin{aligned} -2 \simeq \frac{A_t}{m_{\tilde{t}}} \quad &\simeq \quad (0.32\hat{A}_t - 2.13\hat{M}_3 - 0.27\hat{M}_2 - 0.03\hat{M}_1)\Big[0.66\hat{m}_{\tilde{t}}^2 + 5.15\hat{M}_3^2 \\ &\qquad +0.11\hat{M}_2^2 + 0.02\hat{M}_1^2 + 0.19\hat{A}_t\hat{M}_3 + 0.04\hat{A}_t\hat{M}_2 - 0.05\hat{A}_t^2\Big]^{-1/2} \\ &= \quad (-4.80\hat{M}_3 - 0.03\hat{M}_1)\Big[2.16\hat{M}_3^2 + 0.02\hat{M}_1^2\Big]^{-1/2} \end{aligned} \tag{2.18}$$

which leads to $\hat{M}_1 \simeq 15\hat{M}_3$, again assuming $\hat{M}_2 \simeq -\hat{A}_t$. It is now possible to compute the ratio of the soft trilinear coupling with the gluino mass at the EWSB scale,

$$\frac{A_t}{M_3} \simeq \frac{0.32\hat{A}_t - 2.13\hat{M}_3 - 0.27\hat{M}_2 - 0.03\hat{M}_1}{2.88\hat{M}_3} \simeq -1.8. \tag{2.19}$$

These results agree well with the numerical results presented in section 2.4.2.

Note that a GUT scale model which predicts degenerate and negative squark and slepton soft masses at the GUT scale would need very large wino and bino masses in comparison to the gluino mass in order to drive the slepton soft masses to positive values under RG running to the EWSB scale [85]. This is due to the small coefficients of the bino and wino masses in the β-functions of the slepton soft masses. It is interesting that the MFT region prefers the bino mass larger than the wino mass and, in turn, the wino mass larger than the gluino mass.

Although this cancelation pattern holds to a good approximation for higher messenger scales, $\hat{m}_{\tilde{t}}^2$ does not exactly cancel $\hat{M}_3^2$ as the messenger scale decreases. For lower messenger scales, $\hat{m}_{\tilde{t}}^2$ becomes less tachyonic while $\hat{M}_3^2$ increases, allowing the stop masses to be driven positive faster under RG running to the EWSB scale. Moreover, the coefficient of $\hat{M}_3^2$ in the expression for m_Z^2 (2.5) decreases significantly, as can be seen in Figure 2.1. Therefore the cancelation pattern in $\Delta(m_Z^2, \hat{m}_{H_u}^2)$ discussed above does not hold since the $\hat{m}_{\tilde{t}}^2$ contribution decreases while the $\hat{M}_3^2$ term gives a comparable contribution for all messenger scales (except for very small messenger scales). On the other hand, being a supersymmetric parameter, $\hat{\mu}$ and its coefficient in equation (2.5) does not change much for different messenger scales. Compared to $\hat{M}_3^2$ and $\hat{m}_{\tilde{t}}^2$, its contribution becomes important at lower messenger scales and a lower FT can be obtained by canceling the three contributions together. The other relations in the above cancelation pattern holds to a good approximation for lower messenger scales, although for $M_S \lesssim 10^5$ the cancelation pattern becomes more involved.

2.4.4 Summary of Phenomenological Implications

The above analysis shows that the MTMSSM has small values for μ, the stop masses and the gluino mass. The gluino in the MTMSSM is around 335 GeV for $M_S = M_{\mathrm{GUT}}$, but heavier for lower M_S. There is large mixing in the stop-sector which introduces a significant splitting between the two physical stop masses. They have masses of around 115 GeV and 475 GeV respectively, see Table 2.1. Thus the MTMSSM may have a stop as the LSP. However, as mentioned before, μ can be chosen to be small enough so that a neutralino is the LSP without affecting FT by much.

At the Large Hadron Collider, gluino pair-production in the MTMSSM is thus rather large and comparable to top quark pair-production. The production of $\tilde{t}_1\tilde{t}_1$ is also of the same order.

The gluinos are Majorana particles, and can decay into the lightest stop via $\tilde{g}\tilde{g} \to tt\tilde{t}_1\tilde{t}_1$ producing same-sign top quarks 50% of the time. The top quarks each decay into Wb, and the events with two same-sign top quarks will contain two same-sign leptons if the W decays leptonically. If a neutralino and a chargino are lighter than the stop, the decay $\tilde{t}_1 \to \chi_1^+ b$ is possible, with χ_1^+ further decaying into a neutralino and soft jets or leptons. The events thus also contain missing energy and a number of b-jets, some of which are soft if the $\tilde{t}_1 - \chi_1^+$ mass splitting is small.

If $\tilde{t}_1$ is the LSP a number of further interesting signatures are possible, see [86]. The lighter stop can either be pair-produced directly or from gluino decays. Even though it is the lightest SM superpartner, it may decay into a lighter goldstino $\tilde{G}$ via the flavor-violating decay $\tilde{t}_1 \to c\tilde{G}$ or via the three-body decay $\tilde{t}_1 \to bW\tilde{G}$. The decay rate depends on the messenger scale, with lower messenger scales leading to larger decay rates. For reasonable messenger scales, its decay length easily exceeds the hadronization length scale, and the stop in general hadronizes before it decays [86]. For messenger scales less than a few hundred TeV, the decay length is small enough so that the decay products seem to originate from the interaction region. The three-body decay leads to a similar signature as the top decay but can be distinguished from it, see [87]. For larger messenger scales, $\tilde{t}_1$ decays inside a hadronized mesino or sbaryon and a variety of interesting signatures are possible [86], including mesino-anti-mesino oscillations [88].

Another interesting possibility is the direct pair-production of the heavier stop $\tilde{t}_2$. Since the two physical stop masses are split by a large amount, the decay mode $\tilde{t}_2 \to \tilde{t}_1 + Z$ is kinematically allowed and has a sizeable branching ratio [89]. The resulting signature depends on the $\tilde{t}_1$ decay channel as discussed above. For χ_1^+ and χ_0^1 lighter than $\tilde{t}_1$, the authors of [89] propose to look for the inclusive signature $Z(l^+, l^-)bb\not{E}_T X$, where the two leptons l^+ and l^-

have an invariant mass equal to the Z-mass. Detecting this signature would give evidence for the maximal-mixing scenario but requires a large integrated luminosity (at least $\mathcal{O}(100\ \mathrm{fb}^{-1})$) [89]. Since the mass difference between $\tilde{t}_1$ and the LSP is small in the MTMSSM this signature will be very hard to see since the jet from the decay $\tilde{t}_1 \to \chi_1^+ b$ is soft which makes it more difficult to separate the signal from the SM background [89].

An alternative way to measure the parameters in the stop-sector is to use the Higgs boson as a probe [90]. A measurement of the Higgs mass and its production rate in the gluon fusion channel allows the average of the two stop soft masses as well as the stop mixing to be determined in many regions of the still allowed MSSM parameter space, and especially in regions where the FT is small [90].

2.4.5 Fine-Tuning with Respect to Other Parameters

This subsection briefly discusses other parameters that may in principle contribute to the FT.

If the goal is to find the MFT region of a model and make a prediction of what parameter region is preferred for the model from a FT point of view, there is no reason to include the FT of experimentally known parameters such as g_Y, g_2 ,g_3, or λ_t. Taking into account the known parameters in the minimization procedure would most likely lead to other MFT values for all parameters, including MFT values for the known parameters which would in all likelihood not match the experimental values.

If the goal, however, is to find the FT of a given model, one should in principle include contributions from experimentally known parameters. For example, FT with respect to λ_t, $\Delta(m_Z^2, \lambda_t(M_S))$, may give a large contribution to the total FT due to the large top mass. Indeed, with the MFT values for $M_S = M_{\mathrm{GUT}}$, $\Delta(m_Z^2, \lambda_t(M_{M_{\mathrm{GUT}}})) \simeq 8$. This, however, increases the total FT only by a small amount from 22.1 to 23.5.

What about FT with respect to m_{12}^2 and $\tan\beta$? These parameters are unknown and in principle they should be included in the minimization procedure. With the help of equation (2.3) and symmetries, it is however easy to see that $\Delta(m_Z^2, m_{12}^2(M_S)) = 0$. Indeed m_{12}^2 does not appear directly in the expression for m_Z^2. Furthermore it breaks a $U(1)_{\mathrm{PQ}}$- and a $U(1)_R$-symmetry and consequently does not feed back into any other β-functions since no other parameter breaks both symmetries. Thus m_{12}^2 cannot appear in equation (2.3) and is therefore completely free, which allows m_A to be chosen accordingly as discussed in Section 2.2.

The FT of $\tan\beta$ has not been taken into account in the minimization procedure since an explicit expression for m_Z^2 can only be obtained assuming a specific value for $\tan\beta$, because λ_t

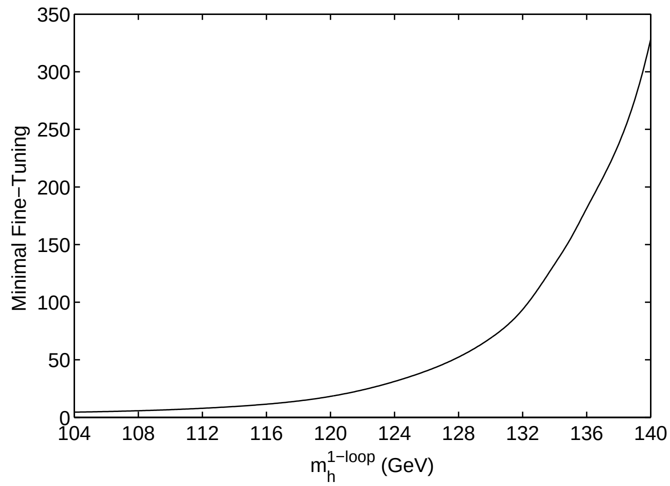

Figure 2.7: The minimal fine-tuning as a function of the lower bound on the Higgs mass m_h, where the calculation of m_h only includes the one-loop corrections from the top-stop sector ($\tan\beta = 10$, $m_A = 250$ GeV, $m_t = 170.9$ GeV).

depends on $\tan\beta$ through m_t. Moreover, since $\tan\beta$ is then a free parameter the approximation leading to equation (2.4) may not be valid anymore and $m^2_{H_d}$ should be reintroduced. Contributions from bottom/sbottom and tau/stau sectors should also be included if $\tan\beta$ becomes large.

2.5 Minimal Fine-Tuning as a Function of the Higgs Mass

The Higgs mass m_h is the most important low-energy constraint that determines the amount of minimal fine-tuning (MFT). It is therefore interesting to look at how the MFT is affected when the lower bound on m_h is changed. Figure 2.7 shows a plot of the MFT as a function of the lower bound on m_h, where the calculation of m_h is the same one used in the FT minimization described in Section 2.4.1, and only includes the one-loop corrections from the top-stop sector (with $m_A = 250$ GeV, $\tan\beta = 10$, $m_t = 170.9$ GeV, and $M_S = M_{\rm GUT}$). The Higgs mass calculated with the one-loop corrections will be denoted by $m_h^{1\ell}$. The region of MFT always saturates the bound on $m_h^{1\ell}$ and has negative A_t. The minimal FT is about 1% for $m_h^{1\ell} \simeq 132$ GeV.

There are, however, other important one-loop and two-loop corrections that can significantly affect m_h, and these need to be included in order to get a more accurate idea of how the MFT changes as a function of the lower bound on m_h. With these additional corrections, m_h is not anymore a symmetric function of the stop-mixing parameter $X_t = A_t - \mu\cot\beta \simeq A_t$, where the latter approximation is good for sizeable $\tan\beta$. It can be up to 5 GeV larger for $X_t = +2m_{\tilde{t}}$ than for $X_t = -2m_{\tilde{t}}$, the difference arising from non-logarithmic two-loop contributions to m_h, see [91, 92, 93]. Moreover, large chargino masses, i.e. large values of M_2 and μ, can give important negative contributions to m_h [94]. These corrections are also not included in $m_h^{1\ell}$. Two-loop corrections that allow the gluino mass to affect m_h can also be important but are smaller in general - this will be ignored in the following discussion since the impact on the results presented below is negligible.

The MFT spectrum that was found with the minimization procedure may be used to calculate m_h with `FeynHiggs`. The `FeynHiggs` estimate for m_h will be denoted by $m_h^{\mathtt{FH}}$. The result is the solid black line in Figure 2.8. This MFT spectrum characteristically has large chargino masses and a negative value for A_t near the "natural" maximal mixing scenario.

Comparing the solid black line in Figure 2.8 with the curve in Figure 2.7 shows the well-known fact that the higher-order corrections to m_h are extremely important. There are two additional very striking features. First of all, as $m_h^{\mathtt{FH}}$ increases and approaches 120 GeV, the FT increases enormously. Any further small increase in the Higgs mass results in an enormous increase in the FT. The reason is that as $m_h^{\mathtt{FH}}$ approaches 120 GeV here, it only grows logarithmically as a function of the stop masses. The stop masses therefore become exponentially large and thus increase the FT at least exponentially (see also [62]).

The second striking feature of this curve is that the value of the Higgs mass at which the FT starts to increase enormously is rather low (the MFT is already 1% for $m_h^{\mathtt{FH}} \simeq 119$ GeV). This value of m_h may be increased by just under 2 GeV by choosing larger $\tan\beta$ and m_A (recall that throughout this discussion $\tan\beta = 10$ and $m_A = 250$ GeV). Note that the latest Tevatron top mass value ($m_t = 170.9$ GeV) has been used in the calculation, and a slightly different value can also change m_h by a few GeV.

An obvious question is whether the MFT region is significantly different if $m_h^{\mathtt{FH}}$ were used in the minimization procedure instead of $m_h^{1\ell}$ (the former is too complicated to be used). For MSSM spectra that give small m_h this is certainly not the case, since there is not a very large discrepancy between the two Higgs mass estimates $m_h^{1\ell}$ and $m_h^{\mathtt{FH}}$. The difference between the two Higgs mass estimates becomes significant, however, for MSSM spectra that give a large m_h, and the approximation $m_h^{\mathtt{FH}}$ can be substantially smaller than $m_h^{1\ell}$. Also, as mentioned above, $m_h^{\mathtt{FH}}$ can be substantially larger for positive A_t (near maximal mixing) than for negative A_t (near "natural" maximal mixing), and increases as the chargino masses decrease. On the other hand, $m_h^{1\ell}$ remains unaffected by the sign of A_t and the size of the chargino masses. It is thus possible that the MFT region does not coincide with the region obtained in the above

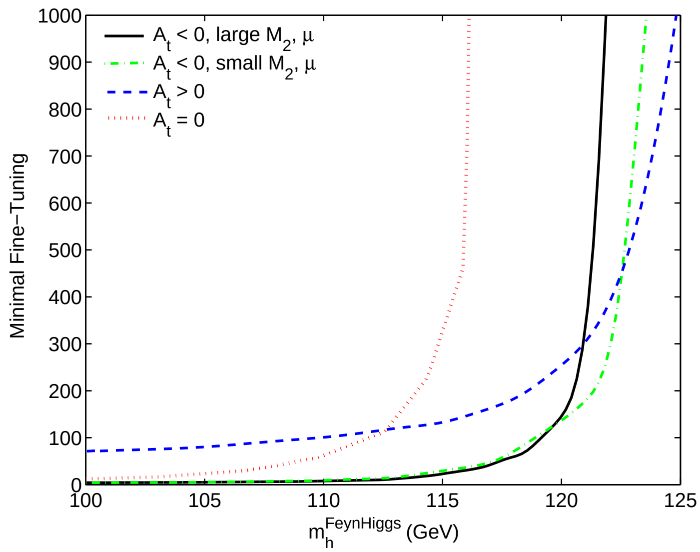

Figure 2.8: The minimal fine-tuning as a function of the lower bound on the Higgs mass m_h calculated with `FeynHiggs` 2.6.0 ($\tan\beta = 10$, $m_A = 250$ GeV, $m_t = 170.9$ GeV). Throughout this paper the fine-tuning is minimized subject to a constraint on m_h, where m_h is estimated with a one-loop formula as described in Section 2.4.1. The different lines arise from different assumptions made about A_t, or μ and M_2, when minimizing the fine-tuning. These different assumptions give rise to different low-energy spectra that present the least fine-tuned parameter choices satisfying these assumptions. These low-energy spectra may then be used in `FeynHiggs` to calculate m_h. Although M_2, μ and the sign of A_t do not affect the one-loop estimate of m_h which only contains the dominant corrections, they do affect the `FeynHiggs` estimate of m_h. For the solid black line no constraint was set on A_t, and μ and M_2 were only required to be above 100 GeV. It is the same line as in Figure 2.7, but with m_h estimated by `FeynHiggs` instead of the one-loop formula. The dashed blue line assumes A_t is positive and near maximal mixing, also with M_2 and μ only required to be above 100 GeV. The dash-dot green curve makes no assumption about A_t but sets $\mu = 100$ GeV and $M_2 = 100$ GeV. The dotted red line assumes $A_t = 0$, and again only requires μ and M_2 to be larger than 100 GeV. Further details and explanations are given in the text.

minimization procedure as the lower bound on m_h increases. This is indeed the case, as will now be discussed.

The FT may be minimized with the constraint that the chargino masses are small. Since the effect of varying μ and M_2 on the FT are noticeable but not substantial, the resulting spectrum will be characterized by gluino and stop masses that are only slightly larger than those obtained in the MFT region discussed in this paper. The value of A_t is still negative. This spectrum may be used to calculate $m_h^{\texttt{FH}}$. The result is shown by the dash-dot green curve in Figure 2.8. For $m_h^{\texttt{FH}}$ not too large, the solid black curve lies below the dash-dot green curve because the MFT region has large values of M_2, see Section 2.4. As $m_h^{\texttt{FH}}$ increases further, however, the FT becomes very large since the stop masses become exponentially large. Smaller chargino masses lead to larger values of $m_h^{\mathtt{FH}}$, and the two curves show that for m_h just below 120 GeV, a smaller FT may be obtained by decreasing the size of M_2. This behavior cannot be captured by $m_h^{1\ell}$ which is unaffected by a change in the chargino masses. Note that the transition between the two regions described by the two curves is smooth, and that it occurs when the MFT is already more than 1%.

Next, the FT may be minimized with the constraint that A_t is positive and near maximal mixing. The resulting low-energy spectrum is characterized by small chargino and gluino masses. This spectrum may then be used to calculate $m_h^{\mathtt{FH}}$, and the MFT as a function of this value of $m_h^{\mathtt{FH}}$ is displayed by the dashed blue line in Figure 2.8. Comparing the solid black line or dash-dot green line with the dashed blue line, it is clear that for small $m_h^{\mathtt{FH}}$ the MFT region has negative values of A_t. Even though negative A_t might be expected to always give less FT than positive A_t due to the IR quasi-fixed point, the increase in $m_h^{\mathtt{FH}}$ by several GeV by making A_t positive is substantial, and as $m_h^{\mathtt{FH}}$ approaches about 123 GeV, the two curves cross. Thus, there is a transition from $A_t \simeq -2m_{\tilde{t}}$ to $A_t \simeq +2m_{\tilde{t}}$ of the minimal fine-tuned region as $m_h^{\mathtt{FH}}$ increases. This behavior is again not captured by $m_h^{1\ell}$ which is independent of the sign of A_t. The transition occurs when the minimal FT is already quite large (about 0.2%).

This transition from negative to positive A_t is not smooth, in the sense that the first derivative of the curve at the transition point is not continuous[5]. To show this, the FT may be minimized with the constraint $A_t = 0$. The resulting low-energy spectrum may then again be used to calculate $m_h^{\mathtt{FH}}$, and the result is shown by the dotted red line in Figure 2.8. The value of $m_h^{\mathtt{FH}}$ for vanishing stop-mixing, $A_t = 0$, is much lower than for the two maximal mixing scenarios, $A_t \simeq \pm 2m_{\tilde{t}}$, and it is clear that the MFT region does not interpolate smoothly between them as a function of A_t.

The main point of the analysis in this section is that although the MSSM is already fine-tuned at least at about the 5% level (if the messenger scale equals the GUT scale), there is not much room left for the Higgs mass to increase before the FT becomes much worse.

Note that for a lower messenger scale the Higgs mass can have a slightly larger value before the MFT begins to increase enormously. For example, for $M_S = 200$ TeV, the MFT is 1% for $m_h \simeq 123$ GeV. So even for a lower messenger scale the Higgs mass cannot be that much beyond 120 GeV before the MFT increases dramatically.

[5] One may perhaps refer to this as the *first order phase transition of fine-tuning.*

2.6 Conclusions

This paper presented the minimally tuned Minimal Supersymmetric Standard Model (MTMSSM). The MSSM parameter region that has the minimal model-independent fine-tuning (FT) of EWSB was found. Model - independent means that no relations were assumed between the soft SUSY breaking parameters at the scale at which they are generated (the messenger scale). Instead, all of the important parameters were allowed to be independent and free at the messenger scale, and were taken to contribute to the total FT of the EWSB scale. The messenger scale itself was varied between 2 TeV and $M_{\rm GUT}$ and the effect of this on the minimal FT was presented.

The most important parameters that contribute to the tuning are $|\mu|^2$, $m^2_{H_u}$, the gaugino masses M_1, M_2 and M_3, the stop soft masses $m^2_{\tilde{t}_L}$ and $m^2_{\tilde{t}_R}$, and the stop soft trilinear coupling A_t. The MSSM spectra which lead to the minimal model-independent FT were found by numerically minimizing the FT expression subject to constraints on the Higgs, stop, and gaugino masses (the Higgs mass was found to always be the most important low-energy constraint). The high-energy spectra are characterized by tachyonic stop soft masses, even for messenger scales as low as 2 TeV (but note that threshold effects in the RG-running were neglected throughout). The potential existence of charge and/or color breaking minima turns out not to be a problem. The gluino mass, M_3, is much smaller than the wino mass, M_2, and M_2 in turn is much smaller than the bino mass M_1. The low-scale spectra are characterized by negative A_t near the maximal mixing scenario that maximizes the Higgs mass. The large stop mixing leads to a large splitting between the two stop mass eigenstates. Interesting phenomenological signatures include the possibility of a stop LSP.

The minimal FT was also found as a function of the lower bound on the Higgs mass (with the messenger scale set to $M_{\rm GUT}$). Although in the numerical minimization procedure the dominant one-loop expression for m_h was used as a constraint, the resulting least fine-tuned spectra were used to calculate m_h more accurately with `FeynHiggs`. A plot of the minimal FT as a function of m_h was presented. There are several striking features of this plot. For m_h larger than about 120 GeV the FT increases very rapidly. This value of m_h is rather low, perhaps surprisingly so. It is only slightly dependent on the parameters in the Higgs sector. Near it, the value of A_t in the least FT region also makes a sudden transition from lying near $-2m_{\tilde{t}}$ to lying near $+2m_{\tilde{t}}$, where $m_{\tilde{t}}$ is the average of the two stop soft masses. The upshot of this particular analysis is that although the MSSM is already fine-tuned at least at about the 5% level (if the messenger scale equals the GUT scale), there is not much room left for the Higgs mass to increase before the FT becomes much worse. The magnitude and rate of increase of the minimal FT as m_h increases beyond about 120 GeV is very striking.

2.7 Appendix: Semi-numerical Solutions of the MSSM One-Loop RG-Equations

This appendix reviews the procedure for solving the MSSM one-loop RG equations semi-numerically [63, 64]. The low scale M_0 is set to be m_Z, and the high (messenger) scale M_S is taken to lie anywhere between m_Z and $M_{\rm GUT}$. Threshold corrections are neglected when solving the RG-equations.

The main goal is to obtain an expression for m_Z^2 in terms of high-scale input parameters as in equation (2.5). Assuming that $\tan\beta$ is not too small, this requires solving $|\mu(m_Z)|^2$ and $m_{H_u}^2(m_Z)$ in terms of high-scale parameters (for moderate values of $\tan\beta$, $m_{H_d}^2$ may be neglected, see equation (2.4)). The fine-tuning may then be calculated and naturally expressed in terms of high-scale parameters as in equation (2.10). However, in order to minimize the fine-tuning taking into account low-scale constraints on the Higgs, stop, and gaugino masses, it is more appropriate to rewrite the fine-tuning expression in terms of low scale parameters. This requires that μ as well as all the soft supersymmetry breaking parameters appearing in equation (2.10) be written in terms of low scale parameters.

In solving the RG-equations, only the contributions from the third generation particles will be included, since the third generation Yukawa couplings are much larger than those from the first and second generations. Moreover, the contributions from the bottom/sbottom and tau/stau sectors are neglected as $\tan\beta$ is taken to be not too large.

The high-scale parameters may in general be written in terms of low scale-parameters as

$$m_i^2(M_S) = \sum_{j,k} c_{ijk}(\tan\beta, M_0, M_S)\, m_j(M_0)\, m_k(M_0). \tag{2.20}$$

For example, for $M_S = M_{\rm GUT}$, the expressions for the most important high-scale parameters written in terms of low-scale parameters are

$$\hat{M}_i = d_i\,M_i \qquad \{d_1,d_2,d_3\} = \{2.42, 1.22, 0.35\} \tag{2.21}$$

$$\hat{A}_t = 3.15\,A_t + 2.33\,M_3 + 1.03\,M_2 + 0.26\,M_1 \tag{2.22}$$

$$\begin{aligned}\hat{m}^2_{H_u} = {} & 2.07\,m^2_{H_u} + 1.07\,m^2_{\tilde{t}_L} + 1.07\,m^2_{\tilde{t}_R} + 0.19\,M_3^2 - 0.98\,M_2^2 \\ & - 0.31\,M_1^2 + 3.38\,A_t^2 + 3.69\,A_t\,M_3 + 1.19\,A_t\,M_2 + 0.24\,A_t\,M_1 \\ & + 0.76\,M_3\,M_2 + 0.15\,M_3\,M_1 + 0.05\,M_2\,M_1 + 0.06\,S_Y\end{aligned} \tag{2.23}$$

$$\begin{aligned}\hat{m}^2_{\tilde{t}_L} = {} & 0.36\,m^2_{H_u} + 1.36\,m^2_{\tilde{t}_L} + 0.36\,m^2_{\tilde{t}_R} - 0.72\,M_3^2 - 0.81\,M_2^2 \\ & - 0.06\,M_1^2 + 1.13\,A_t^2 + 1.23\,A_t\,M_3 + 0.40\,A_t\,M_2 + 0.08\,A_t\,M_1 \\ & + 0.25\,M_3\,M_2 + 0.05\,M_3\,M_1 + 0.02\,M_2\,M_1 + 0.02\,S_Y\end{aligned} \tag{2.24}$$

$$\begin{aligned}\hat{m}^2_{\tilde{t}_R} = {} & 0.72\,m^2_{H_u} + 0.72\,m^2_{\tilde{t}_L} + 1.72\,m^2_{\tilde{t}_R} - 0.65\,M_3^2 - 0.18\,M_2^2 \\ & - 0.46\,M_1^2 + 2.26\,A_t^2 + 2.46\,A_t\,M_3 + 0.80\,A_t\,M_2 + 0.16\,A_t\,M_1 \\ & + 0.50\,M_3\,M_2 + 0.10\,M_3\,M_1 + 0.04\,M_2\,M_1 - 0.09\,S_Y\end{aligned} \tag{2.25}$$

$$\hat{\mu} = 0.95\,\mu. \tag{2.26}$$

Similar type of expressions hold for low-scale parameters as a function of high-scale parameters. The gauge couplings g_α, $\alpha \in \{1,2,3\}$, and the top Yukawa coupling λ_t are fixed at the low scale by their experimental values [69]. Section 2.7.1 gives the solution of their RG-equations.

The MSSM one-loop β-functions that need to be solved come in three different functional forms [95]. The RG-equations of the gaugino masses M_α, the supersymmetric Higgsino mass μ, and S_Y are of the form

$$\frac{dm_i}{dt} = f_i(\lambda_t, g_\alpha)\,m_i, \quad m_i \in \{M_\alpha, \mu, S_Y\}, \tag{2.27}$$

where $t = \ln(M_S/M_0)$. Their solution is given by

$$m_i(t) = m_i(0)\,\exp\int_0^t dt'\,f_i(\lambda_t, g_\alpha). \tag{2.28}$$

The stop soft trilinear coupling has the functional form

$$\frac{dA_t}{dt} = a(\lambda_t)\,A_t + b(g_\alpha, M_\alpha). \tag{2.29}$$

The solution of this equation is more involved due to the presence of both homogeneous and inhomogeneous terms, and requires the solution for the gaugino masses (2.28). It may be written as (see Section 2.7.3)

$$A_t(t) = e^{\int dt' a(\lambda_t)}\,A_t(0) + e^{\int dt' a(\lambda_t)}\int_0^t dt' e^{-\int dt'' a(\lambda_t)}\,b(g_\alpha, M_\alpha). \tag{2.30}$$

Finally, the RG-equations of the up-type Higgs soft mass and the stop soft masses form a system of coupled inhomogeneous differential equations,

$$\frac{dm_i^2}{dt} = \sum_j u_{ij}(\lambda_t) m_j^2 + v_i(g_\alpha, M_\alpha, S_Y, A_t), \quad m_i^2 \in \{m_{H_u}^2, m_{\tilde{t}_L}^2, m_{\tilde{t}_R}^2\}. \tag{2.31}$$

This may be solved (see Section 2.7.4) using the solutions for the gaugino masses and S_Y (2.28) as well as the solution for the stop soft trilinear coupling (2.30),

$$m_i^2(t) = \left(e^{\int dt' u(\lambda_t)} m^2(0) + e^{\int dt' u(\lambda_t)} \int_0^t dt' e^{-\int dt'' u(\lambda_t)} v(g_\alpha, M_\alpha, S_Y, A_t) \right)_i . \tag{2.32}$$

2.7.1 Appendix: Gauge and Yukawa Couplings

The one-loop β-functions for the gauge and top Yukawa couplings in the MSSM are

$$\begin{aligned} 8\pi^2 \beta_{g_\alpha^2} &= b_\alpha \, g_\alpha^4, \quad \{b_Y, b_2, b_3\} = \{11, 1, -3\} && (2.33) \\ 16\pi^2 \beta_{\lambda_t} &= \lambda_t \left(6\,\lambda_t^2 - \frac{16}{3}\, g_3^2 - 3\, g_2^2 - \frac{13}{9}\, g_Y^2 \right). && (2.34) \end{aligned}$$

Their solutions are

$$\begin{aligned} g_\alpha^2(t) &= g_\alpha^2(0)\, \xi_\alpha^{-1}(t) && (2.35) \\ \lambda_t^2(t) &= \lambda_t^2(0)\, E(t; \vec{n}_0)\, G(t; \vec{n}_0)^{-1}, && (2.36) \end{aligned}$$

where $\vec{n}_0 = \left(\frac{13}{9b_1}, \frac{3}{b_2}, \frac{16}{3b_3} \right) = \left(\frac{13}{99}, 3, -\frac{16}{9} \right)$, and for future convenience the functions

$$\begin{aligned} \xi_\alpha(t) &= 1 - \frac{b_\alpha}{8\pi^2}\, g_\alpha^2(0) t && (2.37) \\ E(t; \vec{n}) &= \prod_{\alpha=1}^{3} \xi_\alpha^{(\vec{n})_\alpha}(t) && (2.38) \\ F(t; \vec{n}) &= \int_0^t dt'\, E(t'; \vec{n}) && (2.39) \\ G(t; \vec{n}) &= 1 - \frac{3}{4\pi^2}\, \lambda_t^2(0)\, F(t; \vec{n}) && (2.40) \end{aligned}$$

have been introduced. The solution (2.36) is analytic if g_2 and g_Y are set to zero [96, 97], whereas non-zero values of g_2 and g_Y require a numerical integration.

2.7.2 Appendix: Gaugino Masses, μ-term and S_Y

The RG-equations for the gaugino masses, μ and S_Y are

$$\begin{aligned} \beta_{M_\alpha} &= \frac{M_\alpha}{g_\alpha^2}\, \beta_{g_\alpha^2} && (2.41) \\ 16\pi^2 \beta_\mu &= \mu \left(3\,\lambda_t^2 - 3\, g_2^2 - g_Y^2 \right) && (2.42) \\ 8\pi^2 \beta_{S_Y} &= g_Y^2 \sum_{\text{scalars i}} \left(\frac{Y_i}{2} \right)^2 S_Y . && (2.43) \end{aligned}$$

The general solution is of the form (2.28), and may be written as

$$M_\alpha(t) = M_\alpha(0)\,\xi_\alpha^{-1}(t) \tag{2.44}$$

$$\mu(t) = \mu(0)\,G(t;\vec{n}_0)^{-\frac{1}{4}}\,\xi_2^{\frac{3}{2}}(t)\,\xi_1^{\frac{1}{22}}(t) \tag{2.45}$$

$$S_Y(t) = S_Y(0)\,\xi_1^{-1}(t) \tag{2.46}$$

with the notation of Section 2.7.1. The solutions for the gaugino masses and S_Y are analytic while μ must be solved numerically unless the contributions from g_2 and g_Y are neglected.

2.7.3 Appendix: Stop Soft Trilinear Coupling

The β-function of the stop soft trilinear coupling is

$$8\pi^2\beta_{A_t} = \left(6\,\lambda_t^2\,A_t - \frac{16}{3}\,g_3^2\,M_3 - 3\,g_2^2\,M_2 - \frac{13}{9}\,g_Y^2\,M_1\right). \tag{2.47}$$

Using the solutions for the gaugino masses (2.44), this equation may be integrated and written as

$$A_t(t) = \frac{1}{G(t;\vec{n}_0)}\left[A_t(0) + \sum_{\alpha=1}^{3}(\vec{n}_0)_\alpha\frac{M_\alpha(0)}{\xi_\alpha(t)}\Big(G(t;\vec{n}_0) - \xi_\alpha(t)\,G(t;\vec{n}_0 - \vec{e}^{\alpha})\Big)\right] \tag{2.48}$$

where $(\vec{e}^{\alpha})_\beta = \delta_\beta^\alpha$ are the usual unit vectors. If g_2 and g_Y are zero, the solution does not require a numerical integration.

2.7.4 Appendix: Up-type Higgs Soft Mass and Stop Soft Masses

The β-functions of $m_{H_u}^2$, $m_{\tilde{t}_L}^2$ and $m_{\tilde{t}_R}^2$ are

$$\begin{aligned} 8\pi^2\beta_{m^2_{H_u}} &= 3\lambda_t^2\left[m_{H_u}^2 + m_{\tilde{t}_L}^2 + m_{\tilde{t}_R}^2 + |A_t|^2\right] \\ &\qquad -3\,g_2^2\,|M_2|^2 - g_Y^2\,|M_1|^2 - \frac{1}{2}\,g_Y^2\,S_Y \qquad (2.49)\\ 8\pi^2\beta_{m^2_{\tilde{t}_L}} &= \lambda_t^2\left[m_{H_u}^2 + m_{\tilde{t}_L}^2 + m_{\tilde{t}_R}^2 + |A_t|^2\right] \\ &\qquad -\frac{16}{3}\,g_3^2\,|M_3|^2 - 3\,g_2^2\,|M_2|^2 - \frac{1}{9}\,g_Y^2\,|M_1|^2 - \frac{1}{6}\,g_Y^2\,S_Y \qquad (2.50)\\ 8\pi^2\beta_{m^2_{\tilde{t}_R}} &= 2\lambda_t^2\left[m_{H_u}^2 + m_{\tilde{t}_L}^2 + m_{\tilde{t}_R}^2 + |A_t|^2\right] \\ &\qquad -\frac{16}{3}\,g_3^2\,|M_3|^2 - \frac{16}{9}\,g_Y^2\,|M_1|^2 - \frac{2}{3}\,g_Y^2\,S_Y\,. \qquad (2.51) \end{aligned}$$

They form a system of coupled inhomogeneous differential equations. Note that A_t appears quadratically in these β-functions which gives cross-terms between $M_\alpha(0)$ and $A_t(0)$ (see equation (2.48)). The equations can be solved as in (2.32) but it is possible to simplify the analysis by the change of variables

$$X = m_{H_u}^2 - m_{\tilde{t}_L}^2 - m_{\tilde{t}_R}^2 \tag{2.52}$$

$$Y = m_{H_u}^2 - 3m_{\tilde{t}_L}^2 \tag{2.53}$$

$$Z = m_{H_u}^2 + m_{\tilde{t}_L}^2 + m_{\tilde{t}_R}^2 . \tag{2.54}$$

In terms of the new variables, the β-functions are

$$8\pi^2 \beta_X = \frac{32}{3}\, g_3^2\, |M_3|^2 + \frac{8}{9}\, g_Y^2\, |M_1|^2 + g_Y^2\, S_Y \tag{2.55}$$

$$8\pi^2 \beta_Y = 16\, g_3^2\, |M_3|^2 + 6\, g_2^2\, |M_2|^2 - \frac{2}{3}\, g_Y^2\, |M_1|^2 \tag{2.56}$$

$$8\pi^2 \beta_Z = 6\lambda_t^2 Z + 6\lambda_t^2 |A_t|^2 - \frac{32}{3}\, g_3^2\, |M_3|^2 - 6\, g_2^2\, |M_2|^2 - \frac{26}{9} g_Y^2 |M_1|^2 . \tag{2.57}$$

In this form, β_X and β_Y are easily integrated since they have no homogeneous term (which is due to the fact that the corresponding matrix u_{ij} in (2.31) has rank = 1)

$$\begin{aligned} X(t) &= X(0) - \frac{16}{9}\, M_3^2(0)\, \left(\xi_3^{-2}(t) - 1\right) \\ &\qquad + \frac{4}{99}\, M_1^2(0)\, \left(\xi_1^{-2}(t) - 1\right) + \frac{1}{11}\, S_Y(0)\, \left(\xi_1^{-1}(t) - 1\right) \end{aligned} \tag{2.58}$$

$$\begin{aligned} Y(t) &= Y(0) - \frac{8}{3}\, M_3^2(0)\, \left(\xi_3^{-2}(t) - 1\right) \\ &\qquad + 3\, M_2^2(0)\, \left(\xi_2^{-2}(t) - 1\right) - \frac{1}{33}\, M_1^2(0)\, \left(\xi_1^{-2}(t) - 1\right) . \end{aligned} \tag{2.59}$$

The equation for Z requires a numerical integration (even if g_2 and g_Y are zero)

$$\begin{aligned} Z(t) &= \frac{1}{G(t;\vec{n}_0)} \Bigg[Z(0) - \sum_{\alpha=1}^{3} (\vec{n}_0)_\alpha \frac{M_\alpha^2(0)}{\xi_\alpha^2(t)} \Big(G(t;\vec{n}_0) - \xi_\alpha^2(t)\, G(t;\vec{n}_0 - 2\vec{e}^{\,\alpha}) \Big) \\ &\qquad + \frac{3}{4\pi^2} \lambda_t^2(0) \int_0^t dt'\, E(t';\vec{n}_0)\, |A_t(t')|^2 \Bigg] . \end{aligned} \tag{2.60}$$

The solutions for $m_{H_u}^2$, $m_{\tilde{t}_L}^2$ and $m_{\tilde{t}_R}^2$ in terms of X, Y and Z are then

$$m_{H_u}^2(t) = \frac{1}{2}\Big(X(t) + Z(t) \Big) \tag{2.61}$$

$$m_{\tilde{t}_L}^2(t) = \frac{1}{6}\Big(X(t) - 2Y(t) + Z(t) \Big) \tag{2.62}$$

$$m_{\tilde{t}_R}^2(t) = \frac{1}{3}\Big(-2X(t) + Y(t) + Z(t) \Big) . \tag{2.63}$$

2.8 Appendix: Fine-tuning Components

This appendix lists for completeness the expressions for the fine-tuning of m_Z^2 with respect to M_3^2, M_2^2, M_1^2, μ^2, A_t^2, $m_{H_u}^2$, $m_{\tilde{t}_L}^2$ and $m_{\tilde{t}_R}^2$. The fine-tuning components as a function of high-scale parameters are easily found from the fine-tuning measure, equation (2.8), with the observable m_Z^2 written as in equation (2.5). For $M_S = M_{\rm GUT}$, the fine-tuning components are

$$\begin{aligned}
m_Z^2\Delta(m_Z^2,\hat{M}_3^2) &\simeq 5.24\hat{M}_3^2+0.23\hat{M}_3\hat{M}_2+0.03\hat{M}_3\hat{M}_1-0.38\hat{A}_t\hat{M}_3 && (2.64)\\
m_Z^2\Delta(m_Z^2,\hat{M}_2^2) &\simeq -0.44\hat{M}_2^2+0.23\hat{M}_3\hat{M}_2+0.01\hat{M}_2\hat{M}_1-0.08\hat{A}_t\hat{M}_2 && (2.65)\\
m_Z^2\Delta(m_Z^2,\hat{M}_1^2) &\simeq -0.01\hat{M}_1^2+0.03\hat{M}_3\hat{M}_1+0.01\hat{M}_2\hat{M}_1-0.01\hat{A}_t\hat{M}_1 && (2.66)\\
m_Z^2\Delta(m_Z^2,\hat{\mu}^2) &\simeq -2.19\hat{\mu}^2 && (2.67)\\
m_Z^2\Delta(m_Z^2,\hat{A}_t^2) &\simeq 0.22\hat{A}_t^2-0.38\hat{A}_t\hat{M}_3-0.08\hat{A}_t\hat{M}_2-0.01\hat{A}_t\hat{M}_1 && (2.68)\\
m_Z^2\Delta(m_Z^2,\hat{m}_{H_u}^2) &\simeq -1.32\hat{m}_{H_u}^2 && (2.69)\\
&\simeq -m_Z^2-\,2.19\,\hat{\mu}^2+\,1.36\,\hat{m}_{\tilde{t}}^2+\,5.24\,\hat{M}_3^2\\
&\quad -0.44\,\hat{M}_2^2+\,0.46\,\hat{M}_3\,\hat{M}_2-\,0.77\,\hat{A}_t\,\hat{M}_3-\,0.17\,\hat{A}_t\,\hat{M}_2\\
&\quad -0.01\hat{M}_1^2+\,0.22\,\hat{A}_t^2\\
m_Z^2\Delta(m_Z^2,\hat{m}_{\tilde{t}_L}^2) &\simeq 0.68\hat{m}_{\tilde{t}_L}^2 && (2.70)\\
m_Z^2\Delta(m_Z^2,\hat{m}_{\tilde{t}_R}^2) &\simeq 0.68\hat{m}_{\tilde{t}_R}^2. && (2.71)
\end{aligned}$$

Here it is understood that the absolute value of the right-hand sides of each of these equations is meant to be taken. The EWSB relation, equation (2.7), was used to eliminate $\hat{m}_{H_u}^2$. It is natural to eliminate $\hat{m}_{H_u}^2$ instead of $\hat{\mu}^2$ or any other soft supersymmetry breaking parameters since $\hat{\mu}^2$ is supersymmetric while the other soft supersymmetry breaking parameters are not involved in the EWSB equation at the EW scale. With the help of equations (2.21)-(2.26), it is now straightforward to rewrite the FT expression (2.10) in terms of low-scale parameters.

Chapter 3

Spontaneous Symmetry Breaking in Supersymmetry

3.1 Introduction

In this chapter we discuss in detail the findings of the work done in [29].

Although the extension of the R_ξ-gauge to supersymmetric gauge theories has been studied previously [98, 99, 100, 101] confusion still remains about the results. Ovrut and Wess [98] extended the R_ξ-gauge to spontaneously broken $SU(N_c)$ super Yang-Mills with matter and computed the superpropagators. They did not however calculate the vertices nor did they stress the non-local behavior of these gauges. Later Marcus, Sagnotti and Siegel [99] and Siegel [100] used equivalent gauge-fixing terms in the context of ten-dimensional Yang-Mills theory and four-dimensional $N = 1$ superspace Gervais-Neveu gauge respectively. Recently Goldhaber, Rebhan, van Nieuwenhuizen and Wimmer [101] discussed the supersymmetric extension of the R_ξ-gauge and pointed out that non-local terms appear in the action. They concluded that one might not be able to construct a local R_ξ-gauge theory in the superFeynman gauge due to the presence of non-local terms.

This paper re-introduces the R_ξ-gauge for supersymmetric Yang-Mills with matter and shows that the theory is well-defined at one-loop in general gauge. The effectiveness of supersymmetric R_ξ-gauge relies on the projection operator for chiral fields [98] which however introduces non-local terms in the gauge-fixing term as described in [101]. These non-local terms show up in two different parts of the action, in the gauge-fixing action and the ghost action. Most of these terms become gauge-dependent mass terms for quark and ghost superfields while non-zero vacuum expectation values give vector superfield mass term. This is analogous to usual R_ξ-gauge [102] and Higgs mechanism [103, 104, 105] in non-supersymmetric theories. The non-local terms left are all of the same form and correspond to vertices between one quark superfield and two ghost superfields. To one-loop, non-local contributions to the effective action are well-defined, the non-renormalization theorem of supersymmetric theories forcing several non-local diagrams to give a zero contribution. Remaining contributions are mostly finite, the most divergent diagrams are only logarithmically divergent and do not require additional counterterms.

The massive vector superfields encountered in these theories are interesting on their own. Indeed, supersymmetry (SUSY) could be the theory beyond the standard model of particles and it is not excluded that electroweak symmetry breaking happens at energy scales higher than SUSY breaking. In this scenario massive vector superfields would be generated, which signals SUSY as the theory beyond the standard model.

The paper is constructed as follows. In section 3.2 the R_ξ-gauge is introduced for $SU(N_c)$ super Yang-Mills theory with fundamental matter and the superpropagators and vertices in general gauge are computed. In section 3.3 non-local contributions to the effective action at one-loop are computed from superFeynman diagrams. The effects of these non-local terms are discussed and it is argued that higher-order corrections should have the same form. Notation conventions follow [98] and are gathered in appendix 3.5 with other useful identities. The computation of the ghost action is left for appendix 3.6.

3.2 $SU(N_c)$ supersymmetric QCD with matter

The starting point is $SU(N_c)$ supersymmetric QCD with N_f flavors of quarks Q_{in} in a given representation R (in general complex, reducible) of the gauge group ($i, j = 1, \ldots, N_f$ are flavor indices and $n, m = 1, \ldots, \dim R$ are gauge group index). The gauge group representation R carried by the quarks is chosen such that anomalies cancel. The SUSY Yang-Mills action is given by

$$S_{\text{inv}} = \frac{1}{16g^2C_2(A)}\text{Tr}\left(\int d^6z\; W^\alpha W_\alpha + h.c.\right) + \int d^8z\; \overline{Q}_i e^V Q_i. \tag{3.1}$$

The quarks $Q_{in}(z)$ are chiral superfields and the gauge bosons $V_{nm}(z) = V^a(z)T^a_{nm}$ are vector superfields. Here $a, b = 1, \ldots, N_c^2 - 1$ are indices in the adjoint representation A of the gauge group and T^a_{nm} are the generators of the gauge group in the representation R. The generators of the vector superfield action are in the adjoint representation where $T(A) = C_2(A)$ (see appendix 3.5) and the normalization is chosen such that the rescaling $V \to 2gV$ leads to the canonical normalization. For simplicity the superpotential is set to zero. This avoids further complications due to additional propagators between (anti-)chiral quark superfields. From the super field strength $W_\alpha = -\frac{1}{4}\bar{D}^2(e^{-V}D_\alpha e^V)$ the vector superfield action can be rewritten in a more convenient way as an integral over full superspace

$$\begin{aligned} S_V &= \frac{1}{16g^2C_2(A)}\text{Tr}\left(\int d^6z\; W^\alpha W_\alpha + h.c.\right) \\ &= -\frac{1}{64g^2C_2(A)}\text{Tr}\left(\int d^6z\; \left(-\frac{\bar{D}^2}{4}\right)\left(\bar{D}^2(e^{-V}D^\alpha e^V)(e^{-V}D_\alpha e^V)\right) + h.c.\right) \qquad (3.2) \\ &= -\frac{1}{64g^2C_2(A)}\text{Tr}\left(\int d^8z\; \bar{D}^2(e^{-V}D^\alpha e^V)(e^{-V}D_\alpha e^V) + h.c.\right). \end{aligned}$$

An interesting phenomenon is the SUSY analog [98] of the Higgs mechanism [103, 104, 105] where quarks have non-zero vacuum expectation values. These theories, which have massive vector superfields, could be relevant if e.g. electroweak symmetry breaking happens at higher energy scales than SUSY breaking. With that in mind, the quark vacuum expectation values are chosen such that they do not break SUSY nor Poincaré invariance. The simplest choice is

$$Q_{in}(z) = q_{in} + \Phi_{in}(z) \tag{3.3}$$

where q_{in} are constrained by the auxiliary field equations of motion. The phenomenon giving rise to non-zero quark expectation values is not of interest here. Expanding the action leads to

$$S_{\text{inv}} = -\frac{1}{64g^2C_2(A)}\mathrm{Tr}\left(\int d^8z\, \bar{D}^2(e^{-V}D^\alpha e^V)(e^{-V}D_\alpha e^V) + h.c.\right) + \int d^8z\, (\overline{q}_i + \overline{\Phi}_i)e^V(q_i + \Phi_i). \tag{3.4}$$

In order to cancel quark superfield/vector superfield cross-terms, one introduces the chiral gauge-fixing term

$$F^a = \bar{D}^2V^a + 32g^2\xi\left(\frac{\bar{D}^2}{16\partial^2}\right)\overline{\Phi}_iT^aq_i \tag{3.5}$$

which is, as component notation shows, the SUSY analog of the non-SUSY R_ξ-gauge. F^a is chosen chiral since gauge transformations have a chiral parameter Λ^a. This choice of gauge-fixing term takes advantage of the chiral field projection operator $P_2 = \frac{\bar{D}^2D^2}{16\partial^2}$ with $P_2\Phi(z) = \Phi(z)$. However, as shown by the second term of equation (3.5), it forces the introduction of non-local terms in the action which can spoil the consistency of the theory in these gauges. This non-locality will be studied more carefully in the following section. The generating functional is gauge-fixed following the general procedure of the functional determinant

$$\Delta(V) = \int \mathbb{D}\Lambda\mathbb{D}\overline{\Lambda}\,\delta[F(V^{\Lambda,\overline{\Lambda}}) - f]\delta[\overline{F}(V^{\Lambda,\overline{\Lambda}}) - \overline{f}]. \tag{3.6}$$

Averaging over f and $\overline{f}$ with a Gaussian weight factor results in the $SU(N_c)$ superQCD generating functional

$$\begin{aligned} Z &= \frac{1}{N}\int \mathbb{D}f\mathbb{D}\overline{f}\mathbb{D}V\mathbb{D}\Phi\mathbb{D}\overline{\Phi}\mathbb{D}\widetilde{\Phi}\mathbb{D}\overline{\widetilde{\Phi}}\,\exp\left(-\frac{i}{32g^2\xi}\int d^8z\,\overline{f}^af^a\right)\Delta^{-1}(V)\Delta(V)e^{iS_{\text{inv}}} \\ &= \int \mathbb{D}V\mathbb{D}\Phi\mathbb{D}\overline{\Phi}\mathbb{D}\widetilde{\Phi}\mathbb{D}\overline{\widetilde{\Phi}}\mathbb{D}c\mathbb{D}\overline{c}\mathbb{D}c'\mathbb{D}\overline{c}'\,e^{iS_{\text{inv}}+iS_{\text{GF}}+iS_{\text{FP}}} \end{aligned} \tag{3.7}$$

where the gauge-fixing action (coming from the Gaussian weight factor and the functional determinant) and the ghost action (coming from the inverse of the functional determinant) are

(see appendix 3.6)

$$S_{\text{GF}} = \int d^8z \left(-\frac{1}{64g^2\xi C_2(A)}\text{Tr}V\{D^2,\bar{D}^2\}V - \overline{q}_i V\Phi_i - \overline{\Phi}_i V q_i - 2g^2\xi(\overline{q}_i T^a\Phi_i)\frac{1}{\partial^2}(\overline{\Phi}_i T^a q_i)\right) \quad (3.8)$$

$$S_{\text{FP}} = \int d^8z \left(\frac{1}{C_2(A)}\text{Tr}\left[(c'+\overline{c}')(\mathcal{L}_{V/2}[(c+\overline{c}) + \coth(\mathcal{L}_{V/2})(c-\overline{c})])\right]\right. \quad (3.9)$$
$$\left. -2g^2\xi\left[(\overline{q}_i + \overline{\Phi}_i)\overline{c}\left(\frac{1}{\partial^2}c'\right)q_i + \overline{q}_i\left(\frac{1}{\partial^2}\overline{c}'\right)c(q_i+\Phi_i)\right]\right).$$

The gauge-fixing action generates the terms needed to cancel the quark superfield/vector superfield cross-terms. However, in both the gauge-fixing and ghost actions, the gauge-fixing term also leads to non-local terms as stated above. Most of the non-local terms consist of only two fields (two quark or two ghost superfields) and will therefore modify the propagators, in this case by generating mass terms. The non-local terms consisting of more than two fields are at first sight problematic. Only two vertices are of this kind, corresponding to interactions between one quark superfield and two ghost superfields. Their effects will be investigated in the next section, after the propagators and vertices are obtained.

The free and interacting parts of the actions are easily found by expansion. For the vector superfield, the free action can be simplified using projection operators (see appendix 3.5)

$$S_V^0 = \int d^8z \left(V^a\left[\frac{1}{64g^2}\left(D^\alpha\bar{D}^2D_\alpha + \bar{D}_{\dot\alpha}D^2\bar{D}^{\dot\alpha} - \frac{1}{\xi}\{D^2,\bar{D}^2\}\right)\delta^{ab} + \frac{\mathcal{M}^{2ab}}{4g^2}\right]V^b + \overline{q}_i V q_i\right)$$
$$= \frac{1}{2}\int d^8z\left(V^a\left[-\frac{1}{2g^2}\left(P_T + \frac{1}{\xi}P_0 - \frac{\mathcal{M}^2}{\partial^2}\right)^{ab}\partial^2\right]V^b\right) + \int d^8z\, \overline{q}_i V q_i \quad (3.10)$$

which gives the propagator

$$\langle 0|T\{V^a(z_1)V^b(z_2)\}|0\rangle = -2ig^2\left[\left(\frac{1}{\partial_1^2 - \mathcal{M}^2}\right)^{ab}P_T + \xi\left(\frac{1}{\partial_1^2 - \xi\mathcal{M}^2}\right)^{ab}P_0\right]\delta_{12}. \quad (3.11)$$

The quark superfield free action is simply

$$S_\Phi^0 = \int d^8z\left(\overline{\Phi}_i\Phi_i - 2g^2\xi(\overline{q}_i T^a\Phi_i)\frac{1}{\partial^2}(\overline{\Phi}_i T^a q_i)\right)$$
$$= \frac{1}{2}\int d^8z\left(\overline{\Phi}_{in}\left[\delta_{ij}\delta_{nm} - \xi\frac{M^2_{in,jm}}{\partial^2}\right]\Phi_{jm} + \Phi_{in}\left[\delta_{ij}\delta_{nm} - \xi\frac{M^2_{jm,in}}{\partial^2}\right]\overline{\Phi}_{jm}\right) \quad (3.12)$$

and the free propagator becomes (notice that since the superpotential is zero no free propogators between Φ and Φ or between $\overline{\Phi}$ and $\overline{\Phi}$ appear)

$$\langle 0|T\{\Phi_{in}(z_1)\overline{\Phi}_{jm}(z_2)\}|0\rangle = i\left(\frac{\partial_1^2}{\partial_1^2 - \xi M^2}\right)_{in,jm}P_2\delta_{12} = i\left[\delta_{ij}\delta_{nm} + \xi M^{2ab}_{in,jm}\left(\frac{1}{\partial_1^2 - \xi\mathcal{M}^2}\right)^{ab}\right]P_2\delta_{12}. \quad (3.13)$$

Finally the ghost superfield free action is

$$S_g^0 = \int d^8z\left(\frac{1}{k}\text{Tr}\left[\overline{c}'c - c'\overline{c}\right] - 2g^2\xi\left[\overline{q}_i\left(\frac{1}{\partial^2}\overline{c}\right)c'q_i + \overline{q}_i\overline{c}'\left(\frac{1}{\partial^2}c\right)q_i\right]\right)$$
$$= \int d^8z\left(\overline{c}'^a\left[\delta^{ab} - \xi\frac{\mathcal{M}^{2ab}}{\partial^2}\right]c^b - c'^a\left[\delta^{ab} - \xi\frac{\mathcal{M}^{2ba}}{\partial^2}\right]\overline{c}^b\right) \quad (3.14)$$

leading to the propagators

$$\langle 0|T\{c^a(z_1)\overline{c}'^b(z_2)\}|0\rangle \;=\; i\left(\frac{\partial_1^2}{\partial_1^2-\xi\mathcal{M}^2}\right)^{ab} P_2\delta_{12} \tag{3.15}$$

$$\langle 0|T\{\overline{c}^a(z_1)c'^b(z_2)\}|0\rangle \;=\; -i\left(\frac{\partial_1^2}{\partial_1^2-\xi\mathcal{M}^2}\right)^{ba} P_1\delta_{12}. \tag{3.16}$$

Here $M^{2ab}_{in,jm} = 2g^2(\overline{q}_jT^b)_m(T^aq_i)_n$ and the vector and ghost superfield mass matrix is $\mathcal{M}^{2ab} = \sum M^{2ab}_{in,in}$ while the quark superfield mass matrix is $M^2_{in,jm} = \sum M^{2aa}_{in,jm}$. As pointed out before all non-local terms involving exactly two superfields modify the free propagators by generating mass terms. This occurs since the projection operators $\{P_T, P_1, P_2\}$ of the free propagators absorb the extra $\frac{1}{\partial^2}$ factor of these non-local terms to produce the corresponding mass terms. Therefore the only non-local terms left are in the interacting actions and involve one quark and two ghost superfields

$$\begin{aligned} S_V^{\text{int}} &= \frac{1}{64g^2C_2(A)}\mathrm{Tr}\left[\int d^8z\,\left(\bar{D}^2D^\alpha V[V,D_\alpha V] - \frac{1}{4}[V,D^\alpha V]\bar{D}^2[V,D_\alpha V]\right.\right. && (3.17)\\ &\quad \left.\left.-\frac{1}{3}\bar{D}^2D^\alpha V[V,[V,D_\alpha V]]+\cdots\right)+h.c.\right] + \int d^8z\,\overline{q}_i\left[\frac{V^3}{3!}+\frac{V^4}{4!}+\cdots\right]q_i \\ S_\Phi^{\text{int}} &= \int d^8z\,\left(\overline{q}_i\left[\frac{V^2}{2}+\cdots\right]\Phi_i + \overline{\Phi}_i\left[\frac{V^2}{2}+\cdots\right]q_i + \overline{\Phi}_i\left[V+\frac{V^2}{2}+\cdots\right]\Phi_i\right) && (3.18)\\ S_g^{\text{int}} &= \frac{1}{C_2(A)}\mathrm{Tr}\int d^8z\,\left(\frac{1}{2}(c'+\overline{c}')[V,c-\overline{c}] + \frac{1}{12}(c'+\overline{c}')[V,[V,c-\overline{c}]]\cdots\right) && (3.19)\\ &\quad -2g^2\xi\int d^8z\,\left[\overline{\Phi}_i\overline{c}\left(\frac{1}{\partial^2}c'\right)q_i + \overline{q}_i\left(\frac{1}{\partial^2}\overline{c}'\right)c\Phi_i\right]. \end{aligned}$$

Notice that, apart from non-locality issues, the Higgs mechanism in SUSY theories is similar to the Higgs mechanism in non-SUSY theories. It leads to gauge-dependent mass terms for quark and ghost superfields and to quark superfield/ghost superfield/ghost superfield interactions as in non-SUSY theories. In addition notice that all non-local terms disappear in superLorentz gauge ($\xi = 0$). Consequently one can undertake all computations in this specific gauge without worrying about non-locality. The next section is devoted to show that the non-local vertices are well-behaved in the effective action at one-loop in any gauge.

3.3 Non-local terms in the effective action at one-loop

The goal here is to compute one-loop contributions to the effective action coming from non-local terms in general gauge. The interest lies in terms that could spoil the locality of the theory at one-loop. By inspection the only possible divergent diagrams involving non-local vertices can be grouped according to their external superfields (here the zero superpotential decreases greatly the number of diagrams).

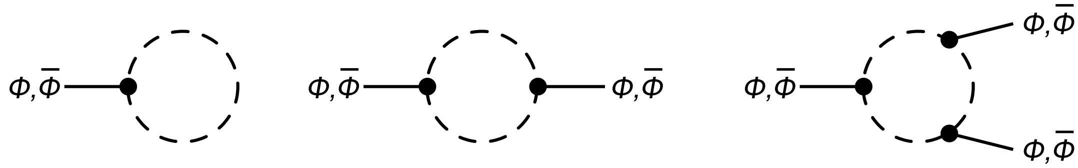

Figure 3.1: Diagrams renormalizing the superpotential.

The first group shown in figure 3.1 corresponds to diagrams renormalizing the superpotential. They are all exactly zero by the chirality properties of the external superfields, as anticipated from the non-renormalization theorem of SUSY theories. For example, in the case of external chiral quark superfields $\Phi(z)$, after integrating by parts all covariant derivatives on one δ-function and on quark chiral superfields, one ends up with integrals of chiral superfields with projection operators over full superspace. These simplify ($P_T\Phi(z) = 0$, $P_1\Phi(z) = 0$ and $P_2\Phi(z) = \Phi(z)$) and give integrals of naked chiral superfields over full superspace, which are identically zero. The same is true of anti-chiral quark superfields $\overline{\Phi}(z)$ with P_2 replaced by P_1. Consequently no superpotential is generated, as expected in perturbation theory of SUSY theories and the non-local vertices do not affect the theory at this level.

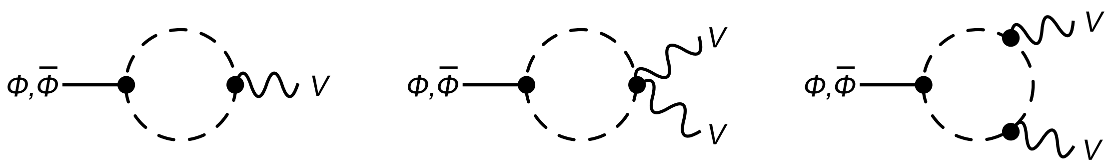

Figure 3.2: Diagrams renormalizing the interactions between one quark superfield and any number of vector superfields.

The second group of diagrams of figure 3.2 renormalizes the interactions between one quark superfield and any number of vector superfields. The number of external vector superfields is arbitrary since vector superfields have mass dimension zero in SUSY. By gauge invariance all the diagrams in this group lead to the same infinite contributions. For example, the first diagram of figure 3.2 with external chiral quark superfield Φ gives

$$2 \times \frac{i^2}{2} \int d^8z_1 d^8z_2 \left\langle \frac{1}{2C_2(A)} \mathrm{Tr}\overline{c}'(z_1)[V(z_1), c(z_1)](-2g^2\xi)\overline{q}_i \left(\frac{1}{\partial_2^2}\overline{c}'(z_2)\right) c(z_2)\Phi_i(z_2) \right\rangle$$
$$= -ig^2\xi f^{abc}(\overline{q}_i T^d T^e)_n \int \frac{d^4p}{(2\pi)^4}\frac{d^4k}{(2\pi)^4} d^4\theta\, V^a(-p,\theta) \left(\frac{1}{(p+k)^2+\xi\mathcal{M}^2}\right)^{cd} \left(\frac{1}{k^2+\xi\mathcal{M}^2}\right)^{eb} \Phi_{in}(p,\theta)$$
$$= -ig^2\xi f^{abc}(\overline{q}_i T^c T^b)_n \int \frac{d^4p}{(2\pi)^4}\frac{d^4k}{(2\pi)^4} d^4\theta\, V^a(-p,\theta)\frac{1}{k^2(p+k)^2}\Phi_{in}(p,\theta) + \text{finite}. \quad (3.20)$$

With respect to non-SUSY theories, this diagram is equivalent to its non-SUSY analog since

$$\int d^4\theta\ V(\theta)\Phi(\theta) \supset \int d^4\theta\ (-\theta\sigma^\mu\bar{\theta}A_\mu)(i\theta\sigma^\nu\bar{\theta}\partial_\nu\phi). \tag{3.21}$$

It also fulfills the same goal, i.e. it cancels gauge-dependent terms in figure 3.3. Moreover it is only logarithmically divergent as expected in SUSY theories. This divergence has the same form as the field strength renormalization divergence thus it should be taken care off by the same counterterm. Therefore the theory seems unaffected by non-locality issues for this group of diagrams.

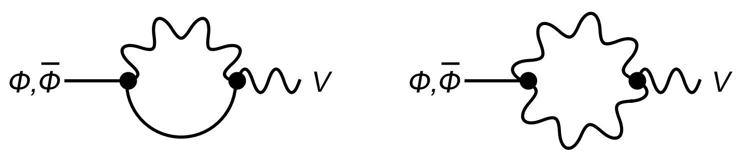

Figure 3.3: Other relevant diagrams which renormalize the interactions between one quark superfield and one vector superfield.

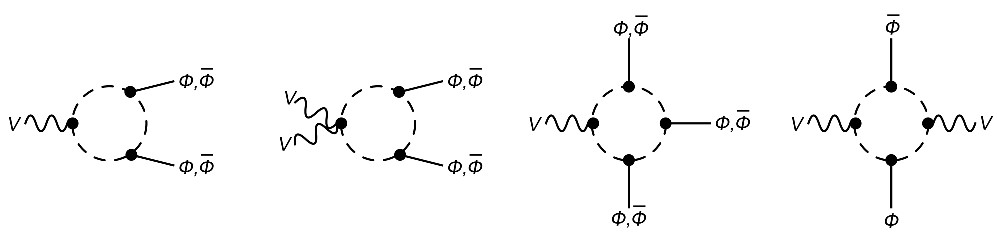

Figure 3.4: Diagrams renormalizing the interactions between two or more quark superfields and any number of vector superfields.

The third group (see figure 3.4) consists of diagrams with two or three external quark superfields (chiral or anti-chiral) and any number of vector superfields. A simple computation shows that these diagrams are all finite and thus do not spoil the theory. Indeed, since quark superfields and quark vacuum expectation values have mass dimension one, these diagrams have to be finite by dimensional analysis.

The fourth and last group of diagrams of figure 3.5 is defined by unphysical processes where ghost superfields appear on external legs. These diagrams are the most dangerous since the non-locality may lie on the external legs. However, diagrams with non-local factors on external legs become local since the non-local factors disappear in the integration process. Indeed, integration by parts pushes the appropriate covariant derivatives on the external ghost superfields with a $\frac{1}{\partial^2}$ factor which gives rise to the appropriate projection operators. By the chirality properties

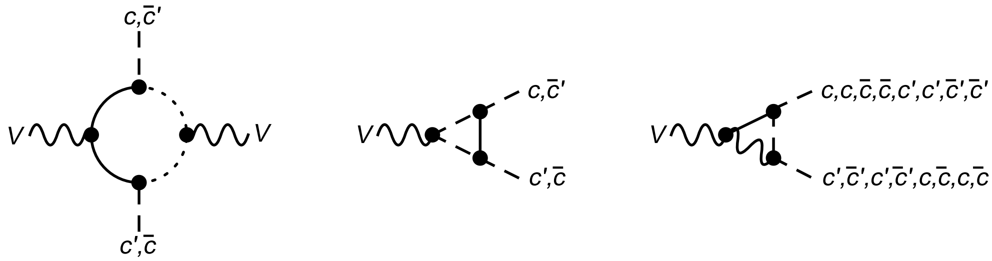

Figure 3.5: Diagrams involving external ghost superfields.

of the ghost superfields, the non-local factor then disappears. For example, the second diagram of 3.5 with external chiral ghost superfields c and c' contains

$$\begin{aligned}
&\int d^8z_1 d^8z_2 d^8z_3 \left(\frac{\partial_2^2}{\partial_2^2-\xi M^2}\right)_{in,jm} P_2\delta_{12}^8 \left(\frac{\partial_1^2}{\partial_1^2-\xi\mathcal{M}^2}\right)^{ab} P_1\delta_{13}^8 \\
&\qquad\qquad\qquad \times \left(\frac{\partial_2^2}{\partial_2^2-\xi\mathcal{M}^2}\right)^{cd} P_1\delta_{23}^8 \frac{1}{\partial_1^2} c'^e(z_1)c^f(z_2)V^g(z_3) \\
&= \int d^8z_1 d^8z_2 d^8z_3 \left(\frac{\partial_2^2}{\partial_2^2-\xi M^2}\right)_{in,jm} P_2\delta_{12}^8 \left(\frac{1}{\partial_1^2-\xi\mathcal{M}^2}\right)^{ab} \delta_{13}^8 \\
&\qquad\qquad\qquad \times \left(\frac{\partial_2^2}{\partial_2^2-\xi\mathcal{M}^2}\right)^{cd} P_1\delta_{23}^8 \frac{\bar{D}_1^2 D_1^2}{16\partial_1^2} c'^e(z_1)c^f(z_2)V^g(z_3)
\end{aligned} \tag{3.22}$$

where P_1 is naturally integrated by parts on the ghost superfield $c'^e(z_1)$ leading to $P_2c'^e(z_1) = c'^e(z_1)$. Moreover, by dimensional analysis these diagrams are all finite.

From this analysis the theory thus seems well-defined at one-loop in any gauge. Moreover, by similar considerations one expects the theory to be well-defined at any order in perturbation theory. In fact, in physical processes ghosts never occur as external fields and thus have to be contracted. This helps the analysis since ghost propagators carry an extra ∂^2 factor in their numerator which cancels the non-local $\frac{1}{\partial^2}$ contributions of the vertices. These diagrams should then have a clear meaning. For unphysical processes with external ghost superfields the $\frac{1}{\partial^2}$ factor of non-local vertices is taken care of by covariant derivatives and the chiral properties of the ghost superfields. In the end non-local effects only seem to generate less divergent quantum corrections and as a result additional counterterms are not required. These reasons suggest that spontaneously broken $SU(N_c)$ superQCD with matter is well-defined in general gauge in perturbation theory.

3.4 Conclusion

Supersymmetric R_ξ-gauge for super Yang-Mills theory with spontaneously broken gauge group leads to subtleties which deserve investigation. The chiral choice of the gauge-fixing term introduces non-local terms which could spoil the locality of the theory. It is shown here that these terms do not threaten the consistency of the theory at one-loop. In fact, it parallels quite closely the non-SUSY case. Indeed, non-zero quark vacuum expectation values lead to vector mass terms by the Higgs mechanism and part of the newly introduced non-local terms give rise to gauge-dependent mass terms for quark and ghost superfields. Moreover the remaining non-local vertices result in analogous non-SUSY quantum corrections. The non-renormalization theorem forces some of the corrections related to non-locality to be exactly zero while the non-zero diagrams left over are at worst logarithmically divergent and cancel gauge-dependent terms in well-behaved diagrams. No additional counterterms seems to be required. Adding a non-zero superpotential brings more free propagators but the general idea stays the same. Simplified computations can be performed in the superLorentz gauge where all problematic non-local terms disappear and the theory gives expected results for the β-function of the gauge coupling. Unfortunately the computation is long and tedious and won't be reported here. Other choices of gauge groups do not seem to complicate the problem further.

3.5 Appendix: Notation

The notation conventions used throughout the paper (see [98]) are reported here. The group generators T^a in the representation R are chosen hermitian and satisfy the following identities

$$[T^a, T^b] = i f^{abc} T^c \tag{3.23}$$

$$\mathrm{Tr}(T^a T^b) = T(R)\delta^{ab} \tag{3.24}$$

$$(T^a T^a)_{nm} = C_2(R)\delta_{nm} \tag{3.25}$$

$$f^{acd} f^{bcd} = C_2(A)\delta^{ab} \tag{3.26}$$

$$T(A) = C_2(A). \tag{3.27}$$

$$\tag{3.28}$$

f^{abc} are the structure constants and $T(R), C_2(R)$ are the Casimir coefficients of the representation R. In superspace the compact notation is $\delta_{12} = \delta^8(z_1 - z_2) = \delta^4(x_1 - x_2)\delta^4(\theta_1 - \theta_2) = \delta^x_{12}\delta^\theta_{12}$.

Several useful identities for integrals over superspace are (some make sense only in integrals)

$$
\begin{aligned}
D_1^\alpha \delta_{12} &= -D_2^\alpha \delta_{12} && (3.29)\\
D_1^2 \delta_{12} &= D_2^2 \delta_{12} && (3.30)\\
\delta_{12}^\theta \bar{D}_1^2 D_1^2 \delta_{12} &= \delta_{12}^\theta \bar{D}_2^2 D_2^2 \delta_{12} = 16\delta_{12} && (3.31)\\
\delta_{12}^\theta D_1^2 \bar{D}_1^2 \delta_{12} &= \delta_{12}^\theta D_2^2 \bar{D}_2^2 \delta_{12} = 16\delta_{12} && (3.32)\\
\delta_{12}^\theta D_1^\alpha \bar{D}_1^2 D_{1\alpha} \delta_{12} &= \delta_{12}^\theta D_2^\alpha \bar{D}_2^2 D_{2\alpha} \delta_{12} = 16\delta_{12} && (3.33)\\
D^2 \bar{D}^2 D^2 &= 16\partial^2 D^2 && (3.34)\\
\bar{D}^2 D^2 \bar{D}^2 &= 16\partial^2 \bar{D}^2 && (3.35)\\
\{D_\alpha, \bar{D}_{\dot\alpha}\} &= -2i\sigma^\mu_{\alpha\dot\alpha}\partial_\mu && (3.36)\\
\sigma^\mu_{\alpha\dot\alpha}\bar{\sigma}_\nu^{\dot\alpha\alpha} &= -2g^{\mu\nu} && (3.37)\\
[D_\alpha, \bar{D}^2] &= -4i\sigma^\mu_{\alpha\dot\alpha}\partial_\mu \bar{D}^{\dot\alpha} && (3.38)\\
[\bar{D}_{\dot\alpha}, D^2] &= 4i\sigma^\mu_{\alpha\dot\alpha}\partial_\mu D^\alpha && (3.39)\\
D_\alpha D_\beta &= \frac{1}{2}\epsilon_{\alpha\beta} D^2 && (3.40)\\
\bar{D}_{\dot\alpha} \bar{D}_{\dot\beta} &= -\frac{1}{2}\epsilon_{\dot\alpha\dot\beta} \bar{D}^2. && (3.41)
\end{aligned}
$$

From the δ_{12}^θ-function reduction formulae (A.5-7), one can focus only on integrals with naked δ-functions and one δ-function with four covariant derivatives. One also introduces the projection operators $P_i = \{P_1, P_2, P_T\}$,

$$P_1 = \frac{D^2\bar{D}^2}{16\partial^2} \qquad P_2 = \frac{\bar{D}^2 D^2}{16\partial^2} \qquad P_0 = P_1 + P_2 \tag{3.42}$$

and

$$P_T = -\frac{D^\alpha \bar{D}^2 D_\alpha}{8\partial^2} = -\frac{\bar{D}_{\dot\alpha} D^2 \bar{D}^{\dot\alpha}}{8\partial^2}. \tag{3.43}$$

As their name implies they obey the following relations

$$\sum_{i=\{1,2,T\}} P_i = 1 \qquad P_i P_j = \delta_{ij} P_j. \tag{3.44}$$

Moreover chiral superfields $\Phi(z)$ obey

$$P_T \Phi(z) = 0 \qquad P_1 \Phi(z) = 0 \qquad P_2 \Phi(z) = \Phi(z). \tag{3.45}$$

Two additional operators given by

$$P_+ = \frac{D^2}{4(\partial^2)^{\frac{1}{2}}} \qquad P_- = \frac{\bar{D}^2}{4(\partial^2)^{\frac{1}{2}}} \tag{3.46}$$

are helpful in inverting matrix with covariant derivatives (see [98]). Those are useful when one has a non-zero superpotential which mixes chiral quark superfields together. Finally Fourier transforms are defined as

$$A(x,\theta) = \int \frac{d^4k}{(2\pi)^4}\, A(k,\theta)e^{-ik\cdot x} \tag{3.47}$$

and integrals over half superspace are converted into integrals over full superspace with the help of

$$\int d^4x d^2\theta \left(-\frac{1}{4}\bar{D}^2\right) F = \int d^4x d^2\theta d^2\bar{\theta}\; F. \tag{3.48}$$

This is possible since derivatives in superspace are the same than integrals.

3.6 Appendix: Ghost action

The ghost action is found by usual techniques. Using integral representations of δ-functions the functional determinant can be written as

$$\begin{aligned}\Delta(V) &= \int \mathbb{D}\Lambda\mathbb{D}\overline{\Lambda}\; \delta[F(V^{\Lambda,\overline{\Lambda}}) - f]\delta[\overline{F}(V^{\Lambda,\overline{\Lambda}}) - \overline{f}] \\ &= \int \mathbb{D}\Lambda\mathbb{D}\overline{\Lambda}\mathbb{D}\Lambda'\mathbb{D}\overline{\Lambda}'\; \exp\left(\int d^8z \left[\Lambda'^a \left(\frac{\delta F}{\delta\Lambda}\Lambda + \frac{\delta F}{\delta\overline{\Lambda}}\overline{\Lambda}\right)^a + \overline{\Lambda}'^a \left(\frac{\delta\overline{F}}{\delta\Lambda}\Lambda + \frac{\delta\overline{F}}{\delta\overline{\Lambda}}\overline{\Lambda}\right)^a\right]\right)\end{aligned} \tag{3.49}$$

where Λ' and $\overline{\Lambda}'$ are general superfields* and the derivatives are to first order in the gauge parameters. From the field transformation properties

$$\begin{aligned} Q_i &\rightarrow Q'_i = e^{-i\Lambda}Q_i \\ e^V &\rightarrow e^{V'} = e^{-i\overline{\Lambda}}e^V e^{i\Lambda}\end{aligned} \tag{3.50}$$

the variations and appropriate derivatives are easily found (here $\mathcal{L}_X Y = [X,Y]$)

$$\begin{aligned}\Delta(V) = \int \mathbb{D}\Lambda\mathbb{D}\overline{\Lambda}\mathbb{D}\Lambda'\mathbb{D}\overline{\Lambda}'\; \exp\Bigg(i\int d^8z\; \Big[&\Lambda'^a\bar{D}^2(\mathcal{L}_{V/2}[(\Lambda+\overline{\Lambda}) + \coth(\mathcal{L}_{V/2})(\Lambda-\overline{\Lambda})])^a \\ &+\overline{\Lambda}'^a D^2(\mathcal{L}_{V/2}[(\Lambda+\overline{\Lambda}) + \coth(\mathcal{L}_{V/2})(\Lambda-\overline{\Lambda})])^a \\ &+\Lambda'^a\bar{D}^2\frac{2g^2\xi}{\partial^2}(\overline{q}_i + \overline{\Phi}_i)\overline{\Lambda}T^a q_i - \overline{\Lambda}'^a D^2\frac{2g^2\xi}{\partial^2}\overline{q}_i T^a\Lambda(q_i+\Phi_i)\Big]\Bigg).\end{aligned} \tag{3.51}$$

To invert it, one uses anti-commuting superfields b^a, $\overline{b}^a$, c^a and $\overline{c}^a$ instead of commuting superfields Λ'^a, $\overline{\Lambda}'^a$, Λ^a and $\overline{\Lambda}^a$ respectively, which gives

$$\begin{aligned}\Delta^{-1}(V) &= \int \mathbb{D}c\mathbb{D}\overline{c}\mathbb{D}b\mathbb{D}\overline{b}\; \exp\Bigg(i\int d^8z\; \Big[b^a\bar{D}^2(\mathcal{L}_{V/2}[(c+\overline{c}) + \coth(\mathcal{L}_{V/2})(c-\overline{c})])^a \\ &\quad +\overline{b}^a D^2(\mathcal{L}_{V/2}[(c+\overline{c}) + \coth(\mathcal{L}_{V/2})(c-\overline{c})])^a \\ &\quad +b^a\bar{D}^2\frac{2g^2\xi}{\partial^2}(\overline{q}_i+\overline{\Phi}_i)\overline{c}T^a q_i - \overline{b}^a D^2\frac{2g^2\xi}{\partial^2}\overline{q}_i T^a c(q_i+\Phi_i)\Big]\Bigg) \qquad (3.52) \\ &= \int \mathbb{D}c\mathbb{D}\overline{c}\mathbb{D}c'\mathbb{D}\overline{c}'\; e^{iS_{\rm FP}}.\end{aligned}$$

*Unlike the gauge parameters Λ and $\overline{\Lambda}$ which are chiral and anti-chiral superfields respectively.

Here integration by parts was used to write the general anti-commuting superfields b and $\overline{b}$ as chiral and anti-chiral anti-commuting superfields $c' = \bar{D}^2 b$ and $\overline{c}' = D^2 \overline{b}$. The ability to write the ghost action only in terms of chiral and anti-chiral ghost superfields was expected since the gauge-fixing term is chiral. The ghost action is

$$\begin{aligned} S_{\text{FP}} \quad = \quad & \int d^8 z \left(\frac{1}{C_2(A)} \text{Tr} \left[(c' + \overline{c}')(\mathcal{L}_{V/2}[(c + \overline{c}) + \coth(\mathcal{L}_{V/2})(c - \overline{c})]) \right] \right. \\ & \left. -2g^2 \xi \left[\left(\frac{1}{\partial^2} \left[(\overline{q}_i + \overline{\Phi}_i)\overline{c} \right] \right) c' q_i + \overline{q}_i \overline{c}' \left(\frac{1}{\partial^2} \left[c(q_i + \Phi_i) \right] \right) \right] \right) \end{aligned} \tag{3.53}$$

where the generators in the first term are chosen to be in the adjoint representation A of the gauge group. Notice again the presence of non-local terms $\frac{1}{\partial^2}$ in S_{FP}, as for S_{GF}.

Chapter 4

Undetected Higgs Decays in Supersymmetry

4.1 The little hierarchy problem and its solutions

In this chapter we discuss in detail the findings of the work done in collaboration with T. Banks and L. Carpenter [9].

The minimal supersymmetric extension of the standard model (MSSM) predicts a light Higgs boson. While theory predicts a tree level Higgs mass which is at most the mass of the Z boson, the current experimental lower bound from LEP [107] is 114.4 GeV. Evading the experimental lower bound requires significant one loop corrections which can be achieved only by fine tuning of parameters [108]. This *little hierarchy problem*, while nowhere near as severe as the original gauge hierarchy problem, has excited a lot of theoretical interest. A variety of solutions has been proposed [109]. Some of them introduce new degrees of freedom to enhance the contributions to the Higgs mass, while others allow for non-standard decays of the Higgs, which would have been missed at LEP. The latter can greatly alter the experimental search strategy for the Higgs and supersymmetry (SUSY) at the LHC.

In this paper, we will pursue the suggestion of [111] and [112], that the Higgs can decay into light gauginos, which in turn decay via renormalizable lepton number violating couplings, into jets plus neutrinos. This decay would have been missed at LEP if the Higgs is between $85-100$ GeV, and the gauginos are less than half the Higgs mass. We will discuss the FermiLab constraints on this scenario in this paper, as well as constraints on like sign dilepton decays of the Higgs, which inevitably accompany the decays with neutrinos. We find that there are plausible models in which the branching ratios for like sign dileptons are small enough to evade the strong, model independent, bounds from FNAL.

Our purpose is to go beyond the work of [112] in two ways. First of all, we incorporate the L violating mechanism for hiding the Higgs into gauge mediated SUSY breaking models. Secondly, we also exploit the lepton number violating operators to generate the neutrino masses. The seesaw mechanism for generating neutrino masses, requires one to introduce a new mass scale, an order of magnitude or so below the unification scale $M_U \sim 2 \times 10^{16}$ GeV[1]. Renormalizable lepton number violating operators in SUSY can provide a natural alternative [114]. Our aim is to see whether this can be combined with gauge mediation and simultaneously hide the Higgs.

We will find that certain restrictions must be placed on the L violating operators in order to achieve all of these goals. Most of our considerations are quite general, but we will specialize to the Pentagon model [115] in order to investigate whether an appropriate discrete symmetry can be found, which automatically implies these restrictions. We will also assume, as in the Pentagon model, that we have a singlet chiral field S, with an SH_uH_d coupling. This changes the tree level prediction for the lightest Higgs, and allows us to have a Higgs obeying the model independent OPAL lower bound of 82 Gev for the Higgs mass, even when $\tan\beta \sim 1$. This is important, because we find that we need such a value of $\tan\beta$ in order for our model to predict a like sign dilepton signal compatible with the model independent bounds for the Tevatron. For $\tan\beta \sim 1$ it is natural for the lightest neutralino to decouple approximately from charged leptons. We will discuss this in detail below.

Our attitude toward the magnitude of the possible L violating operators is influenced by our knowledge of the Yukawa couplings in the standard model. Many of these are surprisingly small. Given the strong constraints on flavor changing neutral currents, we think that the most plausible explanation of Yukawa textures is the Froggatt-Nielsen mechanism [116] operating near the unification scale. It then seems clear that the flavor structure of L violating operators will be similarly constrained. Rather than trying to formulate a full high energy theory of these textures, we merely take away the lesson that dimensionless L violating couplings might be anomalously small, and that one of them might be much larger than all the others.

The MSSM also contains dimension two L violating operators, analogous to the μ term, with H_d replaced with a linear combination of L_i. Clearly, an explanation of the magnitude of the dimension two parameter is necessary to a complete low energy theory. We will adopt the philosophy of the NMSSM, in which this parameter is the vacuum expectation value (VEV) of a low energy singlet, and the bare dimension two couplings are forbidden by a discrete symmetry.

Other recent analyses of hard to find Higgs decays can be found in [117].

4.2 Constraints on $h^0 \to \chi^0\chi^0 : \chi^0 \to (\tau, \nu_\tau)jj$

We want to investigate the LEP bound on the Higgs mass in the MSSM where the lightest Higgs boson is produced by Higgs- strahlung of the Z boson (or maybe through Z or W-fusion

[1]It has been suggested that this scale arises naturally, as $M_{seesaw} = \frac{M_U^2}{m_P}$ [113].

processes). The cascade decay we are interested in consists of the decay of the lightest Higgs to two next-to-lightest SUSY particle (NLSP) neutralinos followed by an R-parity violating (RPV) decay of each neutralino to one third generation lepton plus two quarks. We do the computation in the narrow-width limit where the cascade is divided into a two-body decay and two three-body decays.

4.2.1 BR of the lightest Higgs to two neutralinos

The partial decay width $\Gamma(h^0 \to \chi_i^0 \chi_j^0)$ is given by

$$\Gamma(h^0 \to \chi_i^0 \chi_j^0) = \frac{\lambda^{1/2}(m_{h^0}^2, m_{\chi_i^0}^2, m_{\chi_j^0}^2)}{16\pi m_{h^0}^3 \times 2^{\delta_{ij}}} \Big(2|Y^{ij}|^2(m_{h^0}^2 - m_{\chi_i^0}^2 - m_{\chi_j^0}^2) \\ -2[(Y^{ij})^2 + (Y^{ij*})^2] m_{\chi_i^0} m_{\chi_j^0}\Big) \tag{4.1}$$

where

$$\lambda(x,y,z) = x^2 + y^2 + z^2 - 2xy - 2xz - 2yz \tag{4.2}$$

$$Y^{ij} = \frac{1}{2}(-N_{i3}^* \sin\alpha - N_{i4}^* \cos\alpha)(gN_{j2}^* - g'N_{j1}^*) + \{i \leftrightarrow j\}. \tag{4.3}$$

Here N diagonalizes the neutralino mass matrix M_{χ^0} which can be written at tree level as

$$M_{\chi^0} = \begin{pmatrix} M_1 & 0 & -g'v_d/\sqrt{2} & g'v_u/\sqrt{2} \\ 0 & M_2 & gv_d/\sqrt{2} & -gv_u/\sqrt{2} \\ -g'v_d/\sqrt{2} & gv_d/\sqrt{2} & 0 & -\mu \\ g'v_u/\sqrt{2} & -gv_u/\sqrt{2} & -\mu & 0 \end{pmatrix} \tag{4.4}$$

where $N^* M_{\chi^0} N^{-1} = \mathrm{diag}(m_{\chi_1^0}, m_{\chi_2^0}, m_{\chi_3^0}, m_{\chi_4^0})$ with $|m_{\chi_1^0}| < |m_{\chi_2^0}| < |m_{\chi_3^0}| < |m_{\chi_4^0}|$.

The total decay width is expected to be dominated by decays of the lightest Higgs to neutralinos (when kinematically allowed), thus the branching ratio can be approximated as

$$\mathrm{BR}(h^0 \to \chi_i^0 \chi_j^0) = \frac{\Gamma(h^0 \to \chi_i^0 \chi_j^0)}{\Gamma(h^0 \to \mathrm{all})} \sim \frac{\Gamma(h^0 \to \chi_i^0 \chi_j^0)}{\Gamma(h^0 \to \mathrm{SM}) + \Gamma(h^0 \to \mathrm{neutralinos})}. \tag{4.5}$$

4.2.2 BR of the neutralino to one lepton plus two quarks

The decay of the neutralino to one lepton plus two quarks occurs through the R-parity violating vertex $\lambda'_{ijk}\epsilon_{ab}L_i^a Q_j^b \bar{D}_k \subset \mathcal{W}$. Since squarks are assumed much heavier than sleptons, decays with off-shell squarks are sub-dominant contributions to the partial decay widths. Moreover, assuming there is no mixing in the sfermion sector $\tilde{f}_L$ and $\tilde{f}_R$ are mass eigenstates. This reduces the number of Feynman diagrams since only left-handed sleptons and sneutrinos are relevant to the R-parity violating vertex $\lambda'_{ijk}\epsilon_{ab}L_i^a Q_j^b \bar{D}_k$. Thus only decays with off-shell $\tilde{\ell}_{Li}$ or $\tilde{\nu}_i$ are possible. Finally, since the kinematically allowed final state standard model fermions (for a NSLP neutralino with mass $m_{\chi_1^0} \sim 30$ GeV only the top quark is excluded as a final state fermion) are much lighter than any sparticles, one can compute the partial decay widths in the limit of vanishing fermion masses. This introduces a maximal error of the order $\mathcal{O}\left(\frac{m_b}{m_{\chi_1^0}}\right) \sim 0.13$ for a NLSP neutralino with mass $m_{\chi_1^0} \sim 30$ GeV. With these assumptions, the partial decay width computations simplify greatly and one can get analytical results.

Thus, with these assumptions, the partial decay widths $\Gamma(\chi_l^0 \to \ell_i u_j \bar{d}_k) = \Gamma(\chi_l^0 \to \bar{\ell}_i \bar{u}_j d_k)$ and $\Gamma(\chi_l^0 \to \nu_i d_j \bar{d}_k) = \Gamma(\chi_l^0 \to \bar{\nu}_i \bar{d}_j d_k)$ are

$$\Gamma(\chi_l^0 \to \ell_i u_j \bar{d}_k) = \frac{N_c m_{\chi_l^0}(|c_1|^2 + |c_2|^2)}{1024\pi^3}\left[6\rho - 5 + 2(\rho-1)(3\rho-1)\ln\left(\frac{\rho-1}{\rho}\right)\right] \tag{4.6}$$

$$\Gamma(\chi_l^0 \to \nu_i d_j \bar{d}_k) = \frac{N_c m_{\chi_l^0}|c_1|^2}{1024\pi^3}\left[6\rho - 5 + 2(\rho-1)(3\rho-1)\ln\left(\frac{\rho-1}{\rho}\right)\right] \tag{4.7}$$

where

$$c_1 = \sqrt{2}\lambda'_{ijk}(gT_3^{f_i}N_{l2}^* + g'Y_{f_i}^H N_{l1}^*) \tag{4.8}$$

$$c_2 = \lambda'_{ijk}\frac{m_{\ell_i}}{v_d}N_{l3} \tag{4.9}$$

$$\rho = \left(\frac{m_{\tilde{f}_i}}{m_{\chi_l^0}}\right)^2. \tag{4.10}$$

Here $N_c = 3$ is the number of colors and Martin's notation is used for the hypercharge, i.e. $Q = T_3 + Y^H$ [118]. Moreover, the first term in c_1 represents the fermion/sfermion coupling to the wino, the second term in c_1 represents the fermion/sfermion coupling to the bino and c_2 represents the fermion/sfermion coupling to the higgsino. The following table reviews the needed hypercharges,

particle	Y^H	T_3	Q
ℓ	$-\frac{1}{2}$	$-\frac{1}{2}$	-1
ν	$-\frac{1}{2}$	$\frac{1}{2}$	0

(4.11)

Since the dominant decay of the lightest Higgs is expected to be $h^0 \to \chi_1^0\chi_1^0$, the NLSP neutralino decay is the one of interest. The total decay width for the NLSP neutralino is dominated by the kinematically allowed R-parity violating vertex processes discussed above,

$$\Gamma(\chi_1^0 \to \text{all}) \sim \sum_{i,j,k}\left[\Gamma(\chi_1^0 \to \ell_i u_j \bar{d}_k) + \Gamma(\chi_1^0 \to \nu_i d_j \bar{d}_k) + \text{antiparticles}\right] \tag{4.12}$$

$$= 2\sum_{i,j,k}\left[\Gamma(\chi_1^0 \to \ell_i u_j \bar{d}_k) + \Gamma(\chi_1^0 \to \nu_i d_j \bar{d}_k)\right] \tag{4.13}$$

where the sums over u_j is limited to $j = \{1, 2\}$ since the top quark is not kinematically allowed.

Thus the relevant branching ratios are

$$\mathrm{BR}(\chi_1^0 \to \ell_i u_j \bar{d}_k) = \frac{\Gamma(\chi_l^0 \to \ell_i u_j \bar{d}_k)}{\Gamma(\chi_1^0 \to \text{all})} \tag{4.14}$$

$$\mathrm{BR}(\chi_1^0 \to \nu_i d_j \bar{d}_k) = \frac{\Gamma(\chi_l^0 \to \nu_i d_j \bar{d}_k)}{\Gamma(\chi_1^0 \to \text{all})} \tag{4.15}$$

with the same results for final state antiparticles. Notice that the neutralino decay to the gravitino (mass $m_{3/2}$),

$$\Gamma(\chi_1^0 \to X\tilde{G}) = \frac{m_{\chi_1^0}^5}{48\pi m_P^2 m_{3/2}^2}\left(1 - \frac{m_X^2}{m_{\chi_1^0}^2}\right)^4, \tag{4.16}$$

is sub-dominant in our direct gauge mediation model. This will be quantified in the next section.

4.2.3 Total branching ratio in the regime $\tan\beta \sim 1$: Numerical example

The total branching ratio for one particular final state in the cascade decay of interest is simply the product of the appropriate branching ratios (in the narrow-width limit). For example, for the cascade decay $h^0 \to \chi_1^0\chi_1^0 \to \ell_{i_1} u_{j_1} \bar{d}_{k_1} \ell_{i_2} u_{j_2} \bar{d}_{k_2}$ the total branching ratio is

$$\mathrm{BR}(h^0 \to \ell_{i_1} u_{j_1} \bar{d}_{k_1} \ell_{i_2} u_{j_2} \bar{d}_{k_2}) = \mathrm{BR}(h^0 \to \chi_1^0\chi_1^0)\mathrm{BR}(\chi_1^0 \to \ell_{i_1} u_{j_1} \bar{d}_{k_1})\mathrm{BR}(\chi_1^0 \to \ell_{i_2} u_{j_2} \bar{d}_{k_2}). \tag{4.17}$$

Our interest lies in decays with final state tau leptons and tau neutrinos since these processes have not been studied extensively at LEP. We will evaluate these branching ratios in the limit $\tan\beta \sim 1$, as is predicted in the Pentagon model. We do this here because it turns out that in this regime, the like sign dilepton contribution to Higgs decay is naturally suppressed. The FNAL bounds on this process will be more difficult to satisfy for larger values of $\tan\beta$.

Following [111] we want the lightest neutralino χ_1^0 to be mostly bino. This can be achieved with $M_1 = 50$ GeV, $M_2 = 250$ GeV and $\mu = +150$ GeV which lead to the following masses

particle	χ_1^0	χ_2^0	χ_3^0	χ_4^0	$\chi_1^\pm$	$\chi_2^\pm$
mass (in GeV)	30	125	150	300	105	295

(4.18)

and mixing matrix

$$N = \begin{pmatrix} -0.89 & 0.15 & -0.30 & 0.30 \\ -0.44 & -0.48 & 0.54 & -0.54 \\ 0 & 0 & 0.71 & 0.71 \\ -0.09 & 0.86 & 0.35 & -0.35 \end{pmatrix}. \tag{4.19}$$

Close to the Higgs decoupling limit this leads to $\mathrm{BR}(h^0 \to \chi_1^0\chi_1^0) \sim 0.9$ for m_{h^0} between $85-100$ GeV. Figure 4.1 shows the branching ratios $\mathrm{BR}(h^0 \to \chi_1^0\chi_1^0)$ and $\mathrm{BR}(h^0 \to b\bar{b})$ as a function of the Higgs mass for a mixing angle $\alpha = -\frac{\pi}{8}$. Here, since $\tan\beta = 1$, we go slightly away from the Higgs decoupling limit in order to satisfy the experimental bound on $\xi^2 \mathrm{BR}(h^0 \to b\bar{b})$ with $\xi = \sin(\beta - \alpha)$ for m_h as low as 85 GeV [107].

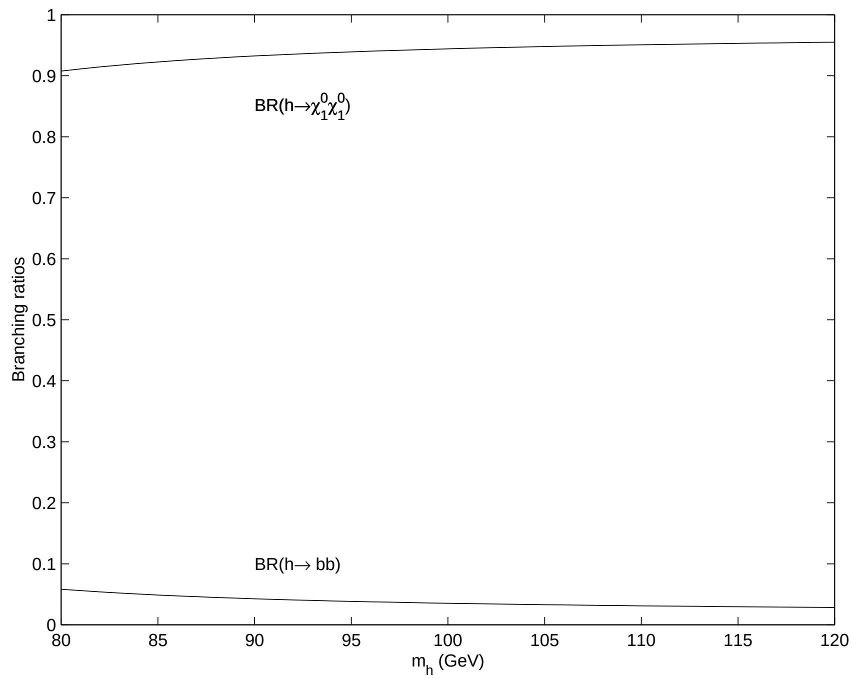

Figure 4.1: Branching ratio of $h^0 \to \chi_1^0\chi_1^0$ (upper line) and $h^0 \to b\bar{b}$ (lower line) as a function of the Higgs mass (in GeV) for $M_1 = 50$ GeV, $M_2 = 250$ GeV, $\mu = +150$ GeV, $\tan\beta = 1$ and $\alpha = -\frac{\pi}{8}$.

Using PDG bounds [119] on the masses of the sleptons, appropriate values for the masses of the sneutrinos[2]

$$\begin{array}{r|ccc|ccc} \text{particle} & \tilde{\ell}_1 = \tilde{e} & \tilde{\ell}_2 = \tilde{\mu} & \tilde{\ell}_3 = \tilde{\tau} & \tilde{\nu}_1 = \tilde{\nu}_e & \tilde{\nu}_2 = \tilde{\nu}_\mu & \tilde{\nu}_3 = \tilde{\nu}_\tau \\ m \text{ (in GeV)} & 73 & 94 & 81.9 & 75 & 75 & 75 \end{array} \tag{4.20}$$

and for the R-parity violating coupling [114]

$$\lambda'_{ijk} = 0 \;\forall\, i = \{1,2\},\; j,k = \{1,2,3\} \tag{4.21}$$

$$(\lambda'_{3jk}) = \begin{pmatrix} 0.001 & 0.001 & 0 \\ 0.001 & 0.001 & 0 \\ 0 & 0 & 0 \end{pmatrix} \tag{4.22}$$

one obtains $\mathrm{BR}(\chi_1^0 \to \tau u_j \bar{d}_k) = 0.019 \;\forall\, j,k = \{1,2\}$, $\mathrm{BR}(\chi_1^0 \to \nu_\tau d_j \bar{d}_k) = 0.11 \;\forall\, j,k = \{1,2\}$ and zero otherwise. The difference between the branching ratios comes from the mixing matrix

[2]For $\tan\beta = 1$, theory forces the sneutrinos to be almost degenerate with the sleptons. However from the non-SM invisible width of the Z-boson sneutrinos could be as light as 45 GeV.

N and the quantum numbers T_3 and Y^H. Indeed, since the sneutrino is almost degenerate with the stau one can forget about the ρ-dependent part of the decay width and focus on the c_1-bino and wino contributions to the decay width. The c_1-bino contributions to the branching ratio for τ and ν_τ are the same *but* the c_1-wino contributions to the branching ratio for τ and ν_τ have opposite sign due to the weak isospin charges. From the mixing matrix one can see that the contributions partly cancel for τ and add up for ν_τ. Though smaller, the c_1-wino contributions are about a third of the c_1-bino contributions which leads to a suppression

$$\frac{\mathrm{BR}(\chi_1^0 \to \tau u_j \bar{d}_k)}{\mathrm{BR}(\chi_1^0 \to \nu_\tau d_j \bar{d}_k)} \sim \frac{|c_{1,\tau}|^2}{|c_{1,\nu_\tau}|^2} \sim \frac{(-1+3)^2}{(1+3)^2} \sim \frac{1}{4}. \tag{4.23}$$

This kind of suppression is generic in the region of the parameter space where the lightest neutralino is light and mostly bino and the lightest chargino satisfies the lower bound on its mass since the mixing matrix does not change by much.

Notice also that the c_2-higgsino contribution to the charged lepton decay width is small due to the lepton mass suppression factor in the limit $\tan\beta \sim 1$ and can thus be neglected. This leads to an even bigger decoupling of the neutralinos to the charged leptons and more easily evades the FNAL bounds.

As shown before the branching ratios for antiparticles in the final state are the same. Thus the total branching ratios for the following cascade decays are

$$\mathrm{BR}(h^0 \to \tau\tau + 4\text{ jets}) \sim 0.0055 \tag{4.24}$$

$$\mathrm{BR}(h^0 \to \tau\nu_\tau + 4\text{ jets}) \sim 0.03 \tag{4.25}$$

$$\mathrm{BR}(h^0 \to \nu_\tau\nu_\tau + 4\text{ jets}) \sim 0.17 \tag{4.26}$$

with $m_{h^0} \sim 90$ GeV and $\alpha = -\frac{\pi}{8}$. Here any group of particles associated to the neutralino decay products can be changed to its antiparticle counterpart without changing the branching ratios. Thus one obtains like sign ditau (or di-antitau) events with the same branching ratio then tau-antitau events. The total decay width of the Higgs and the NLSP neutralino are

$$\Gamma(h^0 \to \text{all}) \quad \sim \quad 0.02 \text{ GeV} \tag{4.27}$$

$$\Gamma(\chi_1^0 \to \text{all}) \quad \sim \quad 0.11 \cdot 10^{-10} \text{ GeV} \tag{4.28}$$

and this may lead to displaced vertices since $c\tau_{\chi_1^0 \to \text{all}} \sim 19\ \mu$m.

As mentioned previously, the neutralino to gravitino decay is sub-dominant, even for small R-parity violating couplings. Indeed the decay widths ratio is parametrically

$$\frac{\Gamma(\chi_1^0 \to \gamma\tilde{G})}{\Gamma(\chi_1^0 \to (\tau,\nu_\tau)jj)} \sim \frac{64\pi^2 m_{\chi_1^0}^4 |N_{11}|^2}{3N_c m_P^2 m_{3/2}^2 (g\lambda')^2} \left[6\rho - 5 + 2(\rho-1)(3\rho-1)\ln\left(\frac{\rho-1}{\rho}\right)\right]^{-1}. \tag{4.29}$$

This is of order 10^{-2} and leads to a neutralino to gravitino branching ratio of order 10^{-3} and thus can be safely neglected. Here the decay product is mostly photon and the gravitino mass is assumed to be $m_{3/2} \sim 1$ eV. Cosmological constraints on light gravitinos restrict their mass to be $< 10-20$ eV. Within the Pentagon model, the additional hypothesis of Cosmological SUSY Breaking gives $m_{3/2} \sim \Lambda^{1/4} \sim 10^{-3}$ eV. For such super-light gravitinos, the gravitino decay channel of the gaugino, which is ruled out experimentally for light gauginos, would dominate, and our scenario would not be viable.

4.2.4 $\tan\beta \sim 1$ and the little hierarchy problem

The reader familiar with the supersymmetric standard model may be a bit confused at this point. We have invoked R-parity violating couplings to weaken the experimental bound on the Higgs mass, in order to avoid the little hierarchy problem. However, our discussion of like sign dilepton constraints used the Pentagon model relation $\tan\beta \sim 1$ to motivate the decoupling of light neutralinos from charged leptons. In the MSSM, the lightest Higgs mass vanishes at tree level when $\tan\beta = 1$. Fortunately, our model is not even approximately the MSSM. If we compute the Higgs sector potential neglecting Pentagon model corrections to the Kahler potential of S (which is plausible if g_S is small), we find the potential for the scalar components of neutral chiral superfields

$$V = \frac{g_1^2 + g_2^2}{8}(|H_u|^2 - |H_d|^2)^2 + |g_\mu S|^2(|H_u|^2 + |H_d|^2) + |k g_S \Lambda_5^2 + g_\mu H_u H_d + g_T S^2|^2, \quad (4.30)$$

where k is a strong Pentagon interaction correction, of order 1. This potential has a hypercharge Goldstone boson if the Higgs fields have nonzero VEVs, but all the other scalars are massive, with mass determined by a combination of the couplings and the large scale $\Lambda_5 \sim 1$ TeV. To obtain Higgs VEVs of the right order of magnitude, we must take g_S small, but the other Yukawa couplings are bounded only by perturbative unification[3]. The latter constraint probably does not allow one to make the Higgs mass large enough to evade the conventional bounds, but there is no problem in evading the model independent bounds of ~ 82 GeV on the Higgs mass. R-parity violating Higgs decays then make the conventional bound irrelevant.

4.2.5 Gaugino mass relationships and the chargino mass bound

There is a strict lower mass bound of 102.7 GeV set on charginos that decay through RPV operators. We note that if we assume the minimal gauge mediated prediction for the gaugino

[3] In fact, the Pentagon model, or any other model with 5 messengers, and a TeV scale threshold, has problems with perturbative unification, irrespective of the size of these Yukawas.

mass ratio, a chargino of 102.7 GeV would make it impossible to have neutralinos less than 50 GeV. In order to allow neutralinos of less than half the Higgs mass and satisfy the chargino mass bound, we must alter the minimal gauge mediation predictions for gaugino masses. We present here a simple method proposed by [120] of adding to the hidden sector multiple scalar fields which get supersymmetric and non-supersymmetric masses, and coupling them with different strengths to parts of a single 10 and $\overline{10}$ of messengers. The superpotential is thus

$$W = r_i X_i u\overline{u} + \gamma_i X_i q\overline{q} + \lambda_i X_i l\overline{l} \tag{4.31}$$

for

$$X_i = x_i + \theta^2 F_i \tag{4.32}$$

The resulting gaugino eigenstates are determined by three mass parameters instead of a single mass parameter in the minimal case. The parameters are,

$$\Lambda_l = \frac{\lambda_i F_i}{\lambda_i x_i}, \quad \Lambda_q = \frac{\gamma_i F_i}{\gamma_i x_i}, \quad \Lambda_u = \frac{r_i F_i}{r_i x_i} \tag{4.33}$$

and the resulting gaugino mass parameters are

$$M_1 = \frac{1}{2}\frac{\alpha_1}{4\pi}\left(\frac{4}{3}\Lambda_q + 2\Lambda_l + \frac{8}{3}\Lambda_u\right), \quad M_2 = \frac{3}{2}\frac{\alpha_2}{4\pi}\Lambda_q, \quad M_3 = \frac{1}{2}\frac{\alpha_3}{4\pi}(\Lambda_u + 2\Lambda_q) \tag{4.34}$$

Here we have changed the ordinary gaugino mass ratio with minimal extra structure and it is easy to get a M_1 much lighter than M_2.

We note also that within the Pentagon model, we do not expect minimal gauge mediation predictions for gaugino masses to be valid.

4.3 Bounds on jets + $\not{E}_T$

We will now assess the effects of current Tevatron and LEP searches on the viability of our Higgs decays. In particular there are five searches with relevant final states: Tevatron's inclusive search with like sign dilepton events, Tevatron's measurement of the ditop cross-section, LEP's search for cascade decays of the Higgs, LEP's Higgs to WW^* search and direct searches for neutralinos with R-parity violation.

4.3.1 Like sign dileptons

The Tevatron inclusive search for new physics with like sign dilepton events [121] is a strong model independent bound that must be evaded. The CDF collaboration looked at a data sample

Decay channel	Experiment	Bound	Search
–	Tevatron	< 10 events for 1 fb^{-1}	$p\overline{p}$ collisions
$bbqq+ \not{E}_T$	Tevatron	$\sigma < 3$ pb	$t\bar{t}$ production cross-section
$bbbb+ \not{E}_T$	LEP	$m_{h^0} < 84.5$ GeV (worst case)	ZH_2H_2 cascade decay
$q\overline{q}'q\overline{q}'+ \not{E}_T$	LEP	$m_{h^0} > 105$ GeV	WW^* with invisible Z decay
–	LEP	$\sigma < 1$ pb	direct neutralino search

Table 4.1: Higgs mass and production cross-section bounds for various searches.

of 1 fb^{-1} and observed no significant excess in an inclusive selection or in a SUSY-optimized selection. The SUSY-optimized selection requires large missing transverse energy and is thus irrelevant in our model since we get like sign dilepton events without missing transverse energy. The expected number of events in the inclusive selection is 33.2 ± 4.7 while the observed number of events is 44. Our model could explain this slight excess. Indeed, light Higgs production cross-section at the Tevatron is around 1 pb which would lead to an extra number of like sign dilepton events of about 10 (without taking into account any cuts). However, one must remember that the Tevatron search focused on first and second generation leptons while our like sign dilepton events are ditau events which are more subtle to study.

4.3.2 Tevatron $t\bar{t}$ search

The Tevatron $t\bar{t}$ [122] search in principle looks very similar to our signal; it places limits on the $t\bar{t}$ production cross-section by looking for multi-jet events with two b quarks in the final state and with missing energy, which is not found in the b quark direction. There are several reasons to expect this search to be insensitive to our decay. First, since the Higgs is produced close to threshold at the Tevatron, the decay products are all relatively soft. The most missing energy we expect is from final states with two neutrinos of about 15 GeV. Since the decay products are isotropically distributed, it is unlikely that the two neutrinos will be found in the same hemisphere, and the total missing energy vector will not be large enough to pass missing energy cuts in this search. However, the most important remark is that the Higgs production cross-section in the regime of interest is a few picobarns [123]. The same can be said for the direct neutralino production cross-section. The two sigma error bars for the $t\bar{t}$ production cross-section at Tevatron are about 3 pb. Thus, the jet plus missing energy events found by Tevatron, are all consistent with coming from top and cannot put strong bounds on $LQ\bar{D}$ couplings, even if a significant number of events were to pass the missing energy cut. Finally, there is a question about how many b quarks are in the final state. The Fermilab search insisted on two b tagged jets as one of their primary cuts. Since the flavor structure of the $LQ\bar{D}$ couplings is undetermined, we could easily construct models, which further suppressed b jets. Thus gaugino decays through lepton number violation could have easily escaped detection. However, since the missing energy threshold is small, if there are too many tagged b's in the event it will be discarded as QCD background. Therefore events with four b's in the final state are less likely to be picked up by this search.

4.3.3 Higgs cascade decays

LEP conducted three searches which have bearing on these decays. One is the cascade decay $e^+e^- \rightarrow H_2Z \rightarrow H_1H_1Z$. In the case of invisible Z decay and $H_1 \rightarrow b\bar{b}$ there is a four jet plus missing energy signal. This search only applies to final states with a maximum number of b quarks. Details may be found in [111]. This channel, as detailed in figure 12, puts a bound on the Higgs mass of less than 85 GeV. Reconstruction of the missing Z may further reduce the sensitivity of this search down to OPAL's inclusive limit, which is 82 GeV [126]. LEP also conducted a search in the channel $hZ \rightarrow WW^*Z$ where the Z decays invisibly and the W's decay to qq' [127]. This search is not applicable to final states where all four quarks are the same flavor, or to final states where the quarks are all up type or down type. For example, this search is insensitive to our 4b plus missing energy final state. When the search is applicable to our final states, it can only put a bound of 105 GeV on the Higgs mass. We detail the Higgs mass limits and production cross-section limits in the table above.

Having convinced ourselves that current searches do not rule out our scenario, we note that the kinematics of the gaugino decays are sufficiently different from the top decays, and that one could imagine finding them in a dedicated search. One could attempt a search without b tagging, but simple searches for jets plus significant missing energy are very difficult. In the standard 4b search the Higgs, which decays to $b\bar{b}$, is produced in association with one or two b quarks [125]. This search required at least 3 b-tags, but overall it was not very sensitive since it was sensitive to the 3b background. The best chance might be to assume that the Higgs decays have the maximal number of b's in the final state, and to modify the Tevatron 4b Higgs search to be sensitive to missing energy [124]. One may imagine a similar search which requires multiple b tags and a missing energy cut. This scenario faces the same problem that we detailed in the ditop measurement above, the smallness of the missing energy vector. The missing energy at the Tevatron must be more than what we would expect from semi-leptonic b decay, and more than what would result from the mis-measurement of a 4 b event with no missing energy. Passing these cuts with low energy neutrinos is a problem. Searches at LHC seem to be even more problematic, but we note that Kaplan and Rehermann have proposed searching for Higgs decays through neutralino LSP's into multi jet final states using the LHCb experiment [128]. LHCb catches events highly boosted in the forward direction, has maximal b acceptance, and has a p_T trigger which can be as low as 2 GeV. As in the B violating 6 jet decays of the Higgs [111], it may be possible to search for lepton number violating decays of the gaugino at LHCb, with missing energy and multiple b tags.

4.3.4 Direct searches for neutralinos

Direct searches for neutralinos with R-parity violation [129] put bounds on the neutralino cross-section for direct three body decays. Since our model leads to a new production mechanism for neutralinos, it is natural to investigate these bounds. The Higgs boson production cross-section and the neutralino pair production cross-section at an e^+e^- collider are around 300 fb each [130]. Since the direct searches for neutralinos with R-parity violation give an upper bound of about 2 pb for the neutralino pair production cross-section, our model escapes direct neutralino search bounds easily.

4.4 Neutrino masses

The lepton number violating operators, which we have invoked to hide the decays of a light Higgs boson, might also be the source of neutrino masses. There is a large literature (see [131] and references therein) on the use of renormalizable L violating terms in the MSSM to generate neutrino masses. Indeed, some of the strongest constraints on the L violating couplings we have used come from the requirement that the neutrino masses they generate not be too large. For instance, the numerical example of section 4.2.3 leads to a $\lambda'\lambda'$ loop neutrino mass of about $1.5 \cdot 10^{-3}$ eV for squark of about 250 GeV [131]. Obviously one needs a more involved flavor structure to generate all neutrino masses since only the third generation neutrino mass is generated in our model.

A survey of the literature indicates that bilinear L violating terms of the form $L_i H_u$ are the dominant source of neutrino masses in a generic model. However, to be consistent one should require that all B and L violating terms which could lead to unobserved processes are forbidden by a symmetry. We do not know how to make a general analysis of such symmetries without committing ourselves to a specific model. Thus we will restrict our attention to the Pentagon model [115], though we expect that a similar analysis could be done for any specific model of gauge mediation. We will find, that within the context of the Pentagon model, the symmetries we utilize will forbid terms of the form L_iH_u but allow L_iH_uS (where S is the singlet of the Pentagon). If S has a vacuum expectation value (VEV), this will generate a tree level mass for one neutrino. The dominant contribution to the other two neutrino masses comes from loop corrections involving the $LQ\bar{D}$ couplings that hide the Higgs decay. There is thus a potential understanding of a $2-1$ hierarchy among the three neutrino masses, as seems to be indicated by experiment. However, we emphasize that both the magnitude of the L_iH_uS term, and the $LQ\bar{D}$ couplings is determined by high energy physics beyond the range of the present analysis. Therefore, a proper understanding of the structure of the neutrino mass matrix really requires unification scale physics.

The original Pentagon model was designed to eliminate all baryon and lepton number violating operators of dimension ≤ 5, except for the neutrino seesaw term. This led to a $\mathbb{Z}_4$ R symmetry with two possible generation independent charge assignments. In order to admit renormalizable lepton number violating terms we must change the symmetry and the charge assignments. We will assume an R symmetry group $\mathbb{Z}_N$. Therefore in the following all equations are understood modulo N and the R-charge of a given field is denoted by the name of the field itself.

4.4.1 Independent R-charges

The aim of this subsection is to express the R-charges of all the fields of the Pentagon in terms of the R-charges of a minimal set of fields. The appropriate restricted set is somewhat arbitrary but a rather convenient one comes naturally from the model. First, the crucial $SP\tilde{P}$ and SH_uH_d terms lead to

$$SP\tilde{P} \quad \Rightarrow \quad P + \tilde{P} = 2 - S \tag{4.35}$$

$$SH_uH_d \quad \Rightarrow \quad H_u = 2 - S - H_d. \tag{4.36}$$

The important Yukawa couplings give

$$LH_d\bar{E} \quad \Rightarrow \quad \bar{E} = 2 - L - H_d \tag{4.37}$$

$$QH_u\bar{U} \quad \Rightarrow \quad \bar{U} = 2 - Q - H_u \tag{4.38}$$

$$QH_d\bar{D} \quad \Rightarrow \quad \bar{D} = 2 - Q - H_d. \tag{4.39}$$

Thus one can rewrite everything as a function of the restricted set $\{S, L, Q, H_d\}$ as

$$P + \tilde{P} = 2 - S \tag{4.40}$$

$$H_u = 2 - S - H_d \tag{4.41}$$

$$\bar{E} = 2 - L - H_d \tag{4.42}$$

$$\bar{U} = S - Q + H_d \tag{4.43}$$

$$\bar{D} = 2 - Q - H_d. \tag{4.44}$$

This set is dubbed extended since anomaly conditions will generate relations between the four different R-charges of the set.

Anomaly conditions

The anomaly conditions of the Pentagon model are

$$SU(5)_P \Rightarrow 5(P + \tilde{P}) = 0 \tag{4.45}$$

$$SU(3)_C \Rightarrow 6Q + 3(\bar{U} + \bar{D}) + 5(P + \tilde{P}) = 0 \tag{4.46}$$

$$SU(2)_L \Rightarrow H_u + H_d + 9Q + 3L + 5(P + \tilde{P}) = 0. \tag{4.47}$$

Using the relations obtained from the restricted set $\{S, L, Q, H_d\}$ of independent R-charges these can be rewritten as

$$SU(5)_P \Rightarrow 5(S - 2) = 0 \tag{4.48}$$

$$SU(3)_C \Rightarrow 3(S + 2) = 0 \tag{4.49}$$

$$SU(2)_L \Rightarrow 2 - S + 9Q + 3L = 0. \tag{4.50}$$

The last anomaly condition leads to an unextended restricted set of independent R-charges by removing one R-charge in the extended restricted set. Due to the modulo N form of the equations the easiest one to remove is S but it is more convenient to keep everything written in function of the extended restricted set $\{S, L, Q, H_d\}$. Indeed one can easily solve the anomaly conditions as a function of S. Thus it is more practical to eliminate Q instead as shown later. The first two anomaly conditions can be combined as

$$0 = 5(S - 2) = 3(S + 2) + 2(S - 8) = 2(S - 8). \tag{4.51}$$

For $N = 2n + 1$ one has $S = 8$ and the first two anomaly conditions force $N|30$ thus $N = \{3, 5, 15\}$. For $N = 2n$ one has $S = 8$ or $S = 8 - n$. For the case $S = 8$ the first two anomaly conditions force $N|30$ thus $N = \{2, 6, 10, 30\}$. For the case $S = 8 - n$ the first two anomaly conditions lead to

$$N \quad | \quad (30 - 5n) \tag{4.52}$$

$$N \quad | \quad (30 - 3n) \tag{4.53}$$

thus $N = \{4, 12, 20, 60\}$.

4.4.2 Superpotential terms and RPV terms

Using the extended restricted set the possible S^3 superpotential term gives

$$S^3 \Rightarrow 3S - 2 \tag{4.54}$$

where the RHS has to be zero modulo N if and only if the term is allowed. For the RPV terms, the trilinear lepton number violating (TLNV) terms (including the useful SLH_u) give

$$LL\bar{E} \quad \Rightarrow \quad 2L + (2 - L - H_d) - 2 = L - H_d \tag{4.55}$$

$$LQ\bar{D} \quad \Rightarrow \quad L + Q + (2 - Q - H_d) - 2 = L - H_d \tag{4.56}$$

$$SLH_u \quad \Rightarrow \quad S + L + (2 - S - H_d) - 2 = L - H_d. \tag{4.57}$$

and the bilinear lepton number violating (BLNV) term LH_u leads to

$$LH_u \Rightarrow L + (2 - S - H_d) - 2 = L - H_d - S. \tag{4.58}$$

Finally the trilinear baryon number violating (TBNV) term gives

$$\bar{U}\bar{D}\bar{D} \Rightarrow (S - Q + H_d) + 2(2 - Q - H_d) - 2 = S - 3Q - H_d + 2. \tag{4.59}$$

The no-go theorem here states that one cannot allow only specific TLNV terms since all TLNV terms are allowed when any one is allowed.

4.4.3 Dimension five baryon number violating operators

Dimension five baryon number violating (D5BNV) operators and D-terms lead to

$$\begin{aligned}
QQQL &\Rightarrow 3Q + L - 2 && (4.60)\\
QQQH_d &\Rightarrow 3Q + H_d - 2 && (4.61)\\
\bar{U}\bar{U}\bar{D}\bar{E} &\Rightarrow 2(S - Q + H_d) + (2 - Q - H_d) + (2 - L - H_d) - 2 &&\\
&= 2S - 3Q - L + 2 && (4.62)\\
\text{D-term} &\Rightarrow Q + \bar{U} - L = Q + (S - Q + H_d) - L = S - L + H_d && (4.63)\\
\text{D-term} &\Rightarrow \bar{U} + \bar{E} - \bar{D} = (S - Q + H_d) + (2 - L - H_d) - (2 - Q - H_d) &&\\
&= S - L + H_d && (4.64)
\end{aligned}$$

where the last two equations come from D-terms.

4.4.4 Overall solutions

From the last two sections one can group together terms that lead to the same equation as a function of the R-charges of the extended restricted set. One has seven different sets labeled G_1 to G_7,

$$\begin{aligned}
G_1 = \{S^3\} &\Rightarrow 3S - 2 && (4.65)\\
G_2 = \{LL\bar{E}, LQ\bar{D}, SLH_u\} &\Rightarrow L - H_d && (4.66)\\
G_3 = \{LH_u, \text{D-terms}\} &\Rightarrow L - H_d - S && (4.67)\\
G_4 = \{\bar{U}\bar{D}\bar{D}\} &\Rightarrow S - 3Q - H_d + 2 && (4.68)\\
G_5 = \{QQQL\} &\Rightarrow 3Q + L - 2 && (4.69)\\
G_6 = \{QQQH_d\} &\Rightarrow 3Q + H_d - 2 && (4.70)\\
G_7 = \{\bar{U}\bar{U}\bar{D}\bar{E}\} &\Rightarrow 2S - 3Q - L + 2 && (4.71)
\end{aligned}$$

where group G_2 consists of all TLNV terms exclusively, group G_4 of the TBNV term and groups G_5 to G_7 of D5BNV terms. Using these sets and the extra $SU(2)_L$ anomaly relation $2 - S + 9Q + 3L$ to eliminate Q the solutions are given in table 4.2 where the TLNV set $G_2 \Rightarrow L - H_d$ does not simplify. Notice that no extra relation comes from the $SU(2)_L$ anomaly condition for $N = 3$. The removal of Q from the extended restricted set is more subtle for the cases $N = \{15, 20, 30, 60\}$. For $N = 15$ one has $9Q + 3L = 15k + 6 \Rightarrow 3Q + L = 5k + 2$ $(k \in \mathbb{Z})$ thus $3Q = \{2 - L, 7 - L, 12 - L\}$. For $N = 20$ one has $9Q + 3L = 20k' + 16 \Rightarrow$ $3Q + L = \frac{1}{3}(20k' + 16) = 20k + 12$ with $k' = 3k + 1$ $(k \in \mathbb{Z})$ thus $3Q = 12 - L$. For $N = 30$

N	S	$SU(2)_L$	G_1	G_3	G_4	G_5	G_6	G_7
2	0	$Q = L$	0	$L - H_d$	$L - H_d$	0	$L - H_d$	0
3	2	none	1	$L - H_d - 2$	$1 - H_d$	$L - 2$	$H_d - 2$	$-L$
4	2	$Q = L$	0	$L - H_d - 2$	$L - H_d$	2	$-(L - H_d - 2)$	2
5	3	$Q = 3L - 1$	2	$L - H_d - 3$	$L - H_d - 2$	0	$-(L - H_d)$	1
6	2	$3Q = 3L$	4	$L - H_d - 2$	$3L - H_d - 2$	$-2(L + 1)$	$3L + H_d - 2$	$2L$
10	8	$Q = 3L + 4$	2	$L - H_d - 8$	$L - H_d - 2$	0	$-(L - H_d)$	6
12	2	$3Q = 3L$	4	$L - H_d - 2$	$4 - 3L - H_d$	$4L - 2$	$3L + H_d - 2$	$-4L + 6$
15	8	$9Q = 6 - 3L$	7	$L - H_d - 8$	$10 - 3Q - H_d$	$3Q + L - 2$	$3Q + H_d - 2$	$-3Q - L + 3$
	8	$3Q = 2 - L$	7	$L - H_d - 8$	$L - H_d + 8$	0	$-(L - H_d)$	1
	8	$3Q = 7 - L$	7	$L - H_d - 8$	$L - H_d + 3$	5	$-(L - H_d - 5)$	-4
	8	$3Q = 12 - L$	7	$L - H_d - 8$	$L - H_d - 2$	10	$-(L - H_d - 10)$	-9
20	18	$9Q = 16 - 3L$	12	$L - H_d - 18$	$-3Q - H_d$	$3Q + L - 2$	$3Q + H_d - 2$	$-3Q - L + 18$
	18	$3Q = 12 - L$	12	$L - H_d - 18$	$L - H_d - 12$	10	$-(L - H_d - 10)$	6
30	8	$9Q = 6 - 3L$	22	$L - H_d - 8$	$10 - 3Q - H_d$	$3Q + L - 2$	$3Q + H_d - 2$	$-3Q - L + 18$
	8	$3Q = 2 - L$	22	$L - H_d - 8$	$L - H_d + 8$	0	$-(L - H_d)$	16
	8	$3Q = 12 - L$	22	$L - H_d - 8$	$L - H_d - 2$	10	$-(L - H_d - 10)$	6
	8	$3Q = 22 - L$	22	$L - H_d - 8$	$L - H_d - 12$	20	$-(L - H_d - 20)$	-4
60	38	$9Q = 36 - 3L$	52	$L - H_d - 38$	$40 - 3Q - H_d$	$3Q + L - 2$	$3Q + H_d - 2$	$-3Q - L + 18$
	38	$3Q = 12 - L$	52	$L - H_d - 38$	$L - H_d + 28$	10	$-(L - H_d - 10)$	6
	38	$3Q = 32 - L$	52	$L - H_d - 38$	$L - H_d + 8$	30	$-(L - H_d - 30)$	-14
	38	$3Q = 52 - L$	52	$L - H_d - 38$	$L - H_d - 12$	50	$-(L - H_d - 50)$	-34

Table 4.2: Allowed R-charges.

one has $9Q + 3L = 30k + 6 \Rightarrow 3Q + L = 10k + 2$ $(k \in \mathbb{Z})$ thus $3Q = \{2 - L, 12 - L, 22 - L\}$. Finally for $N = 60$ one has $9Q + 3L = 60k + 36 \Rightarrow 3Q + L = 20k + 12$ $(k \in \mathbb{Z})$ thus $3Q = \{12 - L, 32 - L, 52 - L\}$.

Looking at the previous table one sees that only the cases $N = \{2, 4\}$ allow for the S^3 term set G_1. In the case of interest to us, i.e. allowing TLNV terms set G_2 (thus $H_d = L$) while prohibiting sets G_3 to G_7, one can find a solution only for $N = \{12, 15, 20, 30, 60\}$ (notice that G_3 is not a problem unless $N = 2$). For example the case $N = 3$ is not a solution since prohibiting G_5 and G_7 forces $L = 1$ which allows the unwanted G_4 while the case $N = 12$ is a solution since the sets G_5, G_6 and G_7 do not constrain L but G_4 forces $L \neq \{1, 4, 7, 10\}$ which is possible. The specific R-charges for the five possible cases are then computable. In this framework it is therefore impossible to allow only TLNV terms set G_2 along with the S^3 term set G_1. It is however possible to allow only TLNV terms set G_2.

4.4.5 Constraints on $\langle S \rangle$

In light of the previous computations one can engineer the appropriate Pentagon superpotential

$$\begin{aligned} \mathcal{W} &= (m_{\text{ISS}} + g_S SY)P\tilde{P} + g_\mu S H_u H_d + \lambda_L H_d L \bar{E} + \lambda_u H_u Q \bar{U} + \lambda_d H_d Q \bar{D} \\ &\quad + \frac{1}{2}\lambda L L \bar{E} + \lambda' L Q \bar{D} + g_\epsilon S L H_u. \end{aligned} \tag{4.72}$$

If S gets a VEV then *one* neutrino mass is mostly due to the SLH_u term while the Higgs is hidden by the $LQ\bar{D}$ term. This comes from the specific form of the tree level neutrino mass matrix (rank = 1) and thus only one neutrino is massive which is good to generate a hierarchy. Loop diagrams from the $LL\bar{E}$ and $LQ\bar{D}$ terms give masses to the other neutrinos (see [131]). There is also an effective μ term and thus no light higgsinos.

On the other hand, it may be a challenge to give a VEV to S if there is no S^3 term. If there is no S VEV then we could get both neutrino masses and Higgs decay to jets plus missing energy from the $LQ\bar{D}$ term, but we are likely to have an unacceptable light higgsino. A model without a VEV for S could generate all neutrino masses through loops involving the $LQ\bar{D}$ couplings, and could hide the Higgs via these same couplings. However, it would probably have an unacceptable light higgsino.

4.5 Conclusions

We have seen that gauge mediated models with lepton number violation can in principle hide the Higgs and generate an acceptable neutrino mass spectrum simultaneously. Our attempt to find a model in which the appropriate couplings followed from a discrete symmetry of the low energy theory was not completely successful.

The problem we encountered was specific to embedding the lepton violating scenario into the framework of the Pentagon model, but we anticipate some general features. In particular, it seems hard to find models where low energy symmetries allow $LQ\bar{D}$ operators, but forbid $LL\bar{E}$ operators. One has to rely on a high energy Froggatt-Nielsen mechanism, combined with SUSY non-renormalization theorems, to explain the suppression of the latter, which are significantly more constrained.

There will also be an inevitable connection between the origin of neutrino masses in R-parity violating models and the μ term of the MSSM. Our analysis indicates that it may be hard to explain the value of μ in terms of a low energy singlet VEV in these lepton number violating models.

Nonetheless, we think that gauge mediated models with renormalizable lepton number violation could offer considerable insight into two puzzles of the standard model. We have barely scratched the surface of this general class of models, and they deserve further investigation.

Chapter 5

Metastable Supersymmetry Breaking

5.1 Introduction

In this chapter we discuss in detail the findings of the work done in collaboration with R. Essig, K. Sinha, G. Torraba and M. Strassler [15].

Relaxing the requirement that supersymmetry breaking occurs in the true vacuum (see e.g. [132]–[134]) can help overcome many of the constraints of dynamical supersymmetry breaking with no supersymmetric vacua [135]. Recently, Intriligator, Seiberg and Shih [14] have shown that metastable dynamical supersymmetry breaking is rather generic and easy to achieve. They found that metastable vacua occur in supersymmetric QCD (SQCD), in the free magnetic range, when the quarks have small masses,

$$W = \mathrm{tr}\big(m\tilde{Q}Q\big)\,. \tag{5.1}$$

This has opened many new avenues for model building and gauge mediation; see [136]–[152] for some examples of recent work, and [153] for a review and a more complete list of references.

It is not possible to build a phenomenologically viable model of gauge mediation using directly the ISS superpotential (5.1). This is due to an unbroken R-symmetry that forbids non-zero gaugino masses. A natural question is then how the phenomenology changes when the superpotential is a more general polynomial in $\tilde{Q}Q$. While this has been considered before for some particular superpotential deformations (see e.g. [141, 144, 146, 150, 151]), a more detailed account of the space of metastable vacua and the low energy phenomenology is needed. For instance, the light fermions of the model have not been fully explored. The aim of this work is to analyze the IR properties of the theory and its phenomenology in the presence of a generic $U(N_f)$-preserving polynomial superpotential

$$W = m\,\mathrm{tr}(Q\tilde{Q}) + \frac{1}{2\Lambda_0}\,\mathrm{tr}\,\big[(Q\tilde{Q})^2\big] + \frac{1}{2\Lambda_0}\,\gamma\big[\mathrm{tr}\,(Q\tilde{Q})\big]^2 + \dots\ , \tag{5.2}$$

where $\Lambda_0 \gg \Lambda$ is some large UV scale, γ is an order one coefficient, and '…' are sextic and higher dimensional operators.

Deforming (5.1) by a generic polynomial in $\tilde{Q}Q$ breaks R-symmetry explicitly at tree level, and additional supersymmetric vacua are introduced [13]. The supersymmetric vacua for a single trace superpotential were analyzed in detail in [146], where it was found that the magnetic theory has classical supersymmetric vacua with various possible unbroken subgroups of the magnetic gauge group. This should be contrasted with the case of ISS, Eq. (5.1), where the magnetic gauge group is completely Higgsed and supersymmetry is broken classically by the rank condition.

After taking into account one loop quantum corrections in the magnetic theory, one finds the deformed theory also has metastable vacua at low energies [146]. The dynamical reason for this is that the deformations to the magnetic superpotential come from irrelevant operators in the electric theory, which are parametrically suppressed. Therefore, we end up with a controllable deformation of the ISS construction in the IR. These vacua break R-symmetry spontaneously, and in phenomenologically interesting regions of parameter space the spontaneous breaking is much larger than the explicit breaking.

Since supersymmetric vacua allow for unbroken magnetic gauge groups, one might expect the same to occur for metastable vacua. However, the metastable vacua in the theories we explore below have a completely broken magnetic gauge group; vacua with unbroken subgroups of the magnetic gauge group do not occur. This is in some disagreement with [146] and it would be interesting to see how this effect appears in the brane constructions of metastable vacua [154].

Next we will analyze the phenomenological properties of the spectrum, with particular attention to the light fermions, including the Standard Model gauginos and a multiplet of fermions from the "meson" superfield $M = \tilde{Q}Q$. If the superpotential contains only single traces of powers of M, the singlet and adjoint parts of the meson superfield $M = \tilde{Q}Q$ have the same one loop effective action. The singlet fermion is the Goldstino, and must be massless at one loop through a cancellation of its nonzero tree level mass against a one loop correction. The adjoint fermions (or more precisely, a certain subset thereof) have the same tree and one loop effective action, and so their masses arise only at two loops (and/or through equally small mixing effects.) Consequently their masses are small compared with those of the Standard Model gauginos, which arise at one loop.

In this paper we will be considering the case where the embedding of the Standard Model gauge group into the $U(N_f)$ flavor group endows these fermions with Standard Model quantum numbers. With such light masses, these fermions would already have been observed, and so these models would be phenomenologically unacceptable.

We are therefore led to consider a multitrace deformation of the superpotential; in particular, we must take $\gamma \neq 0$ in Eq. (5.2). Then the cancellation between the tree level and one loop masses for the Goldstino fails for the adjoint fermions, leaving them with masses proportional to γ. The phenomenology of direct gauge-mediated models based on this theory is quite rich, since the adjoint fermions may be lighter or heavier than the Standard Model gauginos, depending on γ. Mixing between these fermions and the gauginos is negligibly tiny, due to a charge-conjugation symmetry in (5.2). We will briefly discuss some of the interesting phenomenological properties of such a scenario, leaving the details to a forthcoming publication [155].

The various sections are arranged as follows. In Section 5.2, we discuss the moduli space of SQCD with the superpotential Eq. (5.2), keeping only terms up to quartic order in the electric fields. In Section 5.3, we review SQCD without deformations (ISS), with emphasis on the spectrum and associated phenomenological issues. In Section 5.4, we study single trace deformations of the ISS superpotential, that is, the case $\gamma = 0$. We show that all metastable vacua have a magnetic gauge group that is completely Higgsed, and we discuss the spectrum, showing it is unacceptable for phenomenology. Next, in Section 5.5 we consider $\gamma \neq 0$, describing the spectrum in detail. Finally, Section 5.6 contains a brief overview of the phenomenology of and constraints on such models. Various computations are shown in detail in the Appendix.

5.2 SQCD with a multitrace superpotential

In this section, we analyze the symmetries and supersymmetric vacua of SQCD in the presence of a generic $U(N_f)$-preserving polynomial superpotential.

Supersymmetric QCD with gauge group $SU(N_c)$ and N_f flavors $(Q_i, \tilde{Q}_j)$ with equal masses m has a global symmetry group

$$SU(N_f)_V \times U(1)_V \tag{5.3}$$

under which $(Q_i,\, \tilde{Q}_i)$ transform as $(\square_{+1},\, \overline{\square}_{-1})$. There is also a discrete $\mathbb{Z}_2$ charge conjugation symmetry $Q_i \leftrightarrow \tilde{Q}_i$. For phenomenological applications we will later weakly gauge a subgroup of $SU(N_f)_V$ and identify it with the Standard Model gauge groups. We will also gauge $U(1)_V$ to remove a Nambu-Goldstone boson.

The most general quartic superpotential preserving this symmetry is of the form

$$W = m\,\mathrm{tr}(Q\tilde{Q}) + \frac{1}{2\Lambda_0}\,\mathrm{tr}\left[(Q\tilde{Q})^2\right] + \frac{1}{2\Lambda_0}\,\gamma\Big[\mathrm{tr}\,(Q\tilde{Q})\Big]^2 . \tag{5.4}$$

We will typically consider $\Lambda_0 \gg \Lambda \gg m$, and take γ to be of order one or smaller. We will not consider sextic or higher operators, since they are suppressed by higher powers of Λ_0 and would not affect our discussion. The nonrenormalizable superpotential (5.4) could be generated from a renormalizable theory, for example by integrating out fields with masses $\sim \Lambda_0$ that couple to $Q\tilde{Q}$.

Let us consider the theory in various limits. First, for $W = 0$ there is a moduli space of vacua parameterized by mesons and baryons modulo classical constraints. The global symmetry is enhanced to $SU(N_f)_L \times SU(N_f)_R \times U(1)_V$, and there is a non-anomalous $U(1)_R$ symmetry as well as an anomalous $U(1)_A$ axial current.

For $m/\Lambda \neq 0$ but $\Lambda_0 \to \infty$, the superpotential is renormalizable, and the theory has an exact classical $U(1)_R$ symmetry which is anomalous at the quantum level.[1] The non-anomalous symmetries of the model are

	$SU(N_f)_V$	$U(1)_R$	$U(1)_V$
Q_i	$\square$	$+1$	$+1$
$\tilde{Q}_i$	$\bar{\square}$	$+1$	-1
$\Lambda^{3N_c-N_f}$	0	$2N_c$	0

plus the $\mathbb{Z}_2$ charge conjugation. The F-term relations lift the moduli space and the only vacuum is at the origin.

On the other hand, for $m \neq 0$ and Λ_0 large but finite, all R-symmetries are explicitly broken at the classical level. New discrete supersymmetric vacua appear in the regime

$$\tilde{Q}\,Q \sim m\Lambda_0\,.$$

5.2.1 Magnetic dual

Below the scale Λ, the theory is described by an effective theory, called the "dual magnetic theory", with gauge group $SU(\tilde{N}_c)$, singlet mesons Φ_{ij}, and N_f fundamental flavors $(q_i, \tilde{q}_j)$; we define $\tilde{N}_c \equiv N_f - N_c$. The theory has a positive beta function and is weakly-coupled in the infrared. After an appropriate change of variables, the classical tree level superpotential reads

$$W = h\,\mathrm{tr}(q\Phi\tilde{q}) - h\mu^2\,\mathrm{tr}\,\Phi + +\frac{1}{2}h^2\mu_\phi\Big(\mathrm{tr}\,\Phi^2 + \gamma(\mathrm{tr}\,\Phi)^2\Big)\,. \tag{5.5}$$

where the first trace is over magnetic color and the remaining traces are over flavor indices. The relation with the electric variables is (roughly)

$$\Lambda\Phi \sim \tilde{Q}Q,\; h\,\mu^2 \sim \Lambda m\;,\; h^2\,\mu_\phi \sim \frac{\Lambda^2}{\Lambda_0}\,.$$

[1] There is also an approximate non-anomalous R-symmetry "$U(1)_{R'}$" which is restored as $m \to 0$, but we will not need to consider this symmetry.

More details may be found in [14].

As in ISS, we restrict to small quark masses $m \ll \Lambda$. We will also restrict ourselves to the range

$$\Lambda_0 \gg \sqrt{\frac{\Lambda}{m}}\,\Lambda\,, \tag{5.6}$$

which guarantees that $h\mu_\phi \ll \mu$. This will be needed to have long-lived metastable vacua. There are nonperturbative corrections to the superpotential (5.5), but they are all small enough not to affect our calculations given (5.6).

Also, these conditions ensure that the symmetries of the model at the scale Λ are approximately $SU(N_f)_L \times SU(N_f)_R \times U(1)_V \times U(1)_{R'}$, broken to $SU(N_f)_V \times U(1)_V$ only by effects of order m/Λ and Λ/Λ_0. Therefore, to an excellent approximation, both the superpotential *and* the Kähler potential satisfy the larger symmetry group, under which the trace and traceless parts of Φ_{ij} transform as a single irreducible multiplet. We will work only to leading non-vanishing order in the symmetry-breaking effects from non-zero m and non-infinite Λ_0.

Furthermore, the discrete $\mathbb{Z}_2$ charge-conjugation symmetry of the electric theory appears as the transformation

$$\Phi \to \Phi^T\,,\ q_i \leftrightarrow \tilde{q}_i\ . \tag{5.7}$$

This transformation plays an important role in the phenomenology of gauge mediation models based on (5.5), and indeed in other ISS-related models (see e.g. [161]).

As in the electric theory, the R-symmetry is explicitly broken, and we expect new supersymmetric vacua parametrically at μ^2/μ_ϕ. Indeed, the solutions to the F-term constraints

$$\begin{aligned}\big(-h\mu^2 + h^2\mu_\phi\gamma\,\mathrm{tr}\,\Phi\big)\, I_{N_f\times N_f} + h^2\mu_\phi\,\Phi + h\,\tilde{q}q &= 0\\ q\Phi = \Phi\tilde{q} &= 0\,,\end{aligned} \tag{5.8}$$

are

$$\langle h\,\Phi\rangle = \frac{1}{1+(N_f-k)\gamma}\,\frac{\mu^2}{\mu_\phi}\begin{pmatrix} 0_{k\times k} & 0_{k\times(N_f-k)} \\ 0_{(N_f-k)\times k} & I_{(N_f-k)\times(N_f-k)}\end{pmatrix} \tag{5.9}$$

and

$$\langle \tilde{q}q\rangle = \frac{1}{1+(N_f-k)\gamma}\,\mu^2\begin{pmatrix} I_{k\times k} & 0_{k\times(N_f-k)} \\ 0_{(N_f-k)\times k} & 0_{(N_f-k)\times(N_f-k)}\end{pmatrix} \tag{5.10}$$

with $k = 1, \ldots, N_f - N_c$. (Here I represents the identity matrix, and a subscript $r \times s$ indicates a block matrix of the corresponding size.) The appearance of the extra parameter k classifying different classical vacua has been observed for $\gamma = 0$ by [146]. In particular, for $k < N_f - N_c$ there is an unbroken magnetic gauge group $SU(N_f - N_c - k)$.

5.3 Metastable DSB in the R-symmetric limit

In the next three sections, we will analyze the IR dynamics of (5.5) in three steps. First, we review the ISS model [14], the R-symmetric limit $\mu_\phi = 0$, which corresponds to an electric SQCD with massive flavors and no irrelevant operators. We will highlight the spectrum and associated phenomenological problems. In Section 5.4, we show how these problems are not entirely solved by making μ_ϕ non-zero but leaving $\gamma = 0$. Finally, in Section 5.5, we show how the theory with $\gamma \neq 0$ resolves the remaining problems.

5.3.1 The model and its spectrum

The ISS model considers massive SQCD near the origin in field space in the free magnetic range $N_c + 1 \leq N_f < \frac{3}{2} N_c$, where the theory has a dual magnetic description with superpotential

$$W = -h\mu^2 \operatorname{tr} \Phi + h\operatorname{tr}(q\Phi\tilde{q}) \,. \tag{5.11}$$

At the classical level the theory breaks supersymmetry by the rank condition. We parametrize the fields by

$$\Phi = \begin{pmatrix} Y_{\tilde{N}_c \times \tilde{N}_c} & Z^T_{\tilde{N}_c \times N_c} \\ \tilde{Z}_{N_c \times \tilde{N}_c} & X_{N_c \times N_c} \end{pmatrix} \tag{5.12}$$

$$q^T = \begin{pmatrix} \chi_{\tilde{N}_c \times \tilde{N}_c} \\ \rho_{N_c \times \tilde{N}_c} \end{pmatrix} \,,\ \tilde{q} = \begin{pmatrix} \tilde{\chi}_{\tilde{N}_c \times \tilde{N}_c} \\ \tilde{\rho}_{N_c \times \tilde{N}_c} \end{pmatrix} \,, \tag{5.13}$$

where $\tilde{N}_c = N_f - N_c$ is the rank of the magnetic gauge group. The classical moduli space of vacua is parametrized by $\langle \chi\tilde{\chi} \rangle = \mu^2 \, I_{\tilde{N}_c \times \tilde{N}_c}$ and $\langle X \rangle$. The other fields have vanishing expectation values. In the rest of the paper we will restrict to metastable vacua with maximal unbroken global symmetry, by choosing the ansatz

$$\langle X \rangle = X_0 \, I_{N_c \times N_c} \,,\ \langle \chi \rangle = q_0 \, I_{\tilde{N}_c \times \tilde{N}_c} \,,\ \langle \tilde{\chi} \rangle = \tilde{q}_0 \, I_{\tilde{N}_c \times \tilde{N}_c} \,. \tag{5.14}$$

It will be checked that this is a self-consistent choice.

The vev for $\chi\tilde{\chi}$ breaks the gauge group $SU(\tilde{N}_c)_G$ completely, with the breaking pattern

$$SU(\tilde{N}_c)_G \times SU(N_f)_V \times U(1)_V \to SU(\tilde{N}_c)_V \times SU(N_c) \times U(1)' \,. \tag{5.15}$$

(Here all groups except $SU(\tilde{N}_c)_G$ are global; we remind the reader that $\tilde{N}_c = N_f - N_c$). The reduction of the global symmetry group leads to $2N_c\tilde{N}_c + 1$ Nambu-Goldstone modes. The fields $(\rho, \tilde{\rho}, Z, \tilde{Z})$ are charged under $U(1)'$, which plays the role of a messenger number symmetry. See [14] for a more detailed discussion.

The flat directions X are not protected by holomorphy or symmetries and, as we shall review shortly, become massive at one loop. (A field with these properties is called a "pseudo-modulus" [14].) In particular, X is stablized at the origin. Near the origin of moduli space the rank condition imposes

$$|F_X| = |h\mu^2|\,, \tag{5.16}$$

and the scale of supersymmetry breaking is

$$V_{min} = N_c\,|h^2\mu^4|\,. \tag{5.17}$$

To analyze the spectrum of the theory, it is convenient to rewrite the superpotential in terms of the component fields,

$$\begin{aligned} W &= -h\mu^2 \operatorname{tr} X + h \operatorname{tr} \begin{pmatrix} \rho & Z \end{pmatrix} \begin{pmatrix} X & \mu \\ \mu & 0 \end{pmatrix} \begin{pmatrix} \tilde{\rho} \\ \tilde{Z} \end{pmatrix} \\ &\quad + h\mu \operatorname{tr}\big[Y(\chi + \tilde{\chi})\big] + h \operatorname{tr}\big(\chi Y \tilde{\chi} + \rho \tilde{Z} \tilde{\chi} + \chi Z \tilde{\rho}\big)\,. \end{aligned} \tag{5.18}$$

The spectrum consists of three sectors, each consisting of fields satisfying $\mathrm{Str}\, M^2 = 0$.

(1) *The* (ρ, Z) *sector*: Treating X as a background superfield, the (ρ, Z) supersymmetric mass matrix is

$$M_f = \begin{pmatrix} hX & h\mu \\ h\mu & 0 \end{pmatrix} \tag{5.19}$$

while the bosonic matrix is computed, as usual, including off-diagonal blocks with F-terms.

There are $2N_c\tilde{N}_c$ Dirac fermions that come from $(\psi_\rho,\, \psi_Z)$ and $(\psi_{\tilde{\rho}},\, \psi_{\tilde{Z}})$. Near the origin of field space, their masses are of order $h\mu$, from (5.19). The scalars combine into $4N_c\tilde{N}_c$ complex fields, which are linear combinations of $(\rho, Z, \tilde{\rho}^*, \tilde{Z}^*)$. There are $N_c\tilde{N}_c$ complex Nambu-Goldstone bosons from the combinations $\mathrm{Re}\,(\rho + \tilde{\rho})$ and $\mathrm{Im}\,(\rho - \tilde{\rho})$. The $3N_c\tilde{N}_c$ remaining complex scalars have splittings of order, and centered around, $h\mu$. The numerical coefficients adjust to preserve $\mathrm{Str}\, M^2 = 0$.

This sector will play the role of the messenger sector in gauge mediation applications. Once a subgroup of the flavor symmetry is identified with the Standard Model, and gauged with couplings g_{SM}, the Nambu-Goldstone modes will acquire a one loop mass of order $g_{SM}\mu/(4\pi)$. (In particular, we will study the case where $SU(N_c)$ is gauged — see Eq.(5.15).) The lightest state will be stable in the full theory, since the messenger sector is protected by the non-anomalous $U(1)'$ messenger number.

(2) *The* (Y, χ) *sector*: Fermions from $Y, (\chi + \tilde{\chi})$ form $\tilde{N}_c^2$ Dirac fermions with mass $\sim h\mu$. The traceless part[2] of the chiral superfield $(\chi - \tilde{\chi})$, which contains the NG bosons $\mathrm{Im}\,(\chi' - \tilde{\chi}')$,

[2] We denote traceless fields with primes; for instance X' is the traceless part of X.

is eaten by the superHiggs mechanism when the magnetic group is gauged.

The field $\mathrm{Im}\,\mathrm{tr}(\chi-\tilde{\chi})$ is a NG boson associated to the breaking of $U(1)_V$. The field $\mathrm{Re}\,\mathrm{tr}(\chi-\tilde{\chi})$ corresponds to a pseudo-modulus, which will be lifted at one loop. The fermion from $\mathrm{tr}\,(\chi-\tilde{\chi})$ is massless. This sector has a supersymmetric spectrum at tree level.

The massless fields from $\mathrm{tr}\,(\chi-\tilde{\chi})$ would be phenomenologically forbidden. This forces us to gauge $U(1)_V$, so that the superfield $\mathrm{tr}\,(\chi-\tilde{\chi})$ is eaten by the $U(1)_V$ gauge boson and at tree level acquires a mass of order $g_V\mu$.

(3) *The X sector*: X is a flat direction, with massless fermionic partner at tree level. In particular, $\psi_{\mathrm{tr}\,X}$ is the Goldstino.

One loop contributions from heavy particles lift the pseudo-moduli. The fields $(Y,\chi,\tilde{\chi})$ do not couple at tree level to the supersymmetry breaking sector, so they do not contribute to the one loop effective potential for the pseudo-moduli. Because we are in the regime where $|F_X| = |h\mu^2|$ is of order the square of the messenger masses, the effect of integrating out the messengers does not have a simple expression in superspace, and it is more convenient to work directly with nonsupersymmetric expressions. The bosonic action is given by the usual Coleman-Weinberg formula [156]

$$V_{CW} = \frac{1}{64\pi^2}\,\mathrm{STr}\,M^4\log\frac{M^2}{\Lambda^2}\,. \tag{5.20}$$

Near the origin of moduli space $X \ll \mu$, the potential is approximated by [14]

$$V_{CW} \approx \frac{a}{2}\,|h^4\mu^2|\,\mathrm{tr}\,\left(\mathrm{Re}\,\frac{1}{\sqrt{2}}[\chi-\tilde{\chi}]\right)^2 + b|h^4\mu^2|\,\mathrm{tr}\,(X^\dagger X) \tag{5.21}$$

with

$$a = \frac{\log 4-1}{8\pi^2}\,N_c\,,\quad b = \frac{\log 4-1}{8\pi^2}\,\tilde{N}_c\,. \tag{5.22}$$

Therefore, in the ISS model the pseudo-moduli are consistently stabilized at the origin and R-symmetry is preserved. In this approximation, the one loop mass of the bosonic field X is given by

$$m^2_{CW} = b|h^4\mu^2| = \frac{\log 4-1}{8\pi^2}\,\tilde{N}_c\,|h^4\mu^2|\,. \tag{5.23}$$

5.3.2 Phenomenological problems

One could try to use the ISS construction as the supersymmetry breaking sector in models of direct gauge mediation. However, since R-symmetry is preserved in the metastable vacuum, Majorana masses for the Standard Model gauginos are forbidden. The same applies to the fermions ψ_X and $\psi_{\chi-\tilde{\chi}}$, which may have SM quantum numbers after embedding the SM gauge group into the flavor symmetry group of the model. For these reasons, this model does not give an acceptable phenomenology.

There are various ways of improving this situation (see, for instance, [157]–[160]). One very interesting proposal [161] is that the gauginos could come from Dirac fermions, whose mass is not constrained to vanish by an unbroken R-symmetry. This idea was applied to the ISS model in [162], by adding new fields and interactions to the superpotential. Dirac masses appear from one loop diagrams mixing the MSSM Weyl gauginos with the new Weyl fermions. One problem with this approach is that doubling the number of fields (in order to have Dirac fermions) creates a Landau pole close to the messenger scale. In this case, corrections from the microscopic theory may become important.

Another possibility is to deform the superpotential by higher powers of the meson superfield, explicitly breaking the R-symmetry at tree level [141, 144, 146]. We consider this possibility in detail below.

5.4 Single trace deformation

We begin by considering the superpotential Eq. (5.5) with $\gamma = 0$, that is, with only a single trace perturbation:

$$W = -h\mu^2 \,\mathrm{tr}\,\Phi + h\mathrm{tr}(q\Phi\tilde{q}) + \frac{1}{2}h^2\mu_\phi \,\mathrm{tr}\,(\Phi^2)\,. \tag{5.24}$$

This model was discussed in [146], where it was suggested that new metastable vacua, with unbroken magnetic group, appear around $X \sim \mu$. However, this region of parameter space is subtle, because higher order corrections to (5.21) become important. We will have two new things to say about this model.

(1) By considering the full logarithmic one loop potential (5.20), it is possible to show that the metastable vacua with unbroken magnetic gauge group are actually unstable. Thus, one is led to study only the ISS-like vacuum where the magnetic gauge group is completely Higgsed.

(2) Gauginos indeed become massive at one loop in this model, as expected from the R-symmetry breaking. However (ignoring some subtleties which we will discuss later) the adjoint fermions $\psi_{X'}$ become massive only at two loops, because diagrammatic cancellations that make the Goldstino $\psi_{\mathrm{tr}\,X}$ massless at one loop also force the adjoint fermions $\psi_{X'}$ to be massless at this order. This provides the main motivation for studying non-zero γ below.

	Fermions				Bosons			
	Weyl mult.	mass	$U(N_c)$	$SU(\tilde{N}_c)_D$	Real mult.	mass	$U(N_c)$	$SU(\tilde{N}_c)_D$
tr$X$	1	$h^2\mu_\phi$	1_0	1	2	$h^2\mu_\phi$	1_0	1
X'	$N_c^2 - 1$	$h^2\mu_\phi$	Adj$_0$	1	$2(N_c^2 - 1)$	$h^2\mu_\phi$	Adj$_0$	1
Y, χ, $\tilde{\chi}$	$\tilde{N}_c^2$ $\tilde{N}_c^2$ $\tilde{N}_c^2 - 1$ 1	$\mathcal{O}(h\mu)$ $\mathcal{O}(h\mu)$ $g_{\mathrm{mag}}\mu$ 0	1_0 1_0 1_0 1_0	Adj Adj Adj 1	$2\tilde{N}_c^2$ $2\tilde{N}_c^2$ $2(\tilde{N}_c^2 - 1)$ 1 1	$\mathcal{O}(h\mu)$ $\mathcal{O}(h\mu)$ $g_{\mathrm{mag}}\mu$ 0_{NGB} 0	1_0 1_0 1_0 1_0 1_0	Adj Adj Adj 1 1
Z,$\tilde{Z}$, ρ, $\tilde{\rho}$	$2N_c\tilde{N}_c$ $2N_c\tilde{N}_c$	$\mathcal{O}(h\mu)$ $\mathcal{O}(h\mu)$	$\square_1+\overline{\square}_{-1}$ $\square_1+\overline{\square}_{-1}$	$\square+\overline{\square}$ $\square+\overline{\square}$	$2N_c\tilde{N}_c$ $2N_c\tilde{N}_c$ $2N_c\tilde{N}_c$ $2N_c\tilde{N}_c$	0_{NGB} $\mathcal{O}(h\mu)$ $\mathcal{O}(h\mu)$ $\mathcal{O}(h\mu)$	$\square_1$ $\overline{\square}_{-1}$ $(\square_1+$ $\overline{\square}_{-1})$	$\overline{\square}$ $\square$ $(\overline{\square}+$ $\square)$

Table 5.1: The classical mass spectrum, grouped in sectors with Str $M^2 = 0$. Since supersymmetry is spontaneously broken only after including one loop effects, there is no Goldstino at tree level. g_{mag} is the magnetic gauge coupling. A subscript "NGB" indicates the particle is massless because it is a Nambu-Goldstone boson. Subscripts in the third column indicate the charge under the $U(1)$ subgroup. Note this table gives the spectrum before the Standard Model gauge group is gauged.

5.4.1 Metastable supersymmetry breaking

The classical supersymmetric vacua are obtained by setting $\gamma = 0$ in (5.9) and (5.10). In order to analyze the effect of the deformation on the ISS metastable vacuum, the cases $k = N_f - N_c$ and $k < N_f - N_c$ have to be distinguished.

Case $k = N_f - N_c$

This is the analog of the ISS construction, with no unbroken gauge group. The fields are parameterized as in Eqs. (5.12) and (5.13). We will now review why a metastable vacuum appears at a distance of order μ_ϕ/b away from the origin [146].

As a starting point, set $V_{CW} \to 0$. Due to the classical deformation, X is no longer a flat direction, unlike the ISS case. Rather, the origin $X_0 \sim 0$ is at the side of a paraboloid of classical curvature $|h^2\mu_\phi|^2$. In other words, the origin is unstable against classical flow of X_0 toward the supersymmetric vacua discussed before. The tree level spectrum near the origin is shown in Table 5.1.

In order to create a local minimum, the quantum contribution $V_{CW} \sim m_{CW}\,|X_0|^2$ should overwhelm the curvature of the classical potential, i.e., $m_{CW} \gg |h^2\,\mu_\phi|$. This rather interesting effect, where a one loop contribution stabilizes a classical runaway direction, was analyzed in [145]. Here, the stabilization of X_0 can occur naturally, since μ_ϕ, arising from a nonrenormalizable operator in the microscopic theory, is parametrically small. The condition that the one loop potential introduces a supersymmetry breaking minimum,

$$\epsilon \equiv \frac{m_{cl}^2}{m_{CW}^2} \approx \left|\frac{\mu_\phi^2}{b\mu^2}\right| \ll 1\,, \tag{5.25}$$

is naturally satisfied.

The potentials at tree level and at one loop, as a function of X_0, are shown in Figure 5.1. As seen from the figure, the tree level potential (lower magenta curve), which is obtained from the superpotential in (5.24), has no supersymmetry breaking minimum. A metastable minimum is created near the origin once the one loop quantum corrections in the form of V_{CW} are included (upper blue curve).

As a result of the competition between the classical and quantum contributions, a metastable vacuum is created at

$$hX_0 \approx \frac{\mu^2\mu_\phi^*}{b|\mu|^2 + |\mu_\phi|^2}\ ,\ q_0\tilde{q}_0 = \mu^2\,; \tag{5.26}$$

see Eq. (5.14) for the notation. As expected, X_0 is proportional to the explicit R-symmetry breaking parameter μ_ϕ. However, it is larger than this by the inverse loop factor $1/b$. This follows from the fact that the minimum appears from balancing a tree level linear term of order $\mu^2\,\mu_\phi$ against a one loop quadratic term of order $b\mu^2$.

The pattern of symmetry breaking in this vacuum is

$$SU(\tilde{N}_c)_G \times SU(N_f)_V \times U(1)_V \to SU(\tilde{N}_c)_V \times SU(N_c) \times U(1)'\,, \tag{5.27}$$

where only the messengers transform under $U(1)'$. Unlike the ISS construction, here $X_0 \neq 0$, so that the R-symmetry is both explicitly and spontaneously broken, *with the latter dominating* since $|hX_0| \gg |\mu_\phi|$.

Case $k < N_f - N_c$

The possibility of metastable vacua with $k < N_f - N_c$ is very interesting; coupling this to the MSSM, it would imply unbroken gauge groups in the hidden sector. Properties of such configurations were discussed in [146]. Unfortunately, we will now show that there are generically no metastable vacua in this regime.

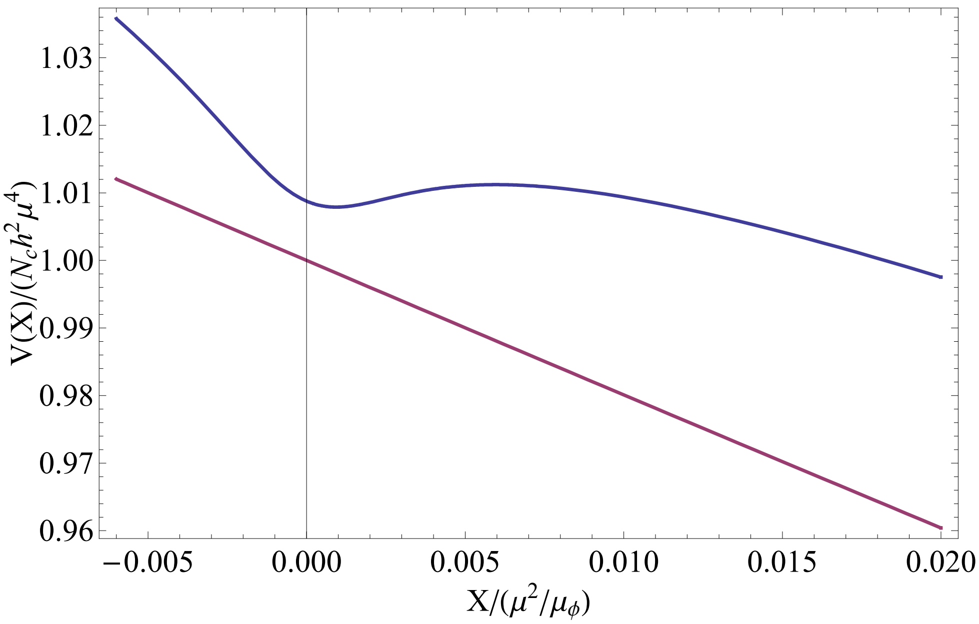

Figure 5.1: Metastable vacuum near $X \sim 0$, for a single trace quadratic deformation of the superpotential (i.e. $\gamma = 0$). All parameters have been chosen to be real. The bottom (magenta) line is the tree level potential, while the top (blue) line shows the tree level potential plus one loop Coleman-Weinberg corrections. The X-axis has been normalized such that the position of the tree level supersymmetric vacuum lies at $X/(\mu^2/\mu_\phi) = 1$. Notice how the one loop corrections create a (metastable) minimum near the origin.

Such vacua should be of the form

$$\Phi = \begin{pmatrix} 0 & 0 \\ 0 & X_{(N_f-k)\times(N_f-k)} \end{pmatrix} \ , \ \tilde{q}q = \begin{pmatrix} \mu^2 I_{k\times k} & 0 \\ 0 & 0 \end{pmatrix} . \tag{5.28}$$

The parametrization of the fluctuations is slightly more involved,

$$\Phi = \begin{pmatrix} Y_{k\times k} & Z_{k\times(N_f-k)} \\ \tilde{Z}_{(N_f-k)\times k} & X_{(N_f-k)\times(N_f-k)} \end{pmatrix} \ , \ q = \begin{pmatrix} V_{k\times k} & T_{k\times(\tilde{N}_c-k)} \\ P_{(N_f-k)\times k} & \varphi_{(N_f-k)\times(\tilde{N}_c-k)} \end{pmatrix} \tag{5.29}$$

and similarly for $\tilde{q}$. As in the case $k = N_f - N_c$, the expectation values are chosen to be of the form

$$\langle X \rangle = X_0 \, I_{(N_f-k)\times(N_f-k)} \ , \ \langle V \rangle = q_0 \, I_{k\times k} \ , \ \langle \tilde{V} \rangle = \tilde{q}_0 \, I_{k\times k} \, .$$

The new fields $(\varphi, \tilde{\varphi})$ and $(T, \tilde{T})$ do not exist for $k = N_f - N_c$. They are fundamental flavors of the unbroken magnetic group $SU(N_f - N_c - k)$.

As was found in [146], positivity of the bosonic mass matrix of $(\varphi, \tilde{\varphi})$ implies

$$|X_0|^2 \geq |\mu^2 - h\mu_\phi X_0| \, .$$

This places us in the regime $X_0 \gtrsim \mu$. In this regime, the quadratic approximation (5.21) to the Coleman-Weinberg potential is no longer valid. For $X_0/\mu \sim 1$, all the higher order terms in V_{CW} give contributions comparable to (5.21). In other words, it is necessary to use the full expression appearing in Eq. (5.20).

Therefore, to establish the existence of such vacua, a detailed analysis of V_{CW} is required. As shown in the Appendix, all such vacua are unstable once the full form of V_{CW} is included. The intuitive reason for this is that at large X_0 the logarithmic growth of V_{CW} cannot overwhelm the quadratic terms in the classical potential. A similar behavior was found in [145].

The plot of $V_{tree} + V_{CW}$ for this case is almost the same as that of Figure 5.1. For sufficiently large $|X_0/\mu| > 1$, the classical falling potential dominates the logarithmic rise of the V_{CW}, and no critical points are found until the supersymmetric vacuum is reached.

Summarizing, metastable states occur only for $k = N_f - N_c$. The fields have expectation values Eq. (5.26), breaking the magnetic gauge group completely at the scale μ.

5.4.2 Light fermions

We therefore return to the one remaining vacuum, the ISS-like case with $k = N_f - N_c$. From the previous analysis, the bosons from X and the traceless part of $\chi - \tilde{\chi}$ acquire masses of order m_{CW}. The aim of this section is to compute the fermion masses at one loop, and show that $\psi_{X_{ij}}$ remains massless at this order, contrary to naive expectations from R-symmetry breaking.

First we explore one loop effects involving the Goldstino $\psi_{\mathrm{tr}\,X}$. At tree level it has a nonvanishing mass $h^2\mu_\phi$. We are not expanding around a critical point of the classical potential, but rather one of the full one loop potential, and therefore the Goldstino should become massless only once one loop effects are included. This implies that the one loop diagram has to give

$$m^{1-loop}_{\psi_{\mathrm{tr}\,X}} \approx -h^2\mu_\phi\,, \tag{5.30}$$

such that $m^{tree}_{\psi_{\mathrm{tr}\,X}} + m^{1-loop}_{\psi_{\mathrm{tr}\,X}} \approx 0$. Indeed, the explicit evaluation of the one loop diagram in the Appendix corroborates (5.30). These results are approximate because we are neglecting (subleading) mixings with other singlet fermions; see below and the Appendix.

At a first glance it is surprising that the one loop contribution can be equal to the tree level one. This is so because the one loop diagram is of order

$$\frac{h^2}{16\pi^2}\, h\, X_0\,.$$

However, since $hX_0 \sim \mu_\phi/b$, with b defined in Eq. (5.22), we obtain the result (5.30). This is another manifestation of the pseudo-runaway behavior discussed in the previous section.

Next, notice that within the classical superpotential (5.24), X_{ij} only appears in single traces. On the other hand, the one loop contribution is a single trace of a function of X_{ij}, because it comes from exponentiating bosonic and fermionic determinants (denoted by Δ) arising from messengers in the fundamental representation of $SU(N_c)$. Therefore, the full one loop effective action

$$S_{eff}(X,\psi_X) = S_{tree} + \mathrm{Tr}\left(\log\Delta\right)$$

can be written as a single trace of products of X_{ij} and its superpartner. This means that *the tree level plus one loop* contribution to the masses of the X fields must be of the form $\mathrm{Tr}(X^\dagger X)$, and therefore the singlet and adjoint parts of X get identical masses through one loop. The same is true for the fermionic partners of X: at one loop the masses of the singlet $\psi_{\mathrm{tr}\,X}$ and the adjoint $\psi_{X'}$ are the same. Diagrammatically, there is a cancellation between the tree level Weyl mass and the one loop correction.

We note two small subtleties. First, we have assumed here that the kinetic terms for the singlet and adjoint parts of X have the same normalization. This is true to a very good approximation. We assumed $m \ll \Lambda \ll \Lambda_0$, which ensured that the high-energy theory's approximate $SU(N_f)\times SU(N_f)$ symmetry is only weakly broken to $SU(N_f)_V$ at the scale Λ. Under this larger symmetry, the singlet and adjoint transform as a single irreducible representation, assuring equally normalized kinetic terms, up to negligible order(μ/Λ) corrections.

Second, and irreducibly, the Goldstino is not quite $\psi_{\mathrm{tr}\,X}$. As discussed in more detail in the Appendix, it mixes slightly with the fields $\psi_{\mathrm{tr}\,Y}$ and $\psi_{\mathrm{tr}\,(X+\tilde{X})}$, with mixing angles of order a one loop factor, $\sim 1/16\pi^2$ and $\sim X_0/(16\pi^2\mu)$, respectively. Consequently the tree level and one loop ψ_X masses fail to cancel precisely, though by an amount that is one further loop-order suppressed. Thus our statement that the ψ_X masses vanish at one loop is effectively correct.

5.4.3 Phenomenology of the $\gamma = 0$ model

After gauging a subgroup of the flavor group $SU(N_c)$ — see Eq. (5.15) — and identifying it with the Standard Model gauge group, the adjoint fermions $\psi_{X'}$ will carry Standard Model gauge charges. The fact that they are approximately massless at one loop is unacceptable phenomenologically. They do become massive at two loop order, through the above-mentioned mixings, and through explicit two loop diagrams. For example, Standard Model gauge bosons, which do not impact the singlet $\psi_{\mathrm{tr}\,X}$, generate for the other fields a two loop mass of order

$$m_{\psi_{X'}} \;\sim\; g^2\,\frac{X_0}{(16\pi^2)^2} \;\sim\; g^2\,\frac{\mu_\phi}{16\pi^2}\;. \tag{5.31}$$

But the Standard Model gauginos have a one loop mass of order $X_0/16\pi^2 \sim \mu_\phi$. Importantly, the charge conjugation symmetry discussed in Section 5.2 forbids significant mixing between λ and ψ_X, so the masses for the $\psi_{X'}$ fields cannot be raised through mixing effects. *Consequently, requiring the gauginos are at a scale $\sim$ 1 TeV implies the $\psi_{X'}$ would be so light that they would have already been observed.*

5.5 The deformation with $\gamma \neq 0$

Clearly the root of this phenomenological problem lies in treating $\psi_{X'}$ and the Goldstino $\psi_{\mathrm{tr}\,X}$ on the same footing in the tree level superpotential. A solution is to allow non-zero γ,

$$W = h\mathrm{tr}(q\Phi\tilde{q}) - h\mu^2\,\mathrm{tr}\,\Phi + \frac{1}{2}h^2\mu_\phi\Big(\mathrm{tr}\,(\Phi^2) + \gamma(\mathrm{tr}\,\Phi)^2\Big)\,. \tag{5.32}$$

such that the two have different tree level masses. Then the total one loop mass for $\psi_{X'}$ becomes proportional to $\gamma\mu_\phi$.

The motivation for considering non-zero γ

$$W = -h\mu^2\,\mathrm{tr}\,\Phi + h\mathrm{tr}(q\Phi\tilde{q}) + \frac{1}{2}h^2\mu_\phi\Big(\mathrm{tr}\,(\Phi^2) + \gamma(\mathrm{tr}\,\Phi)^2\Big)\,, \tag{5.33}$$

extends beyond phenomenological utility. No symmetry enforces $\gamma = 0$ once μ_ϕ or even μ are non-zero, so it is quite natural for γ to be nonzero.[3]

Let us now analyze the metastable vacua of the theory. For $h\mu_\phi \ll \mu$ (and for $|\gamma|$ roughly of order 1), the Coleman-Weinberg potential is approximately as in ISS. The only stable local minimum occurs for $k = N_f - N_c$. The multitrace deformation adds a term proportional to the identity matrix to W_Φ, so we obtain

$$q_0\tilde{q}_0 = \mu^2 - h\mu_\phi\,N_c\,\gamma\,X_0\,. \tag{5.34}$$

$$hX_0 \approx \frac{\mu^2\mu_\phi^*(1+N_c\gamma^*)}{b|\mu^2| + |\mu_\phi|^2 + f(\gamma,\gamma^*)} \tag{5.35}$$

with

$$f(\gamma,\gamma^*) = |\mu_\phi|^2\big[N_c\,(\gamma+\gamma^*) + N_c^2\,|\gamma|^2\big]\,.$$

In the limit $h\mu_\phi \ll \mu$, the effect of γ is qualitatively unimportant:

$$hX_0 \approx \frac{\mu^2\mu_\phi^*(1+N_c\gamma^*)}{b|\mu|^2}\;,\; q_0\tilde{q}_0 \approx \mu^2\,, \tag{5.36}$$

so that $|hX_0| \gg |\mu_\phi|$. While $\gamma \neq 0$ does not alter the qualitative features of the vacuum, it is important, when computing the spectrum, that the precise values (5.34) and (5.35) be used.

---

[3] Considering the preserved symmetries, one might wonder why the coefficients of $q\Phi\tilde{q}$ should be taken precisely equal. The point is that the physical couplings are constrained by the approximate $SU(N_f)_L \times SU(N_f)_R$ in the electric theory, which is still valid at and just below the scale Λ. In other words, the $\mu \to 0$ and $\mu_\phi \to 0$ limit implies equal couplings. Nothing comparable favors $\gamma = 0$.

5.5.1 Spectrum

We now analyze the spectrum in the metastable vacuum. As in Section 5.4, the Goldstino is not massless at tree level. Some of the one loop diagrams exactly cancel the tree level contributions and for this reason we discuss directly the tree level plus one loop results.

We first consider the fermions of the pseudo-modulus X. The singlet fermion (the Goldstino) is massless at one loop. For the adjoint fermions, the tree level mass $h^2\mu_\phi$ is partially canceled against the one loop contribution, and the full mass is of order

$$m_{\psi_{X'}} \approx h^2\mu_\phi \, N_c\gamma \, . \tag{5.37}$$

Of course this vanishes in the limit $\gamma \to 0$, as required from Section 5.4.

Interestingly, we will see in Section 5.6 that the Majorana gaugino masses are proportional to $(1 + N_c\gamma)$. By changing the dimensionless parameter γ, the adjoint fermions may thus be made lighter or heavier than the gauginos. This allows a variety of spectra with different phenomenological signatures, see Section 5.6.

As for the bosons of X, both the adjoint and one component of the singlet acquire one loop masses of order m_{CW}; see Eq. (5.23). The other part of the singlet, $\mathrm{Arg}(X)$, is a massive R-axion. This is because X has a large nonzero expectation value $X_0 \sim 16\pi^2\mu_\phi \gg \mu_\phi$, which spontaneously breaks the approximate $U(1)_R$ symmetry at a scale much larger than any explicit breaking. The mass of the R-axion is given by

$$m_a^2 = \frac{2\sqrt{N_c}}{N_c|X_0|} \, \mathrm{Re}\left[h\mu^2 \, (h^2\mu_\phi)^*\right] \sim b|h^4 \, \mu^2| \, . \tag{5.38}$$

This is of the same order as the one loop mass m_{CW}, Eq. (5.23).

Finally, the $(Y, \chi, \tilde{\chi})$ and $(Z, \tilde{Z}, \rho, \tilde{\rho})$ sectors are as in Section 5.3.1. We remind the reader that we have gauged the $U(1)_V$ symmetry, and g_V denotes its gauge coupling. The (otherwise massless) fields from $\mathrm{tr}(\chi - \tilde{\chi})$ acquire masses of order $g_V\mu$, as shown in the table. Furthermore, the NG bosons from (ρ, $\tilde{\rho}$, Z, $\tilde{Z}$) acquire a one loop mass of order $g_{SM}\mu/4\pi$ once the Standard Model is gauged, as a subgroup of the flavor symmetry group. The lightest of these is stable due to the unbroken messenger number $U(1)'$ from Eq. (5.27).

5.5.2 Lifetime of the metastable vacuum

Here we check that the metastable non-supersymmetric vacuum can be sufficiently long-lived. This vacuum can decay to the ISS-like supersymmetric vacuum with $k = N_f - N_c$, or to the supersymmetric vacua with $k < N_f - N_c$ (see Section 5.2.1). The decay to the vacua with

	Fermions				Bosons			
	Weyl mult.	mass	$U(N_c)$	$SU(\tilde{N}_c)_D$	Real mult.	mass	$U(N_c)$	$SU(\tilde{N}_c)_D$
tr$X$	1	0	1_0	1	1 1	$\mathcal{O}(m_{CW})$ $\mathcal{O}(\sqrt{b}h^2\mu)$	1_0 1_0	1 1
X'	N_c^2-1	$h^2\mu_\phi N_c\gamma$	Adj_0	1	$2(N_c^2-1)$	$\mathcal{O}(m_{CW})$	Adj_0	1
Y, χ, $\tilde{\chi}$	$\tilde{N}_c^2$ $\tilde{N}_c^2$ $\tilde{N}_c^2-1$ 1	$\mathcal{O}(h\mu)$ $\mathcal{O}(h\mu)$ $g_{\mathrm{mag}}\mu$ $g_V\mu$	1_0 1_0 1_0 1_0	Adj Adj Adj 1	$2\tilde{N}_c^2$ $2\tilde{N}_c^2$ $2(\tilde{N}_c^2-1)$ 2	$\mathcal{O}(h\mu)$ $\mathcal{O}(h\mu)$ $g_{\mathrm{mag}}\mu$ $g_V\mu$	1_0 1_0 1_0 1_0	Adj Adj Adj 1
Z,$\tilde{Z}$, ρ, $\tilde{\rho}$	$2N_c\tilde{N}_c$ $2N_c\tilde{N}_c$	$\mathcal{O}(h\mu)$ $\mathcal{O}(h\mu)$	$\square_1+\overline{\square}_{-1}$ $\square_1+\overline{\square}_{-1}$	$\square+\overline{\square}$ $\square+\overline{\square}$	$2N_c\tilde{N}_c$ $2N_c\tilde{N}_c$ $2N_c\tilde{N}_c$ $2N_c\tilde{N}_c$	0_{NGB} $\mathcal{O}(h\mu)$ $\mathcal{O}(h\mu)$ $\mathcal{O}(h\mu)$	$\square_1$ $\overline{\square}_{-1}$ $(\square_1+$ $\overline{\square}_{-1})$	$\overline{\square}$ $\square$ $(\overline{\square}+$ $\square)$

Table 5.2: The mass spectrum, including one loop corrections (but without Standard Model gauge interactions), grouped in sectors with Str $M^2 = 0$. Notice the appearance of the Goldstino in the tr (X) sector. The details of the spectrum are described further in the text. Notation is as in Figure 1.

$k < N_f - N_c$ requires changing the expectation value of (some of the elements of) $q\tilde{q}$, from $h\mu^2$ to 0. This is strongly suppressed by the quartic potential term $V = \ldots + |hq\tilde{q}|^2$. The dominant decay channel will be to the supersymmetric vacuum with $k = N_f - N_c$, which we now analyze.

The lifetime of the vacuum may be estimated using semiclassical techniques and is proportional to the exponential of the bounce action, e^B [163]. We will see that the tunneling takes place in the direction of tr X, in a region where $q\tilde{q} \approx \mu^2$ is almost constant. The potential as a function of tr X, including the one loop quantum corrections from the Coleman-Weinberg potential, is given in the Appendix and shown in Figure 5.1. It may be modeled as a triangular barrier, and the bounce action may be estimated using the results in [164].

We will see in the next section that, in order to have large enough gaugino masses but a low SUSY-breaking scale and low sfermion masses, the ratio μ_ϕ/μ cannot be made too small. Nonetheless, it is useful to first analyze the bounce action in the limit $\mu_\phi \ll \mu$, where it is clear the vacuum is parametrically stable.

The dimensionful parameters controlling the shape of the potential are μ and μ_ϕ. We assume h, γ, N_f, and N_c are all of order 1. The SUSY vacua are parametrically far away from the metastable vacua in the limit

$$\epsilon \equiv \left| \frac{\mu_\phi^2}{b\mu^2} \right| \ll 1 \ . \tag{5.39}$$

In this limit, the calculation of the bounce action is very similar to that done in [145], as long as only $\mathrm{tr}\, X$ varies. Let us assume $q\tilde{q}$ is essentially constant.

The metastable SUSY-breaking vacuum lies at $X_0 \sim \mu_\phi/b$, the peak of the potential is near $X_{\text{peak}} \sim b\mu^2/\mu_\phi$, and the SUSY vacuum is at $X_{\text{susy}} \sim \mu^2/\mu_\phi$, where phases and $\mathcal{O}(1)$ numbers have been ignored. Moreover, the potential difference between the peak and the metastable SUSY-breaking minimum is roughly $V(X_{\text{peak}}) - V(X_0) \sim b\,\mu^4$, much smaller than $V(X_0) - V(X_{\text{susy}}) \sim \mu^4$. The results of [164] then show that the field tunnels not to the SUSY vacuum directly but rather to $X_{\text{tunnel}} \gtrsim X_{\text{peak}}$. For this value of X_{tunnel}, Eq. (5.8) implies $q\tilde{q} \approx \mu^2$, and thus $q\tilde{q}$ indeed stays approximately constant in the tunneling region. This confirms that the results in [164] apply.

In the limit $\epsilon \ll 1$, the bounce action scales parametrically as

$$B \sim \frac{(X_{\text{tunnel}})^4}{V(X_{\text{peak}}) - V(X_0)} \sim b\,\frac{1}{\epsilon^2}, \tag{5.40}$$

where we have neglected some numerical factors, see [164]. Thus, $B \to \infty$ as $\epsilon \to 0$, and the metastable vacuum can be made parametrically long-lived.

In Section 5.6, we will see that in order to obtain sfermion masses that are roughly of the same size as gaugino masses, we need to take $\mu_\phi \sim b\mu$ (and thus $\epsilon \sim b$.) In this regime X_0, X_{peak} and X_{tunnel} are all parametrically of order bX_{SUSY}. A numerical study is required to determine the existence and lifetime of the metastable vacuum. Taking the gaugino masses to lie at their experimental lower bound, of order 100 GeV, we find that the existence of a metastable vacuum sets a lower bound on the sfermion masses — typically a few TeV for the squarks and at least a few hundred GeV for the right-handed sleptons. Once such a metastable vacuum is obtained, it is easy to make the bounce action larger than the required 400 by a small increase (of order 5%) in the sfermion masses. The details of the spectrum, together with a more precise estimate of the lower bound on the sfermion masses, and the implications for the tuning of electroweak symmetry breaking, will be given in [155].

5.6 Comments on the phenomenology

This section briefly discusses some of the phenomenology associated with the multitrace deformation of the ISS model, equation (5.32). The details will be left to a forthcoming publication [155].

The ISS-like supersymmetry breaking models are interesting from a phenomenological point of view due to the presence of the large global symmetry group

$$SU(\tilde{N}_c)_V \times SU(N_c) \times U(1)' . \tag{5.41}$$

A model of direct gauge mediation can be built by weakly gauging a subgroup of (5.41) and identifying it with the Standard Model (SM) gauge group. The fields ρ, Z, $\tilde{\rho}$, and $\tilde{Z}$ in (5.12) and (5.13) act as messengers that mediate the supersymmetry breaking effects to the visible sector. Loops involving these messengers can give non-zero masses to the scalar superpartners of the SM fermions and, provided there is no unbroken R-symmetry, non-zero Majorana fermion masses to the gauginos.

In this section, we will consider gauging the $SU(3) \times SU(2) \times U(1)$ subgroup of $SU(N_c)$ for $N_c = 5$ in the $\gamma \neq 0$ model, and identifying it with the SM gauge group. (The effect of gauging a subgroup of $SU(\tilde{N}_c)_V$ will be discussed in [155].)

Under the SM gauge group $SU(3)_C \times SU(2)_L \times U(1)_Y$, the adjoint field X' decomposes as

$$X' = X_{\mathbf{24}} = X_{(\mathbf{8},\mathbf{1})_0} \oplus X_{(\mathbf{1},\mathbf{3})_0} \oplus X_{(\mathbf{3},\mathbf{2})_{-5/6}} \oplus X_{(\bar{\mathbf{3}},\mathbf{2})_{5/6}} \oplus X_{(\mathbf{1},\mathbf{1})_0} . \tag{5.42}$$

The fermions from the superfields $X_{(\mathbf{8},\mathbf{1})_0}$, $X_{(\mathbf{1},\mathbf{3})_0}$, and $X_{(\mathbf{1},\mathbf{1})_0}$ carry the same gauge charges as the gluino, wino, and bino, respectively, and the first two could be directly produced at colliders.[4] Also, there are new light fermions from the superfields $X_{(\mathbf{3},\mathbf{2})_{-5/6}}$ and $X_{(\bar{\mathbf{3}},\mathbf{2})_{5/6}}$; these are stable unless given new interactions, and require a special discussion below.

5.6.1 Phenomenology of $\psi_{X'}$ and λ

A very important property of the model is that *the gauginos and the adjoint $\psi_{X'}$ do not mix.* This is due to the fact that λ and $\psi_{X'}$ have charge conjugation transformations that differ by a sign,

$$C(\psi_{X'_{ij}}) = \psi_{X'_{ji}} \ , \ C(\lambda_{ij}) = -\lambda_{ji} . \tag{5.43}$$

This discrete symmetry forbids any mixing at low orders between the two sets of fermions. More precisely, C-violation in the SM allows λ and $\psi_{X'}$ to mix, but this occurs only at three loops and is thus negligibly small.

Let us estimate the gaugino and $\psi_{X'}$ masses. As discussed in Section 5.5.1, the metastable vacuum has an approximate R-symmetry that is spontaneously broken through the non-zero

[4]The X bosons in (5.42) get a mass of order $\sqrt{b}h^2\mu \sim \mathcal{O}(10 \text{ TeV})$ from the Coleman-Weinberg potential and are thus rather heavy. If produced in the early Universe, they would have decayed promptly into ψ_X and a gaugino, excepting gauge singlets which would decay a bit more slowly through higher dimension operators.

vev $X_0 \sim (1+N_c\gamma)\mu_\phi/b$, where $b \sim 1/(16\pi^2)$ is a loop factor (5.22). Therefore, gauginos obtain a one loop mass of order

$$m_\lambda \sim \frac{g^2}{16\pi^2}\, X_0 \sim g^2\,(1+N_c\gamma)\mu_\phi\,. \tag{5.44}$$

Neglecting $\mathcal{O}(1)$ numbers and factors of the gauge coupling g, an interesting phenomenology is obtained for

$$m_\lambda \sim \mathcal{O}\,(1\ \text{TeV})\,, \tag{5.45}$$

i.e. for

$$\mu_\phi \sim \mathcal{O}(1\ \text{TeV}). \tag{5.46}$$

The $\psi_{X'}$ also obtain a mass at one loop, which, using equation (5.37), is of order

$$m_{\psi_{X'}} \sim h^2\,\mu_\phi\,N_c\,\gamma \sim \gamma\,\times\,\mathcal{O}\,(1\ \text{TeV})\,, \tag{5.47}$$

neglecting factors of h and g and other $\mathcal{O}(1)$ numbers. By adjusting γ, $\psi_{X'}$ can be made heavier or lighter than λ, leading to very different collider signatures as we will discuss next.

The $\psi_{X'}$ do not mix with the Standard Model gauginos at a level that determines their decays. Instead, if they are heavy enough, they can decay (promptly) into a gaugino and a gauge boson through the dimension five operator $\psi_{X'}\sigma^{\mu\nu}\lambda F_{\mu\nu}$:

$$\psi_{X'} \to \lambda + \text{gauge boson}\,. \tag{5.48}$$

The gauginos can decay through all the usual supersymmetric decay modes, and/or through the standard coupling of each gaugino to a gauge boson and Goldstino:

$$\lambda \to \psi_{\mathrm{tr}\,X} + \text{gauge boson} \tag{5.49}$$

If instead the $\psi_{X'}$ are lighter than the gauginos, then the gauginos will decay into the $\psi_{X'}$ plus a gauge boson via the above-mentioned operator. The $\psi_{X'}$ decays to a gauge boson and an off-shell gaugino. The precise decay modes and the lifetime of the $\psi_{X'}$ depend on the details of the spectrum, and will be discussed further in [155].

From (5.42), we see that there are *new* $(\mathbf{3},\mathbf{2})$ *fermions*, with charges $(\mathbf{3},\mathbf{2})_{-5/6}$ and $(\bar{\mathbf{3}},\mathbf{2})_{5/6}$. By binding to quarks, these form hadrons, some of which are charged. The lightest of these novel hadrons, whether charged or neutral, would be stable in the model as described so far. But this would be ruled out, since these hadrons would have been created in the early Universe, violating the bounds on the existence of heavy stable particles [165, 166]. These fermions must thus be made to decay through additional baryon-number violating operators in the superpotential and/or the Kähler potential. In [155], we will show that additional dimension five Kähler potential terms, coupling the adjoint X' to SM quarks and leptons, can allow the $(\mathbf{3},\mathbf{2})$ fermions to decay without affecting Big-Bang Nucleosynthesis or violating current bounds on proton decay.

5.6.2 Sfermion masses, the SUSY-breaking scale and a light gravitino

Since the supersymmetry breaking scale is $|\sqrt{F}| = |\sqrt{h}\mu|$ and the mass scale of the messengers is of the same order, the soft scalar masses are roughly given by

$$m_S \sim \frac{g^2}{16\pi^2}\,\mu\,. \tag{5.50}$$

Comparing this to (5.44), the sfermions and gauginos have similar masses if

$$\mu_\phi \sim \mu/(16\pi^2). \tag{5.51}$$

We recall that the existence and longevity of the metastable vacuum requires $\mu_\phi \ll \mu$, see Section 5.5.2.

More concretely, there is an interesting parameter region characterized by (5.51) and a low supersymmetry breaking scale

$$\sqrt{F} \approx \mu \sim \mathcal{O}\,(100 - 200 \text{ TeV})\,. \tag{5.52}$$

In this case, the heaviest sfermions (squarks) have masses of a few TeV, the lightest sfermions (right-handed sleptons) haves masses of a few hundred GeV, the gaugino masses are of order several hundred GeV, and there is a large enough lifetime for the metastable vacuum. The gravitino mass is

$$m_{3/2} \sim \frac{F}{\sqrt{3}M_{\mathrm{Pl}}} \sim \mathcal{O}(1\text{–}10 \text{ eV})\,, \tag{5.53}$$

where $M_{\mathrm{Pl}} \simeq 2.4\times10^{18}$ GeV is the reduced Planck mass. Such a light gravitino does not violate any cosmological or astrophysical constraints [172].

5.6.3 Further comments on the spectrum

As discussed in Section 5.5, the messenger sector (ρ, $\tilde\rho$, Z, $\tilde Z$) contains $2N_c\tilde N_c$ real NG bosons, all of which become massive at one loop after weakly gauging the flavor symmetry. In the parameter range (5.52), this mass is of order of several TeV. The $U(1)'$ messenger number in (5.27) forbids the decay of the lightest of these messenger particles, which is thus stable. If the lightest messenger is neutral and weakly interacting and has an appreciable relic density, it would have a tree-level coupling to nuclei via Z-boson exchange and would have been seen at a dark matter direct detection experiment [167]-[171]. If the stable state is charged and/or colored, the experimental constraints are even stronger [165, 166]. Thus experimental constraints rule out the possibility that the lightest messenger is dark matter; this will be investigated further in [155].

We also note that the SM gauge couplings have a Landau pole well below the GUT scale, due to the presence of extra matter charged under the SM gauge group. As one runs up to the high scale, the $SU(3)_C$ gauge coupling blows up first at about 10^9 (10^7) GeV for $\tilde{N}_c = 1$ (3), so that new physics has to enter at or below this scale. Larger values of $\tilde{N}_c$ lower this scale to the point that it affects our discussion materially. See [173] for a recent discussion of the Landau pole problem in ISS-like SUSY-breaking models.

5.6.4 Illustrative choices of parameters

We postpone a careful study of the various constraints to [155], but preliminarily it appears possible to satisfy simultaneously all of the conditions considered above. For example, for $\tilde{N}_c = 1$,[5] the parameters of the electric theory Eq. (5.4) that are consistent with (5.51) and (5.52) are m of order 0.01–10 TeV, $\Lambda \sim 10^{3-5}$ TeV, and $\Lambda_0 \sim 10^{6-9}$ TeV. With these choices, the models appear to have no insuperable problem below the scale of the Landau pole.

On the other hand, for $\tilde{N}_c \geq 3$, Λ has to be below 10^3 TeV, and the ratio m/Λ is not parametrically small. In this case, the corrections from the microscopic theory are not guaranteed to be small, and the violations of the approximate symmetries may be large. In particular, the cancellations described in section 5.4.2 may be imperfect, requiring a more elaborate analysis. However, the argument for nonzero γ still holds, and its effects can still dominate, in which case the phenomenology outlined here will be largely unchanged.

5.6.5 Summary

While these models are not yet entirely plausible, they represent an advance over the models with $SU(N_c)$ gauged and $\gamma = 0$, which as we showed are excluded by the presence of overly-light charged and colored fermions. We have demonstrated that with $\gamma \neq 0$, it is possible to obtain models with a long-lived metastable vacuum, a spectrum with all standard model superpartners in the TeV range, and with no obvious unresolvable conflict with any experiment.

[5] In this case, the magnetic gauge group is trivial and, after a field redefinition, the superpotential is given by (5.5) plus $\det \Phi/\Lambda^{N_c-2}$. For $N_c > 2$ this term is negligible near the origin, so our analysis is self-consistent.

The minimal versions of these models have new TeV-scale fermions in the adjoint representations of the Standard Model gauge group that do not mix with standard model gauginos. They also have squarks and sleptons significantly heavier than the gauginos, and exotic stable hadrons which must be made to decay through additional interactions. They also suffer from the ubiquitous intermediate-scale Landau pole for standard model gauge couplings. We will pursue various associated model-building issues, and study in more detail the phenomenology of these models in [155].

5.7 Appendix: One loop calculations

In this appendix we collect the one loop calculations for the ISS model with multitrace quadratic deformations. The superpotential is

$$W = h \operatorname{tr} q\Phi\tilde{q} - h\mu^2 \operatorname{tr}\Phi + \frac{1}{2}h^2\mu_\phi \operatorname{tr}\Phi^2 + \frac{1}{2}h^2\mu_\phi\gamma\,(\operatorname{tr}\Phi)^2 \tag{5.54}$$

where $\Phi = \Phi_{N_f\times N_f}$, $q = q_{\tilde{N}_c\times N_f}$ and $\tilde{q} = \tilde{q}_{N_f\times\tilde{N}_c}$.

5.7.1 Appendix: Messenger sector

Let us consider separately the cases $k = N_f - N_c$ and $k < N_f - N_c$ (see Section 5.4.1).

Case $k = N_f - N_c$

The parametrization of the metastable minima is given by Eqs. (5.12) and (5.13). Around these minima the superpotential is

$$\begin{aligned} W \;=\;& hq_0\tilde{q}_0 \operatorname{tr} Y - h\mu^2 \operatorname{tr} Y - h\mu^2 \operatorname{tr} X + h \operatorname{tr} q_0 Y\tilde{\chi} + h\tilde{q}_0 \operatorname{tr}\chi Y \\ &+hq_0 \operatorname{tr} Z\tilde{\rho} + h\tilde{q}_0 \operatorname{tr}\rho\tilde{Z} + \frac{1}{2}h^2\mu_\phi\left(\operatorname{tr} Y^2 + \gamma(\operatorname{tr} Y)^2\right) + h^2\mu_\phi \operatorname{tr} Z\tilde{Z} \\ &+\frac{1}{2}h^2\mu_\phi\left(\operatorname{tr} X^2 + \gamma(\operatorname{tr} X)^2\right) + h^2\mu_\phi\gamma \operatorname{tr} X \operatorname{tr} Y \\ &+h \operatorname{tr}\chi Y\tilde{\chi} + h \operatorname{tr}\rho X\tilde{\rho} + h \operatorname{tr}\rho\tilde{Z}\tilde{\chi} + h \operatorname{tr}\chi Z\tilde{\rho} \end{aligned} \tag{5.55}$$

and the non-zero F-term is

$$\partial_{X_{ij}} W = \left(-h\mu^2 + h^2\mu_\phi(1+N_c\gamma)X_0\right)\delta_{ij}\,. \tag{5.56}$$

We recall the ansatz (5.14),

$$\langle X\rangle = X_0\, I_{N_c\times N_c}\;,\;\langle\chi\rangle = q_0\, I_{\tilde{N}_c\times\tilde{N}_c}\;,\;\langle\tilde{\chi}\rangle = \tilde{q}_0\, I_{\tilde{N}_c\times\tilde{N}_c}\,. \tag{5.57}$$

The $q_0\tilde{q}_0$ vev completely Higgses the dual gauge group $SU(\tilde{N}_c)_G$ and the $U(1)_V$. To determine X_0, one must compute the Coleman-Weinberg potential from the tree level masses of the messenger sector. The ansatz (5.57), which will be checked self-consistently, simplifies the computations since the mass eigenstates are then independent of their flavor index. One can thus suppress color and flavor indices in the following.

The messenger sector contains the fields ρ, $\tilde{\rho}$, Z and $\tilde{Z}$, that couple to the non-zero F-term. Let us define

$$\hat{\psi} = \begin{pmatrix} \psi_\rho & \psi_Z \end{pmatrix}^T \qquad \hat{\tilde{\psi}} = \begin{pmatrix} \psi_{\tilde{\rho}} & \psi_{\tilde{Z}} \end{pmatrix}^T \qquad \hat{\phi} = \begin{pmatrix} \rho & Z & \tilde{\rho}^* & \tilde{Z}^* \end{pmatrix}^T \tag{5.58}$$

for the messenger gauge eigenstates. The Weyl fermions combine into Dirac fermions and the messenger masses can be written as

$$\mathcal{L}_{mess,mass} = -\hat{\tilde{\psi}} M_{mess,f} \hat{\psi} - h.c. - \hat{\phi}^\dagger M^2_{mess,b} \hat{\phi} \tag{5.59}$$

where the messenger mass matrices are

$$M_{mess,f} = h \begin{pmatrix} X_0 & q_0 \\ \tilde{q}_0 & h\mu_\phi \end{pmatrix}, \quad M^2_{mess,b} = \begin{pmatrix} M^\dagger_{mess,f} M_{mess,f} & -h^* F^*_X \\ -hF_X & M_{mess,f} M^\dagger_{mess,f} \end{pmatrix} \tag{5.60}$$

and

$$-F^*_X = h \begin{pmatrix} -\mu^2 + h\mu_\phi(1+N_c\gamma)X_0 & 0 \\ 0 & 0 \end{pmatrix}. \tag{5.61}$$

For $\tilde{q}_0 = q_0$ the fermionic and bosonic messenger masses are ($\sigma = \pm 1$ and $\eta = \pm 1$)

$$m^2(X_0) = |h|^2 \Bigg(|q_0|^2 + \frac{1}{2}|X_0|^2 + \frac{1}{2}|h\mu_\phi|^2 + \frac{1}{2}\sigma\sqrt{\left(|X_0|^2 - |h\mu_\phi|^2\right)^2 + 4|q_0X_0^* + q_0^* h\mu_\phi|^2} \Bigg) \tag{5.62}$$

$$\tilde{m}^2(X_0) = |h|^2 \Bigg(|q_0|^2 + \frac{1}{2}|X_0|^2 + \frac{1}{2}|h\mu_\phi|^2 + \frac{1}{2}\eta|\mu^2 - h\mu_\phi(1+N_c\gamma)X_0| + \frac{1}{2}\sigma\sqrt{\left(|X_0|^2 - |h\mu_\phi|^2 + \eta|\mu^2 - h\mu_\phi(1+N_c\gamma)X_0|\right)^2 + 4|q_0X_0^* + q_0^* h\mu_\phi|^2} \Bigg). \tag{5.63}$$

The fermion masses have multiplicity $4N_c\tilde{N}_c$ while the complex boson masses have multiplicity $2N_c\tilde{N}_c$.

The messenger mass matrices can be diagonalized by unitary matrices U_f, $\tilde{U}_f$ and U_b such that

$$\psi = U_f \hat{\psi} \qquad \tilde{\psi} = \tilde{U}_f \hat{\tilde{\psi}} \qquad \phi = U_b \hat{\phi} \tag{5.64}$$

where ψ, $\tilde{\psi}$ and ϕ are messenger mass eigenstates. The quadratic lagrangian for the messengers is therefore of the canonical form

$$\mathcal{L}_{mess} = -\sum_{a=1}^{4} \phi_a^\dagger \left(D^2 + \tilde{m}_a^2\right) \phi_a$$
$$+ \sum_{a=1}^{2} \left(\bar{\psi}_a i\bar{\sigma}^\mu D_\mu \psi_a + \bar{\tilde{\psi}}_a i\bar{\sigma}^\mu D_\mu \tilde{\psi}_a - m_a(\tilde{\psi}_a \psi_a + \bar{\tilde{\psi}}_a \bar{\psi}_a)\right). \quad (5.65)$$

Due to the charge conjugation symmetry, it is possible to write the mixing matrices such that $(U_b)_{a\{1,2\}} = (U_b)^*_{a\{3,4\}}$ and $\tilde{U}_f = U_f$. This can be easily seen from the mass matrices for $\tilde{q}_0 = q_0$. This property will be useful when computing one loop corrections to light masses.

Case $k < N_f - N_c$

The fluctuations are parametrized as in Eq. (5.29), so there are extra messenger superfields $(\varphi, \tilde{\varphi})$. The analysis of $(\rho,\, \tilde{\rho},\, Z,\, \tilde{Z})$ proceeds along the same lines as in the case $k = N_f - N_c$, except that the fermion messenger masses have now multiplicity $4(N_f - k)k$ while the complex boson messenger masses have multiplicity $2(N_f - k)k$.

The masses of φ and $\tilde{\varphi}$ are $(\eta = \pm 1)$

$$\begin{aligned} m_\varphi^2(X_0) &= |hX_0|^2 \\ \tilde{m}_\varphi^2(X_0) &= |h|^2 \left(|X_0|^2 + \eta|\mu^2 - h\mu_\phi X_0|\right). \end{aligned} \quad (5.66)$$

The fermion masses have multiplicity $4(N_f - k)(\tilde{N}_c - k)$ while the complex boson masses have multiplicity $2(N_f - k)(\tilde{N}_c - k)$. Importantly, in the limit of small deformation, (5.66) forces $|X_0| \gtrsim |\mu|$ to avoid tachyons.

5.7.2 Appendix: One loop bosonic action

The tree level pseudo-moduli are given by X_0 and $\mathrm{Re}\,\mathrm{tr}(\chi - \tilde{\chi})$, and they are stabilized by one loop contributions. For $\mu_\phi \ll \mu$, the one loop effective potential for $\mathrm{Re}\,\mathrm{tr}(\chi - \tilde{\chi})$ is the same as in [14] (see Eq. (5.21).) As a result, this field is stabilized at the origin and acquires a mass of order $|h^4\mu^2|/(8\pi^2)$.

Let us now analyze the pseudo-modulus X_0; for $k \leq N_f - N_c$, this is a $(N_f - k) \times (N_f - k)$ matrix. The ISS-type vacua correspond to $k = N_f - N_c$. We will argue here that the new metastable vacua corresponding to the case $k < N_f - N_c$ do not exist, as they are located in a region where some of the fields become tachyonic. The only remaining metastable vacua will be the ISS-type vacua.

The one loop correction from integrating out the messenger fields is

$$\begin{aligned} V_{CW} &= \frac{(N_f-k)k}{32\pi^2}\sum_{\sigma,\eta=\pm1}\left[\tilde{m}(X_0)^4\log\frac{\tilde{m}(X_0)^2}{\Lambda^2}-m(X_0)^4\log\frac{m(X_0)^2}{\Lambda^2}\right] \\ &+ \frac{(N_f-k)(\tilde{N}_c-k)}{32\pi^2}\sum_{\eta=\pm1}\left[\tilde{m}_\varphi(X_0)^4\log\frac{\tilde{m}_\varphi(X_0)^2}{\Lambda^2}-m_\varphi(X_0)^4\log\frac{m_\varphi(X_0)^2}{\Lambda^2}\right]. \end{aligned} \tag{5.67}$$

with masses given in Section 5.7.1. We find that the full potential

$$V = V_{tree} + V_{CW} \tag{5.68}$$

has a metastable vacuum if $k = N_f - N_c$, but there are no metastable vacua for $k < N_f - N_c$. Let us discuss in more detail how this occurs.

For $k = N_f - N_c$, the messengers are non-tachyonic for any X_0; see Eq. (5.62). As explained in Section 5.4.1, the metastable vacuum appears because quantum corrections at small X_0 are large enough to overwhelm the slope of the classical potential, which would otherwise push X_0 toward the supersymmetric vacua. The supersymmetry breaking vacuum is located in the range $|X_0/\mu| \lesssim 1$, far from the supersymmetric vacuum.

The situation for $k < N_f - N_c$ is very different, because the messengers $(\varphi, \tilde{\varphi})$ are tachyonic at small X_0; see Eq. (5.66). For $|X_0/\mu| \gtrsim 1$ these tachyons are absent, but in this regime the one loop corrections $V_{CW}(X_0)$ grow only logarithmically with $|X_0|$, and cannot compete with the classical potential to create a metastable vacuum. One may directly check that the Hessian of the potential always has a negative eigenvalue for $|X_0| \gtrsim |\mu|$ (and all values of k). Notice that if one used the quadratic expansion of V_{CW} around the origin $X_0/\mu = 0$, instead of the full logarithmic form, it would suggest the existence of metastable vacua with $k < N_f - N_c$ and $|X_0/\mu| \sim 1$ [146]. But this approximation is inconsistent, and when the full logarithmic dependence of V_{CW} is included, these vacua become unstable and disappear.

Summarizing, only the ISS-type minima with $k = N_f - N_c$ survive, and the adjoint (X') and singlet $(\mathrm{tr}\, X)$ components of the pseudo-modulus X acquire one loop masses

$$m^2_{X'} \approx b\,|h^2\mu|^2 + |h^2\mu_\phi|^2 \tag{5.69}$$

$$m^2_{\mathrm{tr}\,X} \approx b\,|h^2\mu|^2 + |h^2\mu_\phi(1+N_c\gamma)|^2. \tag{5.70}$$

The R-axion, discussed in section 5.5.1, has a mass of this same order, Eq. (5.38). All bosons which were light at tree level thus become heavy at one loop, with masses of order $m_{CW} = \sqrt{b}\,|h^2\mu|$.

5.7.3 Appendix: One loop fermionic action

In this section we discuss the low energy fermionic spectrum of the theory, taking into account one loop effects.

Goldstino

At one loop, the Goldstino appears as a combination of $\psi_{\mathrm{tr}\,X}$, $\psi_{\mathrm{tr}\,Y}$ and $\psi_{\mathrm{tr}\,(\chi+\tilde{\chi})}$, which we now determine. The charge conjugation symmetry forbids mixings with $\psi_{\mathrm{tr}\,(\chi-\tilde{\chi})}$, which is eaten by the $U(1)_V$ gauge fermion and has mass $g_V\mu$.

First, at tree level, in the limit $\mu_\phi = 0$, $\psi_{\mathrm{tr}\,Y}$ and $\psi_{\mathrm{tr}\,(\chi+\tilde{\chi})}$ form a Dirac fermion of mass $h\mu$, while $\psi_{\mathrm{tr}\,X}$ is massless; see Eq. (5.55). When μ_ϕ and γ are nonzero, $\psi_{\mathrm{tr}\,X}$ acquires a mass term proportional to μ_ϕ, and there is a $\psi_{\mathrm{tr}\,X}$-$\psi_{\mathrm{tr}\,Y}$ mixing of order $\gamma\mu_\phi$. There is no linear combination of the fields $\psi_{\mathrm{tr}\,Y}$, $\psi_{\mathrm{tr}\,(\chi+\tilde{\chi})}$ and $\psi_{\mathrm{tr}\,X}$ that is massless at tree level.

Once one loop effects are taken into account, supersymmetry is spontaneously broken, so we should get a massless Goldstino. Since the dominant F-term comes from $F_{\mathrm{tr}\,X}$, the Goldstino will be approximately aligned with $\psi_{\mathrm{tr}\,X}$. Indeed, the tree level plus one loop $\psi_{\mathrm{tr}\,X}\,\psi_{\mathrm{tr}\,X}$ mass element is (using the messenger mass eigenbasis),

$$m_{\psi_{\mathrm{tr}\,X}} = h^2\mu_\phi(1+N_c\gamma) - \frac{2h^2\tilde{N}_c}{16\pi^2}\sum_{j=1}^{4}\sum_{k=1}^{2}(U_f^*)_{k1}\,(\tilde{U}_f^*)_{k1}\,(U_b^*)_{j1}\,(U_b)_{j3}\,I[\tilde{m}_j, m_k] \tag{5.71}$$

where the sums are over messenger fields and

$$I(\tilde{m}_j, m_k) = m_k\left[\ln\left(\frac{\Lambda^2}{m_k^2}\right) - \frac{\tilde{m}_j^2}{\tilde{m}_j^2 - m_k^2}\ln\left(\frac{\tilde{m}_j^2}{m_k^2}\right)\right]. \tag{5.72}$$

It can be checked that the tree and one loop terms in (5.71) largely cancel, leaving only a term of order $\mu_\phi/(16\pi^2)$, of the same size as two loop corrections.

There are also one loop mixings between $\psi_{\mathrm{tr}\,X}$ and $\psi_{\mathrm{tr}\,Y}$, $\psi_{\mathrm{tr}\,(\chi+\tilde{\chi})}$. For simplicity, let us consider first the ISS model, corresponding to the limit $\mu_\phi = 0$. The mass-mixing comes from the two-point function $\psi_{\mathrm{tr}\,X}\,\psi_{\mathrm{tr}\,(\chi+\tilde{\chi})}$, which is allowed by R-symmetry. A calculation along the same lines as in (5.71) shows that this mass-mixing is of order $\mu/(16\pi^2)$. The Goldstino is hence predominantly in the $\psi_{\mathrm{tr}\,X}$ direction, with a small (of order $1/(16\pi^2)$) component along $\psi_{\mathrm{tr}\,Y}$. This implies that in ISS, one loop corrections generate a nonzero F-term

$$|F_{\mathrm{tr}\,Y}| \sim \frac{|F_{\mathrm{tr}\,X}|}{16\pi^2}\,.$$

For μ_ϕ/μ nonzero but small, the Goldstino also has a small component along $\psi_{\mathrm{tr}\,(\chi+\tilde{\chi})}$, with mixing angle of order $|X_0/(16\pi^2\mu)|$. This is smaller than the mixing of $\psi_{\mathrm{tr}\,X}$ and $\psi_{\mathrm{tr}\,Y}$, and is consistent with a one loop F-term

$$|F_{\mathrm{tr}\,(\chi+\tilde{\chi})}| \sim \left|\frac{X_0}{16\pi^2\mu}\right| |F_{\mathrm{tr}\,X}|\,.$$

Gauginos and the fermions $\psi_{X'}$

There are no mixings between the gauginos and the $\psi_{X'}$ fermions at one and two loops, because they are forbidden by charge conjugation. The expression for the one loop gaugino mass is

$$m_\lambda = \frac{2g^2\tilde{N}_c}{16\pi^2} \sum_{c=1}^{2}\sum_{d=1}^{2}\sum_{j=1}^{4}\sum_{k=1}^{2} (U_f^*)_{kc}\,(\tilde{U}_f^*)_{k,d}\,(U_b)_{jc}\,(U_b^*)_{j,d+2}\,I[\tilde{m}_j, m_k]\,. \tag{5.73}$$

which is of order $g^2\mu_\phi$. The one loop computation for the masses of $\psi_{X'}$ is nearly identical to that of $\psi_{\mathrm{tr}\,X}$, given in (5.71), since they have the same interactions with the messenger fields. The result is

$$m_{\psi_{X'}} = h^2\mu_\phi - \frac{2h^2\tilde{N}_c}{16\pi^2} \sum_{j=1}^{4}\sum_{k=1}^{2} (U_f^*)_{k1}\,(\tilde{U}_f^*)_{k1}\,(U_b^*)_{j1}\,(U_b)_{j3}\;I[\tilde{m}_j, m_k] \tag{5.74}$$

The cancellation that occurs in (5.71) occurs here as well, but leaves over a large remainder, of order $|\gamma\mu_\phi|$.

Chapter 6

A Pyramid Scheme for Particle Physics

6.1 Introduction

In this chapter we discuss in detail the findings of the work done in collaboration with T. Banks [10].

Direct gauge mediation models are attractive from a variety of points of view. They are the most straightforward solution to the SUSY flavor problem of the MSSM. The general structure of a direct gauge mediation model is that of a supersymmetric quivering moose with gauge group $G \times SU(1,2,3)$. There are chiral fields F_i^A which transform in irreducible representations of both groups, possibly including singlets which can couple to the non-singlets in the cubic superpotential. The fields that are singlets under G, but not $SU(1,2,3)$, are assumed to be precisely the 3 generations plus two Higgs fields of the MSSM. At the scale Λ_G the G gauge interactions become strong and are assumed to produce a meta-stable SUSY violating state[1].

One of the phenomenological virtues of the MSSM is its successful prediction of coupling constant unification. If we wish to preserve this prediction, to one loop order, then the G-charged chiral fields must lie in complete multiplets of the unified group. Furthermore, there are strong constraints on the gauge group G, and the additional matter content, from the requirement that the standard model gauge couplings remain in the perturbative regime all the way up to the GUT scale. As far as we know, the only phenomenologically viable choice of G which *might* satisfy these constraints is $SU(5)$, and one is led to the Pentagon model [187]. Even in the Pentagon model the dynamics which leads to a phenomenologically viable SUSY violating state is somewhat conjectural. In all other examples that we have studied, there are dramatic clashes with existing experiments - spontaneous breakdown of charge or color, or unobserved light states.

Recently, a careful two loop study of the standard model running couplings has shown [188]

[1] To ensure this, it may be necessary to introduce quadratic terms in the superpotential by hand [179]. Depending on one's theoretical orientation, one may view these as arising from retro-fitting [180] or from Cosmological SUSY Breaking [181].

that the Pentagon is viable only if the scale Λ_5, and the ISS mass terms are both > 1000 TeV. This is incompatible with the original motivation for the Pentagon model, in which it was the low energy implementation of Cosmological SUSY Breaking. For most readers it will be more significant that the lower bound on the SUSY breaking scale pushes up against the forbidden window of gravitino masses. A conservative reading of the literature on cosmological gravitino bounds leads one to conclude that $m_{3/2} < 30$ eV, corresponding to a bound on the highest SUSY breaking scale of order $\sqrt{6} \times 10^2$ TeV. If we raise the scale high enough to get to the high side of the forbidden window for gravitino masses, then we lose the solution to the SUSY flavor problem.

Yet another problem with the Pentagon model surfaced in a recent paper [178]. The pseudo Nambu-Goldstone boson of spontaneously broken penta-baryon number, gets its mass from an operator of dimension 7. If the scale associated with this irrelevant operator is larger than $\sim 10^{10}$ GeV then the PNGB is copiously produced in stars and leads to unobserved stellar cooling[2].

Finally, like most gauge mediated models, the Pentagon model does not have a SUSY WIMP dark matter candidate. One is forced to invoke either a QCD axion, or the scenario mentioned in the previous footnote.

In this paper we will show that all of these problems can be solved simultaneously if we replace unification in $SU(5)$ or some larger group, with *trinification* [174]. We will present an explicit direct mediation model called The Pyramid Scheme, which realizes these ideas. However, we note that the idea of resolving the Landau pole problem of direct mediation with trinification, may be of more general utility.

Trinification and the Pyramid Scheme

In E_6, one generation of standard model fermions is embedded in the [27] representation. E_6 has an $SU_1(3) \times SU_2(3) \times SU_3(3) \rtimes Z_3$ subgroup, under which

$$[27] = (3, 1, \bar{3}) \oplus (\bar{3}, 3, 1) \oplus (1, \bar{3}, 3),$$

with the three groups and representations permuted by the Z_3. $SU_3(3)$ is identified with color, while the electro-weak $SU(2)$ is the upper Cartesian subgroup of $SU_2(3)$. Weak hypercharge is a linear combination of the hypercharge generators of the first and second $SU(3)$ factors. The

[2]It should be noted that if one postulates a scale $\sim 10^8 - 10^{10}$ GeV for the coefficient of the dimension 7 operator, and also a primordial asymmetry in penta-baryon number, then one can get a unified explanation of the baryon asymmetry of the universe, and the origin of dark matter [177].

usual 15 components of the [27] make up a standard model generation, while the Higgs fields $H_{u,d}$ of the MSSM can be obtained in a variety of ways from [27] and [$\bar{27}$] representations of E_6.

The essential idea of trinification, is that, in order to predict gauge coupling unification, it is sufficient, at one loop, to insist that all extra matter between the weak scale and the unification scale, fall into complete multiplets of $SU(3)^3 \rtimes Z_3$, and that there be no strong breaking of this symmetry by Yukawa couplings. The latter requirement is subsumed under the further demand that *all* couplings remain perturbative up to the unification scale, so that one loop renormalization group formulae are a good approximation[3].

Although we have described trinification in terms of embedding in an underlying E_6, it might also be derived in a simple manner from D-brane constructions in Type II string theory, or related geometric engineering models [175]. This notion makes the *Pyramid Scheme*, which we now introduce, particularly natural.

In the Pyramid Scheme we extend the quivering moose of trinification by a fourth $SU(3)$ group, $SU_P(3)$. All standard model fields are singlets of the new group, and we add the new representations

$$\begin{aligned}
\mathcal{T}_1 + \bar{\mathcal{T}}_1 &= (3,1,1,\bar{3}) + (\bar{3},1,1,3), \\
\mathcal{T}_2 + \bar{\mathcal{T}}_2 &= (1,3,1,\bar{3}) + (1,\bar{3},1,3), \\
\mathcal{T}_3 + \bar{\mathcal{T}}_3 &= (1,1,3,\bar{3}) + (1,1,\bar{3},3).
\end{aligned}$$

We call these new matter fields, *trianons*. Note that only the third trianon carries color. Thus, the one loop running of the gauge couplings will be like that in a vanilla gauge mediated model with 3 messengers. One loop perturbative coupling unification will be preserved. The quivering moose of this model has the pyramidal shape of figure 6.1, which accounts for the name.

In a D-brane or geometric engineering construction, trinification corresponds to 3 singular loci (stacks of wrapped D-branes) residing on a set of internal cycles which are permuted by a Z_3 isometry of the compact geometry. We call these the chiral cycles since the chiral fields result from topological intersections of these cycles. The Pyramid Scheme introduces an extra stack of branes, wrapped on a cycle with the appropriate (non-topological) intersection with each of the chiral cycles. The trianon mass terms that we introduce below correspond to small deformations of this extra cycle, so that it no longer intersects the chiral cycles.

[3]Two loop unification in the MSSM works less well than one loop unification, and is subject to unknown unification scale threshold corrections, so we do not consider two loop unification to be a necessary desideratum of a good model.

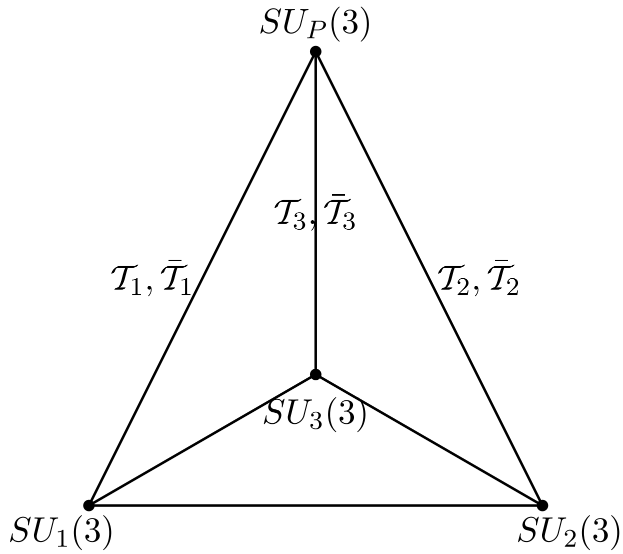

Figure 6.1: Quiver Diagram of the Pyramid Scheme. Standard Model Particles are in broken multiplets running around the base of the pyramid.

As in the Pentagon model, we introduce a chiral field S, singlet under all gauge groups, with superpotential couplings

$$W_S = g_\mu S H_u H_d + \frac{g_T}{3} S^3 + \sum_{i=1}^{3} y_i S \mathcal{T}_i \bar{\mathcal{T}}_i,$$

where the bilinears in the trianon fields are the unique $SU(3)^4$ invariants. The Z_3 symmetry imposes $y_i = y$, independent of i. Strictly speaking, we do not have to impose this much symmetry on the Yukawa couplings, if they are sufficiently small, because they affect gauge coupling running only at two loops. The only inviolable symmetry of this low energy Lagrangian is the low energy gauge symmetry $SU(1,2,3) \times SU_P(3) \times Z_R$[4]. For simplicity however we will assume that the full Pyramid gauge group is broken only by the part of the Lagrangian containing standard model fields, and by the Intriligator-Seiberg-Shih (ISS) [179] trianon mass terms. It is certainly worth exploring more complicated models, in which the gauge symmetry is broken down to the standard model ($\times SU_P(3)$), also in the couplings to S.

The singlet S serves several purposes in the model. Most importantly, the term $|\frac{\partial W}{\partial S}|^2$ ties $SU_L(2) \times U_Y(1)$ breaking to the properties of the meta-stable SUSY violating state of the strong $SU_P(3)$ gauge theory. This predicts $\tan\beta \sim 1$ for the Higgs mixing angle. Secondly, the VEV of S can give rise to the μ term of the MSSM, while F_S generates the B_μ term. We will discuss

[4] Z_R is the discrete R-symmetry required by CSB. We also use it to forbid unwanted dimension 4 and 5 operators in the MSSM. We will discuss it in section 2, below.

mechanisms for generating such VEVs below. We note that the coupling g_μ can ameliorate the little hierarchy problem, but that this might interfere with our desire for a VEV of S.

The rest of this paper is organized as follows. In the next section we find a discrete R-symmetry of the Pyramid model, which outlaws all dimension four and five B and L violating couplings, apart from the neutrino seesaw operator. In section 3 we introduce the ISS mass terms and explore the resulting dynamics of the $SU_P(3)$ gauge theory. We work in the regime where the mass terms for $\mathcal{T}_{1,3}$ are above the $SU_P(3)$ confinement scale Λ_3, while that for $\mathcal{T}_2$ is close to it. This produces a non-trivial Kähler potential for S, and reduces the dynamics to the moduli space non-linear σ model for the $N_F = N_C = 3$ gauge theory with a small mass for the chiral fields. As in the Pentagon model, we assume a meta-stable SUSY violating state of this system, with VEVs for both the pyrma-baryon and pyrmeson fields constructed from $\mathcal{T}_2$. We argue that the extra terms in the potential for S, which come from integrating out $\mathcal{T}_{1,3}$ could lead to a non-zero VEV for this field, if F_S is non-zero. We also find that the gaugino and squark spectra are "squeezed" relative to vanilla gauge mediation models [190], because the colored messengers have a SUSY preserving mass higher than the SUSY breaking scale. We give rough estimates of superpartner masses in this model.

In section 4 we argue that the pyrma-baryons made from $\mathcal{T}_{1,3}$ could be dark matter, if they are produced in the late decay of some other particle with a reheat temperature in the TeV range[5] [22]. The dark matter particles annihilate predominantly to the pseudo Nambu-Goldstone boson (PNGB) of the spontaneously broken pyrma-baryon number, which we call the *pyrmion*. The constituents of the pyrmion do not carry color, and we estimate its mass to be a few MeV, so it can decay only to electrons, positrons, photons and neutrinos. It is possible that this could account for the various dark matter "signals" that have accumulated over the past few years, along the lines of [184]. The mass of the pyrmion is also large enough to avoid constraints from stellar cooling [178]. Section 5 is devoted to conclusions and to many suggestions for further elaboration of this work. In Appendix A we sketch the basis for the revised estimate of the relation between the gravitino mass and the cosmological constant, which we used in the computations of superpartner masses in section 3. In Appendix B we recall, for completeness, the calculation done in [22] of the non-thermal relic density of pyrma-baryons and Appendix C shows some computations.

Throughout this paper we will use the abbreviations, c.c. for cosmological constant, SUSY and SUSic for supersymmetry and supersymmetric, CSB for Cosmological SUSY Breaking,

[5] They could also have the requisite density as a consequence of a primordial asymmetry in one or more of the pyrma-baryon numbers. However, in this case there would be no annihilation signals.

PNGB for pseudo Nambu-Goldstone boson, and LEFT for low energy effective field theory. We will use the phrases *heavy trianons* and *heavy pyrma-baryons* to refer to states constructed from the fields $\mathcal{T}_{1,3}$.

6.2 Discrete R-symmetry: the model

At low energies, the model is $SU_P(3) \times SU(1,2,3)$ where the SM gauge group can be seen as coming from the subgroup $SU(3)^3 \rtimes Z_3 \subset E_6$. In the latter notation, the extra matter fields are

	$SU_1(3)$	$SU_2(3)$	$SU_3(3)$	$SU_P(3)$
$\mathcal{T}_1$	3	1	1	$\bar{3}$
$\bar{\mathcal{T}}_1$	$\bar{3}$	1	1	3
$\mathcal{T}_2$	1	3	1	$\bar{3}$
$\bar{\mathcal{T}}_2$	1	$\bar{3}$	1	3
$\mathcal{T}_3$	1	1	3	$\bar{3}$
$\bar{\mathcal{T}}_3$	1	1	$\bar{3}$	3
S	1	1	1	1

and the model can be represented by the quiver diagram shown in figure 6.1. We want to find an approximate discrete R-symmetry which is exact in the limit of zero ISS masses. We will in fact look for a $U_R(1)$, of which we imagine only a discrete Z_N subgroup is fundamental. A variety of equations below only have to be satisfied modulo N.

The superpotential terms we would like to have in our model are

$$W \supset S\mathcal{T}_i\bar{\mathcal{T}}_i,\ SH_uH_d,\ H_uQ\bar{U},\ H_dQ\bar{D},\ H_dL\bar{E},\ (LH_u)^2$$

which implies that the R-charges satisfy (we denote each R-charge by the name of the corresponding field)

$$\begin{aligned} \mathcal{T}_i + \bar{\mathcal{T}}_i &= 2 - S \\ H_u &= 2 - H_d - S \\ \bar{U} &= H_d + S - Q \\ \bar{D} &= 2 - H_d - Q \\ \bar{E} &= 2 - H_d - L \end{aligned}$$

plus the extra relation from the neutrino seesaw operator. The (approximate) $U_R(1)$ anomaly conditions are

$$\begin{aligned}
SU_P(3)^2U_R(1) &\Rightarrow 2\cdot 3+3(\mathcal{T}_1+\bar{\mathcal{T}}_1+\mathcal{T}_2+\bar{\mathcal{T}}_2+\mathcal{T}_3+\bar{\mathcal{T}}_3-6)=3(2-3S)\\
SU_C(3)^2U_R(1) &\Rightarrow 2\cdot 3+6(Q-1)+3(\bar{U}+\bar{D}-2)+3(\mathcal{T}_3+\bar{\mathcal{T}}_3-2)=0\\
SU_L(2)^2U_R(1) &\Rightarrow 2\cdot 2+(H_u+H_d-2)+9(Q-1)+3(L-1)\\
&\qquad +3(\mathcal{T}_2+\bar{\mathcal{T}}_2-2)=3(3Q+L)-4(S+2)
\end{aligned}$$

which might allow for an S^3 superpotential term if $3S=2 \mod N$.

The dangerous higher-dimensional superpotential and Kähler potential terms can be combined into seven groups (the neutrino seesaw operator is allowed). Operators in each group have the same R-charge (once one takes the $d^2\theta$ for superpotential terms into account).

$$\begin{aligned}
G_1=\{LL\bar{E},\ LQ\bar{D},\ SLH_u\} &\Rightarrow L-H_d\\
G_2=\{LH_u,\ Q\bar{U}\bar{E}H_d,\ \bar{U}\bar{D}^*\bar{E}\} &\Rightarrow L-H_d-S\\
G_3=\{\bar{U}\bar{U}\bar{D}\} &\Rightarrow 3Q+H_d-S-2\\
G_4=\{QQQL\} &\Rightarrow 3Q+L-2\\
G_5=\{QQQH_d,\ QQ\bar{D}^*\} &\Rightarrow 3Q+H_d-2\\
G_6=\{\bar{U}\bar{U}\bar{D}\bar{E}\} &\Rightarrow 3Q+L-2S-2\\
G_7=\{LH_uH_dH_u\} &\Rightarrow L-H_d-2S+2.
\end{aligned}$$

It is possible to forbid all dangerous terms. For example, with $N=5$, and $S=4$, $3Q+L=3$, $L=3+H_d$, and any choice of H_d one finds that all anomaly conditions are satisfied and none of the dangerous terms are allowed. Notice moreover that the S^3 superpotential term and neutrino seesaw operator are allowed by this choice of R-charges. Thus one can engineer a superpotential of the form

$$\begin{aligned}
W=\sum_{i=1}^{3}(m_i+y_iS)\mathcal{T}_i\bar{\mathcal{T}}_i+g_\mu SH_uH_d+\frac{g_T}{3}S^3&\\
+\lambda_uH_uQ\bar{U}+\lambda_dH_dQ\bar{D}+\lambda_LH_dL\bar{E}+\frac{\lambda_\nu}{M}(LH_u)^2+W_0&
\end{aligned}$$

where only the ISS masses m_i and W_0 break the R-symmetry. Note that in this equation $\lambda_{u,d,\nu}$ are all matrices in generation space.

6.3 Breaking R-symmetry and SUSY

We now take into account the dynamical effect of the R-symmetry breaking superpotential

$$\delta W=W_0+m_1\mathcal{T}_1\bar{\mathcal{T}}_1+m_2\mathcal{T}_2\bar{\mathcal{T}}_2+m_3\mathcal{T}_3\bar{\mathcal{T}}_3$$

to the low energy effective Lagrangian. Using conventional effective field theory philosophy, we could ascribe this by the strategy of *retro-fitting* [180]. That is, we imagine that the R-symmetry breaking occurs spontaneously, as a consequence of strong dynamics at a scale $\Lambda_R \gg \Lambda_3$ and that the mass terms arise from irrelevant couplings between this sector and the Pyramid model, and have a size $m_i \sim \frac{\Lambda_R^{d_R}}{M^{d_R - 1}}$, where d_R is the dimension of the operator appearing in lowest dimension R-conserving coupling of the two sectors. M could be either the unification scale or the Planck scale, depending on one's microscopic model for these couplings. W_0 is simply added as a phenomenological fudge to obtain the right value of the cosmological constant. Apart from the exigencies of phenomenology, there is no requirement in this way of thinking, that the operators to be added create a SUSY violating meta-stable state in the low energy theory. Indeed, if one adds operators which do create such a state, one must be careful to engineer the model so that these are the dominant effects of the coupling between the two sectors.

The explanation for δW on the basis of the hypothesis of CSB has a very different flavor. Here, the size of the c.c. and the relation $m_{3/2} = 10K\Lambda^{1/4}$ [6], are fundamental inputs of a microscopic theory of quantum de Sitter space. In order to be consistent with this theory the low energy effective Lagrangian *must* have a meta-stable SUSY violating state[7]. Furthermore, Λ is prescribed by the microscopic theory, and the tuning of W_0 simply implements this prescription in the LEFT.

The $SU_P(3)$ gauge theory is IR free with a small β function. Starting from some unification scale boundary condition, the coupling decreases slowly in the IR. If there were no mass terms m_i it would flow to a free theory and SUSY would be preserved. This could not be the low energy implementation of CSB. We must thus introduce mass terms, in order to produce a dynamical meta-stable SUSY violating state with $m_{3/2} = 10K\Lambda^{1/4}$. In order to do this using the known and conjectured dynamics of $N_F \geq N_C$ SUSY QCD, we take two masses $m_{1,3}$ somewhat larger than the third, m_2. The gauge coupling then becomes strong at a confinement scale Λ_3, and we assume that m_2 is small enough to be treated by chiral perturbation theory in the $N_F = N_C = 3$ moduli space Lagrangian[8]. We must further assume that the unification scale coupling is large enough that m_3/Λ_3 is not too large.

---

[6]See Appendix A for an explanation of the new factor of 10 in this equation. K is for the moment, a "parameter of order 1", which cannot be determined from first principles.

[7]And the Lagrangian must be *above the Great Divide* [21] so that transitions out of this state can be viewed as highly improbable Poincaré recurrences of a low entropy state in a finite system, rather than as an instability.

[8]Another possibility is to take $m_3 > m_{1,2}$. The theory then flows close to an interacting superconformal fixed point and for some range of parameters we may find a calculable meta-stable state. We thank N. Seiberg for explaining this possibility to us. We leave the exploration of this scenario to future work, but note that the meta-stable state has the approximate R-symmetry of ISS vacua, and may be phenomenologically problematic.

The latter assumption, and the choice of m_3 as one of the large masses, is motivated by phenomenology. We will see that taking m_3 somewhat larger than Λ_3 solves one of the fine tuning problems of vanilla gauge mediation. It suppresses the gluino/chargino mass ratio. If m_3 is too large, this suppression produces an unacceptably light gluino.

We can think of the two heavy trianons as analogs of the charmed quark in QCD, while the light one is analogous to the strange quark. For purposes of assessing the nature of the (meta-stable) ground state, we integrate out the heavy trianons, and treat the LEFT by chiral (moduli space) Lagrangian techniques.

For phenomenological reasons, we will take the two heavy trianons to be $\mathcal{T}_{1,3}$. As a consequence the light moduli are color singlets and will give rise to gaugino masses only for the electro-weak gauginos. The gluino mass will be induced by a SUSY breaking mass for $\mathcal{T}_3$, and will be suppressed relative to the chargino masses because this field has a relatively large supersymmetric mass term. This relieves the tension between the experimental lower bound on the chargino mass (which might soon reach 160 GeV as a consequence of the Tevatron trilepton studies [191]), and the large radiative corrections to the Higgs potential coming from heavy gluinos. There will be a similar suppression of the squark to slepton mass ratio, relative to the predictions of vanilla gauge mediation.

The moduli space of the $SU_P(3)$ gauge theory coupled to $\mathcal{T}_2$ consists of a 3×3 complex matrix pyrmeson field, M, transforming in the $[3, \bar{3}]$ of the $SU_L(3) \times SU_R(3)$ chiral flavor group (whose diagonal subgroup contains the action of electro-weak $SU_L(2) \times U_Y(1)$ on the moduli space), and a pair $P, \tilde{P}$ of flavor singlet pyrma-baryon fields which carry opposite values of a new accidental vector-like $U(1)$ quantum number. These are related by a constraint

$$\det M - \Lambda_3 P\tilde{P} = \Lambda_3^3,$$

where Λ_3 is the complex confinement scale of the theory. The Kähler potential is of the form

$$K = |\Lambda_3|^2 h(e_k, x, \tilde{x}),$$

where h is a real permutation invariant function of the variables e_k, the eigenvalues of $Y \equiv \frac{M^\dagger M}{|\Lambda_3|^2}$[9], and of

$$x = \frac{|P|^2}{|\Lambda_3|^2}, \qquad \tilde{x} = \frac{|\tilde{P}|^2}{|\Lambda_3|^2}.$$

The superpotential in the chiral LEFT is $W = W_0 + m_2 \Lambda_3 \operatorname{tr} M$. The matrix M can be expanded as $M = Z\sqrt{\frac{2}{3}} I + Z_a \lambda^a$, where the λ^a are the Gell-Mann matrices. We will look for

[9] Equivalently, a function of $w_k \operatorname{tr} Y^k$, for $k = 1, 2, 3$.

$SU(3)$ invariant states, where $Z_a = 0$. The constraints on the moduli space then imply that $\left(\frac{2}{3}\right)^{3/2} Z^3 = \Lambda_3 P\tilde{P} + \Lambda_3^3$. The superpotential is proportional to Z and the locus $P\tilde{P} = 0$ is supersymmetric. Any SUSY violating meta-stable state will have a non-zero VEV for the pyrma-baryon fields, which we will assume charge conjugation symmetric $\tilde{P} = P$. The constraint then allows us to write both the Kähler potential and superpotential in terms of the unconstrained complex field Z. Our previous remarks about the structure of the Kähler potential imply that it is a function of $Z^\dagger Z$, and that the effective potential is

$$K^{-1}_{Z^\dagger Z} |m_2 \Lambda_3|^2.$$

The existence of a SUSY violating minimum is guaranteed if the positive function $K_{Z^\dagger Z}$ has a maximum at some finite Z. Geometrically, we have a non-compact, circularly symmetric 2-manifold, and we are asking that the length of a tangent vector attains a maximum at some particular radius. We have not been able to find arguments for or against the existence of such a maximum, so we will simply explore the phenomenology of the model, under the assumption that the maximum exists.

It should be noted that we have made several assumptions about the symmetry of the ISS mass terms and of the pyrmeson VEV, which are not required by either fundamental principles or phenomenology. All we are required to preserve in the LEFT is the standard model gauge group, and enough of the trinification structure to guarantee gauge coupling unification. Thus, there is actually a rich class of pyramid schemes to explore in search of a meta-stable state. We only treat the most symmetric of them in this paper.

Given our assumptions, the Pyramid model has two kinds of messengers of gauge mediation, the moduli of the $N_F = N_C = 3$ theory, and the heavy trianons. The scalar fields Z_a will get SUSY violating masses of order m_2, which, apart from $SU(3)$ symmetry, are completely unconstrained and unconnected with the masses of their fermionic partners. Therefore we will obtain one loop masses for the $SU_L(2) \times U_Y(1)$ gauginos, of order

$$m^i_{1/2} = 3 X_i \frac{\alpha_i}{4\pi} m_2.$$

The X_i are "order one" numbers, which cannot be calculated without complete knowledge of the Kähler potential, and the factor of 3 is the dimension of the fundamental representation of $SU_P(3)$. The LEFT of the Z fields has quartic scalar couplings of order $(m_2/\Lambda_3)^2$, so we have a consistent low energy expansion only for

$$m_2 < \sqrt{4\pi}\Lambda_3.$$

Combining the estimate above with the gravitino mass formula

$$m_{3/2} = X_g m_2 \Lambda_3 / m_P = 10 K \Lambda^{1/4},$$

gives several competing equalities and inequalities. Here X_g is a constant which must be calculated from the strongly interacting $SU_P(3)$ gauge theory, while K is a constant of order 1, which must be calculated from the as yet incomplete quantum theory of de Sitter space.

Plausible model independent extensions of the Tevatron trilepton analysis might eventually bound the charged gaugino mass term from below by 160 GeV, which requires

$$19.7 < X_2 \frac{m_2}{\mathrm{TeV}}.$$

To get an idea of how these bounds work, assume that $m_2 = 1.7\Lambda_3$ so that the moduli space Lagrangian is fairly strongly coupled, with a "fine structure constant" of order 1/4. Then $m_2 = 14.9\sqrt{K/X_g}$ TeV and we must have $X_2 > 1.32\sqrt{X_g/K}$ in order to satisfy the chargino mass bound. Setting the square root to $\sqrt{3}$ we obtain $m_2 = 8.6$ TeV and $\Lambda_3 = 5.1$ TeV.

The heavy trianons, $\mathcal{T}_{1,3}$ will also have SUSY violating masses, because of their $SU_P(3)$ couplings to the low energy theory. In particular, since $\mathcal{T}_3$ carries color, we will get squark and gluino masses. In the limit where the SUSic masses of the heavy trianons are $\gg \Lambda_3$, we could calculate the resulting gluino masses by integrating the heavy trianons out to create effective couplings of the form *e.g.*

$$\int d^2\theta \, (W_\alpha^{(3)})^2 f(P/m_3, \tilde{P}/m_3, M/m_3).$$

The F-terms of the light fields would then generate small gluino masses. Symmetries imply that the leading operators are fairly high-dimensional. However, there is no reason to suppose that $m_{1,3} \gg \Lambda_3$. For example, in ordinary QCD, an hypothetical quark with mass of order the rho meson mass, would not be treated by chiral perturbation theory, but neither would it make sense to estimate its effects via the operator product expansion. Thus, we predict a gluino/chargino mass ratio which is definitely smaller than the vanilla gauge mediation result α_3/α_2, and depends sensitively on $m_3/\sqrt{m_2\Lambda_3}$ as that variable becomes large. There will be a similar suppression of the squark to slepton mass ratios. A factor of 2 in m_3/m_2 could easily bring the gluino and squark mass predictions down to the range where they are consistent with experimental lower bounds but do not give large contributions to the Higgs potential. The mass m_1 is not constrained by this analysis.

Our model satisfies the general constraints of Meade *et. al.* [192] and so the SUSY spectrum will satisfy the sum rules and positivity constraints in that paper, with one possible exception.

If, as we hope, the VEV of S turns out to be non-zero, then the Higgs field F terms are non-zero, and these produce extra contributions to squark and slepton masses, whose origin is not gauge mediation. We believe that these are probably negligible, except for the top squarks, because of small Yukawa couplings.

We should also note that if we try to estimate the spectrum by working with the moduli space Lagrangian, we find logarithmic divergences[10]. This violates the rules of [192] because the moduli space Lagrangian is not renormalizable. At very high energies, the moduli space Lagrangian fails to be a good description and the rules of [192] are satisfied. Although none of the order one predictions of the moduli space approach are reliable, because there are corrections of the same order coming from energies around Λ_3 and above[11][192], we believe that this calculation indicates an enhancement factor in the sfermion/gaugino mass ratios of the form $\ln(C\Lambda_3/m_2)$. Our phenomenological estimates do not indicate a large ratio between Λ_3 and m_2, but we don't know the value of C. If there is such a logarithmic enhancement, it would help to clarify one of the key phenomenological issues of this model. General gauge mediation estimates suggest that the NLSP in the Pyramid Scheme is either the bino or the right handed slepton. These two particles have very different discovery signals, so it is important to decide which of the two is lighter. If the log enhancement is there, the bino will be the NLSP, which would imply that LHC will see events with hard $X + l^+l^-\gamma\gamma$, plus missing transverse energy. The origin of these events is the decay of a slepton to the bino and a hard lepton, followed by bino decay to a photon and a longitudinally polarized gravitino. Depending on the structure of the SUSY cascade, we will have other particles, denoted by X in the final state. At LHC strong production cross sections for sparticles dominate, so we might expect X to include at least a dijet. If the cascade passes through the relatively light chargino then there will be W bosons in X, coming from the decay of the chargino into W plus neutralino. The leptons might not even be hard. So the general characterization of final states for a bino NLSP is X plus two hard photons plus missing transverse energy, where X depends on the nature of the SUSY cascade.

The ratio $m^1_{1/2}/m^2_{1/2}$ is given by

$$\frac{m^1_{1/2}}{m^2_{1/2}} = \frac{X_1\alpha_1}{X_2\alpha_2} = 0.5\frac{X_1}{X_2}.$$

It's clear that we can only predict these masses up to a factor of a few. Unfortunately, the unknown strong interaction factors might well affect the phenomenological signals of our model.

The ratio of the right handed slepton mass to that of the bino is $f = Y\ln^{1/2}(\sqrt{4\pi}m_2/\Lambda_3)$.

[10] We thank J.L. Jones for pointing out these logarithms to us.

[11] We thank N. Seiberg for explaining this to us.

Y is another unknown strong interaction factor, and we have used the usual naive dimensional analysis estimate of the cutoff for the moduli space LEFT. If we take $Y = \sqrt{3}$ and $m_2 = 1.7\Lambda_3$, then $f = 2.3$, while for $Y = 1$ and $m_2 = \Lambda_3$ we have $f = 1.12$. It seems likely that the bino will be the NLSP in the Pyramid model. For a 50 GeV bino we need $f \gtrsim 2$ in order to satisfy the experimental bound on the right handed slepton mass.

6.4 The Higgs sector and $SU_L(2) \times U_Y(1)$ breaking

The Higgs sector of our model consists of the two doublets $H_{u,d}$ and the singlet S. The doublets are remnants of some sort of multiplet of the unified group, while the singlet might also be such a remnant, or a singlet under $SU(3)^3$. These low energy Higgs fields are the field content of the NMSSM.

In the approximation that the two heavy trianon masses are $\gg \Lambda_3$, integrating out the trianons and $SU_P(3)$ gauge bosons leads to two distinct contributions to the effective action for the Higgs sector of the NMSSM. The heavy trianon couplings to S give us a non-trivial effective potential for S. In the Coleman-Weinberg (CW) approximation it has the form

$$\sum_{i=1,3} |m_F^i|^4 f(u_i).$$

Here $m_F^i = m_i + y_i S$ and

$$u_i \equiv \frac{|F_S|^2}{|m_F^i|^4}.$$

This expression is valid if the y_i are perturbative and $u_i < 1$. We have

$$f(u) = au - \sum_{n=0}^{\infty} \frac{u^{n+2}}{(n+1)(n+2)(2n+3)}.$$

The linear term comes from the logarithmically divergent one loop wave function renormalization for S. The rest of the potential is a negative, monotonically decreasing convex function of u_i, which becomes complex at $u_i = 1$. This change of behavior represents the breakdown of effective field theory when the masses of scalar components of the heavy trianon fields become smaller than other scales in the theory, like Λ_3 and m_2. Calculation of the potential in this regime is more complicated. Note that when $F_S \neq 0$, the CW potential monotonically decreases as m_F^i are lowered. Thus, these contributions tend to make the S VEV non-zero when $F_S \neq 0$. This tendency competes against the contributions to the potential from Higgs F-terms, which are proportional to $|g_\mu|^2$.

It is important to remark that the one loop contribution from integrating out heavy trianons, could compete with tree level contribution to the potential for S. The theory contains multiple

Yukawa couplings and the tree level contributions to the S potential depend on its self coupling, and its couplings to $H_{u,d}$ and $\mathcal{T}_2$. The CW potential depends on the couplings to the heavy trianons. However, as we will note below, the experimental constraints on the gluino mass, probably force us to choose a value for m_3 at which this one loop calculation of the potential for S is inadequate, and the non-perturbative effects of the $SU_P(3)$ gauge theory must be taken into account.

The second important contribution to the Higgs potential is the non-zero pyrmeson VEV $(\mathcal{T}_2\bar{\mathcal{T}}_2)^i_j \sim \Lambda_3 Z \delta^i_j$. The resulting Higgs potential, including standard model D-terms has an $SU_L(2) \times U_Y(1)$ breaking minimum[12]

$$\begin{aligned} g_\mu H_u H_d &= \sqrt{6} y_2 \Lambda_3 Z, \\ \tan\beta &= 1, \end{aligned}$$

and

$$S = F_S = 0.$$

This minimum breaks SUSY and R-symmetry because of the VEVs of Z and F_Z. Given our estimate $\Lambda_3 \sim 5$ TeV, we need $\frac{y_2}{g_\mu} \sim 0.01$, a perfectly reasonable value for a Yukawa coupling ratio. We assume that all Yukawa hierarchies in the model are explained in terms of unification scale physics, a point of view motivated by the strict bounds on flavor changing processes. Note that BOTH couplings could be much smaller than $y_{1,3}$, though we probably want a fairly substantial value for g_μ, to ameliorate the little hierarchy problem.

The fact that $\tan\beta = 1$ was explained in previous papers on the Pentagon model. When $\langle Z \rangle \neq 0$ and $S = 0$ the potential favors a non-zero value for $H_u H_d$, leaving electromagnetism unbroken. The electroweak D-terms then favor $|H_u| = |H_d|$. The problem with this vacuum state is that it implies $\mu = B_\mu = 0$, which is not viable phenomenologically.

When we include quantum corrections to the potential from loops of high scale $SU_P(3)$ gauge bosons, we obtain couplings between S and Z. We have not calculated these, but if they have the effect of forcing $F_S \neq 0$, due to a coupling to F_Z, then the VEV of S is likely to shift as well, since the CW potential favors non-zero VEV if $F_S \neq 0$. Thus it is at least plausible that we obtain MSSM μ and B_μ terms of the right order of magnitude.

[12] There is also an $SU(2) \times U(1)$ preserving minimum with $S \neq 0$ and $F_S = 0$. SUSY is still broken because $F_Z \neq 0$. In a theory with gravity there is no way for the flat space field theory model to "choose" which of these is the "right" vacuum. We can tune the c.c. to be near zero near any minimum of the potential. The resulting dS space never decays into a state resembling the flat space vacua near other points. It makes Poincaré recurrence transitions to states resembling the dS spaces at higher minima of the potential, and transitions to Big Crunch space-times with negative c.c.. The interpretation of the latter depends on details of the potential. See the subsection on tunneling in this chapter, and the references cited there. Our attitude is that we choose the SUSY breaking $SU(2) \times U(1)$ breaking state, because it resembles our world, and because it *may* obey the rules following from the hypothetical theory of stable dS space.

The lower bound on the gluino mass implies that the approximation $m_3 \gg \Lambda_3$ is unlikely to be valid. Rather, it is likely that m_3 should be thought of as the moral equivalent of a quark mass of order 800 MeV in QCD: too large to be treated by chiral perturbation theory, but too small to integrate out above the confinement scale. In other words, the CW approximation we discussed above is probably inadequate, if the model is to produce an acceptably large gluino mass. The generation of effective μ and B_μ terms is thus mixed up with the strong $SU_P(3)$ gauge dynamics. We consider this to be the single most serious phenomenological deficiency of our model.

To summarize: we have given plausibility arguments that, in an appropriate range of the parameters m_i, the Pyramid Scheme has a SUSY violating, R-symmetry violating meta-stable minimum with a non-zero value for S. It can give rise to a reasonable supersymmetric phenomenology, but detailed calculation of the superpartner spectrum is not possible at this juncture, though it seems likely that a neutralino is the NLSP.

We end this section with a discussion of the tuning of parameters in our model, and its interpretation. Although we do not have a precise calculation of superpartner masses, it seems possible that the Pyramid Scheme does not suffer from a *little hierarchy problem*. It incorporates the NMSSM and the Yukawa coupling $g_\mu S H_u H_d$ can evade the usual bounds on the lightest Higgs mass, even for $\tan\beta \sim 1$. We have presented a mechanism that might generate a VEV for S, and thus an effective μ term. The F-terms of both S and the light pyrmeson can provide a B_μ term of the requisite order of magnitude.

Our required pattern of two trianon masses slightly above Λ_3, with the third in the range of validity of chiral perturbation theory may seem artificial, but in the CSB interpretation of the Pyramid Scheme it is in fact required in order to reproduce the meta-stable state implied by the underlying (but still partly hypothetical) quantum theory of dS space. Perhaps retro-fitters of the Pyramid Scheme would be more hard pressed to justify precisely this pattern of masses, but it is surely no more bizarre than the actual pattern of quark and lepton masses in the standard model. The closeness of $m_{1,3}$ to Λ_3 suggests that the value of the $SU_P(3)$ coupling at the unification scale is fairly large. The $N_F = 9$, $N_C = 3$ beta function is relatively small and positive. This leads to a slow decrease of the coupling as the scale is lowered to that of the heavy trianon masses, $m_{1,3}$. At that point, asymptotic freedom kicks in, with a relatively large beta function and effective coupling, and we quickly reach the non-perturbative regime of the $N_F = N_C = 3$ theory. We have not carried out detailed calculations to see if this explanation of the phenomenologically required coincidence of scales is quantitatively reasonable.

6.4.1 Tunneling to the "SUSY minimum"

Finally we note that, as a flat space field theory, the Pyramid Scheme certainly has supersymmetric vacuum states. In a theory with gravity, given our instructions to tune W_0 so that the cosmological constant in the meta-stable state is almost zero, these states could at best correspond to AdS theories of quantum gravity (superconformal $2+1$ dimensional field theories) with cosmological constant of order $-|m_2\Lambda_3|^2$. They have nothing to do with the evolution of our meta-stable state, and belong to a different quantum theory of gravity, with a different Hamiltonian, if they exist at all. In a theory including gravity, it never makes sense to think about tunneling to the supersymmetric vacuum state of a flat space quantum field theory, from a "meta-stable" de Sitter space.

As shown long ago by Coleman and de Luccia, the actual "decay" of the "meta-stable" de Sitter state proceeds to a Big Crunch space-time in which the low energy effective description breaks down. Two features of this breakdown are worthy of note. First of all, high energy degrees of freedom of the field theory are excited. In particular, even in the moduli space approximation (which is not valid in the Crunching region), the fields do not remain in the vicinity of the negative c.c. minimum, but instead explore the entire potential, as the Big Crunch singularity is approached. This means that no low energy effective field theory description of the endpoint of this tunneling process is valid. Our only clue to the nature of the transition, comes from the covariant entropy bound, a conjectured property of any consistent quantum theory of gravity. This bound restricts the entropy observable by any observer in the crunching region to be less than $\sim \frac{M_P^2}{m_2\Lambda_3}$. It is hard to understand how such a low entropy system could represent the fate of the entire universe.

In [21] it was shown that the space of potentials exhibiting "de Sitter decay" is divided into two classes. In the first class, called *above the Great Divide*, the decay probability behaves like $e^{-\pi(RM_P)^2}$ for large de Sitter radius. These transitions look more like Poincaré recurrences, temporary sojourns in low entropy states of a finite system, than like true decays. This is consistent with the hypothesis of Fischler and one of the present authors (TB) that a stable dS space has a finite number of states. It is also consistent with the low entropy implied for the crunching region by the covariant entropy bound. Thus, within a class of potentials for a meta-stable dS minimum in field theory, the semi-classical dynamics is consistent with the idea of a stable quantum dS space with a finite number of states. The instability of the semi-classical theory is viewed as a Poincaré recurrence.

In the second class of potentials, *below the Great Divide*, no such interpretation is possible, and a low energy theory in this class could not be interpreted as the LEFT of a finite theory of stable dS space. From the CSB point of view, the parameters of the Pyramid Scheme must be chosen to lie in the regime above the Great Divide, where this analysis is applicable. If this is possible, there would be no phenomenological consequences of the SUSY vacuum in the flat space effective field theory. The question of whether there are values of parameters for which the Pyramid Scheme is *above the Great Divide* will be studied in future work.

For those who are interested in viewing the Pyramid Scheme as a model divorced from the ideas of CSB, we can present an estimate of the flat space tunneling amplitude between the meta-stable SUSY violating state and the SUSY vacuum. If the model is *below the Great Divide*, this is probably a reasonable estimate of the actual tunneling amplitude including gravity, although the classical evolution after tunneling is dominated, at long enough times in the future, by high energy gravitational effects. We recall that we chose the "quartic fine structure constant", α_4, of the moduli space Lagrangian to be approximately $\frac{1}{4}$. Both the SUSic vacuum with vanishing pyrma-baryon fields, and the meta-stable state, are singlets under the $SU(3) \times SU(3)$ symmetry of the pyrmeson Lagrangian, so we can assume that the instanton is a singlet everywhere along its trajectory. The action is therefore

$$S = 3\frac{\pi}{\alpha_4}k,$$

where the factor of 3 comes from the trace. There are no other small parameters, so we expect $k \sim 1$. The tunneling probability per unit volume per unit time is thus

$$P \sim e^{-12\pi k}\Lambda_3^4 \sim e^{-12\pi k}\Lambda_3^4.$$

If $\Lambda_3 \sim 5$ TeV and $k \gtrsim 12$, there is low probability of a tunneling event in our horizon volume, since the beginning of the universe. It is not implausible that such a numerical factor could emerge from a precise calculation of the instanton action, but the result is not comforting. We are more concerned about the fact that this tunneling time is much more rapid than the recurrence time. Unless we can show that gravitational effects significantly modify the tunneling calculation, the Pyramid Scheme will not fit into the framework of CSB. We hope to return to this problem in a future paper.

6.5 A Pyramid Scheme for cosmology

Models of gauge mediated SUSY breaking do not have a standard WIMP dark matter candidate. Even in the absence of R-parity violation, the LSP is the gravitino, which is very light. When one imposes the further restriction of consistency with CSB, the gravitino mass is about 10^{-2}

eV. In [22], Banks and collaborators proposed that baryon-like states of the hidden sector could play the role of cold dark matter. For reheat temperatures above the confinement scale of the hidden sector, this was only possible if there was a primordial asymmetry in the hidden sector baryon density.

The discovery of the ISS [179] meta-stable vacua did not fit in with this idea, because in these states SUSY breaking is correlated with spontaneous breakdown of the hidden sector baryon number[13]. In [177], with another set of collaborators, Banks proposed that the PNGB of the spontaneously broken hidden sector baryon number could be the dark matter. This was only possible if there was a primordial asymmetry in this quantum number. Such an asymmetry would automatically generate an ordinary baryon asymmetry, through the mechanism of spontaneous baryogenesis [182], because of the effective coupling of the hidden sector and ordinary baryon number currents, due to gluon exchange. If one bounds the hidden sector asymmetry by insisting that the ordinary baryon asymmetry is no bigger than what is observed, then the dark matter density is also bounded, though the bound is model dependent, and depends on the scale at which hidden sector baryon number is broken. In the Pentagon model, one had to assume the scale associated with the leading penta-baryon number violating operator was between $10^8 - 10^{10}$ GeV, in order to explain the observed dark matter density.

A related astrophysical issue with the PNGB was pointed out in [178]. Rather general arguments show that the effective Yukawa coupling of the PNGB to electrons, violates bounds coming from stellar cooling rates. To avoid this, one must raise the mass of the PNGB to about an MeV, so that it cannot be produced in ordinary stars. In the Pentagon model this again required the scale associated with the leading symmetry violating operator to be in the $10^8 - 10^{10}$ GeV range.

The Pyramid Scheme throws a new light on all of these questions. It has three accidental baryon number like symmetries, corresponding to the three types of trianon. Call the corresponding conserved charges $\mathcal{B}_i$. The dynamics of $SU_P(3)$ spontaneously breaks $\mathcal{B}_2$, but the other two are preserved. The lightest particles carrying $\mathcal{B}_{1,3}$ are standard model singlets, and thus potential dark matter candidates. According to [22] there is a small window of low reheat temperatures, below the confinement scale of $SU_P(3)$ in which non-thermal production of these particles could account for the observed dark matter density[14]. Alternatively, a primordial asymmetry in any of these quantum numbers could be invoked to explain dark matter in a

[13]This correlation persists for the $N_F = N_C$ models, which might have vacua breaking the discrete R-symmetry of the ISS states.

[14]We recapitulate this analysis in Appendix B.

cosmological model with high reheat temperature. One would have to correlate this with the ordinary baryon asymmetry, as in [177], a constraint which was missed in [22]. Whether or not there is a PNGB, a primordial asymmetry in some quantum number implies a cosmological expectation value for the associated charge density. The $\mathcal{B}_i$ currents are all coupled to the ordinary baryon number current via exchange of standard model gauge bosons, and, in combination with electro-weak baryon number violation, the asymmetries in pyrma-baryon numbers can drive spontaneous baryogenesis.

The Pyramid Scheme thus provides us with a wealth of possibilities for explaining both the dark matter in the universe and the asymmetry in ordinary baryon number. In this paper we will only explore one of these directions. We assume that only negligible primordial asymmetries in any of these quantum numbers were generated in the very early universe, and assume a low reheat temperature, so that particles carrying $\mathcal{B}_1$ and/or $\mathcal{B}_3$, can be the dark matter.

These particles have QCD like strong interactions, with confinement scale Λ_3. Their annihilation cross section is energy independent and of order Λ_3^{-2}. Probably the best model for their cosmological behavior is the soliton picture of [183]. By analogy with baryon anti-baryon annihilation in QCD, and more generally with soliton anti-soliton annihilation, we expect the typical final state of the annihilation process to be a state of pyrmions (the PNGB of spontaneously broken $\mathcal{B}_2$) with high multiplicity. This is quite interesting, because the pyrmions are very light (we will estimate their mass below, in the MeV range), and their constituents do not carry color. As a consequence, the pyrmion decay into standard model particles will primarily produce electron positron pairs, photons and neutrinos.

One is tempted to try to associate the behavior of our hypothetical dark matter candidate, with some of the ambiguous signals for dark matter that have accumulated in recent years [176]. In [184] it was emphasized that this data can only be interpreted in terms of a dark matter candidate which decays primarily to leptons, and the authors constructed an ingenious set of models to implement this constraint. Our suggestion is, quite frankly, modeled on theirs, but fits more organically into the framework of gauge mediated SUSY breaking. We will only sketch the outlines of it here, since much more work is needed to see whether it is viable. The Pyramid model in fact predicts a zero temperature cross section for dark matter annihilation which is just what is needed to explain the ATIC, PAMELA and PPB-BETS data. The dimensional analysis/soliton estimate is an energy independent cross section

$$\sigma_0 = \frac{A}{\Lambda_3^2}.$$

Recall that Λ_3 was constrained strongly by the twin requirements of an experimentally acceptable chargino mass and a gravitino mass obeying the CSB formula. A typical value obeying the bounds was $\Lambda_3 \sim 5$ TeV.

The interpretation of the ATIC, PAMELA, PPB-BETS and WMAP haze data in terms of dark matter annihilation requires a low energy cross section

$$\sigma_0^{exp} \sim 0.1\ (\mathrm{TeV})^{-2}.$$

Thus $A \sim 2.5$ would seem to fit the data. We will see below that the multiplicity of e^+e^- pairs per dark matter annihilation is likely to be large, so that an even smaller cross section for dark matter annihilation is actually called for. This would require $A \sim 0.2$ for the multiplicity we estimate below. Our point here is not to make precise fits, but rather to show that the Pyramid Scheme is in the right ballpark to explain the observational evidence for a lepton anti-lepton excess in the galaxy.

Fans of thermal WIMP dark matter will be curious to understand how such a large cross section could be compatible with the correct relic dark matter density. For completeness, we recapitulate the non-thermal dark matter production calculation of [22] in the Appendix. The answer depends on the last reheat temperature of the universe, which must satisfy

$$\Lambda_3 > T_{RH} > 0.1 m_{\mathcal{B}}.$$

It is easy to imagine getting such a low reheat temperature from the decay of a relic scalar, like the supersymmetric partner of the QCD axion [185].

With a low reheat temperature, we must look for a method of creating the baryon asymmetry of the universe which is efficient at low energy. Affleck-Dine baryogenesis is always an option [194], but the Pyramid model has the possibility of creating the asymmetry via spontaneous baryogenesis [182] at the electroweak phase transition [177]. That is, a primordial asymmetry in any of the pyrma-baryon numbers acts, because of couplings $\alpha_3^2 J_\mu^{PB} B^\mu / \Lambda_3^2$ induced by gluon exchange, as a chemical potential for ordinary baryon number. This biases electro-weak baryon number violation, which is in equilibrium above the electro-weak phase transition. The asymmetry is frozen in at $T \sim 100$ GeV $\ll T_{RH}$.

In addition to this, the most suggestive feature in the data is the cut-off on the electron-positron spectrum seen by the ATIC and PPB-BETS detectors [195]. In [184] this was interpreted as showing us the mass of the dark matter particle, and gave rise to an estimate $\sim 600 - 800$ GeV. Our dark matter candidate is $40 - 60$ times as heavy.

Our proposed explanation for this discrepancy, centers around the strong $SU_P(3)$ interactions of our dark matter candidate, and the existence of the pyrmion PNGB. Proton anti-proton annihilation at rest, which should be a reasonable analog of heavy pyrma-baryon annihilation in the contemporary universe, produces final states consisting predominantly of pions. The mean number of pions is 5, with variance 1. Correspondingly, the single pion inclusive momentum distribution is peaked at 0.2 GeV, roughly 1/5 of the proton mass. The experimental peak is pronounced, but reasonably broad. The distribution has dropped by a factor of 10 at 0.8 GeV. Lu and Amado [186] have reproduced many of the features of the annihilation data in terms of a soliton model, in which the $p\bar{p}$ initial state is modeled as a zero baryon number lump of pion field in a Skyrme-like model. Their model gives a peak that is somewhat more narrow than the data.

In a soliton model, the initial state of light mesons after heavy pyrma-baryon annihilation will be a coherent state of the field. The probability of having N particles in such a state is proportional to the square of the average field strength and the variance is of order $\sqrt{N}$. In a soliton model of a QCD like theory, the average momentum per particle is strongly suppressed for $|p| > \Lambda_3$, but would otherwise be randomly distributed. Our dark matter candidate would be a pyrma-baryon consisting of three heavy trianons and would have a mass of order $3m_{1,3}$. Given our estimates this is roughly $30 - 40$ TeV. In the Pyramid Scheme, the final state will consist primarily of pyrmions, which are effectively massless and will have a typical momentum $< \Lambda_3 \sim 5$ TeV. Some of these will be primaries and the rest secondary products of the decays of heavier pyrmesons. Thus, we may expect the pyrmion multiplicity to be very large and the energy to be thermalized by strong final state interactions.

The single particle momentum distribution of N body massless phase space for annihilation of a particle anti-particle pair with total mass $2M$ is peaked at $|p| = 2M/N$ and is a Gaussian of the form

$$P \propto e^{-ax^2},$$

in the rescaled momentum x, around the maximum, with $a = N^2$ for large N[15]. If we take the estimate $\Lambda_3 \sim 5$ TeV from our discussion of superpartner masses, and $m_{1,3} \sim 12$ TeV to assure the massive trianons are outside the range of chiral perturbation theory, then $2M \sim 72$ TeV. This would give a distribution centered at 800 GeV, with an extremely narrow width, for $N \sim 90$, which is ~ 18 times the pion multiplicity from proton anti-proton annihilation. We would interpret the actual distributions seen in the balloon experiments as a broadening of this peak toward the low momentum side by the effects of propagation of electrons and positrons through the galactic medium. The high side of the experimental peak should be identified with

[15] We thank H. Haber for these results.

the position of the narrow peak in the primordial distribution.

The underlying $SU_P(3)$ gauge theory is supersymmetric, and has more degrees of freedom than QCD, all of which can decay or annihilate to the pyrmion. Furthermore, in a soliton model of the annihilation process the probability of a single particle with momentum $> \Lambda_3$ is exponentially suppressed since the particles come from a smooth coherent state. Thus one would guess that the dynamics of the annihilation process forces a minimum of 10 pyrmions to be produced. Furthermore, since many of the final state pyrmions will be produced in secondary decays of heavier pyrmesons, the multiplicity is almost certainly higher than 10, since the dynamical momentum cutoff applies to the primaries. In other words, the high multiplicity required to fit the data on balloon experiments does not seem out of the question. Obviously, much more work on the dynamics of this strongly coupled annihilation process, as well as a complete model of galactic propagation, will be necessary in order to render a complete verdict on our model of the experiments.

Thus, *very roughly* we can produce a spectrum of electrons and positrons consistent with the ATIC, PAMELA and PPB-BETS observations from a heavy pyrma-baryon dark matter candidate decaying into ~ 90 pyrmions, which themselves decay to e^+e^- pairs. To be a good candidate for dark matter the pyrma-baryon abundance of the universe must be non-thermal [22], and could come from a late decaying scalar with a reheat temperature in the TeV range. The details of this, including the relation between the reheat temperature, the low energy annihilation cross section, and the relic abundance, can be found in Appendix B. The low reheat temperature requires us to invent a sub-TeV mechanism for baryogenesis, and the most attractive candidate is spontaneous baryogenesis at the electro-weak phase transition, driven by a primordial asymmetry in one of the pyrma-baryon numbers [177]. Obviously a lot more work is needed to make these remarks into a robust theory, explaining the data on dark matter.

We also note that, should the current observational indications of dark matter annihilation signals prove to be explained by astrophysics [196], the Pyramid Scheme has dark matter scenarios in which there are no annihilation signals. This would be the case if the dark matter were interpreted as a pyrma-baryon excess, as in [22]. The required primordial asymmetry is roughly $\epsilon_{PB} = \frac{T_{eq}}{m_{PB}} \sim 10^{-12} \frac{\mathrm{TeV}}{m_{PB}}$. This is too small to give rise to an adequate asymmetry in baryon number via spontaneous baryogenesis [182, 177]. We could invoke an asymmetry of the spontaneously broken $\mathcal{B}_2$ quantum number to give spontaneous baryogenesis, but would then have to explain why the inflaton preferred to decay mostly into $\mathcal{T}_2$ rather than the other trianons. The Pyramid Scheme can accommodate a wide variety of cosmological scenarios. We hope to explore some of them in future work.

6.5.1 The mass of the pyrmion

To calculate the mass of the pyrmion, we must understand the way in which the pyrma-baryon number $\mathcal{B}_2$ is explicitly broken. The operators

$$B_2 = \det \mathcal{T}_2, \qquad \bar{B}_2 = \det \bar{\mathcal{T}}_2,$$

are invariant under $SU_P(3)$ and the standard model gauge group, and have discrete R-charges satisfying

$$B_2 + \bar{B}_2 = 3(2 - S) \mod N.$$

Recall that $N \geq 5$. We use the freedom to choose the individual pyrma-baryon and anti-pyrma-baryon R-charges to impose

$$B_2 = 2 - S, \qquad \bar{B}_2 = 4 - 2S \mod N.$$

In that case, the dimension 5 operator $\int d^2\theta\, SB_2/M_U$, is the leading $\mathcal{B}_2$ violating operator, which is invariant under all the symmetries of the model. The pyrmion mass will then be of order

$$m_b \sim \frac{\Lambda_3^{3/2}}{{M_U}^{1/2}} \sim 2.5 \text{ MeV}.$$

We have used the estimate $\Lambda_3 \sim 5$ TeV from our discussion of superpartner masses. Thus, the pyrmion can decay only into electrons, positrons, photons, neutrinos and gravitinos.

Note that this estimate also resolves the problem of pyrmion production in stars [178], which could lead to cooling faster than what is observed. An MeV scale pyrmion could at best be produced in supernova explosions.

6.6 Conclusions

We have sketched a new Pyramid Scheme for direct mediation of SUSY breaking. It is based on the same fundamental dynamical assumption as the Pentagon model: the existence of a SUSY and R-breaking meta-stable state of $N_F = N_C$ SUSY QCD, but it has the following advantages:

- It is based on trinification rather than unification in a simple group, and as a consequence predicts completely perturbative coupling unification, with no Landau poles. The full model can be associated with a simple quiver/moose diagram, which should make its implementation in string theory straightforward.

- There exist two unbroken baryon-number like symmetries in the hidden sector, which enable us to construct a number of models of dark matter, along the lines of [22]. In this paper we concentrated on a model in which the dark matter is produced non-thermally, but without a pyrma-baryon asymmetry, in order to be able to model dark matter annihilation signals. Given estimates of the confinement scale of the $SU_P(3)$ gauge group from superpartner masses, the model produces annihilation cross sections of (roughly) the right order of magnitude to explain ATIC, PAMELA and PPB-BETS, and the dark matter annihilates predominantly into pyrmions, the PNGB of the spontaneously broken pyrma-baryon number. The latter particle has a mass in the MeV range and decays only into light leptons and photons. We argued that a model of the annihilation process with a high pyrmion multiplicity ~ 100 in the final state could reproduce the bumps in the ATIC and PPB-BETS data.

- The dark matter scenario requires us to invoke a late decaying particle which reheats the universe to ~ 1 TeV, which implies that we must supplement it with a low scale model for baryogenesis. The most economical scheme would be to postulate a primordial asymmetry in one of the pyrma-baryon numbers (not the one associated with the dark matter candidate). Standard model gauge boson exchange produces current-current couplings between the pyrma-baryon currents and ordinary baryon number, so that a pyrma-baryon asymmetry drives spontaneous baryogenesis [182] at the electro-weak phase transition. Affleck-Dine baryogenesis is another reasonable candidate mechanism.

- The pyrmion mass estimate makes it too heavy to be produced in ordinary stars, avoiding the strong constraints of [178] on models of meta-stable SUSY breaking that rely on the dynamics of $N_F \geq N_C$ SUSY QCD.

- The Pyramid Scheme has three pairs of chiral fields, the trianons $\mathcal{T}_{1,2,3}$ and $\bar{\mathcal{T}}_{1,2,3}$, which are charged under the standard model gauge group. Only one carries color. In order to generate meta-stable SUSY breaking, the masses of two of the trianons must be too large to be treated by chiral perturbation theory. If one of these heavy trianons is the colorful one, then the gluino mass is naturally suppressed relative to that of the charginos, and squark masses suppressed relative to those of leptons. This removes the fine tuning problem of the vanilla gauge mediated spectrum. We note that the gluino mass goes down rapidly with the mass of the heavy colored trianon, so the latter probably cannot be so large as to be safely integrated out above the confinement scale Λ_3.

We want to emphasize that our estimates of the properties of the Pyramid Scheme are rather rough and preliminary. In particular, the discussion of dark matter needs a lot of work before one can make a reliable claim that it accounts for any existing dark matter data. Furthermore, many of the important dynamical questions in the model, such as the existence of the SUSY and R-violating vacuum state, and the generation of appropriate μ and B_μ terms, depend on (currently) incalculable strong $SU_P(3)$ dynamics. The Pyramid Scheme has plausibility, but is not yet a fully going concern. Investors are warned that past performance is no guarantee of future returns.

6.7 Appendix: Cosmological SUSY breaking

In this appendix we explain the extra factor of 10, which appeared in our estimate of $m_{3/2}$ according to the hypothesis of CSB. The variables in the holographic theory of dS space [197, 198] are $N \times N+1$ matrices which are also spinors in 7 compactified dimensions. We denote them by

$$(\psi^P)_i^A, \qquad ([\psi^\dagger]^Q)^j_B.$$

Their quantum algebra is

$$\left[(\psi^P)_i^A, ([\psi^\dagger]^Q)^j_B\right]_+ = \delta_i^j \delta_B^A M^{PQ}.$$

P, Q are compact dimension spinor indices, and M^{PQ} are "sums of wrapped brane charges". Their closed super-algebra with the ψ variables defines the compactification. We call it the quantum algebra on a single pixel of the holographic screen of dS space, or the *pixel algebra* for short. The holographic principle requires that the pixel superalgebra, for fixed values of i, j, A, B has a finite dimensional unitary representation. If D_P is the dimension of the pixel algebra representation then $\ln D_P$ is the entropy per pixel. The total entropy of dS space, $\pi(RM_P)^2$ is then given by

$$\pi(RM_P)^2 = N(N+1)\ln D_P.$$

In previous work, D_P was set equal to 2 because the compactified dimensions were ignored.

We note in passing that this formalism implies that, in a finite radius dS space, compactified dimensions have no moduli. The finite dimensional algebras and representations are subject to the constraint that, as $N \to \infty$ we must obtain (super)-gravitons in the spectrum, following the outline in [197][16]. The classification of such algebras has not yet been attempted, but they must be discrete.

A hint at what is required comes from noting that Calabi-Yau manifolds are symplectic and compact, so that geometric quantization gives a(n ambiguous) map from their function algebras

[16] In fact, in this paper, it was impossible to obtain gravitons (only massless chiral multiplets), because there were no compactified dimensions.

to finite dimensional matrix algebras. This can be easily extended to seven manifolds which are Calabi-Yau bundles over an interval (Horava-Witten compactifications) or circle bundles over a CY_3. The variables of the holographic theory will live in modules over these finite dimensional algebras. From these correspondences one can see that D_P will be related exponentially to the volume of the internal space (in Planck units)[17].

What is $\ln D_P$ in the real world ? In Kaluza-Klein compactification, the volume of the internal space in higher dimensional Planck units (denoted by M_{Pl}), is related to the four dimensional reduced Planck scale m_4 by

$$(V/V_{Pl}) = (m_4/M_{Pl})^2.$$

Witten suggested [193] that $M_{Pl} = 2 \times 10^{16}$ GeV $= M_U$, and used the large volume to explain the discrepancy between the Planck and unification scales. Thus we expect

$$\ln D_P \sim 10^4.$$

To proceed, we recall how [197] extracted particle states from the pixel algebra. The point is simply that $N \times N + 1$ matrices are precisely the spinor bundle over the fuzzy 2-sphere. For finite N, we keep only a finite number, of order N^2 spinor spherical harmonics in the expansion of a section of this bundle. Ignoring the compact dimensions, the pixel variables converge, as $N \to \infty$, to $\psi(\Omega)$, an operator valued measure on the spinor bundle. These are the operators describing a single massless chiral super-particle in four dimensions, with fixed magnitude of the momentum and direction Ω. It is hoped that the incorporation of compact dimensions will allow us to generalize the particle content to include gravitons and gauge bosons.

In order to describe multi-particle states, as well as to obtain variable values of the longitudinal momentum, we introduce block diagonal ψ matrices. The size of an $M \times M + 1$ block is interpreted as its momentum in units of $1/R$. The usual permutation gauge symmetry of the space of block diagonal matrices, is interpreted as particle statistics, and the anti-commutation relations and spinor nature of the ψ operators enforces the right spin statistics connection.

One must make a compromise between the number of particles allowed, and the number of spherical harmonics allowed in the momentum space wave function of a given particle (there must be many if it is to be localizable on the holographic screen[18]). The compromise which leads to the maximal particle entropy is to take blocks of size $M \sim N^{1/2}$. This picture of the

[17]This is just the statement that entropy is volume extensive in the internal dimensions. The holographic reduction is just a feature of the non-compact dimensions.

[18]In experimental particle physics language this is localization in the detector.

typical particle momentum and multiplicity which maximizes the entropy in dS space, can be derived in field theory by maximizing the entropy subject to the constraint that no black holes with radius of order the cosmological horizon are formed.

The super-Poincaré algebra arises in this formalism only as $N \to \infty$ and only for localizable particle states. Corrections to the algebra should then scale like $N^{-1/2}$. In particular, the commutator of the Poincaré Hamiltonian, P_0 and the supercharges Q_a should be of order $N^{-1/2} M_P S_a$ where S_a is an operator with matrix elements of order one. It follows that the gravitino mass is given by a formula

$$m_{3/2} = N^{-1/2} K M_P,$$

with K of order one. Our entropy formula gives

$$\frac{3}{8}\frac{M_P^4}{\Lambda} = \pi (R M_P)^2 = N^2 \ln D_P \approx 10^4 N^2.$$

Comparing these two formulae, we get the one used in the text by lumping a factor $(\frac{8}{3})^{1/4}$ into K.

It should be noted that the Lorentz group arises in this formalism as the conformal group of the sphere. The formalism is exactly rotation invariant for any N and conformal transformations corresponding to boosts of moderate rapidity should not be affected much by restricting the space of functions on the sphere to the first 10^{30} spherical harmonics.

6.8 Appendix: Non-thermal dark matter

This appendix recalls the non-thermal dark matter production scenario described in [22]. We assume that a particle X with $m_X \gg m_{\mathcal{B}}$ decays, with a reheat temperature $T_{RH} < \Lambda_3$. This produces an initial abundance of heavy pyrma-baryons

$$Y_0 = 10^{-2} \frac{T_{RH}}{m_{\mathcal{B}}}.$$

Y_0 is, as usual the number density to entropy density ratio. The first factor in this equation is simply the branching ratio that would appear for a massless pyrma-baryon, while the second suppression factor takes into account the fact that the mass is above the typical energy of decay products after thermalization. The decay is relatively quick, so we can neglect annihilation of pyrma-baryons during the decay process.

Below T_{RH} the pyrma-baryon abundance satisfies a Boltzmann equation driven only by annihilation. Processes which create more pyrma-baryons have already fallen out of equilibrium.

We have

$$\frac{dY}{dx} = -k\frac{Y^2}{x^{5/2}},$$

where $x = m_{\mathcal{B}}/T$, and

$$k = \frac{2\pi m_{\mathcal{B}} m_P \sigma_0 g_{*s}}{75 g_*^{1/2}} \approx (1.4 \times 10^{15}\ \mathrm{TeV}) m_{\mathcal{B}} \sigma_0.$$

g_* is the number of massless degrees of freedom into which the pyrma-baryons annihilate and g_{*s} the number that contribute to the entropy. We have, in the last expression for k, approximated both of these by an average value of 50 and written all remaining dimensionful quantities in TeV units.

The solution for the present day abundance is

$$Y_f^{-1} = Y_i^{-1} + \frac{2k}{3}(x_i^{-3/2} - x_f^{-3/2}).$$

The last term is negligible, and so is the first if T_{RH} is high enough for nucleosynthesis to occur in a normal fashion. Thus

$$Y_f = \frac{10^{-15} m_{\mathcal{B}}^{1/2} T_{RH}^{-3/2} \sigma_0^{-1}}{\mathrm{TeV}}.$$

The observed dark matter density is obtained if

$$Y_f \frac{m_{\mathcal{B}}}{\mathrm{TeV}} = 4.4 \times 10^{-13},$$

so we must have

$$\Lambda_3 > T_{RH} = 0.017 \frac{m_{\mathcal{B}}}{[\sigma_0\ (\mathrm{TeV})^2]^{2/3}} \approx 0.15\, m_{\mathcal{B}}/A^{2/3}.$$

In the last approximate equality we have taken $\Lambda_3 \sim 5$ TeV and used A as the value of $\sigma_0 \Lambda_3^2$. This can be satisfied for heavy pyrma-baryon masses less than

$$m_{\mathcal{B}} < 6.7 A^{2/3} \Lambda_3.$$

Recalling that $m_{\mathcal{B}_3}$ cannot be much bigger than $3\Lambda_3$ (in order to satisfy the bounds on the gluino mass) and that $A \sim 1$, we are able to fit the observed dark matter abundance, the gross features of the dark matter signals in ATIC, PAMELA and PPB-BETS, as well as supersymmetric phenomenology. The parameters of our model are tightly constrained by all of this data.

6.9 Appendix: Some computations

In this appendix we present some computations related to the meta-stable state. Below the scale Λ_3, the relevant superpotential is given by

$$W = \sum_{i=1,3} (m_i + y_i S)\mathcal{T}_i \bar{\mathcal{T}}_i + (m_2 + y_2 S)\Lambda_3 \operatorname{tr} M + g_\mu S H_u H_d + \frac{g_T}{3} S^3 + \ldots$$

where the pyrmeson $\mathcal{T}_2\bar{\mathcal{T}}_2 = \Lambda_3 M$ satisfies the usual quantum moduli space constraint $\det M - \Lambda_3 P\tilde{P} = \Lambda_3^3$ and the heavy trianons $\mathcal{T}_{i=1,3}$ and $\bar{\mathcal{T}}_{i=1,3}$ have to be integrated out. Parametrizing the pyrmeson and the pyrma-baryons as

$$M = Z_a\lambda^a, \qquad P = i\Lambda_3 e^{(q+p)/\Lambda_3}, \qquad \tilde{P} = i\Lambda_3 e^{(q-p)/\Lambda_3}$$

where $Z_0 \equiv Z$, $\lambda^0 = \sqrt{\frac{2}{3}}\, I$ and $\lambda^{a=1,\ldots,8}$ are Gell-Mann matrices, the quantum moduli space constraint can be satisfied for any Z_a and p by fixing q. If $q \neq -\infty$ then p is the NGB of the broken $U(1)_{\mathcal{B}_2}$. The superpotential in terms of the unconstrained fields is simply

$$W = \frac{X}{\Lambda_3}\left[\left(\frac{2}{3}\right)^{\frac{3}{2}} Z^3 + \Lambda_3^3 e^{2q/\Lambda_3} - \Lambda_3^3\right] + \sqrt{6}\Lambda_3(m_2 + y_2 S)Z + g_\mu S H_u H_d + \frac{g_T}{3}S^3 + \ldots$$

where the heavy trianons have been integrated out and $Z_{a\neq 0} = 0$ was assumed. The F-terms are

$$\begin{aligned}
-F_S^\dagger &= \sqrt{6}y_2\Lambda_3 Z + g_\mu H_u H_d + g_T S^2 \\
-F_{H_u}^\dagger &= g_\mu S H_d \\
-F_{H_d}^\dagger &= g_\mu S H_u \\
-F_Z^\dagger &= 2\sqrt{\frac{2}{3}}\frac{XZ^2}{\Lambda_3} + \sqrt{6}\Lambda_3(m_2 + y_2 S) \\
-F_q^\dagger &= 2\Lambda_3 X e^{2q/\Lambda_3} \\
-F_X^\dagger &= \left(\frac{2}{3}\right)^{\frac{3}{2}}\frac{Z^3}{\Lambda_3} + \Lambda_3^2 e^{2q/\Lambda_3} - \Lambda_3^2
\end{aligned}$$

and there is an extra SUSY vacuum at $S_{\rm SUSY} = -\frac{m_2}{y_2}$ and $Z_{\rm SUSY} = -\frac{g_T m_2^2}{\sqrt{6}y_2^3\Lambda_3}$ with q satisfying the quantum moduli space constraint and all other VEVs to zero. The Higgs sector scalar potential has three contributions,

$$V = V_{\rm F-terms} + V_{\rm 1-loop} + V_{\rm D-terms}$$

where

$$\begin{aligned}
V_{\rm F-terms} &= |\sqrt{6}y_2\Lambda_3 Z + g_\mu H_u H_d + g_T S^2|^2 + |g_\mu S|^2(|H_u|^2 + |H_d|^2) \\
&\quad + ((\partial^2 K)^{-1}_{Z^\dagger Z})6|\Lambda_3|^2|m_2 + y_2 S|^2 \\
V_{\rm 1-loop} &= \frac{9}{32\pi^2}\sum_{i=1,3}\sum_{\sigma=\pm 1}\left[m_B^4\log\frac{m_B^2}{\Lambda^2} - m_F^4\log\frac{m_F^2}{\Lambda^2}\right] \\
V_{\rm D-terms} &= \frac{1}{8}(g_1^2 + g_2^2)(|H_u|^2 - |H_d|^2)^2 + \frac{1}{2}g_2^2|H_u^+ H_d^{0\dagger} + H_u^0 H_d^{-\dagger}|^2
\end{aligned}$$

and the fermionic and bosonic masses for the heavy trianons are given by

$$\begin{aligned}
m_F^2 &= |m_i + y_i S|^2 \\
m_B^2 &= |m_i + y_i S|^2 + \sigma|y_i(\sqrt{6}y_2\Lambda_3 Z + g_\mu H_u H_d + g_T S^2)|.
\end{aligned}$$

There are critical points of the potential with $H_u^+ = H_d^- = 0$. Assuming this, the potential becomes invariant under $H_u^0 \leftrightarrow H_d^0$ and thus there are critical points with $H_u^0 = H_d^0$. At critical points like these, the D-term contribution vanishes and the potential simplifies greatly. The existence of a SUSY violating minimum is encoded in the strong dynamics of the $SU_P(3)$ gauge group and is therefore difficult to determine.

Chapter 7

Tunneling Constraints in Cosmological Supersymmetry Breaking

7.1 Introduction

In this chapter we discuss in detail the findings of the work done in collaboration with T. Banks [17].

The central idea of Cosmological SUSY Breaking (CSB) is that the correct quantum theory of stable de Sitter space has the effective cosmological constant (c.c.) as a free parameter. Supersymmetry is an emergent property of the limit $\Lambda \to 0$, with a scaling relation $m_{3/2} = K\Lambda^{1/4}$. Here K is constant of order 10 [199].

The basic framework puts strong constraints on the Low Energy Effective Field Theory (LEFT) in the $\Lambda = 0$ limit. It must be a theory with minimal four dimensional SUSY, as well as an R-symmetry group larger than Z_2. The low energy physics of the model is determined by adding certain R-violating terms to the $\Lambda = 0$ Lagrangian, which must give rise to a stable or meta-stable, SUSY violating state, with gravitino mass satisfying the relation above. Among these terms is a constant superpotential W_0, whose function is to tune the effective c.c. to the value indicated by the formula for $m_{3/2}$. Generally there will also be a SUSY preserving solution of the effective action, with negative cosmological constant.

In gravitational effective field theory, this supersymmetric AdS solution, *has nothing to do with the dS solution.* It is not part of the same quantum system, which has the de Sitter solution. This is seen in two complementary ways. If we consider excitations of the AdS solution, which are normalized and correspond to states, then there are no dS states that are acceptable. Depending on the scales in the potential, one may create localized excitations with fields concentrated near the positive energy minimum, but as one pushes the size of the region to the dS horizon scale, the excitation becomes a black hole [200].

Correspondingly, if following Coleman and De Luccia (CDL) [201], we look at tunneling from dS space "to the negative c.c. region", we do not relax to the AdS background, but instead encounter a big crunch, on a microscopic time scale. Moreover, due to the crunch, the field does not in fact stay localized near the negative c.c. minimum, but instead explores the entire potential until the energy density approaches the Planck scale and effective field theory breaks down. It seems clear that the non-gravitational effective theory, in which the two solutions correspond to two states of the same Hamiltonian system, with one decaying into the other, is not a correct qualitative description of the physics, even when all the scales are far below the Planck scale. However, we shall see that the Euclidean solutions of the non-gravitational field theory *are* good approximations to the gravitational CDL instantons, when the range of field variation is small compared to the Planck scale.

As a consequence, *we will show that the idea, introduced in [202], of using a meta-stable flat space field theory vacuum state as the LEFT of the theory of stable dS space, is wrong.* We argue that the only consistent models must use a LEFT which has *no* SUSic vacuum in the $M_P \to \infty$ limit. Combining the classic results of Nelson and Seiberg [203] with the basic constraints of CSB, we conclude that the low energy Lagrangian must be non-generic – that is, it does not include all terms consistent with symmetries, with coefficients determined by dimensional analysis. We argue that in the context of CSB, the terms in the Lagrangian that violate the fundamental discrete R-symmetry of the $\Lambda = 0$ limit, might well be non-generic. Indeed we already know that this is the explanation, in this context, of the fine tuning of the c.c.. The fundamental requirement for the LEFT is that it reproduces the properties of the underlying quantum theory of stable dS space, which has a finite number of states. Any CDL instantons must be interpretable as a description of recurrences of low entropy states, rather than true instabilities.

We introduce a modified version of the Pyramid Scheme, with non-generic R-violating terms[1], which has no SUSic vacua. This model seems to satisfy all the theoretical constraints of CSB and coupling unification, as well as all phenomenological constraints.

We have also taken the opportunity of this paper to repair another flaw that we discovered in the Pyramid Scheme, namely that the hidden sector gauge coupling has a Landau pole below the GUT scale. The unique way we have discovered to circumvent this is to replace the group at the apex of the Pyramid by $SU_P(4)$, Higgsed to $SU_P(3)$ at about $\lesssim$ 50 TeV. We have not yet investigated the dynamical source of this Higgs mechanism, but it is perhaps encouraging that it occurs at a scale close to the other scales in the model. This revision forces us to change the underlying R-symmetry group and the R-charges of various fields. The simplest model we have found, has a Z_{13} R-symmetry.

[1]We note that *all* versions of the Pentagon model and the Pyramid Scheme secretly invoked the fact that R-violating terms were non-generic, in order to explain the absence of proton decay.

7.1.1 CSB and CDL

The authors of [21] showed that the space of potential energy functions for scalar fields, with $|V| > 0$ at every minimum, as well as at infinity, could be divided into two classes. Consider the lowest dS minimum and add a negative constant to the potential to bring this minimum to zero. The resulting Minkowski solution may or may not have a positive energy theorem, and this is the criterion dividing the two classes. The co-dimension one dividing line is called The Great Divide. It is the subspace of potentials that have a static domain wall solution connecting the Minkowski minimum to an AdS solution. For potentials above the Great Divide, whose Minkowski limit has a positive energy theorem, the probability for the dS "decay" is of order $e^{-S_{dS}}$, where S_{dS} is the entropy of the de Sitter space.

This is consistent with a model of dS space as a quantum system with a finite number of states [204], with the "decay" interpreted as a Poincaré recurrence. The dS vacuum (a high entropy density matrix, not a unique quantum state) is the maximal entropy state of the system, in which the system spends most of its time. It is properly viewed as stable, despite the existence of the instanton.

This interpretation is consistent with another feature of the instanton solution : the maximal causal diamond in the crunching region of the Lorentzian continuation of the instanton, has an area much smaller than that of the dS horizon. That is, if we take the holographic interpretation of physics seriously, the instanton is describing a transition from high to low entropy.

By contrast, when the limiting Minkowski vacuum has no positive energy theorem, no such interpretation is possible. The instanton action is much smaller than the dS entropy and approaches a finite limit as the dS radius goes to infinity. Thus, the low energy effective theory of a model representing a stable, finite dS universe, must have a potential that is above the Great Divide.

In recent work [187, 10], one of us (T.B.) has been pursuing models of low energy SUSY breaking, which employ the meta-stable states of SUSY-QCD discovered by Intriligator, Seiberg, and Shih [179], and hypothetical generalizations of these states to the theory with an equal number of flavors and colors. These models have an R-breaking parameter that controls the scale of SUSY breaking. In the CSB context, one wants to choose this parameter (and the constant in the superpotential) in order to enforce the CSB relation

$$m_{3/2} = K\Lambda^{1/4}, \tag{7.1}$$

between the gravitino mass and the c.c.. One of us argued that these models were above the Great Divide, because when one dials the R-breaking terms to zero, SUSY is restored and the meta-stable vacuum becomes exactly stable. *This argument is wrong.* In this paper, following closely the logic of [21], we show that all models in which the potential connecting a meta-stable state to a negative c.c. point, varies rapidly on the Planck scale, are below the Great Divide, and cannot be the low energy effective theory of a stable dS space.

This means that, at the level of non-gravitational effective field theory, the only models compatible with the constraints of CSB, are those which have *no* supersymmetric vacuum states. Nelson and Seiberg [203] showed that generic Landau-Ginzburg models of chiral superfields had SUSY preserving minima unless they had an exact $U(1)$ R-symmetry. Since the rules of CSB require us to break R-symmetry in the LEFT, a generic model can not obey the requirements of CSB. This may not be as bad as it sounds. The LEFT of stable dS space has two kinds of terms in its Lagrangian. The first are terms that exist even in the $\Lambda \to 0$ limit. These arise through conventional mechanisms and can plausibly be expected to satisfy the requirements of genericity. On the other hand, there are terms whose sole purpose is to make sure that the physics of the LEFT is compatible with that of the underlying, non-field theoretic, quantum theory of dS space. At the most fundamental level, it must be compatible with the idea that this system has a finite number of states, the overwhelming majority of which, resemble the dS vacuum. Transitions out of the dS vacuum should be viewed as recurrences of low entropy states.

In the language of [21] this means that *LEFTs compatible with CSB must be above the Great Divide*. Nelson and Seiberg tell us that they must therefore be non-generic. In the last section of this paper, we will present a modified version of the Pyramid Scheme, with non-generic perturbations, which *is* compatible with CSB.

7.2 Tunneling for meta-stable field theory states

Consider a model of supersymmetric quantum field theory, with a meta-stable SUSY violating state. In terms of a (perhaps composite) set of chiral superfields $\{X_i\}$, the superpotential takes the form

$$W = \mu^3 w(X_i/M) + W_0, \tag{7.2}$$

and the Kähler potential is

$$K = M^2 k(X_i/M, X_i^*/M). \tag{7.3}$$

We assume $M \ll m_P$ and $\mu \ll m_P$. The potential for scalar fields, in SUGRA is then given approximately by

$$V = \left[\frac{\mu^6}{M^2}|w_i(x^i)|^2 - 3\frac{|W_0|^2}{m_P^2}\right] \quad \text{with} \quad x^i = \frac{X_i}{M} \quad \text{and} \quad w_i \equiv \frac{\partial w}{\partial x^i}. \tag{7.4}$$

Naively, this could be a LEFT for CSB if $m_{3/2} = \frac{\mu^3}{M m_P} = K\Lambda^{1/4}$, and $W_0 = m_{3/2}m_P^2 - \mathcal{O}(\Lambda^{3/4})$. However, the world is a tough place, and naïveté often meets with disappointment. In fact, such a field theory cannot describe the behavior of local excitations of a stable dS space. To see this, note that the potential has the form $m^4 v(X/M)$, where $m = \mu(\mu/M)^{1/2}$. The tuning of the c.c. implies that the whole potential has this order of magnitude, except right near the meta-stable minimum.

Define $x \equiv X/M$ and re-scale the space time coordinates by the natural time scale M/m^2, then the Coleman-DeLucia equations for gravitational tunneling read $(u = -v)$ [21]

$$\begin{aligned} &\ddot{x} + 3H\dot{x} + u'(x) = 0 \\ &H = \tfrac{\dot{r}}{r} \\ &\dot{r}^2 = 1 + \epsilon^2 r^2 E \\ &E = \tfrac{1}{2}\dot{x}^2 + u \end{aligned} \tag{7.5}$$

where $\epsilon^2 = M^2/3m_P^2$. The Euclidean space-time metric is

$$ds^2 = dz^2 + \rho^2(z)d\Omega_3^2, \tag{7.6}$$

and r and the dimensionless Euclidean time t are related to ρ and z by scaling out $\frac{M}{m^2}$. For the decay of dS space the instanton geometry is an ovoid. In [21] it was argued that the situation of a potential w.r.t. the great divide was determined by the stability of the Minkowski solution which is produced when we shift the dS minimum to zero. In terms of the parameters above, this corresponds to dropping the term of order $\Lambda^{3/4}$ in W_0.

If, for the Minkowski limit, we set $\epsilon = 0$, then the geometry becomes a semi-infinite cigar. Coleman [205] showed that these equations always have a solution, as long as there is a difference in vacuum energies between the true and false minima. The asymptotic solution of the scalar field equations approaches the Minkowski stationary point of the potential exponentially fast, which indicates that for very small ϵ the Minkowski decay occurs in curved dynamical space-time if the corresponding field theoretic decay occurs in Minkowski space.

In [21], we showed that for small ϵ and small positive vacuum energy, one could match this flat space solution to the solution of the field equations in dS space[2]. The instanton manifold

[2] See also [206].

is almost the full dS sphere. As a consequence, the difference between the instanton action and the dS action approaches the flat space instanton action as the dS radius goes to infinity, up to corrections of order ϵ^2. This shows that if $\epsilon \ll 1$ the potential corresponding to a meta-stable vacuum of a non-gravitational field theory is *below the Great Divide*. Such a potential cannot represent an approximate description of a stable quantum model of dS space. Indeed, such model has a finite number of states [207], the overwhelming majority of which always resemble the dS vacuum. A small number of states, of order $e^{c(RM_P)^{3/2}}$ represent meta-stable local excitations of the dS vacuum. CDL decays of such a system, correspond to recurrences of states whose entropy is constant in the limit $RM_P \to \infty$. The potential representing such decays must be above the Great Divide.

7.3 Low energy models compatible with CSB

We are in the fortunate situation of being presented with a paradox. On the one hand CSB requires the c.c. to be a tunable parameter, which arises at a deeper level as a cosmological initial condition. For small values of the c.c. the local physics of quantum dS space must be describable in terms of an effective SUGRA Lagrangian with spontaneous SUSY breaking. The scale of SUSY breaking is $K\Lambda^{1/4}m_P$. Once we put in the phenomenological lower bounds on superparticle masses, this implies that the mechanism for spontaneous breaking must be understandable in flat space effective field theory. High scale SUSY breaking by F-terms of moduli fields is not allowed.

The tunneling constraint we have just described implies that the flat space EFT cannot have a SUSic vacuum state, since if it did, it would be below the Great Divide[3]. Nelson and Seiberg [203] have shown that generic chiral Landau-Ginzburg models have SUSic ground states unless the LEFT has a continuous $U_R(1)$. However, in CSB it is precisely the explicit breaking of R-symmetries that is supposed to trigger SUSY breaking.

In models implementing CSB, the R-axion might also be light enough to cause phenomenological problems, though this depends on the details of the model and assumptions about the scale and dimension of the lowest dimension operator breaking $U_R(1)$. The universal gravitational contribution, coming from the cancelation of the cosmological constant [208], is too small, given the scale of W_0 required in CSB.

One is thus pushed in the direction of assuming a non-generic LEFT. CSB in fact provides

[3]One possible loophole in this argument is that a model below the Great Divide, could represent CSB, if the flat space action $\sim (\frac{M}{\mu})^4$ were close to $\pi(RM_P)^2$. However, since $M \ll M_P$, this can only occur if $\mu \ll \Lambda^{1/4}$, which is inconsistent with experimental lower bounds on super-particle masses.

a motivation for non-generic corrections. Our usual intuition about parameters in effective field theory comes from integrating out high frequency degrees of freedom with the renormalization group. In CSB, the LEFT has two kinds of terms. Those that exist in the $\Lambda = 0$ limit arise from a model akin to string theory in asymptotically flat space. They satisfy the usual constraints of effective field theory : generic parameters of order one in appropriate units, consistent with all symmetries. All mass scales far below the unification scale should be explained dynamically. By contrast, terms which exist only because of the dS horizon do not obey these rules. We do not understand the quantum theory of dS space well enough to give a full list of the rules they *do* obey. We know that the c.c. should be viewed as an input parameter, which means tuning W_0 in a way that would be anathema to an effective field theorist. We know that the new terms should violate R-symmetry, and that their coefficients should enforce the relation $m_{3/2} = K\Lambda^{1/4}$, with K of order 10. We have just learned that they must spontaneously break SUSY in a stable vacuum.

Previous work has explored the additional constraints of unification and other aspects of phenomenology. The constraint that there must be complete multiplets of a GUT group, at the low scale consistent with CSB, and that these new multiplets do not lead to Landau poles in standard model coupling below the unification scale, is very strong and rules out essentially all extant models of gauge mediated or direct mediated SUSY breaking, including the Pentagon model. These constraints would allow hidden sector gauge groups smaller than $SU_P(5)$, but with a flavor group containing the GUT $SU(5)$ or any larger GUT group, we have not been able to find a model with acceptable dynamics.

The Pyramid Scheme solves this problem by using trinification [174]. GUT multiplets consistent with trinification can add just D_R new vector-like quark multiplets to the colored particle spectrum, where D_R is the representation of the hidden sector gauge group. In the Pyramid Scheme we chose that group to be $SU(3)$ and R to be the fundamental plus anti-fundamental. We will see below that this might need to be modified at higher energy. In the next section we will present a simple generalization of the Pyramid Scheme which satisfies *all* these constraints.

7.4 Pyramid Schemes with a triplet of singlets

The new chiral matter content of the Pyramid Scheme consists of a singlet S and three chiral pairs $\mathcal{T}_i, \tilde{\mathcal{T}}_i$. The gauge group is $SU(3)^4 \rtimes Z_3$. The first $SU(3)$, called $SU_P(3)$, is the hidden sector gauge group, while the rest forms Glashow's trinification group, in which the Z_3 permutes the three $SU(3)$ factors, ensuring coupling unification at the GUT scale. We will be working at energies far below the GUT scale, where this group is broken to the $SU(1,2,3)$ of the standard model. We label the three $SU(3)$ groups of trinification $SU_i(3)$, with $i = 1, 2, 3$. For $i = 2, 3$, the $SU(i)$ of the standard model is the obvious Cartesian subgroup of $SU_i(3)$. Weak hypercharge is a linear combination of a generator of $SU_1(3)$ with the hypercharge generator in $SU_2(3)$. We will occasionally write terms in the Lagrangian that preserve more of the GUT symmetry than is required by general principles. We do this for convenience only. We believe that, as long as we do not introduce huge differences between parameters that are set equal by this choice, the qualitative physics of our model will remain unchanged. Another way to say this is that we have found a variety of Pyramid Schemes, with multiple parameters, which satisfy all of our fundamental and phenomenological constraints. For economy's sake we only write down the simplest one explicitly.

The new models we introduce in this paper replace the singlet S by a triplet of singlets S_i with $i = 1, \ldots, 3$. We imagine that, neglecting GUT symmetry breaking, these triplets transform into each other under the Z_3. However, in this paper we will not attempt to write down a GUT field theory or string compactification which reduces to our model below the scale of GUT symmetry breaking. When the c.c. $\Lambda = 0$, the S_i appear in the superpotential as

$$W_{\{S_i\}} = y_i S_i \mathcal{T}_i \tilde{\mathcal{T}}_i + \beta_i S_i H_u H_d, \tag{7.7}$$

with repeated indices summed.

When Λ is turned on, we add the terms

$$m_i \mathcal{T}_i \tilde{\mathcal{T}}_i + M_i^2 S_i. \tag{7.8}$$

The coefficients in these terms will scale to zero with Λ and are chosen to enforce the relation $m_{3/2} = K\Lambda^{1/4}$.

At high energies, the hidden sector is SUSY QCD with 9 flavors and 3 colors[4]. This model has a vanishing one loop beta function, which is positive at two loops. Thus the coupling slowly decreases as we go down in energy scale. We will assume that $m_{1,3}$ are both $> m_2$. After integrating out the heavy trianons, we have the $N_F = N_C = 3$ model, and we assume that this becomes strongly coupled at a scale Λ_3 just below m_2.

Now let us discuss candidates for the discrete R-symmetry which is part of the rules of the game of CSB. The $(3, 9)$ gauge theory has an anomaly free $U_R(1)$ symmetry under which all the trianon and anti-trianon fields have charge $2/3$. We can choose a discrete subgroup of this,

[4]In order to avoid Landau poles in the hidden sector gauge coupling, we will later contemplate an enhanced hidden sector gauge symmetry, reduced to this one by the Higgs mechanism at a fairly high scale.

and add any cyclic subgroup of the $SU_L(9)\times SU_R(9)\times U_B(1)$ flavor group. We must check that the symmetry is not broken by standard model instantons. Finally, we want to reproduce the success of previous models and use this symmetry to forbid all dimension four and five operators in the MSSM, which violate B or L, apart from the neutrino seesaw operators $(LH_u)^2$. We know that this can be accomplished if we choose $\mathcal{T}_2$, $\tilde{\mathcal{T}}_2$ to have R-charge 0 and S_2 to have R-charge 2.

The low energy superpotential is written in terms of the fields S_i, H_u, H_d and the mesons and baryons of the gauge theory. We parametrize the dimension one meson matrix by

$$M = Ze^{\frac{\lambda_a Z_a}{\Lambda_3}}, \tag{7.9}$$

where λ_a are the eight traceless Gell-Mann matrices. We will search for $SU(3)$ symmetric stationary points, where $Z_a = 0$. The superpotential is

$$W = 3\Lambda_3(m_2 + y_2 S_2)Z + L(Z^3/\Lambda_3 - B\tilde{B} - \Lambda_3^2) + \beta_i S_i H_u H_d + M_i^2 S_i. \tag{7.10}$$

The equations from the variation of B and $\tilde{B}$ either force these fields to be zero or L to vanish. We explore the second alternative first. The variation of Z, for $L = 0$ implies

$$y_2 S_2 + m_2 = 0. \tag{7.11}$$

The variational equations for the S_i imply

$$3\delta_{i2} y_2 \Lambda_3 Z + \beta_i H_u H_d + M_i^2 = 0. \tag{7.12}$$

These are three equations for two unknowns, and have no solution.

Turning to the solution $B = \tilde{B} = 0$, we note that the moduli space constraint now freezes $Z^3 = \Lambda_3^3$, which has 3 solutions. The Z equation fixes L in terms of S_2, but the S_i equations are now three equations for the single unknown $H_u H_d$. Therefore, we do not find any supersymmetric solution on either branch of the moduli space.

This conclusion is unchanged if we explore non-zero values of the adjoint fields Z_a. These appear only through a multiplicative factor Tr $e^{\lambda_a Z_a}$ in the term in the superpotential linear in Z. The variational equations for these fields are of course satisfied when $Z_a = 0$, and there are other solutions. If we are on the branch where $L = 0$ then all values of the Z_a are stationary. None of this changes the fact that there are no solutions of the variational equations for the S_i.

We note that it is the parameters M_i^2 which prevent us from having a supersymmetric solution. If they vanished, then on the branch with $L = 0$ we can solve the S_2 equation by fixing $y_2\Lambda_3 Z + \beta_2 H_u H_d = 0$, and the other equations are both solved by $H_u = H_d = 0$ (which also solves the variational equations for the Higgs fields – equations we have not yet discussed). Therefore, the crucial SUSY violating equations are those which come from varying $S_{1,3}$.

7.5 $SU_P(3)$ Landau pole and $SU_P(4)$ completion

It is interesting to look at the strongly-coupled gauge theory beta function since this sector consists of $SU_P(N_C)$ SQCD with $N_C = 3$ and $N_F = 9$ and is thus not asymptotically free. One can therefore ask what are the lightest ISS masses compatible with a strongly-coupled $SU_P(3)$, such that there is no Landau pole below the GUT scale. As we mentioned earlier, the resulting large ISS mass hierarchy will suggest that we look instead at $SU_P(4)$ which is Higgsed to $SU_P(3)$ at some high scale. To perform the analysis, it is convenient to look at the general case of $SU_P(N_C)$ SQCD with N_F flavors. The β-function for $SU(N_C)$ with N_F fundamental flavors is

$$\beta_g = -\frac{g^3}{16\pi^2}\frac{3N_C - N_F + N_F\gamma}{1 - N_C\frac{g^2}{8\pi^2}} \tag{7.13}$$

$$\gamma = -\frac{g^2}{8\pi^2}\frac{N_C^2 - 1}{N_C} + \mathcal{O}(g^4) \tag{7.14}$$

or in terms of the fine structure constant $\alpha = g^2/4\pi$

$$\beta_{\frac{2\pi}{\alpha}} = \frac{3N_C - N_F + N_F\gamma}{1 - N_C\frac{\alpha}{2\pi}} \tag{7.15}$$

$$\gamma = -\frac{\alpha}{2\pi}\frac{N_C^2 - 1}{N_C} + \mathcal{O}(\alpha^2) \tag{7.16}$$

At first order, the solution is

$$\frac{2\pi}{\alpha(\mu)} = \frac{2\pi}{\alpha(\mu_0)} + (3N_C - N_F)\ln(\mu/\mu_0) \qquad \text{for } N_F \neq 3N_C \tag{7.17}$$

$$\left(\frac{2\pi}{\alpha(\mu)}\right)^2 = \left(\frac{2\pi}{\alpha(\mu_0)}\right)^2 - 6(N_C^2 - 1)\ln(\mu/\mu_0) \qquad \text{for } N_F = 3N_C \tag{7.18}$$

In our case, we expect the hierarchy $\Lambda_3 < m_2 < m_3 < m_1 < M_{\rm GUT}$ where m_3 cannot be too much larger than Λ_3 due to the experimental lower bound on the gluino mass. When m_3 is large, there are no light messengers, which carry color. Thus the strongly-coupled theory has 0 flavors between Λ_3 and m_2, 3 flavors between m_2 and m_3, 6 flavors between m_3 and m_1 and 9 flavors between m_1 and $M_{\rm GUT}$. At leading order, this leads to

$$\begin{aligned}\left(\frac{2\pi}{\alpha(\mu)}\right)^2 &= [9\ln(m_2/\Lambda_3) + 6\ln(m_3/m_2) + 3\ln(m_1/m_3)]^2 - 48\ln(\mu/m_1) \qquad (7.19)\\ &= 9\ln^2(m_1 m_2 m_3/\Lambda_3^3) - 48\ln(\mu/m_1)\end{aligned}$$

where $m_1 < \mu < M_{\rm GUT}$. With the generic numbers $\Lambda_3 = 5$ TeV, $m_2 = 9$ TeV and $m_3 = 12$ TeV, asking for the Landau pole to be above the GUT scale leads to $m_1 \gtrsim 4 \times 10^4$ TeV. This is quite a large hierarchy of scales for the ISS masses. Indeed it is so large that it ruins standard model gauge coupling unification. With this spectrum of trianons, in the one loop approximation, $\alpha_1(M_{\rm GUT})$ is ~ 20 % away from the value it should be for unification.

The best way to circumvent this hierarchy is to assume that the theory is an $SU_P(4)$ with $N_F = 9$ flavors which is Higgsed to the previous $SU_P(3)$ with $N_F = 9$ flavors at a scale determined by the VEV V_4 of a chiral field in the $N_F = 9$, $N_C = 4$ model. Now the (mild) hierarchy of scales becomes $\Lambda_3 < m_2 < m_3 < m_1 < V_4 < M_{\rm GUT}$. Following the same analysis as shown above, the constraint on the VEV follows from

$$\frac{2\pi}{\alpha(\mu)} = \sqrt{9\ln^2(m_1 m_2 m_3/\Lambda_3^3) - 48\ln(V_4/m_1)} + 3\ln(\mu/V_4) \tag{7.20}$$

where $V_4 < \mu < M_{\rm GUT}$.

With $\Lambda_3 = 5$ TeV, $m_2 = 9$ TeV, $m_3 = 12$ TeV and $m_1 = 15$ TeV the theory is well-behaved for $V_4 \lesssim 50$ TeV. The VEV cannot be pushed to very high scales due to the behavior of the beta function when $N_F = 3N_C$.

There are certainly loci on the moduli space of the $N_F = 9$, $N_C = 4$ theory with this pattern of Higgs VEVs. We have not investigated the origin of the potential which might fix the theory at such a point. We have thus exhibited two possible mechanisms for avoiding a Landau pole in the $SU_P(3)$ coupling below the GUT scale, but only one consistent with standard model gauge coupling unification. The enhancement of the hidden sector gauge group introduces scales in the same ballpark as the rest of the energy scales in the model. Adopting it, we incur a debt to explain a new $10 - 100$ TeV scale Higgs mechanism, which we hope to repay at a later date.

7.6 Discrete R-symmetry

The R-charges in the Pyramid Scheme with a triplet of singlets follow the usual rules. Here we look for a R-charge assignment which leads to the vanishing of the 't Hooft operators for $SU_P(4)$. Another constraint comes from the trilinear singlet-Higgs couplings, $S_i H_u H_d$ which cannot be in the Lagrangian for all $i = 1, \ldots, 3$. If they were, all singlets S_i would have the same R-charge and this is prohibited by the vanishing of the $SU_C(3)$ 't Hooft operator. Therefore one has to choose $\beta_3 = 0$ with $\beta_{i=1,2}$ arbitrary and then the $S_{i=1,2}$ singlets share the same R-charge. Denoting the R-charge of a field by the field itself, this implies $S_1 = S_2 \equiv S$. In the

GUT notation, the extra matter fields are

$$
\begin{array}{c|cccc}
 & SU_1(3) & SU_2(3) & SU_3(3) & SU_P(3) \\
\hline
\mathcal{T}_1 & 3 & 1 & 1 & \bar{3} \\
\bar{\mathcal{T}}_1 & \bar{3} & 1 & 1 & 3 \\
\mathcal{T}_2 & 1 & 3 & 1 & \bar{3} \\
\bar{\mathcal{T}}_2 & 1 & \bar{3} & 1 & 3 \\
\mathcal{T}_3 & 1 & 1 & 3 & \bar{3} \\
\bar{\mathcal{T}}_3 & 1 & 1 & \bar{3} & 3 \\
S_{i=1,2,3} & 1 & 1 & 1 & 1.
\end{array}
\tag{7.21}
$$

As explained above, our goal is to find an approximate discrete R-symmetry which is exact in the limit of zero c.c. and which allows only the terms needed in this limit. To simplify the search, we will look at a continuous $U_R(1)$, of which we imagine only a discrete Z_N subgroup is fundamental. Therefore, all the following equations only have to be satisfied modulo N.

The only superpotential terms which are required at the renormalizable level are

$$
W_{\Lambda=0} \supset S_i \mathcal{T}_i \bar{\mathcal{T}}_i,\ S_{i=1,2} H_u H_d,\ H_u Q \bar{U},\ H_d Q \bar{D},\ H_d L \bar{E},\ (L H_u)^2 \tag{7.22}
$$

which implies that the R-charges satisfy

$$
\begin{aligned}
\mathcal{T}_{i=1,2} + \bar{\mathcal{T}}_{i=1,2} &= 2 - S \\
\mathcal{T}_3 + \bar{\mathcal{T}}_3 &= 2 - S_3 \\
H_u &= 2 - H_d - S \\
\bar{U} &= H_d + S - Q \\
\bar{D} &= 2 - H_d - Q \\
\bar{E} &= 2 - H_d - L
\end{aligned}
$$

since $S_{i=1,2} \equiv S$ and the extra relation from the neutrino seesaw operator has still to be taken into account. All remaining renormalizable superpotential terms must be forbidden by the discrete R-symmetry otherwise we would expect them to be in the superpotential with order 1 coefficients in the appropriate units. Moreover, dangerous higher-dimensional B and L violating terms must be forbidden as well by the discrete R-symmetry to insure proton stability on appropriate timescales.

The (approximate) $U_R(1)$ anomaly conditions are

$$\begin{aligned}
SU_P(4)^2U_R(1) \quad &\Rightarrow \quad 2\cdot 4 + 3(\mathcal{T}_1 + \bar{\mathcal{T}}_1 + \mathcal{T}_2 + \bar{\mathcal{T}}_2 + \mathcal{T}_3 + \bar{\mathcal{T}}_3 - 6) \\
&\qquad\qquad = 8 - 6S - 3S_3 \\
SU_C(3)^2U_R(1) \quad &\Rightarrow \quad 2\cdot 3 + 6(Q-1) + 3(\bar{U} + \bar{D} - 2) + 4(\mathcal{T}_3 + \bar{\mathcal{T}}_3 - 2) \\
&\qquad\qquad = 3S - 4S_3 \\
SU_L(2)^2U_R(1) \quad &\Rightarrow \quad 2\cdot 2 + (H_u + H_d - 2) + 9(Q-1) + 3(L-1) \\
&\qquad\qquad +4(\mathcal{T}_2 + \bar{\mathcal{T}}_2 - 2) = 3(3Q+L) - 8 - 5S.
\end{aligned}$$

These lead to the equation $S_3 = 9S - 8$ and the 't Hooft constraints

$$\begin{aligned}
32 - 33S &= 0 \\
3(3Q+L) - 8 - 5S &= 0.
\end{aligned}$$

The dangerous renormalizable and higher-dimensional B and L violating superpotential and Kähler potential terms (note that the neutrino seesaw operator is required) can be combined into 13 groups,

$$\begin{aligned}
G_1 = \{LL\bar{E},\ LQ\bar{D},\ SLH_u\} \quad &\Rightarrow \quad L - H_d \\
G_2 = \{\bar{U}\bar{D}\bar{D}\} \quad &\Rightarrow \quad 3Q + H_d - S - 2 \\
G_3 = \{LH_u,\ Q\bar{U}\bar{E}H_d,\ \bar{U}\bar{D}^*\bar{E},\ H_u^*H_d\bar{E},\ Q\bar{U}L^*\} \quad &\Rightarrow \quad L - H_d - S \\
G_4 = \{S_3LH_u\} \quad &\Rightarrow \quad L - H_d + 8S - 8 \\
G_5 = \{QQQL\} \quad &\Rightarrow \quad 3Q + L - 2 \\
G_6 = \{QQQH_d,\ QQ\bar{D}^*\} \quad &\Rightarrow \quad 3Q + H_d - 2 \\
G_7 = \{\bar{U}\bar{U}\bar{D}\bar{E}\} \quad &\Rightarrow \quad 3Q + L - 2S - 2 \\
G_8 = \{LH_uH_dH_u\} \quad &\Rightarrow \quad L - H_d - 2S + 2 \\
G_9 = \{SLL\bar{E},\ SLQ\bar{D},\ S^2LH_u\} \quad &\Rightarrow \quad L - H_d + S \\
G_{10} = \{S\bar{U}\bar{D}\bar{D}\} \quad &\Rightarrow \quad 3Q + H_d - 2S - 2 \\
G_{11} = \{SS_3LH_u,\ S_3LL\bar{E},\ S_3LQ\bar{D}\} \quad &\Rightarrow \quad L - H_d + 9S - 8 \\
G_{12} = \{S_3\bar{U}\bar{D}\bar{D}\} \quad &\Rightarrow \quad 3Q + H_d - 10S + 6 \\
G_{13} = \{S_3^2LH_u\} \quad &\Rightarrow \quad L - H_d + 17S - 16.
\end{aligned}$$

Moreover, the forbidden renormalizable superpotential terms can be combined into 12 groups,

$$\begin{aligned}
G_{14} = \{\mathcal{T}_1\bar{\mathcal{T}}_1,\ \mathcal{T}_2\bar{\mathcal{T}}_2,\ H_uH_d\} &\quad\Rightarrow\quad S \\
G_{15} = \{\mathcal{T}_3\bar{\mathcal{T}}_3\} &\quad\Rightarrow\quad 9S-8 \\
G_{16} = \{S_3H_uH_d\} &\quad\Rightarrow\quad 8S-8 \\
G_{17} = \{S\} &\quad\Rightarrow\quad S-2 \\
G_{18} = \{S^2\} &\quad\Rightarrow\quad 2S-2 \\
G_{19} = \{S^3\} &\quad\Rightarrow\quad 3S-2 \\
G_{20} = \{S_3\} &\quad\Rightarrow\quad 9S-10 \\
G_{21} = \{S_3^2\} &\quad\Rightarrow\quad 18S-18 \\
G_{22} = \{S_3^3\} &\quad\Rightarrow\quad 27S-26 \\
G_{23} = \{SS_3\} &\quad\Rightarrow\quad 10S-10 \\
G_{24} = \{S^2S_3\} &\quad\Rightarrow\quad 11S-10 \\
G_{25} = \{SS_3^2\} &\quad\Rightarrow\quad 19S-18.
\end{aligned}$$

Operators in each group have the same R-charge (once one takes the $d^2\theta$ for superpotential terms into account). It is possible to forbid all dangerous terms with $N = 13$, and $S = 12$, $Q = 0$, $L = 1$, and $H_d = 3$. With this choice all anomaly conditions are satisfied, only the required terms do not break the discrete R-symmetry and thus none of the dangerous terms are allowed. Notice moreover that the neutrino seesaw operator is allowed as required by this choice of R-charges. Therefore one can engineer a generic superpotential of the form

$$\begin{aligned}
W_{\Lambda=0} = \sum_{i=1}^{3} y_i S_i \mathcal{T}_i\bar{\mathcal{T}}_i + \sum_{i=1}^{2}\beta_i S_i H_u H_d \\
+ \lambda_u H_u Q\bar{U} + \lambda_d H_d Q\bar{D} + \lambda_L H_d L\bar{E} + \frac{\lambda_\nu}{m_P}(LH_u)^2
\end{aligned} \tag{7.23}$$

which is supplemented by the non-generic superpotential

$$\delta W_{\Lambda\neq 0} = \sum_{i=1}^{3}\left(m_i\mathcal{T}_i\bar{\mathcal{T}}_i + M_i^2 S_i\right) + W_0 \tag{7.24}$$

when the c.c. is turned on. Note that in these equations $\lambda_{u,d,L,\nu}$ are all matrices in generation space.

7.7 Conclusions

When combined with fairly broad brush phenomenological requirements, the idea of CSB is constrained in quite a remarkable manner. The strongest constraints come from the combination of the low scale of SUSY breaking required by CSB, and coupling unification. Most models of gauge mediation, both direct and with an intermediate messenger sector, are ruled out. The only models we have found, which satisfy these constraints, are variations on the Pyramid Scheme.

In this paper, we pointed out two new constraints and proposed a class of models that satisfies them. The first constraint comes from the fundamental requirement that the LEFT of a theory of stable dS space, *must* be above the Great Divide. On the other hand, we showed that flat space field theory models, with a meta-stable SUSY violating vacuum and a SUSic vacuum a distance $M \ll m_P$ away in field space (and no unnatural fine tuning besides the tuning of the c.c.), are all below the Great Divide.

CSB *requires* very low scale SUSY breaking, so the only way to achieve this is for the LEFT to have no SUSic vacuum at all. The seminal paper of Nelson and Seiberg shows us that this is achievable in a generic manner, only if the model has an unbroken $U_R(1)$, which is spontaneously broken. This however is *incompatible* with the requirements of CSB, according to which a discrete R-symmetry and a SUSic vacuum are both restored in the $\Lambda = 0$ limit. Explicit R-violating terms are then supposed to remove the SUSic vacuum. We argued that there is no reason to assume those R-violating terms obeyed the rules of quantum field theory naturalness. We exhibited an explicit variation on the Pyramid Scheme, with a separate singlet for each leg of the Pyramid, which satisfied all these requirements.

The second issue we studied was the occurrence of Landau poles below the GUT scale in the hidden sector gauge coupling. We argued that to avoid these, preserving the phenomenological successes of the model, we either had to take one R-violating trianon mass to be very large $\gtrsim 4 \times 10^4$ TeV, or embed $SU_P(3)$ in $SU_P(4)$ with a Higgs mechanism at $\lesssim$ 50 TeV. However, the first idea ruins standard model gauge coupling unification. Thus, the only scheme consistent with CSB, with gauge coupling unification, and with standard model phenomenology is a pyramid with an $SU(4)$ apex, reduced to the $N_F = N_C = 3$ model by a combination of the Higgs mechanism and trianon masses. All of the scales of the model are in the $1 - 100$ TeV regime. We have not yet investigated the dynamical mechanism which could account for this new Higgs mechanism, which breaks $SU_P(4)$ to $SU_P(3)$.

Finally, everything is connected in the Pyramid Scheme, and we were forced to revisit the issue of the discrete R-symmetry group and its role in suppressing dimension four and five operators that violate B and L. The simplest model we found uses a Z_{13} R-symmetry group.

Chapter 8

Gamma Ray Spectra from Dark Matter Annihilation and Decay

8.1 Introduction

In this chapter we discuss in detail the findings of the work done in collaboration with S. Thomas, J. Shelton and Y. Zhao [28].

Recently several experiments (ATIC [23], H.E.S.S. [24, 25], PAMELA [26], FERMI [27]) have detected an anomaly in the cosmic ray electron spectrum, measuring an excess in the high-energy positron flux compared to usual diffusion models. Such an excess was not found for antiprotons [209]. One was thus led to conjecture a new source of primary electrons and positrons. The most likely sources advanced to explain this anomaly are nearby pulsars or dark matter (DM) annihilation/decay [210, 211]. In any case, the issue related to the identity of the new source (pulsars versus DM) will be clarified by the photon spectrum which will be measured by FERMI and announced later this summer. Indeed, there is an irreducible background of gamma ray photons coming from final state radiation (FSR) from electrons and/or positrons. Nearby pulsars would lead to a local photon spectrum while DM would instead generate a diffuse photon spectrum.

The existence of DM is well established, although its particle identity is still unknown. Assuming that DM annihilation/decay is the new source of primary electrons and positrons, several scenarios are possible (see [212, 213, 214, 215, 216, 217, 218, 219, 220, 221, 222, 223, 224, 225, 226, 227, 228, 229, 230, 231, 232, 233, 234, 235, 236] for related work). Apart from FSR of photons, DM might also annihilate/decay directly to photons. Different photon spectra are expected from each annihilation/decay mode and a knowledge of the achievable spectra will help physicists understand the properties of DM at the particle level.

In Section 8.2, we discuss direct production of photons from DM annihilation/decay through subsequent two-body decay chains. In Section 8.3, we study the irreducible photon background from charged particles, considering only the dominant process (either FSR of photons or photon production from higher-order operators). Next, in Section 8.4 we consider direct photon production from taus. Finally, Section 8.5 contains a summary of the results and a comparison of the different photon spectra and total fluxes obtained from the density of states (DOS). Various detailed computations are left for the Appendix.

Since we want to address both annihilation and decay, we compute photon DOS throughout the paper, which it only differs from the spectrum by a constant factor, namely the total number of photons. One can write the DOS as

$$\frac{1}{N_\gamma}\frac{dN_\gamma}{dE_\gamma} = \frac{1}{\langle\sigma v\rangle}\frac{d\langle\sigma v\rangle}{dE_\gamma} \quad \text{or} \quad \frac{1}{N_\gamma}\frac{dN_\gamma}{dE_\gamma} = \frac{1}{\Gamma}\frac{d\Gamma}{dE_\gamma},$$

as distinct from the photon spectra $\frac{dN_\gamma}{dE_\gamma}$. The photon DOS are thus normalized to 1, i.e. $\int dE_\gamma \frac{1}{N_\gamma}\frac{dN_\gamma}{dE_\gamma} = 1$, except for FSR where the DOS is normalized with respect to the zeroth-order annihilation cross-section/decay width (see Section 8.3). Thus, the total number of photons N_γ, given by $N_\gamma = \int dE_\gamma \frac{dN_\gamma}{dE_\gamma}$, can be found from the photon multiplicity. For example, a scenario where DM annihilates/decays to two scalar bosons which subsequently decay to two photons each would have a total number of photons given by $N_\gamma = 4$. Since we focus on the photon DOS, all the results are applicable to both DM annihilation and decay, which can be assessed simultaneously by taking the parameter M to be $2m_{\text{DM}}$ for DM annihilation or m_{DM} for DM decay.

Since backgrounds fall roughly like E_γ^2, we plot the photon DOS as a function of the dimensionless photon energy $2E_\gamma/M$ with an extra E_γ^2 factor. This is consistent with the standard representation used by experiments. The $M/2$ factor appearing in the plots is to make the quantities dimensionless, where $M/2$ usually is the maximal energy a photon can get during a process.

Throughout this paper we assume that DM annihilates/decays only to leptons or photons as indicated by the experiments. Moreover, we assume that DM annihilation always occurs in the s-wave approximation. Under this assumption, we can eliminate the operators that can only contribute in p-wave or higher-order waves when we do operator analysis in later sections. Furthermore, DM annihilation to leptons or photons is allowed whatever the particle identity of DM (scalar boson, fermion or gauge boson). However, with the assumptions that standard model particles are not charged under hidden symmetries and that individual lepton numbers are conserved, DM decay to leptons or photons is allowed only for scalar boson and abelian gauge boson DM.

Issues related to the overall annihilation cross-sections/decay rates (Sommerfeld enhancement, non-thermal DM production, etc) and the irreducible astrophysical photon background (inverse Compton scattering from starlight and CMB, synchrotron radiation from galactic magnetic fields) will not be investigated.

8.2 Direct production of photons through subsequent two-body decay chain

In this section, we analyze direct production of photons through subsequent two-body decay chains produced by DM annihilation/decay. We assume the whole process is a chain with k steps of the form $\phi_{i-1} \to 2\phi_i$, where the last ϕ will decay to two photons, thereby giving $2k$ photons as the final products. In Appendix 8.7, we give a general way to calculate the DOS for two-body decay chains with on-shell intermediate particles. In following subsections, we simply show some results for different scenarios.

8.2.1 $\mathbf{DM + DM \to 2\gamma}$ and $\mathbf{DM \to 2\gamma}$

We first start with the simplest case where DM annihilates/decays directly to two photons. Since DM particles are almost stationary in the galactic frame, the photon DOS is a pure delta function,

$$\frac{1}{N_\gamma}\frac{dN_\gamma}{dE_\gamma} = \delta\left(E_\gamma - \frac{M}{2}\right). \tag{8.1}$$

Since $N_\gamma = 2$ the photon spectrum is simply twice the photon DOS.

8.2.2 $\mathbf{DM + DM \to 2\phi}$ and $\mathbf{DM \to 2\phi}$ followed by $\boldsymbol{\phi \to 2\gamma}$

To compute the photon DOS when DM annihilates/decays to two bosons which subsequently decay to two photons each, we must first boost the DOS obtained in the previous subsection and convolve it with the appropriate DOS of DM annihilation/decay to two bosons as explained in Appendix 8.7. Because the energy of the ϕ boson is always $\frac{M}{2}$ and the direction of the photon in the boson rest frame is uniform, we can simply boost the delta function into the DM center of mass frame to obtain the photon DOS,

$$\frac{1}{N_\gamma}\frac{dN_\gamma}{dE_\gamma} = \frac{2}{M\sqrt{1-\frac{4m_\phi^2}{M^2}}}, \tag{8.2}$$

where the photon energy is between

$$\frac{M}{4}\left(1-\sqrt{1-\frac{4m_\phi^2}{M^2}}\right) < E_\gamma < \frac{M}{4}\left(1+\sqrt{1-\frac{4m_\phi^2}{M^2}}\right)$$

and m_ϕ is the boson mass. As expected the photon DOS is normalized to one and the photon spectrum is four times the photon DOS ($N_\gamma = 4$). Notice that in the limit where $m_\phi = \frac{M}{2}$, in which case the two ϕ bosons are produced *at rest* in the DM center of mass frame, the photon DOS becomes a delta function and matches the photon DOS obtained in the previous subsection. This is easily understood since in this limit the ϕ bosons are stationary and decay to two photons each as in the previous subsection, only the delta function support and the DOS normalization change.

8.2.3 $\mathbf{DM + DM \to 2\phi}$ and $\mathbf{DM \to 2\phi}$ followed by $\boldsymbol{\phi \to 2\pi}$ and $\boldsymbol{\pi \to 2\gamma}$

When DM annihilates/decays to two ϕ bosons which decay to two π bosons and finally decay to two photons, the photon DOS can again be computed by boosting the DOS obtained in the previous subsection and convolving the result with the appropriate DOS of DM annihilation/decay to two bosons. As shown before, the ϕ DOS is a delta function and the π DOS is a step function. However the photon DOS gets complicated since, for a fixed photon energy, not all π with energy in the support of the step function can contribute. Indeed we have to calculate the minimum and maximum allowed π energies which can generate the relevant photon energy and compute the photon DOS accordingly. Detailed computations are discussed in Appendix 8.7. Defining the boson masses as m_ϕ and m_π the photon DOS is

$$\frac{1}{N_\gamma}\frac{dN_\gamma}{dE_\gamma} = A \begin{cases} \ln\left[\frac{E_\pi^{\max}+|\vec{p}_\pi^{\;\max}|}{m_\pi}\frac{2E_\gamma}{m_\pi}\right] & \text{for } E_\gamma^{\min}(E_\pi^{\max}) < E_\gamma < E_\gamma^{\min}(E_\pi^{\min}) \\ \ln\left[\frac{E_\pi^{\max}+|\vec{p}_\pi^{\;\max}|}{E_\pi^{\min}+|\vec{p}_\pi^{\;\min}|}\right] & \text{for } E_\gamma^{\min}(E_\pi^{\min}) < E_\gamma < E_\gamma^{\max}(E_\pi^{\min}) \\ \ln\left[\frac{E_\pi^{\max}+|\vec{p}_\pi^{\;\max}|}{m_\pi}\frac{m_\pi}{2E_\gamma}\right] & \text{for } E_\gamma^{\max}(E_\pi^{\min}) < E_\gamma < E_\gamma^{\max}(E_\pi^{\max}) \end{cases} \tag{8.3}$$

where

$$\begin{aligned} A &= \frac{2}{M\sqrt{1-\frac{4m_\phi^2}{M^2}}\sqrt{1-\frac{4m_\pi^2}{m_\phi^2}}} \\ E_\pi^{\min} &= \frac{M}{4}\left(1-\sqrt{1-\frac{4m_\phi^2}{M^2}}\sqrt{1-\frac{4m_\pi^2}{m_\phi^2}}\right) \\ E_\pi^{\max} &= \frac{M}{4}\left(1+\sqrt{1-\frac{4m_\phi^2}{M^2}}\sqrt{1-\frac{4m_\pi^2}{m_\phi^2}}\right) \end{aligned}$$

and $|\vec{p}_\pi| = \sqrt{E_\pi^2 - m_\pi^2}$. The limits on the photon energy E_γ are found using

$$\begin{aligned} E_\gamma^{\min}(E_\pi) &= \frac{E_\pi}{2}\left(1-\sqrt{1-\frac{m_\pi^2}{E_\pi^2}}\right) \\ E_\gamma^{\max}(E_\pi) &= \frac{E_\pi}{2}\left(1+\sqrt{1-\frac{m_\pi^2}{E_\pi^2}}\right) \end{aligned}$$

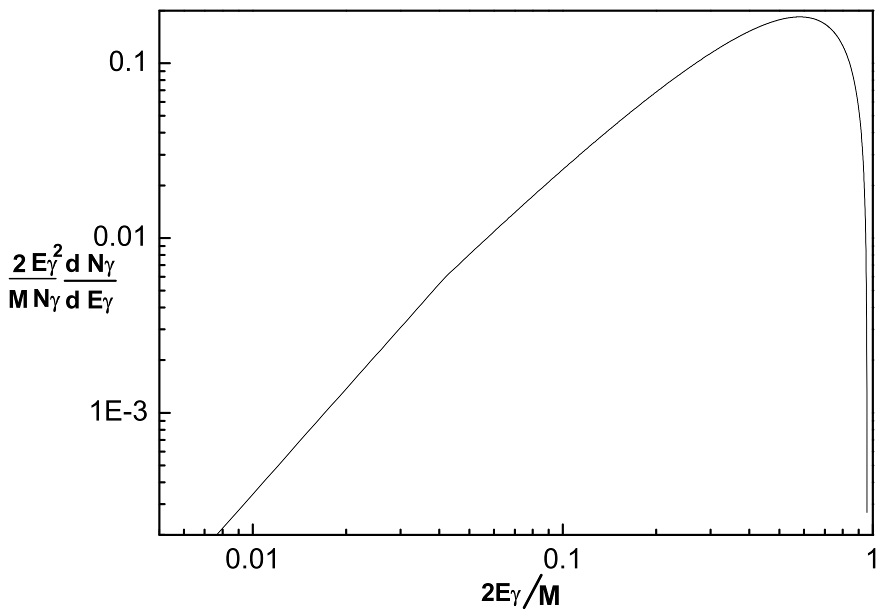

Figure 8.1: Photon spectral distribution for DM + DM $\rightarrow 2\phi$ and DM $\rightarrow 2\phi$ followed by $\phi \rightarrow 2\pi$ and $\pi \rightarrow 2\gamma$ with $M = 2000$ GeV, $m_\phi = 400$ GeV and $m_\pi = 0.14$ GeV. The distributions peaks at $2E_\gamma/M = (E_\pi^{\max} + |\vec{p}_\pi^{\,\max}|)/Me^{1/2}$, where $e \simeq 2.718$; for the parameters here the peak is at $2E_\gamma/M \simeq 0.581$.

where $E_\gamma^{\min}(E_\pi^{\max}) < E_\gamma^{\min}(E_\pi^{\min}) < E_\gamma^{\max}(E_\pi^{\min}) < E_\gamma^{\max}(E_\pi^{\max})$. $E_\gamma^{\min/\max}(E_\pi^{\min})$ is the minimum/maximum photon energy that can be generated by a π boson with minimum energy and similarly for $E_\gamma^{\min/\max}(E_\pi^{\max})$. Again the photon DOS is canonically normalized while the photon spectrum is normalized such that the total number of photons is 8 ($N_\gamma = 8$) and it is shown in figure 8.1 for some given boson masses.

There are three parts in the DOS. The first part of the DOS increases with the photon energy E_γ logarithmically, then in the second part the DOS is constant independent of the photon energy E_γ and in the third part the DOS decreases with the photon energy E_γ logarithmically. With the parameters we chose for figure 8.1, the first part is outside the plot, the second part corresponds to the straight line in the low-energy regime and, since the DOS is not smooth, connects with the third part at the kink located at $2E_\gamma/M = 2E_\gamma^{\max}(E_\phi^{\min}) \simeq 0.04$.

As a consistency check, we can again match the DOS obtained here with the DOS obtained in the previous subsections by taking different limits on the mass ratios. Indeed, by taking the limits $\frac{m_\pi}{m_\phi} = \frac{1}{2}$ or $\frac{m_\phi}{M} = \frac{1}{2}$ (but not both) the DOS becomes a step function because, in such limits, there are two particles produced *at rest* in the center of mass frame of the parent particle(s). Moreover in the limit where both $\frac{m_\pi}{m_\phi} = \frac{1}{2}$ and $\frac{m_\phi}{M} = \frac{1}{2}$ the DOS becomes a delta function since, in that limit, DM annihilates/decays to two stationary ϕ bosons, and both ϕ decay to two stationary π bosons, which finally decay to a total of eight photons, each of them taking $\frac{1}{8}$ of the initial energy M.

If we take generic values for the two mass ratios $\frac{m_\pi}{m_\phi}$ and $\frac{m_\phi}{M}$, the third part of the DOS, which decreases as $-\ln(E_\gamma)$, dominates the DOS (it has the largest support). Also, adding more steps to the decay chain results in a softer photon DOS, a general trend which is intuitively expected since the total energy is distributed among a larger number of particles.

8.2.4 DM + DM $\to N\phi$ and DM $\to N\phi$ followed by $\phi \to 2\gamma$

Finally, we study DM annihilation/decay to N ϕ bosons which then decay to two photons each. The computation is done in the massless limit, i.e. $m_\phi = 0$. This scenario occurs for example when two strongly-coupled bound states annihilate to very light pseudo Nambu-Goldstone bosons (pions in the QCD analogy) which then decay to two photons [10]. In the massless limit, the ϕ boson DOS, assuming constant matrix element, can be computed by dimensional analysis and is given by

$$\frac{1}{N_\phi}\frac{dN_\phi}{dE_\phi} = \frac{2(N-1)(N-2)(M-2E_\phi)^{N-3}2E_\phi}{M^{N-1}} \tag{8.4}$$

where $0 < E_\phi < \frac{M}{2}$. Therefore the photon DOS is simply

$$\frac{1}{N_\gamma}\frac{dN_\gamma}{dE_\gamma} = \frac{2(N-1)(M-2E_\gamma)^{N-2}}{M^{N-1}} \tag{8.5}$$

where $0 < E_\gamma < \frac{M}{2}$ (more detail is given in Appendix 8.7). The photon DOS is canonically normalized and the photon spectrum is normalized to $N_\gamma = 2N$. When $N = 2$ this result is equivalent to the scenario discussed in subsection 8.2.2, equation (8.2), with $m_\phi = 0$. The photon DOS for different N is shown in figure 8.2. One can easily see that the width grows with N.

8.3 Photons from final states with charged particles

In this section, we analyze the irreducible photon background coming from charged particles, considering only the dominant process, i.e. either FSR of photons or direct photon production from higher-order operators.

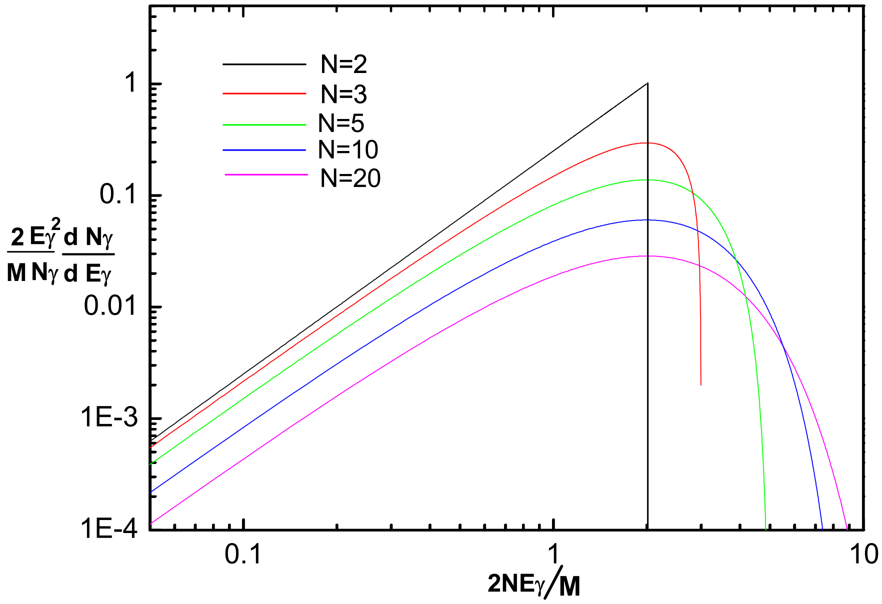

Figure 8.2: Photon spectral distributions for $\mathrm{DM} + \mathrm{DM} \to N\phi$ and $\mathrm{DM} \to N\phi$ followed by $\phi \to 2\gamma$ in the limit $M \gg m_\phi$, for $N = 2, 3, 5, 10$ and 20. All the distributions peak at $2NE_\gamma/M = E_\gamma/(E_\gamma^{\max}/N) = 2$.

For DM annihilation, FSR is the dominant process unless DM is a scalar boson or a Majorana fermion which annihilates directly to an electron-positron pair. For DM decay, FSR is the dominant process unless DM is a scalar boson which decays directly to an electron-positron pair. Indeed, in these specific cases FSR is small due to a large chiral suppression (in the s-wave approximation for the annihilation scenarios), and might or might not be the dominant process according to the typical scale of the leading higher-order operators.

Here we will study two different modes which contribute to the photon DOS: DM annihilation/decay to one electron-positron pair and DM annihilation/decay to one boson pair which subsequently decay to one electron-positron pair each.

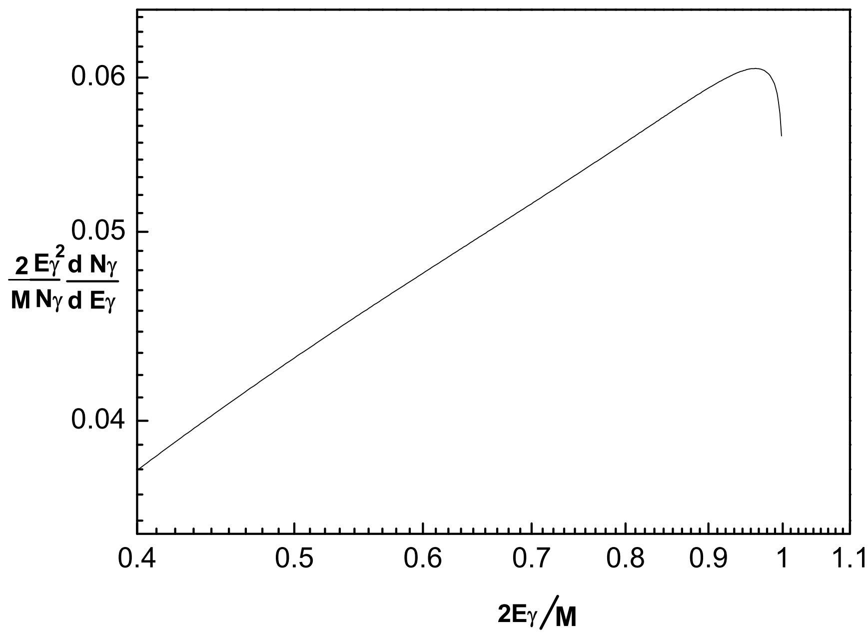

Figure 8.3: Photon spectral distribution for $\mathrm{DM}+\mathrm{DM} \to e^+ + e^- + \gamma$ and $\mathrm{DM} \to e^+ + e^- + \gamma$ from FSR with $M = 2000$ GeV. The distribution peaks at $2E_\gamma/M = x$ where x is the solution of $x(x^2-2x+2)/[(1-x)(3x^2-4x+2)] = \ln\left[M^2(1-x)/m_e^2\right]$; for the parameters here the peak is at $2E_\gamma/M \simeq 0.962$.

8.3.1 $\mathrm{DM}+\mathrm{DM} \to e^+ + e^- + \gamma$ and $\mathrm{DM} \to e^+ + e^- + \gamma$

Final state radiation of photons

For direct DM annihilation/decay to one electron-positron pair, the photon DOS from FSR of a single photon from the electron or the positron, in the collinear limit (a formula at leading order in the electron mass is given in Appendix 8.8), is simply given by [237]

$$\frac{1}{N_\gamma}\frac{dN_\gamma}{dE_\gamma} \simeq \frac{\alpha}{\pi}\left(\frac{M^2+(M-2E_\gamma)^2}{M^2E_\gamma}\ln\left[\frac{M(M-2E_\gamma)}{m_e^2}\right]\right) \tag{8.6}$$

where $E_d < E_\gamma < \frac{M}{2}\left(1-\frac{4m_e^2}{M^2}\right)$ and the DOS is shown in figure 8.3. Since this DOS has a logarithmic soft divergence, we choose to normalize it with respect to the zeroth order approximation in α, i.e. $\sigma_{\mathrm{DM}+\mathrm{DM}\to e^+ + e^-}$ for annihilation and $\Gamma_{\mathrm{DM}\to e^+ + e^-}$ for decay. Notice here that the photon spectrum is the same than the photon DOS.

Direct photon production from higher-order operators

Photons from FSR off electrons may not always be the leading contribution to the spectrum. The smallness of the electron mass can lead to a large chiral suppression for FSR relative to other processes, which may cause the leading photon-generating process to be one where photons are directly generated associated with the e^+e^- pair. In a low-energy effective theory, one can write such processes as higher-order operators, assuming the particle mediating the process is heavy. We will show below that, when the scale of the higher order operators M_{int} is low, there is a regime where the higher-order operators dominate over FSR for the following scenarios: direct scalar boson or Majorana fermion DM s-wave annihilation to one electron-positron pair and direct scalar boson DM decay to one electron-positron pair.

For all three scenarios (scalar boson DM annihilation, Majorana fermion DM annihilation and scalar boson DM decay), the higher-order operators share a common piece constructed from Standard Model fields, given by $e^\dagger\bar{\sigma}^\mu eF^{\alpha\beta}$ or $\bar{e}^\dagger\sigma^\mu\bar{e}F^{\alpha\beta}$. The only differences in the higher-order operators are in the piece constructed from DM fields. However, in the s-wave approximation, the DM piece only contributes different constant coefficients to the spectra of these scenarios. Since we are calculating the DOS instead of the spectrum, that difference will be exactly canceled by normalization. Thus, all three scenarios yield a common expression for the DOS.

Within our assumptions, the photon DOS from the leading contact interactions (as discussed below) is given by

$$\frac{1}{N_\gamma}\frac{dN_\gamma}{dE_\gamma} = \frac{320(M-2E_\gamma)E_\gamma^3}{M^5} \tag{8.7}$$

in the limit of vanishing electron mass, where $E_\gamma^{\max} = M/2$. The photon distribution for this spectrum is shown in figure 8.4. The photon energy varies in the range $0 < E_\gamma < \frac{M}{2}$ and the DOS is normalized to 1. Once again, the photon spectrum is the same as the photon DOS in this case.

Final state radiation versus direct photon production

When scalar boson or Majorana fermion DM annihilates directly to one electron-positron pair or scalar boson DM decays directly to one electron-positron pair, higher-order operators dominate photon production for small M_{int} while FSR dominates for large M_{int}. Here we give the leading operators responsible for both processes in each DM scenario and determine the critical scale M^*_{int} below which higher order operators are the dominant contribution to the photon DOS. We use two-component spinor notation [238].

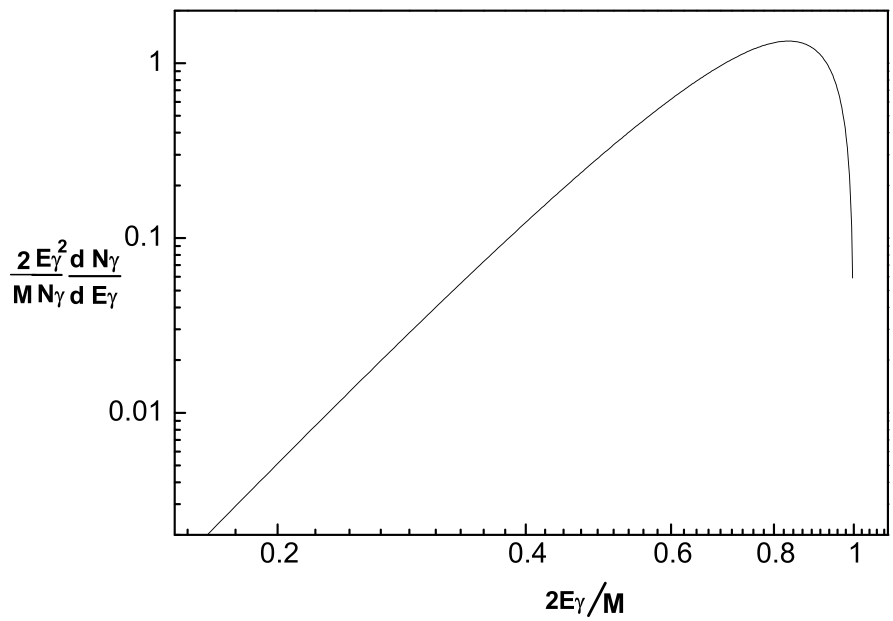

Figure 8.4: Photon spectral distribution for $\mathrm{DM}+\mathrm{DM} \to e^+ + e^- + \gamma$ and $\mathrm{DM} \to e^+ + e^- + \gamma$ from the leading short-range contact interaction for scalar boson or Majorana fermion s-wave annihilation, or scalar boson decay, in the limit $M \gg m_e$. The distribution peaks at $2E_\gamma/M = E_\gamma/E_\gamma^{\max} = 5/6$.

For scalar boson DM ϕ annihilating directly to one electron-positron pair, FSR is generated mainly by the dimension 6 operator

$$\mathcal{L}_{\mathrm{FSR}} \supset \frac{hm_e}{M_{\mathrm{int}}^2}\phi^\dagger\phi(\bar{e}e + \bar{e}^\dagger e^\dagger), \tag{8.8}$$

while direct photon production is generated from dimension 8 operators through the following effective Lagrangian

$$\mathcal{L}_{\mathrm{eff}} \supset \frac{\sqrt{4\pi\alpha}}{M_{\mathrm{int}}^2}\partial^\mu(\phi^\dagger\phi)(e^\dagger\bar{\sigma}^\nu e)[a_L F_{\mu\nu} + b_L\tilde{F}_{\mu\nu}] + \{L \to R, e \to \bar{e}\} \tag{8.9}$$

where the coupling constants $\{h, a_L, b_L, a_R, b_R\}$ should naturally be order one numbers. A similar operator has also been considered in Ref [233]. The relevant cross-sections are $\langle\sigma_{\mathrm{FSR}}v\rangle \approx c_{\mathrm{FSR}}\alpha\frac{m_e^2}{M_{\mathrm{int}}^4}\ln\left(\frac{4m_\phi^2}{m_e^2}\right)$ and $\langle\sigma_{\mathrm{eff}}v\rangle \approx c_{\mathrm{eff}}\alpha\frac{(2m_\phi)^6}{M_{\mathrm{int}}^8}$, where $c_{\mathrm{FSR}} \propto h^2$ and $c_{\mathrm{eff}} \propto a_L^2 + \cdots$ include the appropriate order one coupling constants together with the factors from the phase space integration.

When Majorana DM χ annihilates directly to one electron-positron pair, FSR is generated mainly by the dimension 6 operator

$$\mathcal{L}_{\rm FSR} \supset \frac{h_L}{M_{\rm int}^2}(\chi^\dagger \bar{\sigma}^\mu \chi)(e^\dagger \bar{\sigma}_\mu e) + \{L \to R, e \to \bar{e}\}, \tag{8.10}$$

while direct photon production is generated from dimension 8 operators through the following effective Lagrangian

$$\mathcal{L}_{\rm eff} \supset \frac{\sqrt{4\pi\alpha}}{M_{\rm int}^4}(\chi^\dagger \bar{\sigma}^\mu \chi)(e^\dagger \bar{\sigma}^\nu e)[a_L F_{\mu\nu} + b_L \tilde{F}_{\mu\nu}] + \{L \to R, e \to \bar{e}\} \tag{8.11}$$

where again the coupling constants $\{h_L, a_L, b_L, h_R, a_R, b_R\}$ should naturally be order one numbers. The relevant cross-sections are $\langle \sigma_{\rm FSR} v\rangle \approx c_{\rm FSR}\alpha \frac{m_e^2}{M_{\rm int}^4} \ln\left(\frac{4m_\chi^2}{m_e^2}\right)$ and $\langle \sigma_{\rm eff} v\rangle \approx c_{\rm eff}\alpha \frac{(2m_\chi)^6}{M_{\rm int}^8}$, where $c_{\rm FSR} \propto h_L^2 + h_R^2$ and $c_{\rm eff} \propto a_L^2 + \cdots$ again include the appropriate order one coupling constants together with the factors from the phase space integration.

Finally, when scalar boson DM ϕ decays directly to one electron-positron pair, FSR is generated mainly by the dimension 5 operator

$$\mathcal{L}_{\rm FSR} \supset \frac{h m_e}{M_{\rm int}}\phi(\bar{e}e + e^\dagger \bar{e}^\dagger) \tag{8.12}$$

while direct photon production is generated from dimension 7 operators through the following effective Lagrangian

$$\mathcal{L}_{\rm eff} \supset \frac{\sqrt{4\pi\alpha}}{M_{\rm int}^3}\partial^\mu \phi (e^\dagger \bar{\sigma}^\nu e)[a_L F_{\mu\nu} + b_L \tilde{F}_{\mu\nu}] + \{L \to R, e \to \bar{e}\} \tag{8.13}$$

where again the coupling constants $\{h, a_L, b_L, a_R, b_R\}$ should naturally be order one numbers. This operator has also been considered in Ref [233]. The relevant decay rates are $\Gamma_{\rm FSR} \approx c_{\rm FSR}\alpha \frac{m_e^2 m_\phi}{M_{\rm int}^2} \ln\left(\frac{m_\phi^2}{m_e^2}\right)$ and $\Gamma_{\rm eff} \approx c_{\rm eff}\alpha \frac{m_\phi^7}{M_{\rm int}^6}$, where again $c_{\rm FSR} \propto h^2$ and $c_{\rm eff} \propto a_L^2 + \cdots$ include the appropriate order one coupling constants together with the factors from the phase space integration.

For all scenarios both processes (final state radiation and direct photon production) have comparable contributions when

$$M_{\rm int}^* \approx M \left(\frac{M}{m_e}\right)^{\frac{1}{2}} \left[\frac{h_L^2 + h_R^2}{a_L^2 + b_L^2 + a_R^2 + b_R^2} \ln\left(\frac{M^2}{m_e^2}\right)\right]^{-\frac{1}{4}} \approx 10^6\,\text{GeV} \tag{8.14}$$

where to assume a numerical estimate we assumed order one coupling constants and $M \approx 1$ TeV. Therefore higher-order operators dominate over FSR for $M_{\rm int} \lesssim M_{\rm int}^*$ while FSR dominates over higher-order operators for $M_{\rm int} \gtrsim M_{\rm int}^*$. Obviously for the scalar boson DM decay the decay rates are taken to be small enough such that DM is long-lived. This is possible if the operator coefficients are small, which occurs for example when the effective dimension of the scalar boson DM is higher. This is the case when the scalar boson DM is a composite field (like a glueball).

In this case, equation (8.14) is still valid since the effective dimensions of the operators for both final state radiation and direct photon production increase together. A more detailed analysis can be found in Appendix 8.9.

8.3.2 $\mathbf{DM + DM} \to 2\phi$ and $\mathbf{DM} \to 2\phi$ followed by $\phi \to e^+ + e^- + \gamma$

Here the computation of the photon DOS involves once more a convolution of the boosted (FSR or higher-order operators) photon DOS obtained in section 8.3.1 with the appropriate DOS of DM annihilation/decay to two bosons as described in Appendix 8.7.

Final state radiation of photons

Defining the boson mass as m_ϕ, the photon DOS from FSR of a single photon from the electrons or the positrons is thus

$$\frac{1}{N_\gamma}\frac{dN_\gamma}{dE_\gamma} \simeq \frac{\alpha}{\pi}\frac{1}{\sqrt{E_\phi^2 - m_\phi^2}}\begin{cases} f\left(\frac{2E_\gamma}{E_\phi - |\vec{p}_\phi|}\right) - f\left(\frac{2E_\gamma}{E_\phi + |\vec{p}_\phi|}\right) & \text{for } E_d < E_\gamma < E_\gamma^{\text{int}} \\ f\left(1 - \frac{4m_e^2}{m_\phi^2}\right) - f\left(\frac{2E_\gamma}{E_\phi + |\vec{p}_\phi|}\right) & \text{for } E_\gamma^{\text{int}} < E_\gamma < E_\gamma^{\text{max}} \end{cases} \tag{8.15}$$

where the function f is

$$f(x) = \frac{x^2 + x - 2}{x}\ln\left(\frac{m_\phi^2(1-x)}{m_e^2}\right) - x + 1 \\ - 2\left[1 - \ln\left(\frac{m_e^2}{m_\phi^2}\right)\right]\ln(x) + 2\,\text{dilog}(1-x) \tag{8.16}$$

and the boson energy and momentum are $E_\phi = \frac{M}{2}$ and $|\vec{p}_\phi| = \frac{M}{2}\sqrt{1 - \frac{4m_\phi^2}{M^2}}$ respectively. The limits on the photon energy are

$$E_\gamma^{\text{int}} = \frac{E_\phi - |\vec{p}_\phi|}{2}\left(1 - \frac{4m_e^2}{m_\phi^2}\right) \quad \text{and} \quad E_\gamma^{\text{max}} = \frac{E_\phi + |\vec{p}_\phi|}{2}\left(1 - \frac{4m_e^2}{m_\phi^2}\right).$$

The photon spectrum is simply twice the photon DOS ($N_\gamma = 2$) which is shown in figure 8.5 for a given boson mass.

Again it is possible to relate the FSR photon DOS of this subsection to the FSR photon DOS of the previous subsection by letting the boson mass approach half the parameter M, i.e. $m_\phi = \frac{M}{2}$. This corresponds to DM annihilation/decay to two bosons *at rest* in the DM center of mass frame which subsequently decay to one electron-positron pair each with a single FSR photon. Notice that, in this limit, the $(E_\phi^2 - m_\phi^2)^{-\frac{1}{2}}$ prefactor in the photon DOS is very important for the matching to work.

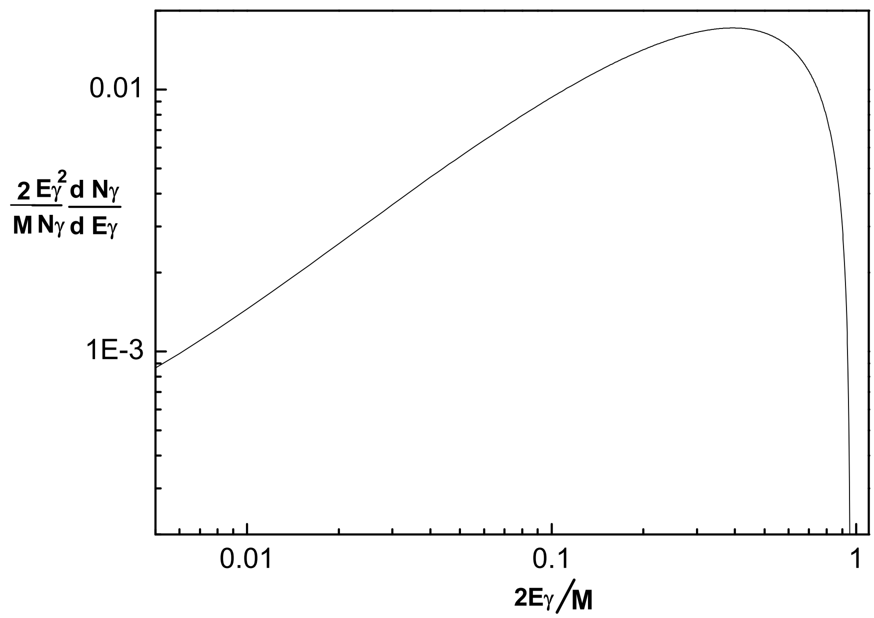

Figure 8.5: Photon spectral distribution for DM + DM $\rightarrow 2\phi$ and DM $\rightarrow 2\phi$ followed by $\phi \rightarrow e^+ + e^- + \gamma$ from FSR with $M = 2000$ GeV and $m_\phi = 400$ GeV. The distribution peaks at $2E_\gamma/M \simeq 0.394$.

Direct photon production from higher-order operators

As previously shown, photon production from scalar boson decay to electron-positron pair is not dominated by FSR when the typical scale of the interactions M_{int} is low. In that case, the photon DOS from higher-order operators is given by

$$\frac{1}{N_\gamma}\frac{dN_\gamma}{dE_\gamma} = \begin{cases} \frac{160[2m_\phi^2(M^2-m_\phi^2)-3M(M^2-2m_\phi^2)E_\gamma]E_\gamma^3}{3m_\phi^8} & \text{for } 0 < E_\gamma < \frac{E_\phi-|\vec{p}_\phi|}{2} \\ \frac{5[(E_\phi+|\vec{p}_\phi|)^4-16(2E_\phi+2|\vec{p}_\phi|-3E_\gamma)E_\gamma^3]}{3|\vec{p}_\phi|(E_\phi+|\vec{p}_\phi|)^4} & \text{for } \frac{E_\phi-|\vec{p}_\phi|}{2} < E_\gamma < \frac{E_\phi+|\vec{p}_\phi|}{2} \end{cases} \tag{8.17}$$

where the boson energy and momentum are $E_\phi = \frac{M}{2}$ and $|\vec{p}_\phi| = \frac{M}{2}\sqrt{1-\frac{4m_\phi^2}{M^2}}$ respectively. The photon DOS, which is shown in figure 8.6, is canonically normalized and the photon spectrum is simply twice the photon DOS ($N_\gamma = 2$). Once more, it is possible to relate the photon DOS obtained in this subsection to the photon DOS obtained in the previous subsection for higher-order operators by taking the limit $m_\phi = \frac{M}{2}$.

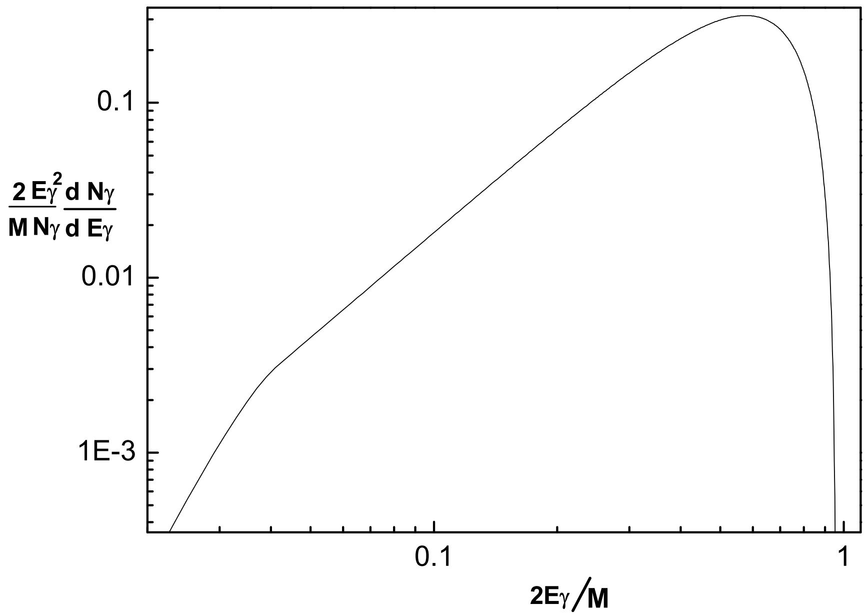

Figure 8.6: Photon spectral distribution for DM + DM $\rightarrow 2\phi$ and DM $\rightarrow 2\phi$ followed by $\phi \rightarrow e^+ + e^- + \gamma$ from the leading short-range contact interaction with $M = 2000$ GeV and $m_\phi = 400$ GeV, and neglecting the electron mass. The distribution peaks at $2E_\gamma/M \simeq 0.577$.

8.4 Photons from taus

Tau leptons represent another interesting decay mode for dark matter annihilation/decay. Since baryon number is conserved in tau decays, and the tau mass is less than the sum of the proton and neutron masses, $m_\tau < m_p + m_n$, tau decays include only (anti)leptons and (anti)mesons, with no (anti)baryons. Dark matter that annihilates/decays preferentially to tau leptons is therefore not necessarily in conflict with stringent limits on the antiproton flux in cosmic rays. However, tau leptons do provide an interesting source of photons since tau decays include a significant fraction of neutral pions, $\tau \rightarrow X + \pi^0$, that subsequently decay to photons, $\pi^0 \rightarrow 2\gamma$.

The average number of π^0 produced in a single τ decay is approximately $\langle N_{\pi^0} \rangle \simeq 0.51$, giving an average of roughly one photon per τ decay, $N_\gamma/N_\tau \simeq 1$. Most π^0 from τ decays come from the hadronic one-prong decay modes $\tau^- \rightarrow \nu_\tau + \rho^- \rightarrow \nu_\tau + \pi^- + \pi^0$ (branching fraction 25.4%) and $\tau^- \rightarrow \nu_\tau + a_1^- \rightarrow \nu_\tau + \pi^- + 2\pi^0$ (branching fraction approximately 9% [239]). These two decay modes account for approximately 85% of all the neutral pions arising from τ decay.

The other main sources of neutral pions are the three-prong mode $\tau^- \to \nu_\tau + 2\pi^- + \pi^+ + \pi^0$ (branching fraction 4.3%) and the one-prong mode $\tau^- \to \nu_\tau + \pi^- + 3\pi^0$ (branching fraction 1.1%), as well as continuum contributions. All branching fractions are taken from the PDG [240]. Below we include only the dominant decays through the ρ and a_1 resonances.

To obtain the photon DOS we first need to obtain the DOS of neutral pions. We have explicitly computed the contribution to the pion spectrum from the principal decay modes, with intermediate ρ and a_1 vector meson resonances. The general τ differential decay rate takes the form

$$d\Gamma \propto \int d\Pi_2(\tau \to \nu_\tau + v)\, dm_v^2\, d\Pi_n(v \to n\pi) \times |\check{\mathcal{M}}_{\mu,\pm}(\tau \to \nu_\tau + v)\mathcal{P}_v^{\mu\nu}(m_v^2)\hat{\mathcal{M}}_\nu(v \to n\pi)|^2 \quad (8.18)$$

The π^0 DOS is obtained by removing a single π^0 from the final state phase space integration. Here $\mathcal{P}_v^{\mu\nu}(m_v^2)$ is the vector meson propagator, $\check{\mathcal{M}}_{\mu,\pm}(\tau \to \nu_\tau + v)$ denotes the matrix element for a τ of helicity $h = \pm\frac{1}{2}$ corresponding to right- or left-handed respectively, to decay to a vector meson, and $\hat{\mathcal{M}}_\nu(v \to n\pi)$ denotes the matrix element for the vector meson to decay to n pions.

First consider the decay through the ρ resonance. Obtaining the pion spectrum from the sequence of two-body cascades $\tau \to \nu + \rho \to \nu + 2\pi$ uses many of the techniques as used in the scalar cascades in Section 8.2. The major differences are first, nonconstant matrix elements, resulting from the nonzero spin of the intermediate ρ, and second, the large decay width of the ρ, which necessitates the use of a Breit-Wigner with a running width. We use a ρ mass and width of $m_{0,\rho} = 770$ MeV and $\Gamma_{0,\rho} = 150$ MeV. Next consider the decay through the a_1 resonance which differs from the ρ mode in that the final decay $a_1 \to 3\pi$ is not two-body. The spectrum of the observed pion therefore requires additional integrations over the phase space of the unobserved pions in the final state. Following [239, 241], we use relatively simple parameterizations given in [242] for both the $a_1 \to 3\pi$ matrix element and running width. We use an a_1 mass and width of $m_{0,a} = 1.22$ GeV and $\Gamma_{0,a} = 420$ MeV.

The photon DOS may be obtained from the pion DOS by convolution, as before. We work in the collinear limit $M \gg m_\tau$ in which the components of the π^0, and therefore photon, momentum transverse to the tau direction of motion in the original annihilation/decay frame are irrelevant. The results for the *normalized* photon DOS under the assumption that the DM annihilates/decays to a single tau-antitau pair are well fit by the parameterized functional form

$$\frac{E_\gamma^{\max}}{N_\gamma}\frac{dN_\gamma}{dE_\gamma} = f(E_\gamma/E_\gamma^{\max})e^{-g(E_\gamma/E_\gamma^{\max})} \quad (8.19)$$

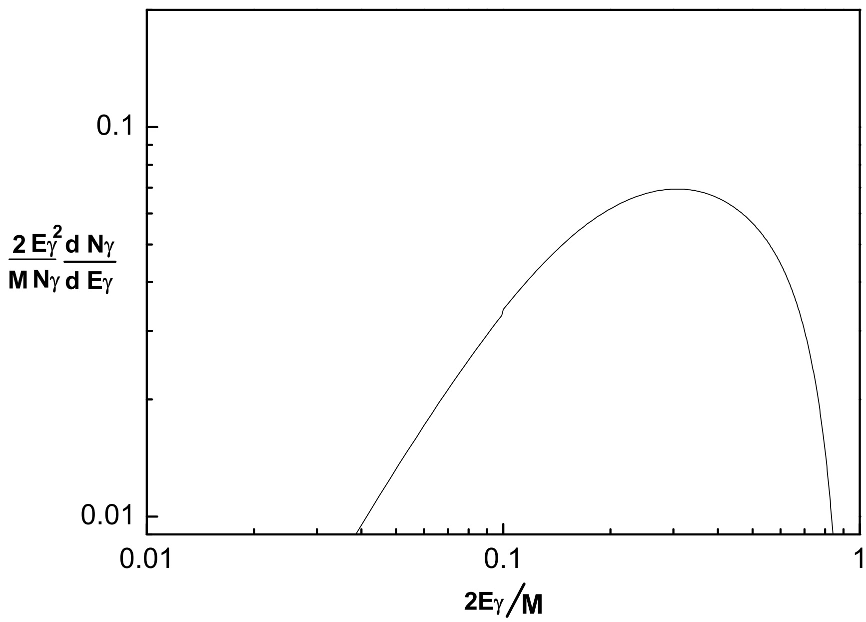

Figure 8.7: Photon spectral distribution for DM + DM $\to 2\tau$ and DM $\to 2\tau$ followed by $\tau \to X + \pi^0$ and $\pi^0 \to 2\gamma$ in the limit $M \gg m_\tau$. The distribution peaks at $2E_\gamma/M = E_\gamma/E_\gamma^{\max} \simeq 0.307$.

where $E_\gamma^{\max} = M/2$, and

$$f(x) = x^a \sum_{n=0}^{4} b_n x^n$$

$$g(x) = \sum_{n=1}^{3} c_n x^n. \tag{8.20}$$

For positive helicity or right-handed taus the best fit parameters are $a_+ = -0.192$, $b_{+,i} = \{4.24, -2.46, -16.96, 35.85, -21.17\}$, $c_{+,i} = \{8.94, -16.10, -19.45\}$, while for negative helicity or left-handed taus the best fit parameters are $a_- = -0.040$, $b_{-,i} = \{6.42, 4.96, -12.65, 0, 0\}$, $c_{-,i} = \{7.36, 0, 0\}$. Similar distributions have also been obtained by fits to pythia decays in [236]. The differences between the photon DOS arising from right- and left-handed taus are only minor. It seems unlikely that a measurement of the photon spectrum alone could ever distinguish the helicity of taus arising from DM annihilation/decay. The photon distribution arising from DM annihilation/decay directly to a single tau-antitau pair and averaging over tau helicity is shown in figure 8.7. In this case the photon spectrum is roughly twice the photon

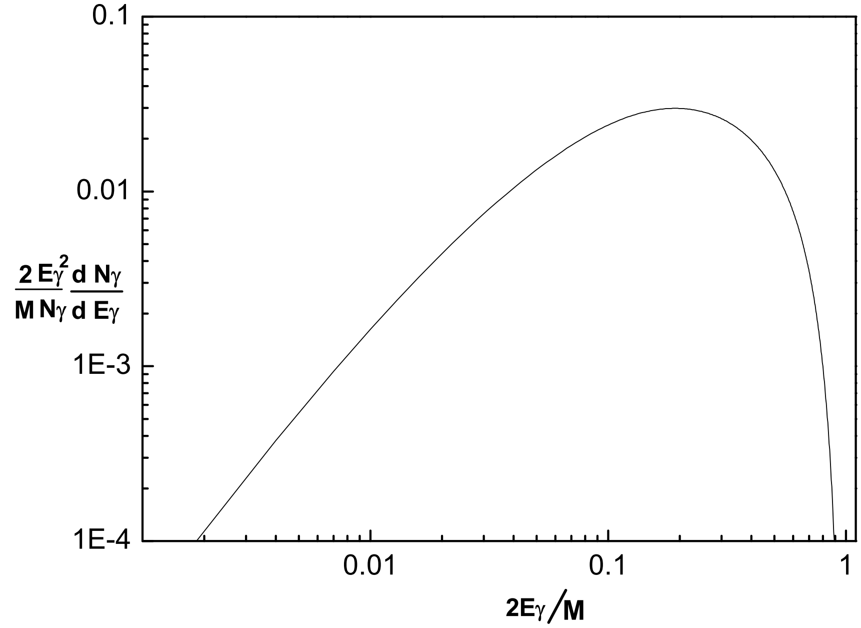

Figure 8.8: Photon spectral distribution for DM + DM $\to 2\phi$ and DM $\to 2\phi$ followed by $\phi \to 2\tau$ and $\tau \to X + \pi^0$ and $\pi^0 \to 2\gamma$ in the limit $M \gg m_\phi \gg m_\tau$. The distribution peaks at $2E_\gamma/M \simeq 0.192$.

DOS, $N_\gamma \simeq 2$, since there is roughly one photon per tau on average and two taus per DM annihilation/decay.

If we assume DM particles annihilate/decay to two intermediate bosons ϕ, each of which subsequently decays to a tau-antitau pair, then we again need to boost the DOS obtained above and convolve it with the appropriate DOS of DM annihilation/decay to two bosons, as explained in Appendix 8.7. The final photon spectral distribution for this case in the collinear limits $M \gg m_\phi \gg m_\tau$, and averaging over tau helicities is shown in figure 8.8. The photon spectrum in this case is roughly four times the photon DOS, $N_\gamma \simeq 4$. We can see that the final photon DOS is softer compared to Fig. 8.7 due to the extra intermediate state.

8.5 Photon spectra and flux

8.5.1 Photon spectra

Strictly speaking, all computations we have performed so far are photon DOS in different scenarios. The different photon DOS are superimposed in figure 8.9. However, in the likely case where several scenarios add up, the different spectra must be added with the appropriate weight. The full photon spectrum obtained is given by

$$\frac{dN_\gamma^{\text{total}}}{dE_\gamma} = \sum_i \text{Br}(i)\frac{dN_\gamma^{(i)}}{dE_\gamma} \tag{8.21}$$

where the sum is over all allowed scenarios i, with photon spectrum $\frac{dN_\gamma^{(i)}}{dE_\gamma}$ and branching ratio $\text{Br}(i)$. In comparing with the background of gamma ray photons, the only difference between DM annihilation and DM decay comes from the power of the DM density profile in the appropriate equations as discussed in the next subsection.

8.5.2 Photon flux

An observation of gamma rays from dark matter annihilation/decay involves not only the spectrum but also the absolute magnitude. The photon flux

$$\Phi_\gamma \equiv \frac{dN_\gamma}{dA\,dt\,d\Omega} \tag{8.22}$$

where dA and $d\Omega$ are the detector area and solid angle elements, can be computed from an integral over the source along the line of sight (los) [243] since gamma rays are not significantly attenuated on galactic length scales. For annihilation of a single species of DM particle that is its own antiparticle the spectral flux is given by

$$\frac{d\Phi_\gamma}{dE_\gamma}(E_\gamma,\Omega) = \frac{\langle\sigma v\rangle}{4\pi m_{\text{DM}}^2}\frac{dN_\gamma}{dE_\gamma}\int_{\text{los}} \rho_{\text{DM}}^2(r,\Omega)dr \tag{8.23}$$

where $\langle\sigma v\rangle$ is the phase space averaged annihilation cross section times velocity, ρ_{DM} is the dark matter density, and dN_γ/dE_γ is the photon spectrum with $N_\gamma = \int dE_\gamma(dN_\gamma/dE_\gamma)$ photons emitted per annihilation. If the DM is composed of distinct particle and antiparticle particle species with equal densities that can annihilate only through the particle-antiparticle channel, the flux equation (8.23) should be multiplied by an additional factor of $\frac{1}{4}$. In terms of dimensionful units the annihilation spectral flux equation (8.23) may be written as

$$\frac{d\Phi_\gamma(E_\gamma,\Omega)/dE_\gamma}{\text{cm}^{-2}\cdot\text{s}^{-1}\cdot\text{sr}^{-1}} \simeq 5.6\times10^{-10}\left(\frac{\langle\sigma v\rangle}{3\times10^{-26}\,\text{cm}^3\cdot\text{s}^{-1}}\right)\left(\frac{100\,\text{GeV}}{m_{\text{DM}}}\right)^2\frac{dN_\gamma}{dE_\gamma}J_2(\Omega) \tag{8.24}$$

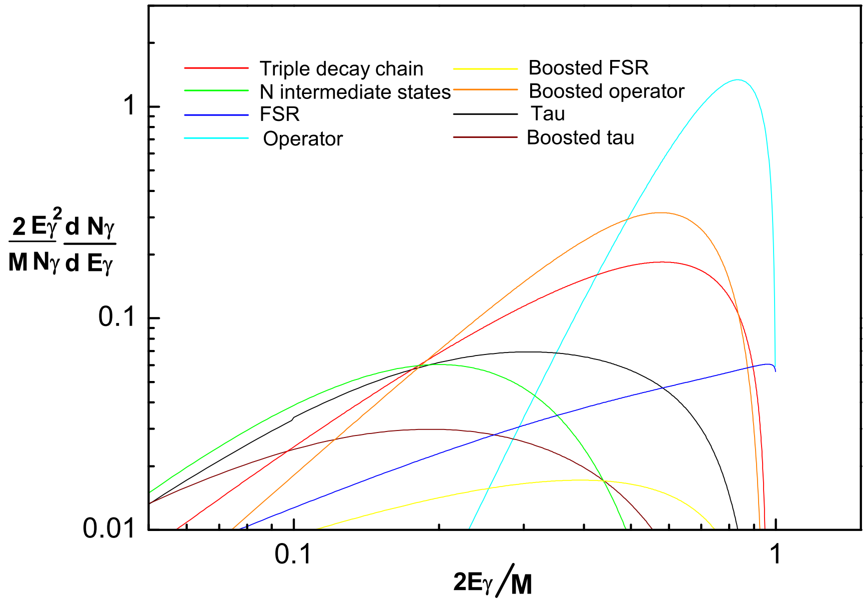

Figure 8.9: Photon spectral disbributions arising from different DM annihilation/decay scenarios for $M = 2000$ GeV, $m_\phi = 400$ GeV and $m_\pi = 0.14$ GeV. For DM annihilation/decay to N intermediate ϕ bosons the limit $M \gg m_\phi$ is presented with $N = 10$. For DM annihilation/decay through intermediate τ's the limits $M \gg m_\tau$ or $M \gg m_\phi \gg m_\tau$ are presented. In each case the photon DOS is normalized to unit probability, except for FSR and Boosted FSR which are normalized with respect to the leading decay without FSR.

where

$$J_2(\Omega) \equiv \frac{1}{8.5\,\mathrm{kpc}}\left(\frac{1}{0.3\,\mathrm{GeV}\cdot\mathrm{cm}^{-3}}\right)^2\int_{\mathrm{los}}\rho^2(r,\Omega)dr \tag{8.25}$$

is a dimensionless order one factor that represents astrophysical parameters.

For decay of a single species of DM the spectral flux is given by

$$\frac{d\Phi_\gamma}{dE_\gamma}(E_\gamma,\Omega) = \frac{\Gamma}{4\pi m_{\mathrm{DM}}}\frac{dN_\gamma}{dE_\gamma}\int_{\mathrm{los}}\rho_{\mathrm{DM}}(r,\Omega)dr \tag{8.26}$$

where Γ is the DM decay rate with $N_\gamma = \int dE_\gamma(dN_\gamma/dE_\gamma)$ photons emitted per decay. In terms of dimensionful units the decay spectral flux may be written as

$$\frac{d\Phi_\gamma(E_\gamma,\Omega)/dE_\gamma}{\mathrm{cm}^{-2}\cdot\mathrm{s}^{-1}\cdot\mathrm{sr}^{-1}} \simeq 6.26\times10^{-9}\left(\frac{\Gamma}{10^{-27}\,\mathrm{s}^{-1}}\right)\left(\frac{100\,\mathrm{GeV}}{m_{\mathrm{DM}}}\right)\frac{dN_\gamma}{dE_\gamma}J_1(\Omega) \tag{8.27}$$

where

$$J_1(\Omega) \equiv \frac{1}{8.5\,\mathrm{kpc}}\left(\frac{1}{0.3\,\mathrm{GeV}\cdot\mathrm{cm}^{-3}}\right)\int_{\mathrm{los}}\rho_{\mathrm{DM}}(r,\Omega)dr \tag{8.28}$$

is a dimensionless order one factor characterizing the astrophysical parameters. With the spectral flux equations (8.23) and (8.26) comparisons with the gamma ray background are straightforward.

8.6 Conclusion

High-energy photons are hardly deflected when they propagate through the galaxy. This is an advantage over charged particles, like electrons and positrons, which interact with the galactic magnetic field. Moreover, once charged particles are accelerated, photons are always produced due to radiation. The different photon spectra which arise in each process can provide information on the process(es) generating the photons. In this paper, we studied the spectra of high-energy photons generated by various dark matter annihilation/decay scenarios including: direct photon production from arbitrary two-body decay chains, final state radiation from charged particles generated by dark matter annihilation/decay, direct photon production together with charged particles from higher-order operators, and the special case where photons are produced from taus generated by dark matter annihilation/decay.

We noted also that, for processes which generate photons and leptons, effective field theory allows a comparison between the spectra from final state radiation and the ones from direct photon production due to higher-order operators. Interestingly, we found that while FSR is the dominant source of photons in most cases, in certain cases (scalar dark matter annihilation/decay and Majorana fermion dark matter annihilation), direct photon production from higher order operators can dominate over final state radiation. In these three cases, for a dark matter mass of $\mathcal{O}(1\,\mathrm{TeV})$, we found that direct photon production from higher-order operators dominates if the scale of the leading operator is lower than $\mathcal{O}(1000\,\mathrm{TeV})$. Finally, it is also very interesting to see that the hardest spectrum among the spectra studied here (see figure 8.9) comes from these exceptions, i.e. direct photon production from higher-order operators.

Once the flux of cosmic gamma rays is measured, an eventual dark matter signal could be compared with the different spectra presented here and a great deal of information on the nature of dark matter at the particle physics level could be deduced.

8.7 Appendix: Density of states

In this appendix we review how the DOS is obtained from general considerations. The DOS for Φ annihilation/decay to ϕ is simply given by

$$\frac{1}{N}\frac{dN}{dE} = \frac{1}{\langle\sigma v\rangle}\frac{d\langle\sigma v\rangle}{dE} \quad \text{and} \quad \frac{1}{N}\frac{dN}{dE} = \frac{1}{\Gamma}\frac{d\Gamma}{dE} \tag{8.29}$$

respectively, and is thus normalized to one. For example, assuming constant averaged matrix element squared, the DOS in the Φ center of mass frame for $2 \to 2$ annihilation in the s-wave approximation and $1 \to 2$ decay is simply obtained from the phase space,

$$\begin{aligned}\frac{1}{N}\frac{dN}{dE} = &\left[\int \frac{d^3p}{EdE}\frac{d^3q}{E'}\delta^{(4)}(P-p-q)\right] \\ &\times \left[\int \frac{d^3p}{E}\frac{d^3q}{E'}\delta^4(M-p-q)\right]^{-1} = \delta\left(E - \frac{M}{2}\right)\end{aligned} \tag{8.30}$$

where $P^\mu = (M,\vec{0})$ with $M = 2m_\Phi$ for Φ annihilation and $M = m_\Phi$ for Φ decay.

For Φ decay in a boosted frame, the DOS follows from Lorentz covariance. Indeed $N \equiv \int dE \frac{dN}{dE}$ is a Lorentz scalar thus $N^{\rm CM} = N^{\rm Boost}$. Therefore one can rewrite the boosted DOS as

$$N^{\rm Boost} = \int dE^{\rm CM} dz^{\rm CM} \frac{dN^{\rm CM}}{dz^{\rm CM}dE^{\rm CM}} = \int dE dz^{\rm CM} \left|\frac{\partial(E^{\rm CM}, z^{\rm CM})}{\partial(E, z^{\rm CM})}\right| \frac{dN^{\rm CM}}{dz^{\rm CM}dE^{\rm CM}}$$

or

$$\frac{1}{N}\frac{dN^{\rm Boost}}{dE} = \int dz^{\rm CM} \left|\frac{\partial(E^{\rm CM}, z^{\rm CM})}{\partial(E, z^{\rm CM})}\right| \frac{1}{N}\frac{dN^{\rm CM}}{dz^{\rm CM}dE^{\rm CM}}. \tag{8.31}$$

Here $z^{\rm CM} = \cos\theta = \hat{p}_\Phi \cdot \hat{p}_\phi^{\rm CM}$ is the angle between the boosted Φ and the unboosted ϕ. Since the DOS in the Φ rest frame is uniform, then $\frac{dN^{\rm CM}}{dz^{\rm CM}dE^{\rm CM}} = \frac{1}{2}\frac{dN^{\rm CM}}{dE^{\rm CM}}$. Finally, the ϕ energy in the Φ center of mass frame is related to the ϕ energy in the boosted frame by

$$E = \frac{1}{m_\Phi}\left(E^{\rm CM}E_\Phi + z^{\rm CM}\sqrt{{E^{\rm CM}}^2 - m_\phi^2}\sqrt{E_\Phi^2 - m_\Phi^2}\right). \tag{8.32}$$

The bounds on E can be found from the bounds in the Φ center of mass frame plus the physical constraint that $-1 < z^{\rm CM} < 1$. Boosting the DOS of the previous example in the frame where Φ has four-momentum $p_\Phi^\mu = E_\Phi(1, \hat{p}_\Phi\sqrt{1 - m_\Phi^2/E_\Phi^2})$, one gets

$$\frac{1}{N}\frac{dN^{\rm Boost}}{dE} = \frac{1}{\sqrt{1 - 4m_\phi^2/m_\Phi^2}}\frac{1}{\sqrt{E_\Phi^2 - m_\Phi^2}} \tag{8.33}$$

where the ϕ energy is bounded by

$$\begin{aligned} E^{\max} &= \frac{E_\Phi}{2}\left[1 + \sqrt{1 - 4m_\phi^2/m_\Phi^2}\sqrt{1 - m_\Phi^2/E_\Phi^2}\right] \\ E^{\min} &= \frac{E_\Phi}{2}\left[1 - \sqrt{1 - 4m_\phi^2/m_\Phi^2}\sqrt{1 - m_\Phi^2/E_\Phi^2}\right]. \end{aligned}$$

Convolution and matching of DOS

For a two-body decay chain $\phi_0 \to 2\phi_1$ to $\phi_{k-1} \to 2\phi_k$ the DOS in the ϕ_0 rest frame can be found by iteration and is given by

$$\begin{aligned}
\frac{1}{N_k}\frac{dN_k}{dE_k} &= \int dE_{k-1}\cdots dE_1 \frac{1}{N_1}\frac{dN_1^{\rm CM}}{dE_1}\frac{1}{N_2}\frac{dN_2^{\rm Boost}}{dE_2}\cdots\frac{1}{N_k}\frac{dN_k^{\rm Boost}}{dE_k} \\
&= \int dE_{k-1}\frac{1}{N_{k-1}}\frac{dN_{k-1}}{dE_{k-1}}\frac{1}{N_k}\frac{dN_k^{\rm Boost}}{dE_k}
\end{aligned} \tag{8.34}$$

where the bounds are complicated functions of the energies. For example, with the same assumptions as above, the two-body decay chain $\phi_0 \to 2\phi_1$ followed by $\phi_1 \to 2\phi_2$ gives

$$\begin{aligned}
\frac{1}{N_2}\frac{dN_2}{dE_2} &= \int dE_1 \frac{1}{N_1}\frac{dN_1}{dE_1}\frac{1}{N_2}\frac{dN_2^{\rm Boost}}{dE_2} \\
&= \int dE_1 \delta\left(E_1 - \frac{m_0}{2}\right)\frac{1}{\sqrt{1-4m_2^2/m_1^2}}\frac{1}{\sqrt{E_1^2-m_1^2}} \\
&= \frac{2}{m_0\sqrt{1-4m_1^2/m_0^2}\sqrt{1-4m_2^2/m_1^2}}
\end{aligned} \tag{8.35}$$

where the ϕ_2 energy is bounded by

$$\begin{aligned}
E_2^{\rm max} &= \frac{m_0}{4}\left[1+\sqrt{1-4m_1^2/m_0^2}\sqrt{1-4m_2^2/m_1^2}\right] \\
E_2^{\rm min} &= \frac{m_0}{4}\left[1-\sqrt{1-4m_1^2/m_0^2}\sqrt{1-4m_2^2/m_1^2}\right].
\end{aligned}$$

By taking limits where intermediate particles are created *at rest* in the center of mass frame of the parent particle, it is possible to match different DOS. Indeed in the limit where $m_{i+1} \to \frac{m_i}{2}$, the decay chain is effectively cut by one step, with all the previous steps being unchanged, the i-th step being deleted and the subsequent steps being modified due to the energy redistribution. The DOS satisfies

$$\begin{aligned}
&\left[\lim_{m_{i+1}\to\frac{m_i}{2}}\frac{1}{N_k}\frac{dN_k}{dE_k}\right]_{m_i=2m_{i+1}} \\
&\qquad = \left[\frac{1}{N_{k-1}}\frac{dN_{k-1}}{dE_{k-1}}\right]_{m_0=\frac{m_0}{2},\ldots,m_{i-1}=\frac{m_{i-1}}{2};m_i=m_{i+1},\ldots,m_{k-1}=m_k}
\end{aligned} \tag{8.36}$$

where the ith step is not included on the LHS. This allows us to check the different DOS formula.

8.8 Appendix: FSR collinear divergence

In the calculation of FSR, it is necessary to deal with the collinear divergence, which appears in the limit of vanishing electron mass. At finite electron mass, the three-body decay rate does not suffer from a collinear divergence and it can be easily computed using Dalitz coordinates

[237]. Here we show the result for $\phi \to e^+ + e^- + \gamma$, where the FSR comes from the following vertex $\frac{hm_e}{M_{\rm int}}\phi(\bar{e}e + \bar{e^\dagger}e^\dagger)$, with decay rate

$$\frac{d\Gamma}{dE_\gamma} = \frac{\alpha h^2 m_e^2}{8\pi^2 M_{\rm int}^2}\left(\frac{m_\phi^2 + (m_\phi - 2E_\gamma)^2}{m_\phi E_\gamma}\ln\left[\frac{m_\phi(m_\phi - 2E_\gamma)}{m_e^2}\right] + \frac{2(m_\phi - 2E_\gamma)}{E_\gamma} + \mathcal{O}(m_e^2)\right). \quad (8.37)$$

Such a spectrum has a soft photon divergence, so we choose to normalize the spectrum with respect to its zeroth order approximation in α, which corresponds to the process $\phi \to e^+ + e^-$, i.e.

$$\frac{1}{N_\gamma}\frac{dN_\gamma}{dE_\gamma} \simeq \frac{1}{\Gamma_{\phi\to e^+ + e^-}}\frac{d\Gamma}{dE_\gamma} \quad (8.38)$$

where $\Gamma_{\phi\to e^+ + e^-} = \frac{h^2 m_e^2 m_\phi}{8\pi M_{\rm int}^2}$.

The first term of the formula comes from long distance contributions since it is not sensitive to the details of the vertex, and it diverges logarithmically when m_e goes to zero. The second term remains finite when the massless limit is taken. This is the term which is dropped in the collinear approximation, where only long distance contributions are kept. In the collinear limit (see equation (8.41)), after the last term of equation (8.37) is dropped, one gets the photon DOS equation (8.6) introduced in section 8.3.

Next, we consider the case where FSR comes from a decay chain with an additional step, i.e. DM annihilates/decays to an intermediate particle ϕ, which subsequently decays to an e^+e^- pair accompanied by a FSR photon.

In a frame where the intermediate particle ϕ has four-momentum $p_\phi^\mu = E_\phi(1, \hat{p}_\phi\sqrt{1 - m_\phi^2/E_\phi^2})$, the boosted DOS can be found from the general formula. However, since the photon is massless, the Jacobian simplifies greatly, leading to

$$\frac{dN_\gamma^{\rm Boost}}{N_\gamma dE_\gamma} = \int \frac{dz^{\rm CM}}{2}\frac{m_\phi}{E_\phi + z^{\rm CM}\sqrt{E_\phi^2 - m_\phi^2}}\frac{dN_\gamma^{\rm CM}}{N_\gamma dE_\gamma^{\rm CM}} \quad (8.39)$$

The integral is easily done using the new variable $w = \frac{m_\phi}{E_\phi + z^{\rm CM}\sqrt{E_\phi^2 - m_\phi^2}}$, in terms of which $E_\gamma^{\rm CM} = wE_\gamma$. The bounds on w can be found from the bounds on $E_\gamma^{\rm CM}$ due to the bounds on E_γ in the original frame and from the physical constraint $-1 < z^{\rm CM} < 1$, giving two different regimes,

$$\frac{m_\phi}{E_\phi + \sqrt{E_\phi^2 - m_\phi^2}} < w < \min\left\{\frac{m_\phi}{E_\phi - \sqrt{E_\phi^2 - m_\phi^2}}, \frac{m_\phi}{2E_\gamma}\left(1 - \frac{4m_e^2}{m_\phi^2}\right)\right\} \quad (8.40)$$

as discussed in the text. Convolving this boosted DOS with the two-body decay DOS one obtains the DOS for DM $\to 2\phi$ followed by $\phi \to e^+ + e^- + \gamma$ mentioned above.

8.9 Appendix: Higher-order operators

In some specific scenarios, FSR suffers a large chiral suppression due to the small electron mass. In these cases, direct photon production from higher-order operators might dominate. In this Appendix we determine the necessary conditions for which direct photon production from higher-order operators dominates over FSR. To reach the most general conclusions, effective field theory is used throughout the analysis. Therefore, the chirality rule, which states that chirality-violating operators must come with an overall mass term, is enforced. Moreover, to evaluate the appropriate FSR annihilation cross-section/decay rate, the collinear limit is taken [244],

$$\frac{dX_{e^+ + e^- + \gamma}}{dx} \simeq \frac{\alpha}{\pi}\left(\frac{1+(1-x)^2}{x}\ln\left[\frac{M^2(1-x)}{m_e^2}\right]\right) X_{e^+ + e^-}$$
$$\Rightarrow X_{\rm FSR} \approx \frac{\alpha}{\pi} X_{e^+ + e^-} \ln\left[\frac{M^2}{m_e^2}\right] \tag{8.41}$$

where $x = 2E_\gamma/M$ and $X = \langle\sigma v\rangle$ with $M = 2m_{\rm DM}$ for DM annihilation or $X = \Gamma$ with $M = m_{\rm DM}$ for DM decay respectively. Notice that for DM annihilation, DM is assumed to be almost at rest, thus the s-wave approximation can be taken. The lowest-dimension electron operators are given in table 8.1. When the operator does not violate chirality, only the operators with e alone are considered since operators mixing e and $\bar{e}$ will lead to chirality-suppressed mixing terms. The photon can either appear in a covariant derivative, which is already taken

$\mathcal{O}(x)$	dim	$\langle e^+e^-\lvert\mathcal{O}\rvert 0\rangle$	$\overline{\lvert\mathcal{M}\rvert^2}$
$m_e(\bar{e}e + e^\dagger\bar{e}^\dagger)$	4	$m_e[(y_- y_+) + (x_-^\dagger x_+^\dagger)]$	$4m_e^2[(p_-\cdot p_+) - m_e^2]$
$im_e(\bar{e}e - e^\dagger\bar{e}^\dagger)$	4	$im_e[(y_- y_+) - (x_-^\dagger x_+^\dagger)]$	$4m_e^2[(p_-\cdot p_+) + m_e^2]$
$m_e(\bar{e}\sigma^{\mu\nu}e + e^\dagger\bar{\sigma}^{\mu\nu}\bar{e}^\dagger)$	4		
$im_e(\bar{e}\sigma^{\mu\nu}e - e^\dagger\bar{\sigma}^{\mu\nu}\bar{e}^\dagger)$	4		
$e^\dagger\bar{\sigma}^\mu e$	3	$(x_-^\dagger\bar{\sigma}^\mu y_+)$	$2[p_-^\mu p_+^{\mu'} + p_+^\mu p_-^{\mu'} - g^{\mu\mu'}(p_-\cdot p_+) + i\epsilon^{\alpha\mu\alpha'\mu'}p_{-\alpha}p_{+\alpha'}]$
$\partial^\nu(e^\dagger\bar{\sigma}^\mu e)$	4		
$i(D^\nu e^\dagger\bar{\sigma}^\mu e - e^\dagger\bar{\sigma}^\mu D^\nu e)$	4		
$\partial^\lambda\partial^\nu(e^\dagger\bar{\sigma}^\mu e)$	5		
$i\partial^\lambda(D^\nu e^\dagger\bar{\sigma}^\mu e - e^\dagger\bar{\sigma}^\mu D^\nu e)$	5		
$D^\lambda D^\nu e^\dagger\bar{\sigma}^\mu e + e^\dagger\bar{\sigma}^\mu D^\lambda D^\nu e$	5		
$i(D^\lambda D^\nu e^\dagger\bar{\sigma}^\mu e - e^\dagger\bar{\sigma}^\mu D^\lambda D^\nu e)$	5		

Table 8.1: Relevant electron-positron operators in the effective Lagrangian approach. The empty boxes correspond to operators which are not needed in the analysis.

into account in the electron operators, or in the field strength tensor as in table 8.2. To simplify the analysis, the Lorentz indices are kept free and are contracted with the appropriate tensors ($g_{\mu\nu}$ or $\epsilon_{\mu\nu\lambda\rho}$) only at the end of the analysis. In this way, one does not have to deal with the complete set of operators at this stage of the analysis (for example, the operator corresponding to the dual field strength tensor can be forgotten).

$\mathcal{O}(x)$	dim	$\langle\gamma\|\mathcal{O}\|0\rangle$	$\overline{\|\mathcal{M}\|^2}$
$F^{\mu\nu}$	2	$i(p_\gamma^\mu \epsilon^{\nu *} - p_\gamma^\nu \epsilon^{\mu *})$	$-(p_\gamma^\mu p_\gamma^{\mu'} g^{\nu\nu'} - p_\gamma^\mu p_\gamma^{\nu'} g^{\nu\mu'} - p_\gamma^\nu p_\gamma^{\mu'} g^{\mu\nu'} + p_\gamma^\nu p_\gamma^{\nu'} g^{\mu\mu'})$

Table 8.2: Relevant photon operators in the effective Lagrangian approach.

Scalar boson DM annihilation to $e^+ + e^- + \gamma$

The relevant lowest-dimension scalar boson operators are given in table 8.3. Combining operators of table 8.3 with operators of table 8.1, the leading operator for FSR seems to be constructed from $\partial^\mu(\phi^\dagger\phi)$ and $(e^\dagger\bar{\sigma}_\mu e)$. It is a dimension 6 operator and it is not explicitly chirality-suppressed. However, in the s-wave approximation, $p_+^\mu = (m_\phi, \vec{p}_e)$ and $p_-^\mu = (m_\phi, -\vec{p}_e)$, thus $\overline{|\langle e^+e^-|(e^\dagger\bar{\sigma}^0 e)|0\rangle|^2} = 2m_e^2$ which is chirality-suppressed. Therefore, the leading FSR operators are dimension 6 but are chirality-suppressed. For example, one such operator can be constructed out of $\phi^\dagger\phi$ and $m_e(\bar{e}e + e^\dagger\bar{e}^\dagger)$. The related FSR cross-section is

$\mathcal{O}(x)$	dim	$\langle 0\|\mathcal{O}\|\phi^\dagger\phi\rangle$	$\overline{\|\mathcal{M}\|^2}$	$\left(\overline{\|\mathcal{M}\|^2}\right)_{\text{s-wave}}$
$\phi^\dagger\phi$	2	1	1	1
$\partial^\mu(\phi^\dagger\phi)$	3	$-i(p_*^\mu + p^\mu)$	$(p_*^\mu + p^\mu)(p_*^{\mu'} + p^{\mu'})$	$4m_\phi^2\delta^{\mu 0}\delta^{\mu' 0}$
$i(\partial^\mu\phi^\dagger\phi - \phi^\dagger\partial^\mu\phi)$	3	$(p_*^\mu - p^\mu)$	$(p_*^\mu - p^\mu)(p_*^{\mu'} - p^{\mu'})$	0

Table 8.3: Relevant scalar boson DM operators for DM annihilation.

$$\langle\sigma_{\mathrm{FSR}} v\rangle \approx c_{\mathrm{FSR}}\alpha \frac{m_e^2}{M_{\mathrm{int}}^4} \ln\left[\frac{4m_\phi^2}{m_e^2}\right] \tag{8.42}$$

where c_{FSR} includes the operator coupling constant and the π factors from the phase space integration.

For direct photon production from higher-order operators to dominate, the operators should not be chirality-suppressed and/or should be of lower dimension. Combining again operators of table 8.3 with operators of tables 8.1 and 8.2 such that one photon can be created in the final state, the leading operators for direct photon production are dimension 8 and are not chirality-suppressed. The operator made out of $\partial^\mu(\phi^\dagger\phi)$, $(e^\dagger\bar{\sigma}_\nu e)$ and $F_{\mu\nu}$ is an example. Following the general rules of effective field theory, a factor of α should be put in front of this type of operators. The related direct photon production cross-section is

$$\langle\sigma_{\mathrm{eff}} v\rangle \approx c_{\mathrm{eff}}\alpha \frac{(2m_\phi)^6}{M_{\mathrm{int}}^8} \tag{8.43}$$

where c_{eff} includes the operator coupling constant and the π factors from the phase space integration[1].

It is now straightforward to compare FSR and direct photon production cross-sections,

$$\langle \sigma_{\text{FSR}} v \rangle \approx \langle \sigma_{\text{eff}} v \rangle \frac{c_{\text{FSR}}}{c_{\text{eff}}} \frac{m_e^2 M_{\text{int}}^4}{(2m_\phi)^6} \ln \left[\frac{4m_\phi^2}{m_e^2} \right] \tag{8.44}$$

which leads to equation (8.14) of section 8.3. Direct photon production from higher-order operators will therefore dominate over FSR when $M_{\text{int}} \lesssim M_{\text{int}}^*$ (see equation (8.14)). In the remaining subsections, the analysis is more concise since it closely follows what has been done here.

Majorana DM annihilation to $e^+ + e^- + \gamma$

The relevant lowest-dimension Majorana operators are given in table 8.4. Combining operators

$\mathcal{O}(x)$	dim	$\langle 0 \vert \mathcal{O} \vert \chi\chi \rangle$	$\overline{\lvert\mathcal{M}\rvert^2}$	$\left(\overline{\lvert\mathcal{M}\rvert^2}\right)_{\text{s-wave}}$
$m_\chi(\chi\chi + \chi^\dagger\chi^\dagger)$	4	$2m_\chi[(x_1 x_2) + (y_1^\dagger y_2^\dagger)]$	$4m_\chi^2[(p_1 \cdot p_2) - m_\chi^2]$	0
$im_\chi(\chi\chi - \chi^\dagger\chi^\dagger)$	4	$2im_\chi[(x_1 x_2) - (y_1^\dagger y_2^\dagger)]$	$4m_\chi^2[(p_1 \cdot p_2) + m_\chi^2]$	$8m_\chi^4$
$m_\chi(\chi\sigma^{\mu\nu}\chi + \chi^\dagger\bar{\sigma}^{\mu\nu}\chi^\dagger)$	4	0	0	0
$im_\chi(\chi\sigma^{\mu\nu}\chi - \chi^\dagger\bar{\sigma}^{\mu\nu}\chi^\dagger)$	4	0	0	0
$\chi^\dagger\bar{\sigma}^\mu\chi$	3	$(y_1^\dagger\bar{\sigma}^\mu x_2) - (y_2^\dagger\bar{\sigma}^\mu x_1)$	$p_1^\mu p_2^{\mu'} + p_2^\mu p_1^{\mu'} - g^{\mu\mu'}(p_1 \cdot p_2) + m_\chi^2 g^{\mu\mu'}$	$2m_\chi^2\delta^{\mu 0}\delta^{\mu' 0}$
$\partial^\nu(\chi^\dagger\bar{\sigma}^\mu\chi)$	4	$-i(p_1^\nu + p_2^\nu) \times$ ibid	$(p_1^\nu + p_2^\nu)(p_1^{\nu'} + p_2^{\nu'}) \times$ ibid	$8m_\chi^4\delta^{\mu 0}\delta^{\mu' 0}\delta^{\nu 0}\delta^{\nu' 0}$
$i(\partial^\nu\chi^\dagger\bar{\sigma}^\mu\chi - \chi^\dagger\bar{\sigma}^\mu\partial^\nu\chi)$	4	$(p_1^\nu - p_2^\nu) \times \{- \to +\}$	$(p_1^\nu - p_2^\nu)(p_1^{\nu'} - p_2^{\nu'}) \times \{+m_\chi^2 \to -m_\chi^2\}$	0

Table 8.4: Relevant Majorana DM operators for DM annihilation. Notice that $\chi\bar{\sigma}^{\mu\nu}\chi = 0$ since χ is a Majorana fermion.

of table 8.4 with operators of table 8.1, the leading order operators for FSR are dimension 6 operators of the form $(\chi^\dagger\bar{\sigma}^\mu\chi)(e^\dagger\bar{\sigma}_\mu e)$. Again, these operators are chirality-suppressed in the s-wave approximation, and thus the related FSR cross-section is

$$\langle \sigma_{\text{FSR}} v \rangle \approx c_{\text{FSR}} \alpha \frac{m_e^2}{M_{\text{int}}^4} \ln \left[\frac{4m_\chi^2}{m_e^2} \right] \tag{8.45}$$

where c_{FSR} includes the operator coupling constant and the π factors from the phase space integration.

Combining operators of table 8.4 with operators of tables 8.1 and 8.2, the leading operators for direct photon production are dimension 8 and are not chirality-suppressed. The operator made out of $(\chi^\dagger\bar{\sigma}^\mu\chi)$, $(e^\dagger\bar{\sigma}^\nu e)$ and $F_{\mu\nu}$ is an example. The related direct photon production cross-section is

$$\langle \sigma_{\text{eff}} v \rangle \approx c_{\text{eff}} \alpha \frac{(2m_\chi)^6}{M_{\text{int}}^8} \tag{8.46}$$

[1] c_{FSR} and c_{eff} have the same phase space factors since both are obtained from a three-particle final state.

where c_{eff} includes the operator coupling constant and the π factors from the phase space integration.

Comparing FSR and direct photon production cross-sections leads to the equivalent of equation (8.44) with the same overall conclusions as scalar boson DM annihilation.

Dirac DM annihilation to $e^+ + e^- + \gamma$

The relevant lowest-dimension Dirac operators are given in table 8.5. Combining operators

$\mathcal{O}(x)$	dim	$\langle 0 \vert \mathcal{O} \vert \eta\bar{\eta} \rangle$	$\overline{\vert\mathcal{M}\vert^2}$	$\left(\overline{\vert\mathcal{M}\vert^2}\right)_{\text{s-wave}}$
$\eta^\dagger \bar{\sigma}^\mu \eta + \bar{\eta}^\dagger \bar{\sigma}^\mu \bar{\eta}$	3	$(y_*^\dagger \bar{\sigma}^\mu x) - (y^\dagger \bar{\sigma}^\mu x_*)$	$p^\mu p_*^{\mu'} + p_*^\mu p^{\mu'} - g^{\mu\mu'}(p \cdot p_*) + m_\eta^2 g^{\mu\mu'}$	$2m_\eta^2 \delta^{\mu 0} \delta^{\mu' 0}$
$\eta^\dagger \bar{\sigma}^\mu \eta - \bar{\eta}^\dagger \bar{\sigma}^\mu \bar{\eta}$	3	$(y_*^\dagger \bar{\sigma}^\mu x) + (y^\dagger \bar{\sigma}^\mu x_*)$	$p^\mu p_*^{\mu'} + p_*^\mu p^{\mu'} - g^{\mu\mu'}(p \cdot p_*) - m_\eta^2 g^{\mu\mu'}$	$2m_\eta^2 [\delta^{\mu 0} \delta^{\mu' 0} - g^{\mu\mu'}]$

Table 8.5: Relevant Majorana DM operators for DM annihilation.

of table 8.5 with operators of table 8.1, the leading order operators for FSR are dimension 6 operators of the form $[(\eta^\dagger \bar{\sigma}^\mu \eta) - (\bar{\eta}^\dagger \bar{\sigma}^\mu \bar{\eta})](e^\dagger \bar{\sigma}_\mu e)$. However, these operators are not chirality-suppressed in the s-wave approximation, and thus the related FSR cross-section is

$$\langle \sigma_{\text{FSR}} v \rangle \approx c_{\text{FSR}} \alpha \frac{4m_\eta^2}{M_{\text{int}}^4} \ln \left[\frac{4m_\eta^2}{m_e^2} \right] \tag{8.47}$$

where c_{FSR} includes the operator coupling constant and the π factors from the phase space integration.

Combining operators of table 8.5 with operators of tables 8.1 and 8.2, the leading operators for direct photon production are dimension 8 and are not chirality-suppressed, as in the Majorana DM annihilation case. The operator made out of $[(\eta^\dagger \bar{\sigma}^\mu \eta) + (\bar{\eta}^\dagger \bar{\sigma}^\mu \bar{\eta})]$, $(e^\dagger \bar{\sigma}^\nu e)$ and $F_{\mu\nu}$ is an example. The related direct photon production cross-section is

$$\langle \sigma_{\text{eff}} v \rangle \approx c_{\text{eff}} \alpha \frac{(2m_\eta)^6}{M_{\text{int}}^8} \tag{8.48}$$

where c_{eff} includes the operator coupling constant and the π factors from the phase space integration.

Comparing FSR and direct photon production cross-sections leads to

$$\langle \sigma_{\text{FSR}} v \rangle \approx \langle \sigma_{\text{eff}} v \rangle \frac{c_{\text{FSR}}}{c_{\text{eff}}} \frac{M_{\text{int}}^4}{(2m_\eta)^4} \ln \left[\frac{4m_\eta^2}{m_e^2} \right] \gg \langle \sigma_{\text{eff}} v \rangle \tag{8.49}$$

and, for order one coefficients, FSR always dominates over direct photon production from higher-order operators.

Gauge boson DM annihilation to $e^+ + e^- + \gamma$

The relevant lowest-dimension gauge boson operators are given in table 8.6. Combining opera-

$\mathcal{O}(x)$	dim	$\langle 0\|\mathcal{O}\|XX\rangle$	$\overline{\|\mathcal{M}\|^2}$	$\left(\overline{\|\mathcal{M}\|^2}\right)_{\text{s-wave}}$
$X^{\mu\nu}X^{\lambda\rho}$	4	$-[(p_1^\mu\epsilon_1^\nu - p_1^\nu\epsilon_1^\mu)(p_2^\lambda\epsilon_2^\rho - p_2^\rho\epsilon_2^\lambda) + \{1 \leftrightarrow 2\}]$		
$D^\kappa(X^{\mu\nu}X^{\lambda\rho})$	5	$-i(p_1^\kappa + p_2^\kappa) \times \text{ibid}$	$(p_1^\kappa + p_2^\kappa)(p_1^{\kappa'} + p_2^{\kappa'}) \times \text{ibid}$	$4m_X^2\delta^{\kappa 0}\delta^{\kappa' 0} \times \text{ibid}$

Table 8.6: Relevant gauge boson DM operators for DM annihilation.

tors of table 8.6 with operators of table 8.1, the leading order operators for FSR are dimension 8 operators of the form $X^{\mu\lambda}X_{\nu\lambda}i(D^\nu e^\dagger\bar{\sigma}_\mu e - e^\dagger\bar{\sigma}_\mu D^\nu e)$. However, these operators are not chirality-suppressed in the s-wave approximation, and thus the related FSR cross-section is

$$\langle\sigma_{\text{FSR}}v\rangle \approx c_{\text{FSR}}\alpha\frac{(2m_X)^6}{M_{\text{int}}^8}\ln\left[\frac{4m_X^2}{m_e^2}\right] \tag{8.50}$$

where c_{FSR} includes the operator coupling constant and the π factors from the phase space integration.

Combining operators of table 8.6 with operators of tables 8.1 and 8.2, the leading operators for direct photon production are dimension 8 and are not chirality-suppressed. The operator made out of $X^{\mu\lambda}X_{\nu\lambda}$ and $i(D^\nu e^\dagger\bar{\sigma}_\mu e - e^\dagger\bar{\sigma}_\mu D^\nu e)$ is an example. The related direct photon production cross-section is

$$\langle\sigma_{\text{eff}}v\rangle \approx c_{\text{eff}}\alpha\frac{(2m_X)^6}{M_{\text{int}}^8} \tag{8.51}$$

where c_{eff} includes the operator coupling constant and the π factors from the phase space integration.

Comparing FSR and direct photon production cross-sections leads to

$$\langle\sigma_{\text{FSR}}v\rangle \approx \langle\sigma_{\text{eff}}v\rangle\frac{c_{\text{FSR}}}{c_{\text{eff}}}\ln\left[\frac{4m_X^2}{m_e^2}\right] \gtrsim \langle\sigma_{\text{eff}}v\rangle \tag{8.52}$$

and, for order one coefficients, FSR always dominates over direct photon production from higher-order operators, although only slightly.

Scalar boson DM decay to $e^+ + e^- + \gamma$

This case follows closely the scalar boson DM annihilation case. The relevant lowest-dimension scalar boson operators are given in table 8.7. Combining operators of table 8.7 with operators of table 8.1, the leading order operators for FSR are dimension 5 operators of the form $m_e\phi(\bar{e}e + e^\dagger\bar{e}^\dagger)$. These operators are chirality-suppressed and thus the related FSR decay rate is

$$\Gamma_{\text{FSR}} \approx c_{\text{FSR}}\alpha\frac{m_e^2 m_\phi}{M_{\text{int}}^2}\ln\left[\frac{m_\phi^2}{m_e^2}\right] \tag{8.53}$$

$\mathcal{O}(x)$	dim	$\langle 0\vert\mathcal{O}\vert\phi\rangle$	$\overline{\vert\mathcal{M}\vert^2}$	$\left(\overline{\vert\mathcal{M}\vert^2}\right)_{\text{s-wave}}$
ϕ	1	1	1	1
$\partial^\mu\phi$	2	$-ip^\mu$	$p^\mu p^{\mu'}$	$m_\phi^2\delta^{\mu 0}\delta^{\mu' 0}$

Table 8.7: Relevant scalar boson DM operators for DM decay.

where c_{FSR} includes the operator coupling constant and the π factors from the phase space integration.

Combining operators of table 8.7 with operators of tables 8.1 and 8.2, the leading operators for direct photon production are dimension 7 and are not chirality-suppressed. The operator made out of $\partial^\mu\phi$, $(e^\dagger\bar{\sigma}^\nu e)$ and $F_{\mu\nu}$ is an example. The related direct photon production decay rate is

$$\Gamma_{\text{eff}} \approx c_{\text{eff}}\alpha\frac{m_\phi^7}{M_{\text{int}}^6} \tag{8.54}$$

where c_{eff} includes the operator coupling constant and the π factors from the phase space integration.

Comparing FSR and direct photon production decay rates leads to the equivalent of equation (8.44) for decay rates,

$$\Gamma_{\text{FSR}} \approx \Gamma_{\text{eff}}\frac{c_{\text{FSR}}}{c_{\text{eff}}}\frac{m_e^2 M_{\text{int}}^4}{(2m_\phi)^6}\ln\left[\frac{4m_\phi^2}{m_e^2}\right], \tag{8.55}$$

with the same overall conclusions as scalar boson DM annihilation.

Abelian gauge boson DM decay to $e^+ + e^- + \gamma$

The relevant lowest-dimension gauge boson operators are given in table 8.8. Combining opera-

$\mathcal{O}(x)$	dim	$\langle 0\vert\mathcal{O}\vert X\rangle$	$\overline{\vert\mathcal{M}\vert^2}$	$\left(\overline{\vert\mathcal{M}\vert^2}\right)_{\text{s-wave}}$
$X^{\mu\nu}$	2	$-i(p^\mu\epsilon^\nu - p^\nu\epsilon^\mu)$		
$\partial^\lambda X^{\mu\nu}$	3	$-ip^\lambda \times$ ibid	$p^\lambda p^{\lambda'} \times$ ibid	$m_X^2\delta^{\lambda 0}\delta^{\lambda' 0} \times$ ibid

Table 8.8: Relevant gauge boson DM operators for DM decay.

tors of table 8.8 with operators of table 8.1, the leading order operators for FSR are dimension 6 operators of the form $\partial^\mu X_{\mu\nu}(e^\dagger\bar{\sigma}^\nu e)$. However, these operators are not chirality-suppressed and thus the related FSR decay rate is

$$\Gamma_{\text{FSR}} \approx c_{\text{FSR}}\alpha\frac{m_X^5}{M_{\text{int}}^4}\ln\left[\frac{m_X^2}{m_e^2}\right] \tag{8.56}$$

where c_{FSR} includes the operator coupling constant and the π factors from the phase space integration.

Combining operators of table 8.8 with operators of tables 8.1 and 8.2, the leading operators for direct photon production are dimension 6 and are not chirality-suppressed. The operator made out of $X^{\mu\nu}$ and $i(D_\nu e^\dagger \bar{\sigma}_\mu e - e^\dagger \bar{\sigma}_\mu D_\nu e)$ is an example. The related direct photon production decay rate is

$$\Gamma_{\text{eff}} \approx c_{\text{eff}} \alpha \frac{m_X^5}{M_{\text{int}}^4} \tag{8.57}$$

where c_{eff} includes the operator coupling constant and the π factors from the phase space integration.

Comparing FSR and direct photon production cross-sections leads to

$$\Gamma_{\text{FSR}} \approx \Gamma_{\text{eff}} \frac{c_{\text{FSR}}}{c_{\text{eff}}} \ln\left[\frac{m_X^2}{m_e^2}\right] \gtrsim \Gamma_{\text{eff}} \tag{8.58}$$

and, for order one coefficients, FSR always dominates over direct photon production from higher-order operators, although only slightly.

DOS for direct photon production from higher-order operators: An example for Majorana DM annihilation

When direct photon production from higher-order operators dominates over FSR, the photon DOS can be obtained from the most general effective Lagrangian. Here we study the case of Majorana DM annihilation to electron-positron pair, $\chi + \chi \to e^+ + e^- + \gamma$. The other cases where direct photon production from higher-order operators dominates over FSR are basically equivalent.

The lowest-dimension operators relevant to $\chi + \chi \to e^+ + e^- + \gamma$ are effective dimension 8 operators due to the chirality rule, and thus only effective mass dimension 8 operators will be considered. The highest possible effective mass dimension for the DM (χ) operators is therefore 4. The photon can either appear in a covariant derivative or in the field strength tensor.

With the help of tables 8.1, 8.2 and 8.4, the minimal set (in the sense that any operator relevant for $\chi + \chi \to e^+ + e^- + \gamma$ can be rewritten as a linear combination of the operators in the minimal set) of operators of the mass dimension 8 effective Lagrangian for the process $\chi + \chi \to e^+ + e^- + \gamma$ can be found.

From the electron operators without covariant derivatives, only the one with mass dimension 3 is relevant, leading to $(\chi^\dagger \bar{\sigma}^\mu \chi)(e^\dagger \bar{\sigma}^\nu e) F^{\lambda\rho}$. From the electron operators with one covariant derivative, only $i(\chi^\dagger\bar{\sigma}^\mu\chi)\partial^\rho(D^\lambda e^\dagger\bar{\sigma}^\nu e - e^\dagger\bar{\sigma}^\nu D^\lambda e)$ survives (there are two different ways of building this operator) since all other operators are either zero to lowest order in m_e from the equations of motion (the σ matrix and the covariant derivative are forced to be contracted together) or vanish in the s-wave. Finally there are only two operators that can be built from the electron operators with two covariant derivatives, which are $(\chi^\dagger\bar{\sigma}^\mu\chi)(D^\rho D^\lambda e^\dagger\bar{\sigma}^\nu e + e^\dagger\bar{\sigma}^\nu D^\rho D^\lambda e)$ and $i(\chi^\dagger\bar{\sigma}^\mu\chi)(D^\rho D^\lambda e^\dagger\bar{\sigma}^\nu e - e^\dagger\bar{\sigma}^\nu D^\rho D^\lambda e)$.

All operators have four Lorentz indices and must therefore be contracted with $g_{\mu\nu}g_{\lambda\rho}$, $g_{\mu\lambda}g_{\nu\rho}$, $g_{\mu\rho}g_{\nu\lambda}$ and $\epsilon_{\mu\nu\lambda\rho}$. Using the equations of motion, this fact leads to an even smaller minimal set (to lowest order in m_e), since $g_{\mu\nu}1 = \sigma_\mu\bar{\sigma}_\nu + 2i\sigma_{\mu\nu}$ and $[D_\mu, D_\nu] = -i\sqrt{4\pi\alpha}F_{\mu\nu}$. Indeed one has

$$
\begin{aligned}
g_{\lambda\rho}(e^\dagger\bar{\sigma}^\nu D^\rho D^\lambda e) &= e^\dagger\bar{\sigma}^\nu(\sigma_\rho\bar{\sigma}_\lambda D^\rho D^\lambda + g\sigma_{\rho\lambda}F^{\rho\lambda})e \sim F^{\lambda\rho}\text{−term} + \mathcal{O}(m_e)\\
g_{\nu\rho}(e^\dagger\bar{\sigma}^\nu D^\rho D^\lambda e) &= g_{\nu\rho}e^\dagger\bar{\sigma}^\nu(D^\lambda D^\rho + [D^\rho, D^\lambda])e \sim F^{\lambda\rho}\text{−term} + \mathcal{O}(m_e)\\
g_{\nu\lambda}(e^\dagger\bar{\sigma}^\nu D^\rho D^\lambda e) &\sim \mathcal{O}(m_e)\\
\epsilon_{\mu\nu\lambda\rho}(e^\dagger\bar{\sigma}^\nu D^\rho D^\lambda e) &= \frac{1}{2}\epsilon_{\mu\nu\lambda\rho}(e^\dagger\bar{\sigma}^\nu[D^\rho, D^\lambda]e) \sim F^{\lambda\rho}\text{−term}
\end{aligned}
$$

thus eliminating all operators with two covariant derivatives. Moreover, the operator with one covariant derivative can be rewritten in terms of two covariant derivatives as $i(\chi^\dagger\bar{\sigma}^\mu\chi)(D^\rho e^\dagger\bar{\sigma}^\nu D^\lambda e - D^\lambda e^\dagger\bar{\sigma}^\nu D^\rho e)$, leading to

$$
\begin{aligned}
g_{\lambda\rho}(D^\rho e^\dagger\bar{\sigma}^\nu D^\lambda e - D^\lambda e^\dagger\bar{\sigma}^\nu D^\rho e) &= 0\\
g_{\nu\rho}(D^\rho e^\dagger\bar{\sigma}^\nu D^\lambda e - D^\lambda e^\dagger\bar{\sigma}^\nu D^\rho e) &\sim \mathcal{O}(m_e)\\
g_{\nu\lambda}(D^\rho e^\dagger\bar{\sigma}^\nu D^\lambda e - D^\lambda e^\dagger\bar{\sigma}^\nu D^\rho e) &\sim \mathcal{O}(m_e)\\
\epsilon_{\mu\nu\lambda\rho}(D^\rho e^\dagger\bar{\sigma}^\nu D^\lambda e - D^\lambda e^\dagger\bar{\sigma}^\nu D^\rho e) &= 2\,\epsilon_{\mu\nu\lambda\rho}(D^\rho e^\dagger\bar{\sigma}^\nu D^\lambda e)\\
&= 2\,\epsilon_{\mu\nu\lambda\rho}[\partial^\rho(e^\dagger\bar{\sigma}^\nu D^\lambda e) - (e^\dagger\bar{\sigma}^\nu D^\rho D^\lambda e)]\\
&\sim \epsilon_{\mu\nu\lambda\rho}\partial^\rho(e^\dagger\bar{\sigma}^\nu D^\lambda e) + F^{\lambda\rho}\text{−term}
\end{aligned}
$$

therefore eliminating three of the four possible operators. Finally, for the operators with $F^{\mu\nu}$, only two operators survive since the field strength tensor is antisymmetric.

Then the minimal set consists of $(\chi^\dagger\bar{\sigma}^\mu\chi)(e^\dagger\bar{\sigma}^\nu e)F_{\mu\nu}$, $(\chi^\dagger\bar{\sigma}^\mu\chi)(e^\dagger\bar{\sigma}^\nu e)\tilde{F}_{\mu\nu}$ and $i\epsilon_{\mu\nu\lambda\rho}\partial^\rho(\chi^\dagger\bar{\sigma}^\mu\chi)(e^\dagger\bar{\sigma}^\nu D^\lambda e)$. In the s-wave approximation, the last term also vanishes, thus leading to only two operators relevant for the mass dimension 8 effective Lagrangian of $\chi + \chi \to e^+ + e_- + \gamma$ (at lowest order in m_e),

$$
\mathcal{L}_{\text{eff}} = \frac{\sqrt{4\pi\alpha}}{M_{\text{int}}^4}(\chi^\dagger\bar{\sigma}^\mu\chi)(e^\dagger\bar{\sigma}^\nu e)[a_L F_{\mu\nu} + b_L\tilde{F}_{\mu\nu}] + \{L \to R, e \to \bar{e}\} \tag{8.59}
$$

where the coupling constants are assumed to be order one numbers. Since the operators do not interfere (they couple the electrons to different photon states), the probability is simply given by

$$\begin{aligned}\overline{|\mathcal{M}|^2} &= -32\pi\alpha(a_L^2+b_L^2+a_R^2+b_R^2)m_\chi^2 M_{\rm int}^{-8} \\ &\qquad \times[(p_\gamma\cdot p_+)(p_\gamma\cdot p_-)-E_\gamma E_+(p_\gamma\cdot p_-)-E_\gamma E_-(p_\gamma\cdot p_+)] \\ &= 64\pi\alpha(a_L^2+b_L^2+a_R^2+b_R^2)m_\chi^3(m_\chi-E_\gamma)M_{\rm int}^{-8} \\ &\qquad \times(2m_\chi^2-2m_\chi E_\gamma-4m_\chi E_+ + E_\gamma^2+2E_\gamma E_+ + 2E_+^2)\end{aligned}$$

where $\vec{p}_- = -\vec{p}_\gamma - \vec{p}_+$, $E_- = \sqrt{E_\gamma^2+E_+^2+2zE_\gamma E_+} = 2m_\chi - E_\gamma - E_+$, $z = \frac{2m_\chi^2-2m_\chi E_\gamma-2m_\chi E_+ + E_\gamma E_+}{E_\gamma E_+}$ and $m_\chi - E_\gamma < E_+ < m_\chi$. Here $z=\cos\theta$ and θ is the angle between the positron and the photon. In the vanishing electron mass limit the annihilation cross-section is thus

$$\frac{d\langle\sigma v\rangle}{dE_\gamma} = \frac{1}{4m_\chi^2}\int_{m_\chi-E_\gamma}^{E_\gamma}\frac{dE_+}{32\pi^3}\overline{|\mathcal{M}|^2} = \frac{\alpha(a_L^2+b_L^2+a_R^2+b_R^2)m_\chi}{3\pi^2 M_{\rm int}^8}(m_\chi-E_\gamma)E_\gamma^3 \tag{8.60}$$

with $0 < E_\gamma < m_\chi$, which gives the DOS mentioned in the text. Notice that the annihilation cross-section vanishes like the cube of the photon energy, E_γ^3, as $E_\gamma \to 0$.

References

[1] E. Gildener, *Gauge Symmetry Hierarchies*, Phys. Rev. D **14**, 1667 (1976).

[2] G. 't Hooft, in Proc. of 1979 Cargèse Institute on *Recent Developments in Gauge Theories*, p.135, Plenum Press, New York 1980.

[3] P. Ramond, Phys. Rev. D **3**, 2415 (1971).

[4] A. Neveu and J. H. Schwarz, Nucl. Phys. B **31**, 86 (1971).

[5] J. L. Gervais and B. Sakita, Nucl. Phys. B **34**, 632 (1971).

[6] E. Witten, *Dynamical Breaking Of Supersymmetry*, Nucl. Phys. B **188**, 513 (1981).

[7] **ALEPH, DELPHI, L3 and OPAL** Collaboration, The LEP Working Group for Higgs Boson Searches, "Search for neutral MSSM Higgs bosons at LEP," hep-ex/0602042.

[8] R. Essig and J. F. Fortin, JHEP **0804**, 073 (2008) [arXiv:0709.0980 [hep-ph]].

[9] T. Banks, L. M. Carpenter and J. F. Fortin, JHEP **0809**, 087 (2008) [arXiv:0804.2688 [hep-ph]].

[10] T. Banks and J. F. Fortin, arXiv:0901.3578 [hep-ph].

[11] S. P. Martin, arXiv:hep-ph/9709356.

[12] M. Dine and A. E. Nelson, Phys. Rev. D **48**, 1277 (1993) [arXiv:hep-ph/9303230].

[13] A. E. Nelson and N. Seiberg, "R symmetry breaking versus supersymmetry breaking," Nucl. Phys. B **416**, 46 (1994) [arXiv:hep-ph/9309299].

[14] K. Intriligator, N. Seiberg and D. Shih, "Dynamical SUSY breaking in meta-stable vacua," JHEP **0604**, 021 (2006) [arXiv:hep-th/0602239].

[15] R. Essig, J. F. Fortin, K. Sinha, G. Torroba and M. J. Strassler, JHEP **0903**, 043 (2009) [arXiv:0812.3213 [hep-th]].

[16] T. Banks, arXiv:hep-th/0007146.

[17] T. Banks and J. F. Fortin, arXiv:0906.3714 [hep-th].

[18] J. D. Bekenstein, Phys. Rev. D **7**, 2333 (1973).

[19] S. W. Hawking, Nature **248**, 30 (1974).

[20] S. W. Hawking, Commun. Math. Phys. **43**, 199 (1975) [Erratum-ibid. **46**, 206 (1976)].

[21] A. Aguirre, T. Banks and M. Johnson, "Regulating eternal inflation. II: The great divide," JHEP **0608**, 065 (2006) [arXiv:hep-th/0603107].

[22] T. Banks, J. D. Mason and D. O'Neil, "A dark matter candidate with new strong interactions," Phys. Rev. D **72**, 043530 (2005) [arXiv:hep-ph/0506015].

[23] J. Chang *et al.*, Nature **456**, 362 (2008).

[24] F. Aharonian *et al.* [H.E.S.S. Collaboration], Phys. Rev. Lett. **101**, 261104 (2008) [arXiv:0811.3894 [astro-ph]].

[25] H. E. S. Aharonian, arXiv:0905.0105 [astro-ph.HE].

[26] O. Adriani *et al.* [PAMELA Collaboration], Nature **458**, 607 (2009) [arXiv:0810.4995 [astro-ph]].

[27] A. A. Abdo *et al.* [The Fermi LAT Collaboration], Phys. Rev. Lett. **102**, 181101 (2009) [arXiv:0905.0025 [astro-ph.HE]].

[28] J. F. Fortin, J. Shelton, S. Thomas and Y. Zhao, arXiv:0908.2258 [hep-ph].

[29] J. F. Fortin, arXiv:0710.2131 [hep-th].

[30] J. R. Ellis, K. Enqvist, D. V. Nanopoulos, and F. Zwirner, "Observables in Low-Energy Superstring Models," *Mod. Phys. Lett.* **A1** (1986) 57.

[31] R. Barbieri and G. F. Giudice, "Upper Bounds on Supersymmetric Particle Masses," *Nucl. Phys.* **B306** (1988) 63.

[32] B. de Carlos and J. A. Casas, "One loop analysis of the electroweak breaking in supersymmetric models and the fine tuning problem," *Phys. Lett.* **B309** (1993) 320–328, hep-ph/9303291.

[33] B. de Carlos and J. A. Casas, "The Fine tuning problem of the electroweak symmetry breaking mechanism in minimal SUSY models," hep-ph/9310232.

[34] G. W. Anderson and D. J. Castano, "Measures of fine tuning," *Phys. Lett.* **B347** (1995) 300–308, hep-ph/9409419.

[35] P. Ciafaloni and A. Strumia, "Naturalness upper bounds on gauge mediated soft terms," *Nucl. Phys.* **B494** (1997) 41–53, hep-ph/9611204.

[36] P. H. Chankowski, J. R. Ellis, and S. Pokorski, "The fine-tuning price of LEP," *Phys. Lett.* **B423** (1998) 327–336, hep-ph/9712234.

[37] K. Agashe and M. Graesser, "Improving the fine tuning in models of low energy gauge mediated supersymmetry breaking," *Nucl. Phys.* **B507** (1997) 3–34, hep-ph/9704206.

[38] K. L. Chan, U. Chattopadhyay, and P. Nath, "Naturalness, weak scale supersymmetry and the prospect for the observation of supersymmetry at the Tevatron and at the LHC," *Phys. Rev.* **D58** (1998) 096004, hep-ph/9710473.

[39] D. Wright, "Naturally nonminimal supersymmetry," hep-ph/9801449.

[40] G. L. Kane and S. F. King, "Naturalness implications of LEP results," *Phys. Lett.* **B451** (1999) 113–122, hep-ph/9810374.

[41] M. Bastero-Gil, G. L. Kane, and S. F. King, "Fine-tuning constraints on supergravity models," *Phys. Lett.* **B474** (2000) 103–112, hep-ph/9910506.

[42] J. A. Casas, J. R. Espinosa, and I. Hidalgo, "The MSSM fine tuning problem: A way out," *JHEP* **01** (2004) 008, hep-ph/0310137.

[43] J. A. Casas, J. R. Espinosa, and I. Hidalgo, "A relief to the supersymmetric fine tuning problem," hep-ph/0402017.

[44] J. A. Casas, J. R. Espinosa, and I. Hidalgo, "Implications for new physics from fine-tuning arguments. I: Application to SUSY and seesaw cases," *JHEP* **11** (2004) 057, hep-ph/0410298.

[45] P. C. Schuster and N. Toro, "Persistent fine-tuning in supersymmetry and the NMSSM," hep-ph/0512189.

[46] R. Dermisek and J. F. Gunion, "Escaping the large fine tuning and little hierarchy problems in the next to minimal supersymmetric model and h $\rightarrow$ a a decays," *Phys. Rev. Lett.* **95** (2005) 041801, hep-ph/0502105.

[47] R. Dermisek and H. D. Kim, "Radiatively generated maximal mixing scenario for the Higgs mass and the least fine tuned minimal supersymmetric standard model," *Phys. Rev. Lett.* **96** (2006) 211803, hep-ph/0601036.

[48] J. A. Casas, J. R. Espinosa, and I. Hidalgo, "Expectations for LHC from naturalness: Modified vs. SM Higgs sector," hep-ph/0607279.

[49] T. Kobayashi, H. Terao, and A. Tsuchiya, "Fine-tuning in gauge mediated supersymmetry breaking models and induced top Yukawa coupling," *Phys. Rev.* **D74** (2006) 015002, hep-ph/0604091.

[50] P. Athron and D. J. Miller, "A New Measure of Fine Tuning," arXiv:0705.2241 [hep-ph].

[51] M. Frank *et al.*, "The Higgs boson masses and mixings of the complex MSSM in the Feynman-diagrammatic approach," hep-ph/0611326.

[52] G. Degrassi, S. Heinemeyer, W. Hollik, P. Slavich, and G. Weiglein, "Towards high-precision predictions for the MSSM Higgs sector," *Eur. Phys. J.* **C28** (2003) 133–143, hep-ph/0212020.

[53] S. Heinemeyer, W. Hollik, and G. Weiglein, "The masses of the neutral CP-even Higgs bosons in the MSSM: Accurate analysis at the two-loop level," *Eur. Phys. J.* **C9** (1999) 343–366, hep-ph/9812472.

[54] S. Heinemeyer, W. Hollik, and G. Weiglein, "FeynHiggs: A program for the calculation of the masses of the neutral CP-even Higgs bosons in the MSSM," *Comput. Phys. Commun.* **124** (2000) 76–89, hep-ph/9812320.

[55] S. Heinemeyer, W. Hollik, H. Rzehak, and G. Weiglein, "The Higgs sector of the complex MSSM at two-loop order: QCD contributions," arXiv:0705.0746 [hep-ph].

[56] Y. Okada, M. Yamaguchi, and T. Yanagida, "Upper bound of the lightest Higgs boson mass in the minimal supersymmetric standard model," *Prog. Theor. Phys.* **85** (1991) 1–6.

[57] J. R. Ellis, G. Ridolfi, and F. Zwirner, "Radiative corrections to the masses of supersymmetric Higgs bosons," *Phys. Lett.* **B257** (1991) 83–91.

[58] H. E. Haber and R. Hempfling, "Can the mass of the lightest Higgs boson of the minimal supersymmetric model be larger than m(Z)?," *Phys. Rev. Lett.* **66** (1991) 1815–1818.

[59] H. E. Haber, R. Hempfling, and A. H. Hoang, "Approximating the radiatively corrected Higgs mass in the minimal supersymmetric model," *Z. Phys.* **C75** (1997) 539–554, hep-ph/9609331.

[60] M. Carena, J. R. Espinosa, M. Quiros, and C. E. M. Wagner, "Analytical expressions for radiatively corrected Higgs masses and couplings in the MSSM," *Phys. Lett.* **B355** (1995) 209–221, hep-ph/9504316.

[61] M. Carena, M. Quiros, and C. E. M. Wagner, "Effective potential methods and the Higgs mass spectrum in the MSSM," *Nucl. Phys.* **B461** (1996) 407–436, hep-ph/9508343.

[62] R. Essig, "Implications of the LEP Higgs bounds for the MSSM stop sector," *Phys. Rev.* **D75** (2007) 095005, hep-ph/0702104.

[63] L. E. Ibanez and C. Lopez, "N=1 Supergravity, the Weak Scale and the Low-Energy Particle Spectrum," *Nucl. Phys.* **B233** (1984) 511.

[64] M. Carena, P. H. Chankowski, M. Olechowski, S. Pokorski, and C. E. M. Wagner, "Bottom-up approach and supersymmetry breaking," *Nucl. Phys.* **B491** (1997) 103–128, hep-ph/9612261.

[65] J. A. Casas, J. R. Espinosa, and I. Hidalgo, "Implications for new physics from fine-tuning arguments. II: Little Higgs models," *JHEP* **03** (2005) 038, hep-ph/0502066.

[66] P. Athron and D. J. Miller, "Fine Tuning in Supersymmetric Models," arXiv:0707.1255 [hep-ph].

[67] A. B. Lahanas and D. V. Nanopoulos, "The Road to No Scale Supergravity," *Phys. Rept.* **145** (1987) 1.

[68] **CDF** Collaboration, "A combination of CDF and D0 results on the mass of the top quark," hep-ex/0703034.

[69] W.-M. Yao *et al.*, "Review of Particle Physics," *Journal of Physics G* **33** (2006) 1+.

[70] M. Drees, R. Godbole, and P. Roy, *Theory & Phenomenology of Sparticles.* World Scientific Publishing Company, 2004.

[71] M. Carena and H. E. Haber, "Higgs boson theory and phenomenology. ((V))," *Prog. Part. Nucl. Phys.* **50** (2003) 63–152, hep-ph/0208209.

[72] S. Heinemeyer, W. Hollik, and G. Weiglein, "The mass of the lightest MSSM Higgs boson: A compact analytical expression at the two-loop level," *Phys. Lett.* **B455** (1999) 179–191, hep-ph/9903404.

[73] G. L. Kane, T. T. Wang, B. D. Nelson, and L.-T. Wang, "Theoretical implications of the LEP Higgs search," *Phys. Rev.* **D71** (2005) 035006, hep-ph/0407001.

[74] R. Kitano and Y. Nomura, "Supersymmetry, naturalness, and signatures at the LHC," *Phys. Rev.* **D73** (2006) 095004, hep-ph/0602096.

[75] P. M. Ferreira, I. Jack, and D. R. T. Jones, "Infrared soft universality," *Phys. Lett.* **B357** (1995) 359–364, hep-ph/9506467.

[76] M. Lanzagorta and G. G. Ross, "Infrared fixed point structure of soft supersymmetry breaking mass terms," *Phys. Lett.* **B364** (1995) 163–174, hep-ph/9507366.

[77] B. Pendleton and G. G. Ross, "Mass and Mixing Angle Predictions from Infrared Fixed Points," *Phys. Lett.* **B98** (1981) 291.

[78] J. M. Frere, D. R. T. Jones, and S. Raby, "Fermion Masses and Induction of the Weak Scale by Supergravity," *Nucl. Phys.* **B222** (1983) 11.

[79] J. P. Derendinger and C. A. Savoy, "Quantum Effects and SU(2) x U(1) Breaking in Supergravity Gauge Theories," *Nucl. Phys.* **B237** (1984) 307.

[80] J. F. Gunion, H. E. Haber, and M. Sher, "Charge / Color Breaking Minima And A-Parameter Bounds In Supersymmetric Models," *Nucl. Phys.* **B306** (1988) 1.

[81] J. A. Casas, A. Lleyda, and C. Munoz, "Strong constraints on the parameter space of the MSSM from charge and color breaking minima," *Nucl. Phys.* **B471** (1996) 3–58, hep-ph/9507294.

[82] C. Le Mouel, "Charge and color breaking conditions associated to the top quark Yukawa coupling," *Phys. Rev.* **D64** (2001) 075009, hep-ph/0103341.

[83] A. Kusenko, P. Langacker, and G. Segre, "Phase Transitions and Vacuum Tunneling Into Charge and Color Breaking Minima in the MSSM," *Phys. Rev.* **D54** (1996) 5824–5834, hep-ph/9602414.

[84] A. Riotto and E. Roulet, "Vacuum decay along supersymmetric flat directions," *Phys. Lett.* **B377** (1996) 60–66, hep-ph/9512401.

[85] R. Dermisek, H. D. Kim, and I.-W. Kim, "Mediation of supersymmetry breaking in gauge messenger models," *JHEP* **10** (2006) 001, hep-ph/0607169.

[86] **SUSY Working Group** Collaboration, R. Culbertson *et al.*, "Low-scale and gauge-mediated supersymmetry breaking at the Fermilab Tevatron Run II," hep-ph/0008070.

[87] C.-L. Chou and M. E. Peskin, "Scalar top quark as the next-to-lightest supersymmetric particle," *Phys. Rev.* **D61** (2000) 055004, hep-ph/9909536.

[88] U. Sarid and S. D. Thomas, "Mesino-antimesino oscillations," *Phys. Rev. Lett.* **85** (2000) 1178–1181, hep-ph/9909349.

[89] M. Perelstein and C. Spethmann, "A collider signature of the supersymmetric golden region," *JHEP* **04** (2007) 070, hep-ph/0702038.

[90] R. Dermisek and I. Low, "Probing the stop sector and the sanity of the MSSM with the Higgs boson at the LHC," hep-ph/0701235.

[91] J. R. Espinosa and R.-J. Zhang, "MSSM lightest CP-even Higgs boson mass to O(alpha(s) alpha(t)): The effective potential approach," *JHEP* **03** (2000) 026, hep-ph/9912236.

[92] M. Carena *et al.*, "Reconciling the two-loop diagrammatic and effective field theory computations of the mass of the lightest CP-even Higgs boson in the MSSM," *Nucl. Phys.* **B580** (2000) 29–57, hep-ph/0001002.

[93] S. Heinemeyer, "MSSM Higgs physics at higher orders," hep-ph/0407244.

[94] M. Carena, S. Heinemeyer, C. E. M. Wagner, and G. Weiglein, "Suggestions for improved benchmark scenarios for Higgs- boson searches at LEP2," hep-ph/9912223.

[95] S. P. Martin and M. T. Vaughn, "Two loop renormalization group equations for soft supersymmetry breaking couplings," *Phys. Rev.* **D50** (1994) 2282, hep-ph/9311340.

[96] C. T. Hill, "Quark and Lepton Masses from Renormalization Group Fixed Points," *Phys. Rev.* **D24** (1981) 691.

[97] M. Lanzagorta and G. G. Ross, "Infrared fixed points revisited," *Phys. Lett.* **B349** (1995) 319–328, hep-ph/9501394.

[98] B. A. Ovrut and J. Wess, "Supersymmetric R(xi) Gauge and Radiative Symmetry Breaking," *Phys. Rev.* **D25** (1982) 409.

[99] N. Marcus, A. Sagnotti, and W. Siegel, "Ten-Dimensional Supersymmetric Yang-Mills Theory in terms of Four-Dimensional Superfields," *Nucl. Phys.* **B224** (1983) 159.

[100] W. Siegel, "SuperYang-Mills theory as a random matrix model," *Phys. Rev.* **D52** (1995) 1035–1041, hep-th/9502163.

[101] A. S. Goldhaber, A. Rebhan, P. van Nieuwenhuizen, and R. Wimmer, "Quantum corrections to mass and central charge of supersymmetric solitons," *Phys. Rept.* **398** (2004) 179–219, hep-th/0401152.

[102] G. 't Hooft, "Renormalizable Lagrangians for Massive Yang-Mills Fields," *Nucl. Phys.* **B35** (1971) 167–188.

[103] P. W. Higgs, "Broken symmetries, massless particles and gauge fields," *Phys. Lett.* **12** (1964) 132–133.

[104] P. W. Higgs, "Broken Symmetries and the Masses of Gauge Bosons," *Phys. Rev. Lett.* **13** (1964) 508–509.

[105] P. W. Higgs, "Spontaneous Symmetry Breakdown Without Massless Bosons," *Phys. Rev.* **145** (1966) 1156–1163.

[106] M. T. Grisaru, W. Siegel, and M. Rocek, "Improved Methods for Supergraphs," *Nucl. Phys.* **B159** (1979) 429.

[107] ALEPH, DELPHI, L3 and OPAL Collaboration, *Search for neutral MSSM Higgs bosons at LEP*, Eur. Phys. J. C **47**, 547 (2006), arXiv:hep-ex/0602042.

[108] R. Essig and J.F. Fortin, *The Minimally Tuned Minimal Supersymmetric Standard Model*, arXiv:0709.0980 [hep-ph]. R. Essig, *Implications of the LEP Higgs bounds for the MSSM stop sector*, Phys. Rev. D **75**, 095005 (2007), arXiv:hep-ph/0702104.

[109] P.C. Schuster and N. Toro, *Persistent fine-tuning in supersymmetry and the NMSSM*, arXiv:hep-ph/0512189. R. Dermisek and J.F. Gunion, *Escaping the large fine tuning and little hierarchy problems in the next to minimal supersymmetric model and $h \to a\ a$ decays*, Phys. Rev. Lett. **95**, 041801 (2005), arXiv:hep-ph/0502105. S. Chang, P.J. Fox and N. Weiner, *Naturalness and Higgs decays in the MSSM with a singlet*, JHEP **0608**, 068 (2006), arXiv:hep-ph/0511250.

[110] S. Chang and N. Weiner, *Nonstandard Higgs Decays with Visible and Missing Energy*, arXiv:0710.4591 [hep-ph]. L.M. Carpenter, D.E. Kaplan and E.J. Rhee, *Reduced fine-tuning in supersymmetry with R-parity violation*, Phys. Rev. Lett. **99**, 211801 (2007), arXiv:hep-ph/0607204.

[111] L.M. Carpenter, D.E. Kaplan and E.J. Rhee, *Reduced fine-tuning in supersymmetry with R-parity violation*, Phys. Rev. Lett. **99**, 211801 (2007), arXiv:hep-ph/0607204.

[112] L.M. Carpenter, D.E. Kaplan and E.J. Rhee, *New Light Windows for Sparticle Masses and Higgs Decays in the R Parity Violating MSSM*, arXiv:0804.1581 [hep-ph].

[113] R. Dermisek and R. Stuart, *Bi-large neutrino mixing and CP violation in an SO(10) SUSY GUT for fermion masses*, Phys. Lett. B **622**, 327 (2005), arXiv:hep-ph/0507045.

[114] R. Barbier *et al.*, *R-parity violating supersymmetry*, Phys. Rept. **450**, 1 (2005), arXiv:hep-ph/0406039.

[115] T. Banks, *Remodeling the pentagon after the events of 2/23/06*, arXiv:hep-ph/0606313.

[116] C.D. Froggatt and H.B. Nielsen, *Hierarchy of Quark Masses, Cabibbo Angles and CP Violation*, Nucl. Phys. B **147**, 277 (1979).

[117] K. Cheung, J. Song and Q.-S. Yan, *Role of h —¿ eta eta in Intermediate-Mass Higgs Boson Searches at the Large Hadron Collider*, Phys. Rev. Lett. **99**, 031801 (2007), arXiv:hep-ph/0703149. K. Belotsky, D. Fargion, M. Khlopov, R. Konoplich and K. Shibaev, *Invisible Higgs boson decay into massive neutrinos of fourth generation*, Phys. Rev. D **68**, 054027 (2003), arXiv:hep-ph/0210153.

[118] S.P. Martin, *A supersymmetry primer*, arXiv:hep-ph/9709356.

[119] A. Heister *et al.* [ALEPH Collaboration], *Absolute lower limits on the masses of selectrons and sneutrinos in the MSSM*, Phys. Lett. B **544**, 73 (2002), arXiv:hep-ex/0207056. DELPHI Collaboration, *Searches for supersymmetric particles in e+ e- collisions up to 208-GeV and interpretation of the results within the MSSM*, Eur. Phys. J. C **31**, 421 (2004), arXiv:hep-ex/0311019.

[120] L. M. Carpenter, M. Dine, G. Festuccia and J. D. Mason, *Implementing General Gauge Mediation*, arXiv:0805.2944 [hep-ph].

[121] CDF Collaboration, *Inclusive search for new physics with like-sign dilepton events in $p\overline{p}$ collisions at $\sqrt{s} = 1.96$ TeV*, Phys. Rev. Lett. **98**, 221803 (2007), arXiv:hep-ex/0702051.

[122] CDF Collaboration, *Measurement of the t anti-t production cross-section in p anti-p collisions at s**(1/2) = 1.96-TeV using missing E(t) + jets events with secondary vertex b-tagging*, Phys. Rev. Lett. **96**, 202002 (2006), arXiv:hep-ex/0603043.

[123] T. Hahn, S. Heinemeyer, F. Maltoni, G. Weiglein and S. Willenbrock, *SM and MSSM Higgs boson production cross-sections at the Tevatron and the LHC*, arXiv:hep-ph/0607308.

[124] J. Nielsen, *Private Communication*.

[125] CDF Collaboration, *Search for Higgs Boson in Association with b-Quarks*, CDF Note 8954 v 1.0. http://www-cdf.fnal.gov/physics/new/hdg/results/3b_susyhiggs_070803/cdf8954_higgs3b_v10.pdf.

[126] G. Abbiendi *et al.* [OPAL Collaboration], *Decay-mode independent searches for new scalar bosons with the OPAL detector at LEP*, Eur. Phys. J. C **27**, 311 (2003), arXiv:hep-ex/0206022.

[127] S. Schael *et al.* [ALEPH Collaboration], *Search for Higgs bosons decaying to W W in e+ e- collisions at LEP*, Eur. Phys. J. C **49**, 439 (2007), arXiv:hep-ex/0605079.

[128] D.E. Kaplan and K. Rehermann, *Proposal for Higgs and Superpartner Searches at the LHCb Experiment*, JHEP **0710**, 056 (2007), arXiv:0705.3426 [hep-ph].

[129] ALEPH Collaboration, *Search for supersymmetry with a dominant R-parity violating $LQ\overline{D}$ coupling in e^+e^- collisions at centre-of-mass energies 130 GeV to 172 GeV*, Eur. Phys. J. C **7**, 383-405 (1999), arXiv:hep-ex/9811033.

[130] W. Oller, H. Eberl and W. Majerotto, *Full one loop corrections to neutralino pair production in e+ e- annihilation*, Phys. Lett. B **590**, 273-283 (2004), arXiv:hep-ph/0402134.

[131] Y. Grossman and S. Rakshit, *Neutrino masses in R-parity violating supersymmetric models*, Phys. Rev. D **69**, 093002 (2004), arXiv:hep-ph/0311310.

[132] H. Murayama, "A model of direct gauge mediation," Phys. Rev. Lett. **79**, 18 (1997) [arXiv:hep-ph/9705271]. S. Dimopoulos, G. R. Dvali, R. Rattazzi and G. F. Giudice, "Dynamical soft terms with unbroken supersymmetry," Nucl. Phys. B **510**, 12 (1998) [arXiv:hep-ph/9705307].

[133] M. A. Luty, "Simple gauge-mediated models with local minima," Phys. Lett. B **414**, 71 (1997) [arXiv:hep-ph/9706554]. M. A. Luty and J. Terning, "Improved single sector supersymmetry breaking," Phys. Rev. D **62**, 075006 (2000) [arXiv:hep-ph/9812290].

[134] T. Banks, "Cosmological supersymmetry breaking and the power of the pentagon: A model of low energy particle physics," arXiv:hep-ph/0510159.

[135] S. D. Thomas, "Recent developments in dynamical supersymmetry breaking," arXiv:hep-th/9801007.

[136] T. Banks, "Remodeling the pentagon after the events of 2/23/06," arXiv:hep-ph/0606313.

[137] A. Amariti, L. Girardello and A. Mariotti, "Non-supersymmetric meta-stable vacua in SU(N) SQCD with adjoint matter," JHEP **0612**, 058 (2006) [arXiv:hep-th/0608063].

[138] M. Dine, J. L. Feng and E. Silverstein, "Retrofitting O'Raifeartaigh models with dynamical scales," Phys. Rev. D **74**, 095012 (2006) [arXiv:hep-th/0608159].

[139] H. Abe, T. Higaki, T. Kobayashi and Y. Omura, "Moduli stabilization, F-term uplifting and soft supersymmetry breaking terms," Phys. Rev. D **75**, 025019 (2007) [arXiv:hep-th/0611024].

[140] M. Dine and J. Mason, "Gauge mediation in metastable vacua," Phys. Rev. D **77**, 016005 (2008) [arXiv:hep-ph/0611312].

[141] R. Kitano, H. Ooguri and Y. Ookouchi, "Direct mediation of meta-stable supersymmetry breaking," Phys. Rev. D **75**, 045022 (2007) [arXiv:hep-ph/0612139].

[142] H. Murayama and Y. Nomura, Phys. Rev. Lett. **98**, 151803 (2007) [arXiv:hep-ph/0612186].

[143] H. Murayama and Y. Nomura, Phys. Rev. D **75**, 095011 (2007) [arXiv:hep-ph/0701231].

[144] C. Csaki, Y. Shirman and J. Terning, "A simple model of low-scale direct gauge mediation," JHEP **0705**, 099 (2007) [arXiv:hep-ph/0612241].

[145] R. Essig, K. Sinha and G. Torroba, "Meta-Stable Dynamical Supersymmetry Breaking Near Points of Enhanced Symmetry," JHEP **0709**, 032 (2007) [arXiv:0707.0007 [hep-th]].

[146] A. Giveon and D. Kutasov, "Stable and Metastable Vacua in SQCD," Nucl. Phys. B **796**, 25 (2008) [arXiv:0710.0894 [hep-th]].

[147] B. K. Zur, L. Mazzucato and Y. Oz, "Direct Mediation and a Visible Metastable Supersymmetry Breaking Sector," arXiv:0807.4543 [hep-ph].

[148] F. q. Xu and J. M. Yang, "An Extension for Direct Gauge Mediation of Metastable Supersymmetry Breaking," arXiv:0712.4111 [hep-ph].

[149] N. Haba and N. Maru, "A Simple Model of Direct Gauge Mediation of Metastable Supersymmetry Breaking," Phys. Rev. D **76**, 115019 (2007) [arXiv:0709.2945 [hep-ph]].

[150] A. Giveon, A. Katz and Z. Komargodski, "On SQCD with massive and massless flavors," JHEP **0806**, 003 (2008) [arXiv:0804.1805 [hep-th]].

[151] A. Giveon, A. Katz, Z. Komargodski and D. Shih, "Dynamical SUSY and R-symmetry breaking in SQCD with massive and massless flavors," JHEP **0810**, 092 (2008) [arXiv:0808.2901 [hep-th]].

[152] K. Intriligator, D. Shih and M. Sudano, "Surveying Pseudomoduli: the Good, the Bad and the Incalculable," arXiv:0809.3981 [hep-th].

[153] K. A. Intriligator and N. Seiberg, "Lectures on Supersymmetry Breaking," Class. Quant. Grav. **24**, S741 (2007) [arXiv:hep-ph/0702069].

[154] A. Giveon and D. Kutasov, "Gauge symmetry and supersymmetry breaking from intersecting branes," Nucl. Phys. B **778**, 129 (2007) [arXiv:hep-th/0703135].

[155] R. Essig, J.-F. Fortin, K. Sinha, M. Strassler, G. Torroba, to appear.

[156] S. R. Coleman and E. Weinberg, "Radiative Corrections As The Origin Of Spontaneous Symmetry Breaking," Phys. Rev. D **7**, 1888 (1973).

[157] S. Abel, C. Durnford, J. Jaeckel and V. V. Khoze, "Dynamical breaking of U(1)R and supersymmetry in a metastable vacuum," Phys. Lett. B **661**, 201 (2008) [arXiv:0707.2958 [hep-ph]].

[158] H. Abe, T. Kobayashi and Y. Omura, "R-symmetry, supersymmetry breaking and metastable vacua in global and local supersymmetric theories," JHEP **0711**, 044 (2007) [arXiv:0708.3148 [hep-th]].

[159] F. Brummer, "A natural renormalizable model of metastable SUSY breaking," JHEP **0707**, 043 (2007) [arXiv:0705.2153 [hep-ph]].

[160] D. Marques and F. A. Schaposnik, "Explicit R-Symmetry Breaking and Metastable Vacua," arXiv:0809.4618 [hep-th].

[161] P. J. Fox, A. E. Nelson and N. Weiner, "Dirac gaugino masses and supersoft supersymmetry breaking," JHEP **0208**, 035 (2002) [arXiv:hep-ph/0206096]. G. D. Kribs, E. Poppitz and N. Weiner, "Flavor in Supersymmetry with an Extended R-symmetry," arXiv:0712.2039 [hep-ph].

[162] S. D. L. Amigo, A. E. Blechman, P. J. Fox and E. Poppitz, "R-symmetric gauge mediation," arXiv:0809.1112 [hep-ph].

[163] S. R. Coleman, "The Fate Of The False Vacuum. 1. Semiclassical Theory," Phys. Rev. D **15**, 2929 (1977) [Erratum-ibid. D **16**, 1248 (1977)].

[164] M. J. Duncan and L. G. Jensen, "Exact tunneling solutions in scalar field theory," Phys. Lett. B **291**, 109 (1992).

[165] P. F. Smith, J. R. J. Bennett, G. J. Homer, J. D. Lewin, H. E. Walford and W. A. Smith, "A Search For Anomalous Hydrogen In Enriched D-2 O, Using A Time-Of-Flight Spectrometer," Nucl. Phys. B **206**, 333 (1982).

[166] M. L. Perl, P. C. Kim, V. Halyo, E. R. Lee, I. T. Lee, D. Loomba and K. S. Lackner, "The search for stable, massive, elementary particles," Int. J. Mod. Phys. A **16**, 2137 (2001) [arXiv:hep-ex/0102033].

[167] S. Dimopoulos, G. F. Giudice and A. Pomarol, "Dark matter in theories of gauge-mediated supersymmetry breaking," Phys. Lett. B **389**, 37 (1996) [arXiv:hep-ph/9607225].

[168] M. W. Goodman and E. Witten, "Detectability of certain dark-matter candidates," Phys. Rev. D **31**, 3059 (1985).

[169] R. Essig, "Direct Detection of Non-Chiral Dark Matter," Phys. Rev. D **78**, 015004 (2008) [arXiv:0710.1668 [hep-ph]].

[170] J. Yoo [CDMS Collaboration], "Results from the CDMS 5-Tower Operation," arXiv:0810.3527 [hep-ex].

[171] J. Angle *et al.* [XENON Collaboration], "First Results from the XENON10 Dark Matter Experiment at the Gran Sasso National Laboratory," Phys. Rev. Lett. **100**, 021303 (2008) [arXiv:0706.0039 [astro-ph]].

[172] M. Viel, J. Lesgourgues, M. G. Haehnelt, S. Matarrese and A. Riotto, "Constraining warm dark matter candidates including sterile neutrinos and light gravitinos with WMAP and the Lyman-alpha forest," Phys. Rev. D **71**, 063534 (2005) [arXiv:astro-ph/0501562].

[173] S. Abel and V. V. Khoze, "Direct Mediation, Duality and Unification," arXiv:0809.5262 [hep-ph].

[174] S. L. Glashow, "Trinification Of All Elementary Particle Forces."

[175] G. K. Leontaris and J. Rizos, "A D-brane inspired trinification model," [arXiv:hep-ph/0603203];

G. K. Leontaris and J. Rizos, "A D-brane inspired trinification model," J. Phys. Conf. Ser. **53**, 722 (2006).

[176] O. Adriani, *et. al.*, (2008), 0810.4995;

S. W. Barwick, *et. al.* (HEAT), Astrophys. J. **482**, L191 (1997) [arXiv:astro-ph/9703192];

J. J. Beatty *et. al.*, Phys. Rev. Lett. **93**, 241102 (2004) [arXiv:astro-ph/0412230];

M. Aguilar *et. al.* (AMS-01), Phys. Lett. **B646f**, 145 (2007) [arXiv:astro-ph/0703154];

J. Chang *et. al.*, (ATIC) (2005), prepared for 29th International Cosmic Ray Conferences, Aug. 03-10, 2005;

D. P. Finkbeiner, Astrophys. J. **614**, 186 (2004) [arXiv:astro-ph/0311547];

G. Dobler, D. P. Finkbeiner, (2007), 0712.1038;

A. W. Strong, R. Diehl, H. Halloin, V. Schonfelder, L. Bouchet, P. Mandrou, F. Lebrun, R. Terrier, Astron. Astrophys. **444**, 495 (2005) [arXiv:astro-ph/0509290].

[177] T. Banks, S. Echols and J. L. Jones, "Baryogenesis, dark matter and the pentagon," JHEP **0611**, 046 (2006) [arXiv:hep-ph/0608104].

[178] T. Banks, H. Haber, "Note on the pseudo-NG-boson of meta-stable SUSY breaking," in preparation.

[179] K. Intriligator, N. Seiberg and D. Shih, "Dynamical SUSY breaking in meta-stable vacua," JHEP **0604**, 021 (2006) [arXiv:hep-th/0602239];

K. Intriligator, N. Seiberg and D. Shih, "Supersymmetry Breaking, R-Symmetry Breaking and Metastable Vacua," JHEP **0707**, 017 (2007) [arXiv:hep-th/0703281].

[180] M. Dine, J. L. Feng and E. Silverstein, "Retrofitting O'Raifeartaigh models with dynamical scales," Phys. Rev. D **74**, 095012 (2006) [arXiv:hep-th/0608159].

[181] T. Banks, *Cosmological breaking of supersymmetry or little Lambda goes back to the future. II,* [arXiv:hep-th/0007146];

T. Banks, *Cosmological breaking of supersymmetry ?,* Int. J. Mod. Phys. A **16**, 910 (2001);

T. Banks, *Supersymmetry, the cosmological constant and a theory of quantum gravity in our universe,* Gen. Rel. Grav. **35**, 2075 (2003), [arXiv:hep-th/0305206];

T. Banks, *SUSY and the holographic screens,* [arXiv:hep-th/0305163];

T. Banks, B. Fiol and A. Morisse, *Towards a quantum theory of de Sitter space,* [arXiv:hep-th/0609062].

[182] A. G. Cohen and D. B. Kaplan, "THERMODYNAMIC GENERATION OF THE BARYON ASYMMETRY," Phys. Lett. B **199**, 251 (1987);

A. G. Cohen and D. B. Kaplan, "SPONTANEOUS BARYOGENESIS," Nucl. Phys. B **308**, 913 (1988).

[183] K. Griest and M. Kamionkowski, "Unitarity Limits on the Mass and Radius of Dark Matter Particles," Phys. Rev. Lett. **64**, 615 (1990).

[184] M. Cirelli, M. Kadastik, M. Raidal and A. Strumia, "Model-independent implications of the e+, e-, anti-proton cosmic ray spectra on properties of Dark Matter," Nucl. Phys. B **813**, 1 (2009) [arXiv:0809.2409 [hep-ph]].

N. Arkani-Hamed, D. P. Finkbeiner, T. Slatyer and N. Weiner, "A Theory of Dark Matter," arXiv:0810.0713 [hep-ph].

[185] T. Banks, M. Dine and M. Graesser, "Supersymmetry, axions and cosmology," Phys. Rev. D **68**, 075011 (2003) [arXiv:hep-ph/0210256].

[186] Y. Lu and R. D. Amado, "Nucleon antinucleon interaction from the Skyrme model," Phys. Rev. C **54**, 1566 (1996) [arXiv:nucl-th/9606002];

Y. Lu, P. Protopapas and R. D. Amado, "Nucleon antinucleon interaction from the Skyrme model. II," Phys. Rev. C **57**, 1983 (1998) [arXiv:nucl-th/9710046].

[187] T. Banks, *Cosmological supersymmetry breaking and the power of the pentagon: A model of low energy particle physics,* [arXiv:hep-ph/0510159];

T. Banks, *Remodeling the pentagon after the events of 2/23/06,* [arXiv:hep-ph/0606313].

[188] J. L. Jones, "Gauge Coupling Unification in MSSM + 5 Flavors," arXiv:0812.2106 [hep-ph].

[189] T. Banks, J. L. Jones, *Moduli Mediation of* $\not{S}$USY *at a Mythical Meta-stable Minimum*, in preparation.

[190] C. Cheung, A. L. Fitzpatrick and D. Shih, "(Extra)Ordinary Gauge Mediation," JHEP **0807**, 054 (2008) arXiv:0710.3585 [hep-ph].

[191] T. Aaltonen *et al.* [CDF Collaboration], "Search for Supersymmetry in $p\bar{p}$ Collisions at $\sqrt{s}$ = 1.96-TeV Using the Trilepton Signature of Chargino-Neutralino Production," arXiv:0808.2446 [hep-ex];

S. Dube, J. Glatzer, S. Somalwar and A. Sood, "An Interpretation of Tevatron SUSY Trilepton Search Results in mSUGRA and in a Model-independent Fashion," arXiv:0808.1605 [hep-ph];

L. M. Carpenter, "Surveying the Phenomenology of General Gauge Mediation," arXiv:0812.2051 [hep-ph].

[192] P. Meade, N. Seiberg and D. Shih, "General Gauge Mediation," arXiv:0801.3278 [hep-ph];

M. Buican, P. Meade, N. Seiberg and D. Shih, "Exploring General Gauge Mediation," arXiv:0812.3668 [hep-ph].

[193] E. Witten, "Strong Coupling Expansion Of Calabi-Yau Compactification," Nucl. Phys. B **471**, 135 (1996) [arXiv:hep-th/9602070].

[194] I. Affleck and M. Dine, "A New Mechanism For Baryogenesis," Nucl. Phys. B **249**, 361 (1985).

[195] J. Chang *et al.*, "An Excess Of Cosmic Ray Electrons At Energies Of 300.800 Gev," Nature **456**, 362 (2008).

[196] S. Profumo, "Dissecting Pamela (and ATIC) with Occam's Razor: existing, well-known Pulsars naturally account for the 'anomalous' Cosmic-Ray Electron and Positron Data," arXiv:0812.4457 [astro-ph].

[197] T. Banks, B. Fiol and A. Morisse, *Towards a quantum theory of de Sitter space,* [arXiv:hep-th/0609062];

[198] T. Banks, "Holographic Space-time from the Big Bang to the de Sitter era," Lectures given at Liouville Gravity and Statistical Models: International conference in memory of Alexei Zamolodchikov, Moscow, Russia, 21-24 Jun 2008. To be published in J. Phys. A. arXiv:0809.3951 [hep-th].

[199] T. Banks, "Holographic Space-time from the Big Bang to the de Sitter era," arXiv:0809.3951 [hep-th].

[200] T. Banks, W. Fischler and S. Paban, "Recurrent nightmares?: Measurement theory in de Sitter space," JHEP **0212**, 062 (2002) [arXiv:hep-th/0210160].

T. Banks, B. Fiol and A. Morisse, "Towards a quantum theory of de Sitter space," JHEP **0612**, 004 (2006) [arXiv:hep-th/0609062].

[201] S. R. Coleman and F. De Luccia, "Gravitational Effects On And Of Vacuum Decay," Phys. Rev. D **21**, 3305 (1980).

[202] T. Banks, "Remodeling the pentagon after the events of 2/23/06," arXiv:hep-ph/0606313.

[203] A. E. Nelson and N. Seiberg, "R symmetry breaking versus supersymmetry breaking," Nucl. Phys. B **416**, 46 (1994) [arXiv:hep-ph/9309299].

[204] T. Banks, "Cosmological breaking of supersymmetry or little Lambda goes back to the future. II," arXiv:hep-th/0007146;

T. Banks and W. Fischler, "M-theory observables for cosmological space-times," arXiv:hep-th/0102077;

T. Banks and W. Fischler, "An holographic cosmology," arXiv:hep-th/0111142;

T. Banks and W. Fischler, "Holographic cosmology 3.0," Phys. Scripta **T117**, 56 (2005) [arXiv:hep-th/0310288];

T. Banks and W. Fischler, "Holographic cosmology," arXiv:hep-th/0405200.

[205] S. R. Coleman,"The Fate Of The False Vacuum. 1. Semiclassical Theory," Phys. Rev. D **15**, 2929 (1977) [Erratum-ibid. D **16**, 1248 (1977)].

[206] R. Bousso, B. Freivogel and M. Lippert, "Probabilities in the landscape: The decay of nearly flat space," Phys. Rev. D **74**, 046008 (2006) [arXiv:hep-th/0603105].

[207] T. Banks, B. Fiol and A. Morisse, "Towards a quantum theory of de Sitter space," JHEP **0612**, 004 (2006) [arXiv:hep-th/0609062].

[208] J. Bagger, E. Poppitz and L. Randall, "The R axion from dynamical supersymmetry breaking," Nucl. Phys. B **426**, 3 (1994) [arXiv:hep-ph/9405345].

[209] O. Adriani *et al.*, Phys. Rev. Lett. **102**, 051101 (2009) [arXiv:0810.4994 [astro-ph]].

[210] M. Cirelli, M. Kadastik, M. Raidal and A. Strumia, Nucl. Phys. B **813**, 1 (2009) [arXiv:0809.2409 [hep-ph]].

[211] N. Arkani-Hamed, D. P. Finkbeiner, T. R. Slatyer and N. Weiner, Phys. Rev. D **79**, 015014 (2009) [arXiv:0810.0713 [hep-ph]].

[212] A. Arvanitaki, S. Dimopoulos, S. Dubovsky, P. W. Graham, R. Harnik and S. Rajendran, arXiv:0812.2075 [hep-ph].

[213] Y. Bai and Z. Han, Phys. Rev. D **79**, 095023 (2009) [arXiv:0811.0387 [hep-ph]].

[214] C. R. Chen, M. M. Nojiri, F. Takahashi and T. T. Yanagida, arXiv:0811.3357 [astro-ph].

[215] C. R. Chen, F. Takahashi and T. T. Yanagida, Phys. Lett. B **671**, 71 (2009) [arXiv:0809.0792 [hep-ph]].

[216] I. Cholis, L. Goodenough and N. Weiner, Phys. Rev. D **79**, 123505 (2009) [arXiv:0802.2922 [astro-ph]].

[217] I. Cholis, D. P. Finkbeiner, L. Goodenough and N. Weiner, arXiv:0810.5344 [astro-ph].

[218] E. J. Chun and J. C. Park, JCAP **0902**, 026 (2009) [arXiv:0812.0308 [hep-ph]].

[219] P. J. Fox and E. Poppitz, Phys. Rev. D **79**, 083528 (2009) [arXiv:0811.0399 [hep-ph]].

[220] P. Grajek, G. Kane, D. Phalen, A. Pierce and S. Watson, arXiv:0812.4555 [hep-ph].

[221] R. Harnik and G. D. Kribs, arXiv:0810.5557 [hep-ph].

[222] M. Ibe, H. Murayama and T. T. Yanagida, Phys. Rev. D **79**, 095009 (2009) [arXiv:0812.0072 [hep-ph]].

[223] J. D. March-Russell and S. M. West, Phys. Lett. B **676**, 133 (2009) [arXiv:0812.0559 [astro-ph]].

[224] J. Mardon, Y. Nomura, D. Stolarski and J. Thaler, JCAP **0905**, 016 (2009) [arXiv:0901.2926 [hep-ph]].

[225] J. Mardon, Y. Nomura and J. Thaler, arXiv:0905.3749 [hep-ph].

[226] P. Meade, M. Papucci, A. Strumia and T. Volansky, arXiv:0905.0480 [hep-ph].

[227] P. Meade, M. Papucci and T. Volansky, arXiv:0901.2925 [hep-ph].

[228] Y. Nomura and J. Thaler, arXiv:0810.5397 [hep-ph].

[229] A. E. Nelson and C. Spitzer, arXiv:0810.5167 [hep-ph].

[230] M. Pospelov and A. Ritz, Phys. Lett. B **671**, 391 (2009) [arXiv:0810.1502 [hep-ph]].

[231] E. Ponton and L. Randall, JHEP **0904**, 080 (2009) [arXiv:0811.1029 [hep-ph]].

[232] S. Shirai, F. Takahashi and T. T. Yanagida, arXiv:0902.4770 [hep-ph].

[233] V. Barger, Y. Gao, W. Y. Keung and D. Marfatia, arXiv:0906.3009 [hep-ph].

[234] I. Cholis, G. Dobler, D. P. Finkbeiner, L. Goodenough, T. R. Slatyer and N. Weiner, arXiv:0907.3953 [astro-ph.HE].

[235] D. P. Finkbeiner and N. Weiner, Phys. Rev. D **76**, 083519 (2007) [arXiv:astro-ph/0702587].

[236] I. Z. Rothstein, T. Schwetz and J. Zupan, JCAP **0907**, 018 (2009) [arXiv:0903.3116 [astro-ph.HE]].

[237] L. Bergstrom, Phys. Lett. B **225**, 372 (1989).

[238] H. K. Dreiner, H. E. Haber and S. P. Martin, arXiv:0812.1594 [hep-ph].

[239] M. Graesser and J. Shelton, JHEP **0906**, 039 (2009) [arXiv:0811.4445 [hep-ph]].

[240] C. Amsler *et al.* [Particle Data Group], Phys. Lett. B **667**, 1 (2008).

[241] B. K. Bullock, K. Hagiwara and A. D. Martin, Nucl. Phys. B **395**, 499 (1993).

[242] J. H. Kuhn and A. Santamaria, Z. Phys. C **48**, 445 (1990).

[243] P. D. Serpico and D. Hooper, arXiv:0902.2539 [hep-ph].

[244] A. Birkedal, K. T. Matchev, M. Perelstein and A. Spray, arXiv:hep-ph/0507194.

Chapter 9

Curriculum Vitae
Jean-François Fortin

Degrees

	Rutgers University, New Brunswick, New Jersey, USA
September 2004 – October 2009	Ph.D., Physics
	Laval University, Québec, Québec, Canada
September 2003 – August 2004	M.S., Physics
September 1999 – August 2003	B.S., Physics Engineering

Positions Held

July 2008 – June 2009	Graduate Assistant, Rutgers University
May 2008	Visiting Student, Santa Cruz Institute for Particle Physics
January 2008 – June 2008	Teaching Assistant, Rutgers University
July 2007 – December 2007	Graduate Assistant, Rutgers University
September 2004 – June 2007	Graduate Fellow, Rutgers University

Publications

- J. F. Fortin, J. Shelton, S. Thomas and Y. Zhao, *Gamma Ray Spectra from Dark Matter Annihilation and Decay*, submitted to Phys. Rev. D, arXiv:0908.2258 [hep-ph].
- T. Banks and J. F. Fortin, *Tunneling Constraints on Effective Theories of Stable de Sitter Space*, submitted to Phys. Rev. D, arXiv:0906.3714 [hep-th].
- T. Banks and J. F. Fortin, *A Pyramid Scheme for Particle Physics*, JHEP **0907**, 046 (2009), arXiv:0901.3578 [hep-ph].
- R. Essig, J. F. Fortin, K. Sinha, M. Strassler and G. Torroba, *Metastable Supersymmetry Breaking and Multitrace Deformations of SQCD*, JHEP **0903**, 043 (2009), [arXiv:0812.3213 [hep-th]].

- T. Banks, L. M. Carpenter and J. F. Fortin, *Undetected Higgs decays and Neutrino Masses in Gauge Mediated, Lepton Number Violating Models*, JHEP **0809**, 087 (2008), [arXiv:0804.2688 [hep-ph]].

- J. F. Fortin, *Spontaneously Broken Gauge Symmetry in SUSY Yang-Mills Theories with Matter*, arXiv:0710.2131 [hep-th].

- R. Essig and J. F. Fortin, *The Minimally Tuned Minimal Supersymmetric Standard Model*, JHEP **0804**, 073 (2008), [arXiv:0709.0980 [hep-ph]].

- J. F. Fortin, P. Mathieu and S. O. Warnaar, *Characters of Graded Parafermion Conformal Field Theory*, Adv. Theor. Math. Phys. **11**, 945 (2007), [arXiv:hep-th/0602248].

- J. F. Fortin, P. Jacob and P. Mathieu, *SM(2,4k) Fermionic Characters and Restricted Jagged Partitions*, J. Phys. A **38**, 1699 (2005), [arXiv:hep-th/0406194].

- J. F. Fortin, P. Jacob and P. Mathieu, *Jagged Partitions*, Ramanujan Journal **10**, 215 (2005), [arXiv:math/0310079].

- J. F. Fortin, P. Jacob and P. Mathieu, *Generating Function for K-restricted Jagged Partitions*, Electronic J. Comb. **12**, 17 (2005), [arXiv:math-ph/0305055].

- L. Bégin, J. F. Fortin, P. Jacob and P. Mathieu, *Fermionic Characters for Graded Parafermions*, Nucl. Phys. B **659**, 365 (2003), [arXiv:hep-th/0301057].